

Regulation of UDP- glucuronosyltransferases by microRNAs

by

Dhilushi D Wijayakumara

*Thesis
Submitted to Flinders University
for the degree of*

Doctor of Philosophy
Department of Clinical Pharmacology
College of Medicine & Public Health
January 2021

Table of Contents

Table of Contents	i
List of Figures	vi
List of Tables	xi
Summary	xii
Declaration	xv
Acknowledgements	xvi
Publications in support of this thesis	xviii
Conference proceedings	xix
Awards in support of this thesis	xx
Abbreviations	xxi

Chapter 1: Review of the literature **1**

1.1 Biotransformation of small lipophilic molecules	1
1.2 Glucuronidation.....	4
1.3 UDP-glucuronosyltransferases.....	6
1.3.1 The UGT multi-gene Family - Nomenclature and Genomic organization.....	6
1.3.2 Human UGT1 family.....	7
1.3.3 Human UGT2 family.....	9
1.3.4 Human UGT8 and UGT3 families.....	11
1.4 Structure, localization and function of UGTs	12
1.5 Substrates of UGTs.....	15
1.6 Tissue specific expression of UGTs	20
1.7 UGTs in steroid target tissues and steroid glucuronidation	24
1.7.1 Androgen glucuronidation in the prostate	25
1.8 UGTs in Carcinogenesis: Impact on cancer risk and Drug metabolism.....	31
1.8.1 Involvement of UGT2B15 and UGT2B17 in Prostate cancer	32
1.9 Transcriptional regulation of UGTs.....	39
1.9.1 Regulation of tissue-specific constitutive expression of UGTs.....	41
1.9.2 Regulation of inducible expression of UGTs	43
1.10 microRNAs.....	48
1.10.1 Overview of miRNA	48
1.10.2 Biogenesis of miRNAs	49
1.10.3 miRNA Target Recognition and Function.....	55
1.10.4 miRNA target prediction	59
1.10.5 Regulation of drug metabolising enzymes (DMEs) by miRNAs.....	63

1.10 Project overview and Experimental Aims.....	66
--	----

Chapter 2: Materials and Methods.....68

2.1 Materials.....	68
2.1.1 Chemicals and Reagents	68
2.1.2 General Buffers	74
2.1.3 Oligonucleotides	75
2.1.4 miRNA mimics and Human Tissue Total RNA	75
2.1.5 Eukaryotic and prokaryotic cell lines.....	76
2.1.6 Luciferase Reporter and Expression Vectors.....	76
2.1.7 Antibodies.....	76
2.2 Methods.....	77
2.2.1 Cell Culture.....	77
2.2.2 Transient Transfection.....	78
2.2.3 Extraction of RNA	79
2.2.3.1 Extraction of RNA from monolayer cells	79
2.2.3.2 Extraction of total RNA, including small RNAs from monolayer cells.....	79
2.2.3.2 Extraction of total RNA from human tissues.....	81
2.2.3 Quantification of mRNA	82
2.2.3.1 Reverse transcription polymerase chain reaction (RT-PCR) of mRNA.....	82
2.2.3.2 Quantification of mRNA by quantitative real-time polymerase chain reaction (qPCR).....	82
2.2.4 Reverse Transcription and quantification of mature and primary miRNAs.....	83
2.2.4.1 Reverse Transcription of mature miRNA.....	83
2.2.4.2 Quantitative RT-PCR of mature miRNA	85
2.2.4.3 Quantitative RT-PCR of primary miRNA.....	85
2.2.5 Site directed mutagenesis	86
2.2.5.1 Polyacrylamide Gel (PAGE) purification of oligonucleotides for.....	86
site directed mutagenesis	86
2.2.5.2 DNA Site directed mutagenesis.....	87
2.2.6 Western Blotting	88
2.2.6.1 Preparation of lysates	88
2.2.6.2 Polyacrylamide gel electrophoresis (PAGE).....	88
2.2.6.3 Development of an antibody specific for UGT2B15 and UGT2B17, and Western Blotting	90
2.2.7 Bacterial culture	91
2.2.8 Restriction digests	92
2.2.9 Ligations and transformations.....	92
2.2.10 Preparation of competent cells.....	93
2.2.11 Plasmid preparations	94
2.2.12 Quantification of RNA/ DNA.....	95
2.2.14 DNA Purification	96
2.2.15 Sequencing.....	96
2.2.16 Luciferase Assays.....	96
2.2.17 Glucuronidation Assays.....	97
2.2.17.1 4-Methylumbelliferone Glucuronidation Assays.....	97
2.2.18 Statistical analysis	97

Chapter 3: Regulation of UGT2B15 and UGT2B17 expression by miRNAs 98

3.1 Introduction 98

3.2 Materials and Methods..... 101

 3.2.1 Luciferase Reporter Construction 101

 3.2.2 Glucuronidation Assays..... 102

 3.2.3 Statistical Analysis 104

3.3 Results..... 105

 3.3.1 3'UTRs of UGT2B15 and UGT2B17 contain putative miRNA target sites..... 105

 3.3.2 The 3'UTRs of UGT2B15 and UGT2B17 are direct targets of miR-376c and UGT2B15 is a direct target of miR-376b and miR-222 in LNCaP cells 115

 3.3.3 MiR-376c reduces both UGT2B15 and UGT2B17 mRNA and protein levels in LNCaP cells..... 124

 3.3.4 MiR-376b and miR-222 reduce UGT2B15 mRNA levels whereas miR-525 reduces both UGT2B15 and UGT2B17 mRNA levels in LNCaP cells..... 126

 3.3.5 MiR-376c reduces glucuronidation activities of both UGT2B15 and UGT2B17 in LNCaP cells..... 129

 3.3.6 UGT2B15 and UGT2B17 mRNA levels are inversely correlated to the levels of miR-376c in human tissues. 134

 3.3.7 UGT2B15 and UGT2B17 mRNA levels are inversely correlated with the levels of miR-376c in prostate cell lines and tissues. 136

 3.3.8 UGT2B15/ UGT2B17 mRNA levels show an inverse relationship to miR-376c levels in normal prostate, primary tumour and metastatic prostate cancer tissues..... 140

3.4 Discussion 144

Chapter 4: Regulation of UGT2B15 EXPRESSION by miR-331-5p 151

4.1 Introduction 151

4.2 Methods..... 152

 4.2.1 Luciferase plasmid Construction..... 152

 4.2.2 Analyses of Prostate Adenocarcinoma (PRAD) and Hepatocellular Carcinoma Data Sets. 153

 4.2.3 Statistical Analysis 154

4.3 Results..... 156

 4.3.1 The 3'UTR of UGT2B15 contains a putative canonical target site for miR-331-5p..... 156

 4.3.2 MiR-331-5p down-regulates UGT2B15 mRNA and glucuronidation activity in human Prostate Cancer cells..... 157

 4.3.3 MiR-331-5p directly binds to the 3'UTR of UGT2B15..... 162

4.3.4 A non-canonical miR-331-5p target site is present in the UGT2B15 3'UTR	166
4.3.5 MiR-331-5p cooperatively regulates UGT2B15 via two target sites.....	169
4.3.6 MiR-331-5p and miR-376c function additively in UGT2B15 regulation.....	171
4.3.7 The expression of miR-331-5p inversely correlates with UGT2B15 mRNA expression in human tissues and hepatocellular carcinoma	174
4.4 Discussion	176

Chapter 5: Regulation of UGT2B7 and UGT2B4 by miRNAs..... 183

5.1 Introduction	183
5.2 Methods.....	185
5.2.1 Luciferase Plasmid Construction	185
5.2.2 Western Blotting	186
5.2.3 Morphine Glucuronidation Assay	187
5.2.4 Data Analyses of Liver Hepatocellular Carcinoma.....	188
5.2.5 Statistical Analysis.....	188
5.3 Results.....	190
5.3.1 The UGT2B7 and UGT2B4 3'UTRs contain putative target sites for miRNAs	190
5.3.2 The 3'UTR of UGT2B7 is a direct target of miR-3664-3p and the 3'UTR of UGT2B4 is a direct target of miR-135a-5p and miR-410-3p in HepG2 cells	196
5.3.3 MiR-3664-3p reduces UGT2B7 mRNA, protein, and glucuronidation activity in human liver HepG2 cells.....	200
5.4 Discussion	210

Chapter 6: Investigation of UGT2B15 and UGT2B17 post-transcriptional regulation by androgens 215

6.1 PART 1: Investigation of the involvement of RNA-binding proteins in UGT2B15 and UGT2B17 regulation	215
6.1.1 Introduction	215
6.1.2 Materials and Methods.....	220
6.1.2.1 PCR amplification of the RBPs from cell lines	220
6.1.2.2 Extraction of pCMV-AUF1 vectors	220
6.1.2.3 Verification of the identity of AUF1 expression vectors.....	221
6.1.2.4 Transient Transfection of AUF1 expression vectors into cell lines	222
6.1.2.5 DHT Treatment of LNCaP and VCaP cells.....	222

6.1.2.6 Primers.....	223
6.1.3 Results.....	223
6.1.3.1 Investigation of RBP expression in human cell lines.....	223
6.1.3.2 Changes in RBP mRNA expression in VCaP and LNCaP cells with DHT treatment.....	225
6.1.3.3 Regulation of UGT2B15 and UGT2B17 mRNA expression by AUF1 isoforms in VCaP and LNCaP cells.	227
6.2 PART 2: Investigation of the role of miRNAs in androgen-induced UGT2B15 and UGT2B17 regulation	231
6.2.1 Results.....	231
6.3 Discussion	235
Chapter 7: General discussion and conclusions	237
Appendix 1: Investigation of SNPs in UGT2B15 and UGT2B17 regulation	249
A1. Introduction	249
A2. Results.....	250
A2.1 Putative miRNA binding to the SNP (rs3100) located in the 3'UTR of UGT2B15	250
A3 Discussion	254
Bibliography.....	257
Appendix 2:.....	291
Appendix 3:.....	309
Appendix 4:.....	323

List of Figures

Chapter 1

Figure 1.1: Glucuronidation reaction.....	5
Figure 1.2: Phylogenetic tree of human UGT members	7
Figure 1.3: The UGT1A family gene locus.....	9
Figure 1.4: The UGT2 family gene locus.....	10
Figure 1.5: Structure of the UDP-glucuronosyltransferase	14
Figure 1.6: UGT expression in liver	21
Figure 1.7: UGT2B enzymes involved in androgen metabolism	27
Figure 1.8: Localization of UGT2B15 and UGT2B17 in prostate tissue by immunohistochemistry	29
Figure 1.9: Androgen metabolism in the prostate.....	30
Figure 1.10: The canonical pathway of miRNA biogenesis.....	51
Figure 1.11: Canonocal miRNA:mRNA interactions	62

Chapter 2

Figure 2.1: Specificity of the UGT2B15/2B17 antibody	91
--	----

Chapter 3

Figure 3.1: The 3'UTRs of both UGT2B15 and UGT2B17 mRNAs contain putative miRNA binding sites	106
Figure 3.2: Expression patterns of UGT2B15, UGT2B17 and predicted miRNAs in ten cell lines	108
Figure 3.3: MiRNAs target 3'UTRs of UGT2B15 and/or UGT2B17 in Du145 cells	111
Figure 3.4: Investigation of new miRNAs that target the 3'UTR of UGT2B17 in Du145, LNCaP and HEK293T cells	113
Figure 3.5: The 3'UTRs of UGT2B15 and/or UGT2B17 contain putative miR-376c, miR-376b and miR-222 binding sites.....	115

Figure 3.6: MiR-376c mimics reduce the activity of the pGL3-promoter construct carrying the UGT2B15 or UGT2B17 3'UTR via their binding to the predicted miR-376c site in prostate cancer LNCaP cells.....	117
Figure 3.7: MiR-376c mimics reduce the activity of the luciferase reporter containing the UGT2B15 or UGT2B17 3'-UTR via their binding to the predicted miR- 376c site in prostate cancer Du145, liver HepG2 and kidney HEK293T cells	119
Figure 3.8: MiR-376b mimics reduce the activity of the pGL3-promoter construct carrying the UGT2B15 3'-UTR via binding to its predicted miR-376b site in prostate cancer LNCaP, Du145 and kidney HEK293T cells	121
Figure 3.9: MiR-222 mimics reduce the activity of the pGL3-promoter construct carrying the UGT2B15 3'-UTR via binding to its predicted miR-222 site in prostate cancer LNCaP, Du145 and kidney HEK293T cells	123
Figure 3.10: miR-376c mimics reduce the mRNA and protein levels of UGT2B15 and UGT2B17 in LNCaP cells.....	125
Figure 3.11: miR-376b and miR-222 mimics reduce UGT2B15 mRNA levels in LNCaP cells.....	127
Figure 3.12: MiR-525 reduces the mRNA levels of UGT2B15 and UGT2B17 via possible binding to target sites in the coding regions of the two UGTs.....	128
Figure 3.13: MiR-376c mimics reduce the testosterone glucuronidating activity of UGT2B15 and UGT2B17 in prostate cancer LNCaP cells.....	129
Figure 3.14: Androsterone is a specific substrate of UGT2B17.....	131
Figure 3.15: MiR-376c mimics reduce the androsterone glucuronidating activity of UGT2B17 and 4-MU glucuronidation activity of UGT2B15 in prostate cancer LNCaP cells.....	133
Figure 3.16: Negative correlation between UGT2B15 and UGT2B17 mRNA levels versus miR-376c in human tissues.....	135
Figure 3.17: Negative correlation between UGT2B15 and UGT2B17 mRNA levels versus miR-376c in androgen receptor–positive prostate cancer cell lines as compared with normal prostate tissues	138
Figure 3.18: Negative correlation between UGT2B15 and UGT2B17 expression versus pri-miR-376c expression in androgen receptor positive prostate cancer cell lines as compared to 18 normal prostate tissue samples	140
Figure 3.19: Relationship between miR-376c versus UGT2B15 and UGT2B17 normal prostate tissues, primary prostate tumours and metastatic prostate tumours.....	142
Figure 3.20: Relationship between miR-222 levels in normal prostate tissues, primary prostate tumours and metastatic prostate tumours.....	143

Chapter 4

Figure 4.1: The putative miR-331-5p binding site in the 3'-UTR of UGT2B15 mRNA	157
Figure 4.2: miR-331-5p reduces UGT2B15 mRNA levels in LNCaP cells	158
Figure 4.3: miR-331-5p reduces UGT2B15 enzymatic activity in LNCaP cells	160
Figure 4.4: miR-331-5p mimics reduce the activity of a luciferase reporter containing the UGT2B15 3'-UTR in LNCaP, Du145, HEK293T and HepG2 cells	163
Figure 4.5: miR-331-5p reduces the activity of a luciferase reporter construct containing the UGT2B15 3'-UTR via a canonical target site (site 1) in LNCaP cells	165
Figure 4.6: Discovery of a noncanonical miR-331-5p target site (site 2) in the UGT2B15 3'-UTR	168
Figure 4.7: Cooperative regulation of UGT2B15 3'-UTR by miR-331-5p via two target sites	170
Figure 4.8: Additive regulation of UGT2B15 3'-UTR by miR-331-5p and miR-376c	173
Figure 4.9: The miR-331-5p and UGT2B15 levels are significantly inversely correlated in a human tissue panel and the TCGA hepatocellular carcinoma cohort.....	175
Figure 4.10: Types of canonical and non-canonical miRNA:mRNA interactions..	178
Figure 4.11: Interaction of 75-150 bp or full-length 3'-UTRs of UGT2B15 and UGT2B17, with miR-331-5p predicted by RNAhybrid	182

Chapter 5

Figure 5.1: The 3'UTRs of UGT2B7 and UGT2B4 mRNAs contain putative miRNA binding sites.....	191
Figure 5.2: Effects of miRNA mimics on a luciferase reporter containing the UGT2B7 3'-UTR or UGT2B4 3'-UTR and expression of miRNAs in HepG2 cells	194
Figure 5.3: The putative interaction of the microRNAs with the 3'UTRs of UGT2B7 and UGT2B4 mRNAs.....	195
Figure 5.4: The UGT2B7 3'-UTR contains a functional miR-3664-3p target site and the UGT2B4 3'-UTR contains a functional miR-135a-5p site and a functional miR-410-3p site.....	198

Figure 5.5: MiR-3664-3p and miR-135a-5p mimics reduce the activity of the pGL3-promoter construct carrying the UGT2B7 and UGT2B4 3'UTR respectively, via their binding to the predicted target site in HuH7 cells	199
Figure 5.6: MiR-3664-3p mimics reduce the expression of endogenous UGT2B7 mRNA	201
Figure 5.7: miR-3664-3p mimics reduce the protein expression of endogenous UGT2B7, and miR-3664 levels are negatively correlated to UGT2B7 mRNA in a tissue RNA panel.....	203
Figure 5.8: miR-135a-5p and miR-410-3p mimics reduce UGT2B4 mRNA levels in HuH7 cells	205
Figure 5.9: Correlation analyses between UGT2B4 and miR-135a-5p (or pri-miR-135a-1/2) levels in normal human liver tissues and liver cancer specimens...	207
Figure 5.10: Negative correlation between UGT2B4 and miR-410-3p in a human tissue panel and a liver cancer cohort.....	209

Chapter 6

Part 1

Figure 6.1.1: Post-transcriptional regulation of gene expression by RBPs and miRNAs at different levels.....	216
Figure 6.1.2: AUF1 isoform detection in AUF1 expression vectors	221
Figure 6.1.3: Expression of RNA-binding proteins in human prostate and breast cancer cell lines.....	224
Figure 6.1.4: Expression of AUF1 isoforms in human prostate and breast cancer cell lines.....	225
Figure 6.1.5: Expression of AUF1 and TIAR in VCaP and LNCaP cells treated with DHT	227
Figure 6.1.6: Target gene expression in AUF1 overexpressed VCaP cells	228
Figure 6.1.7: Changes in UGT2B15 and UGT2B17 mRNA expression in AUF1 overexpressed VCaP cells.....	230

Part 2

Figure 6.2.1: Expression of UGT2B15, UGT2B17 and miRNAs in LNCaP cells treated with DHT	232
Figure 6.2.2: Relationship between miR-135a-5p versus UGT2B15 and UGT2B17 in normal prostate tissues, primary prostate tumours and metastatic prostate tumours.....	233

Figure 6.2.3: 3'UTRs of UGT2B15 and UGT2B17 contain predicted miR-135a-5p binding sites	234
---	-----

Appendix 1

Figure A1: Predicted binding of miRNAs to the the UGT2B15 3'UTR target site where the SNP (rs3100) is located.....	251
--	-----

Figure A2: The position of the SNP, c.1761T>C (rs3100) site in the 3'UTR of UGT2B15	251
---	-----

Figure A3: MiR-3679-5p mimics reduce the activity of the pGL3-reporter construct carrying the UGT2B15 3'UTR containing the C allele of the SNP, rs3100 in LNCaP cells.....	252
--	-----

Figure A4: Luciferase assays in HEK293T cells transfected with miRNA mimics and the reporter construct carrying the UGT2B15 3'UTR with the C allele at the SNP site, or the UGT2B17 3'UTR containing reporter	253
---	-----

Figure A5: UGT2B15 mRNA expression in miR-3679-5p mimic-transfected cells	254
---	-----

Figure A6: SNP (rs3100) is located within the predicted miR-5690 target site in the UGT2B15 3'UTR.....	256
--	-----

List of Tables

Chapter 1

Table 1.1: Selected substrates of UGT1A and UGT2B families.....	15
Table 1.2: Distribution of UGT mRNAs in human tissues	23
Table 1.3: UGTs reported to be associated with certain types of cancers.....	32
Table 1.4: Nuclear receptors, their ligands and their target UGTs.....	45
Table 1.5: miRNA target prediction tools.....	60
Table 1.6: List of miRNAs reported to regulate DME expression	64

Chapter 2

Table 2.1: Reagent used in experimental procedures.....	68
---	----

Chapter 3

Table 3.1: Primers used in this study for mutagenesis, cloning and qPCR (5'–3').....	104
--	-----

Chapter 4

Table 4.1: Primers used in this study for mutagenesis, cloning and qPCR (5'–3').....	154
--	-----

Chapter 5

Table 5.1: Primers used in this study for mutagenesis, cloning and qPCR (5'–3').....	188
--	-----

Chapter 6:

Table 6.1: Primers used in this study for PCR and qPCR (5'–3').....	223
---	-----

Summary

The glucuronidation of lipophilic compounds results in products that are generally more water soluble, thus promoting their detoxification and clearance (Mackenzie et al., 1997). There are four human UDP-glucuronosyltransferase (UGT) families (Mackenzie et al., 2005); however, glucuronidation is primarily carried out by members of the UGT1A and UGT2B subfamilies whose substrates for these enzymes include endogenous bioactive molecules (e.g., bilirubin, steroid hormones, bile acids, retinoids, fatty acids), carcinogens, environmental toxins, and therapeutic drugs (Guillemette, 2003, Mackenzie et al., 2005).

In humans, glucuronidation of androgens (e.g., testosterone and dihydrotestosterone) and their metabolites is carried out mainly by UGT2B15, and UGT2B17 (Turgeon et al., 2001). The androgen/androgen receptor (AR) signaling pathway plays a pivotal role in prostate growth and function; however, excessive androgen signaling contributes to prostate cancer development and progression (Kaarbo et al., 2007). UGT2B15 and UGT2B17 are expressed in the prostate and their glucuronidation of androgens effectively terminates androgen signaling (Chouinard et al., 2008). They are also expressed in liver where they reduce circulating androgen levels. Consistent with their important functions in androgen signaling, altered UGT2B15 and UGT2B17 activity is related to prostate cancer risk and progression (Turgeon et al., 2001, Heinlein and Chang, 2004, Chouinard et al., 2007).

The liver is the primary site of glucuronidation; thus, the control of hepatic UGT expression and activity is of significant biologic and pharmacological interest (Hu et al., 2014b). UGT2B4 and UGT2B7 are both highly expressed in the liver (Congiu et al., 2002, Court, 2010) as well as in extra hepatic tissues where they play important roles in drug metabolism and homeostasis of endogenous bioactive molecules (Hu et al., 2014b, Ohno and Nakajin, 2009). UGT2B7 has high activity toward various endogenous compounds including bile acids, retinoids and steroids (Hu et al., 2014b), as well as exogenous compounds including carcinogens and drugs. Around 35% of the therapeutic drugs that are glucuronidated are UGT2B7 substrates (Williams et al., 2004). UGT2B4 glucuronidates various endogenous compounds as

well as a subset of drugs and toxins; however, UGT2B4 is generally considered to play a more minor role in overall drug metabolism than UGT2B7.

The transcriptional regulation of UGT2B15, UGT2B17, UGT2B7 and UGT2B4 (in the prostate and hepatic models respectively) have been well investigated. However, little is known about the mechanisms controlling these UGTs at the post-transcriptional level. MicroRNAs (miRNAs/miRs) are noncoding small RNAs that mediate post-transcriptional gene regulation through translational repression and/or mRNA degradation (Macfarlane and Murphy, 2010). This project investigated the potential for miRNA to regulate UGT2B15 and UGT2B17 in prostate cancer cells and UGT2B4 and UGT2B7 in liver cancer cells.

Putative target sites for miR-376c, miR-376b, miR-222 and miR-331-5p were identified in the 3'-untranslated regions (UTRs) of the UGT2B15 and/or UGT2B17 mRNAs. In prostate-derived LNCaP cells, miR-376c mimics reduced both UGT2B15 and UGT2B17 mRNA and protein levels and inhibited glucuronidation of the UGT2B15/UGT2B17 substrates testosterone, 4-methylumbelliferone, and androsterone. MiR-376c repressed the activity of luciferase reporters containing UGT2B15 or UGT2B17 3'-UTRs, and this was abrogated by mutating the predicted miR-376c binding sites. Consistent with the idea that miR-376c negatively regulates UGT2B15 and UGT2B17 expression, the level of this miRNA was inversely correlated with UGT2B15/UGT2B17 mRNA levels in normal prostate, primary and metastatic prostate cancer tissues, and in prostate cancer cell lines. Two other miRNAs, miR-222 and miR-376b, also reduced UGT2B15 mRNA levels in LNCaP cells and repressed the UGT2B15 3'-UTR, the latter was abrogated by mutating the relevant miRNA binding sites in the 3' UTR. Levels of miR-222 were inversely correlated with UGT2B15/UGT2B17 mRNAs levels in normal prostate, and primary and metastatic prostate cancers. Endogenous UGT2B15 expression and activity was also repressed by miR-331-5p; however, this miRNA did not alter UGT2B17 expression. Two miR-331-5p binding sites, a canonical target site and a novel non-canonical site, were identified in the UGT2B15 3'UTR and shown to function additively. UGT2B15 and miR-331-5p levels were inversely correlated in a panel of normal human tissues, and in a liver cancer data set, but not in a prostate cancer data set. Overall, these data suggest that miR-376c and miR-331-5p (and possibly miR-

222, miR-376b) are important regulators of UGT2B15 and/or UGT2B17 levels, but may play varying roles in different tissues. Moreover, miR-331-5p mediates differential regulation of the UGT2B15 and UGT2B17 mRNAs. This represents the first evidence for post-transcriptional regulation of UGT2B15 and UGT2B17 by miRNAs in prostate cancer cells and may have importance in regulating AR signaling.

Putative target sites were identified for miR-3664-3p in the UGT2B7 3'-UTR and for miR-135a-5p and miR-410-3p in the UGT2B4 3'-UTR. Transfection of miR-3664-3p mimics in HepG2 liver cancer cells significantly reduced UGT2B7 mRNA and protein levels leading to reduced enzymatic activity. Transfection of miR-135a-5p or miR-410-3p mimics significantly decreased UGT2B4 mRNA levels in Huh7 liver cancer cells. MiR-3664-3p, miR-135a-5p and miR-410-3p directly repressed the UGT2B7 and UGT2B4 3'-UTRs respectively as shown using reporter assays. This repression was abrogated by mutating the relevant miRNA binding sites in the 3'-UTR reporter constructs. The expression levels of miR-410-3p were inversely correlated with UGT2B4 mRNA levels in a cohort of liver hepatocellular carcinoma (371 specimens) and a panel of normal human tissues. Similarly, there was an inverse correlation between miR-135a and UGT2B4 mRNA levels in a panel of 18 normal human liver tissues. Together, these data suggest that miR-135a and miR-410 control UGT2B4 and that miR-3664 controls UGT2B7 expression in liver cancer and/or normal liver cells.

Declaration

I certify that this thesis does not incorporate without acknowledgement any material previously submitted for a degree or diploma in any university; and that to the best of my knowledge and belief it does not contain any material previously published or written by another person except where due reference is made in the text.

Dhilushi D Wijayakumara

Acknowledgements

Major accomplishments in life are seldom achieved without the shining lights of guidance, support and love casted by the people who surround you.

First and foremost, Professor Peter Mackenzie, it has been an absolute pleasure and an honour to have worked with you. I have constantly admired not only your passion and skills as a great scientist but also your kind and caring personality. My gratitude towards you is endless for all the guidance and support you have provided me with during my PhD.

Associate Professor. Robin Meech and Dr. Dong Gui Hu, I have been blessed to have been able to work under your supervision. I couldn't have asked for better co-supervisors to guide me during the most important phase of my career.

Peter, Robin and Dong Gui, from the bottom of my heart, thank you ever so much. I hope I have made all of you proud and I promise to consistently endeavor to emulate the amazing scientists all of you are, for the rest of my career.

To all my current and previous colleagues at the Department of Clinical Pharmacology including Prof. Ross McKinnon, Ms. Anne Rogers, Dr. Andrew Rowland, Ms. Karli Goodwin and Ms. Heather Bailey, thank you very much for all your advice and support. My lovely friends Nuy, Bo, Sara, Negara, Julie Ann, Kushari, Pramod, Lulu, Alex and Siti, I will forever hold on to the fond memories of the days working with all of you. My time at work would not have been the same without you.

My beautiful parents, Amma and Appachchi, words simply cannot express my love and gratitude towards both of you. During my entire PhD, you consistently had faith in me and supported me relentlessly and unconditionally even during times when I seriously felt this achievement was not attainable. I will forever be in your debt. I dedicate my PhD qualification to both of you.

My sisters, Iloshi, Rumesi, Prabhashi and my brother, Sanchitha, thank you for your unwavering love and support always. I am absolutely blessed to have such wonderful siblings. You are the reason I was able to maintain perspective and sanity during this time.

My wonderful boys, Revan, my husband and Savven, my son, thank you for sitting by my side during this long roller coaster of a ride and for the unconditional love and support. You were my anchors whenever the journey got too challenging. I love you. This PhD is yours as much as it is mine.

Publications in support of this thesis

Publications arising directly from this thesis:

Chapter 3

Wijayakumara DD, Hu DG, Meech R, McKinnon RA, Mackenzie PI. (2015) Regulation of Human UGT2B15 and UGT2B17 by miR-376c in Prostate Cancer Cell Lines. *J Pharmacol Exp Ther.* 354(3): 417-25.

Chapter 4

Wijayakumara DD, Mackenzie PI, McKinnon RA, Hu DG, Meech R (2017) Regulation of UDP-Glucuronosyltransferases UGT2B4 and UGT2B7 by MicroRNAs in Liver Cancer Cells. *J Pharmacol Exp Ther.* 361(3):386-397.

Chapter 5

Wijayakumara DD, Mackenzie PI, McKinnon RA, Hu DG, Meech R (2018) Regulation of UDP-Glucuronosyltransferase 2B15 by miR-331-5p in prostate cancer cells involves canonical and non-canonical target sites. *J Pharmacol Exp Ther.* 365(1):48-59.

Additional publications related to the topic of this thesis:

Hu DG, Hickey TE, Irvine C, **Wijayakumara DD**, Lu L, Tilley WD, Selth LA, Mackenzie PI (2014) Identification of androgen receptor splice variant transcripts in breast cancer cell lines and human tissues. *Horm Cancer.* 5(2):61-71.

Hu DG, Selth LA, Tarulli GA, Meech R, **Wijayakumara D**, Chanawong A, Russell R, Caldas C, Robinson JL, Carroll JS, Tilley WD, Mackenzie PI, Hickey TE (2016) Androgen and Estrogen Receptors in Breast Cancer Coregulate Human UDP-Glucuronosyltransferases 2B15 and 2B17. *Cancer Res.* 76(19):5881-5893.

Hu DG, Hulin JA, **Wijayakumara DD**, McKinnon RA, Mackenzie PI, Meech R (2018) Intergenic Splicing between Four Adjacent UGT Genes (2B15, 2B29P2, 2B17, 2B29P1) Gives Rise to Variant UGT Proteins That Inhibit Glucuronidation via Protein-Protein Interactions. *Mol Pharmacol* 94(3):938-952.

Conference proceedings

- Department of Clinical Pharmacology Seminar Series, Flinders University (2013) – Oral Presentation
- 2013 Adelaide Pharmacology Group Meeting, University of South Australia, Adelaide (APG) – Oral presentation
- 2013 Annual Scientific Meeting of the Australasian Society of Clinical and Experimental Pharmacologists and Toxicologists (ASCEPT), Melbourne, VIC – Oral presentation
- 2013 Annual Scientific Meeting of the Australasian Society of Clinical and Experimental Pharmacologists and Toxicologists (ASCEPT), Melbourne, VIC – Poster presentation
- 2014 Annual Meeting of the Australian Society for Medical Research (ASMR), Adelaide, SA – Oral Presentation
- 2014 Combined ASBMB, ASPs, ANZSCDB, NZSBMB and NZSPB Annual Meetings (COMBIO), Canberra, Australia – Poster Presentation
- 2014 Flinders Medical Centre Volunteer Thank you Event, Flinders Centre for Innovation in Cancer – Oral Presentation
- 2015 Annual Meeting of the Australian Society for Medical Research (ASMR), Adelaide, SA – Oral Presentation
- 2015 The 6th European Molecular Biology Organization Meeting (EMBO): Advancing the Life Sciences, Birmingham, United Kingdom – Poster Presentation
- 2015 Annual Scientific Meeting of the Australasian Society of Clinical and Experimental Pharmacologists and Toxicologists (APSA-ASCEPT), Hobart, TAS – Poster presentation

Awards in support of this thesis

- Finders Medical Centre Volunteers PhD scholarship
- Drug Disposition and Response Poster Prize at the Annual Scientific Meeting of the Australasian Society of Clinical and Experimental Pharmacologists and Toxicologists (ASCEPT), Melbourne, VIC, Australia (2013)
- Finalist in Neville Percy Poster Prize (Best poster communication by a Higher Degree student) at the Annual Scientific Meeting of the Australasian Society of Clinical and Experimental Pharmacologists and Toxicologists (ASCEPT), Melbourne, VIC, Australia (2013)
- 2014 Student representative of special interest group: drug development and disposition for ASCEPT
- Finalist in Neville Percy Poster Prize at the Annual Scientific Meeting of the Australasian Society of Clinical and Experimental Pharmacologists and Toxicologists (ASCEPT), Hobart, TAS, Australia (2015)
- Flinders University Research Higher Degree Student Publication Award, 2015
- Australian Government Research Training Program Scholarship (Fee offset)

Grants:

- Flinders Medical Centre Foundation Project Grant (2013)
- Faculty of Health Sciences Student Conference Travel Fund (2013)
- ASCEPT Travel Grant (2013)
- Faculty of Health Sciences Student Conference Travel Fund (2014)
- Research Student Conference Travel Grant (2015)
- Faculty of Health Sciences Student Conference Travel Fund (2015)

Abbreviations

ADCY	Adenylate cyclase
ADT	Androsterone
ADT-G	Androsterone glucuronide
Ago	Argonaute
AKR	Aldo-keto reductase
Amp	Amphicilin
AP-1	Activator protein 1
AR	Androgen receptor
ARE	AU-rich element
ATCC	American Type Culture Collection
ATP	Adenosine triphosphate
AUF	AU-binding factor
BARE	Bile acid response element
BPH	Benign prostatic hyperplasia
bp	Base pair
BRF	Butyrate response factor
CAR	Constitutive androstane receptor
CCR4	Carbon catabolite repressor protein 4
CDCA	Chenodeoxycholic acid
cDNA	Complementary reoxyribonucleic acid
Cdx	Caudal-related homeodomain protein
ChIP	Chromatin immunoprecipitation
CIP	Calf intestinal alkaline phosphatase
COMT	Catechol O-methyl transferases
CRPC	Castrate resistant prostate cancer
CYP	Cytochrome P450
DGCR8	DiGeorge syndrome critical region 8
DH5 α	Doug-Hanahan-5 alpha
DHEA	Dehydroepiandrosterone
DHEA-S	Dehydroepiandrosterone sulphate
DHT	Dihydrotestosterone
3 α -DIOL	5 α -androstane-3 α ,17 β -diol

3 β -DIOL	5 α -androstane-3 β ,17 β -diol
DME	Drug metabolising enzymes
DMEM	Dulbecco's Modified Eagles Medium
DMSO	Dimethyl sulfoxide
DNA	Deoxyribonucleic acid
dNTP	Deoxynucleotide triphosphate
DPE	Downstream core promoter element
DR-1	Direct repeat-1
DTT	Dithiothreitol
EB	Elution buffer
E. coli.	Escherichia coli
EDTA	Ethylenediaminetetraacetic acid
eIF	Eukaryotic initiation factor
EMSA	Electrophoretic mobility shift assays
ER	Endoplasmic reticulum
ER	Estrogen Receptor
ERE	Estrogen response element
ERU	Estrogen response unit
EtOH	Ethanol
FBS	Fetal bovine serum
FOXA1	Forkhead box protein A1
FXR	Farnesoid X receptor
GAPDH	Glyceraldehyde-3-phosphate dehydrogenase
glucuronide	β -D-glucopyranosiduronic acid
GST	Glutathione-S-transferase
HEK	Human embryonic kidney
HNF	Hepatocyte nuclear factor
hnRNP	Heterogeneous nuclear ribonucleoprotein
HPLC	High-performance liquid chromatography
HPR	Horseradish Peroxidase
HSD	Hydroxysteroid dehydrogenase
Inr	Initiator region
kb	Kilobase
kDa	KiloDaltons
KSRP	KH-type splicing regulatory protein

LB	Luria-Bertani media
LCA	Lithocholic acid
LIHC	Liver hepatocellular carcinoma
M3G	Morphine-3-glucuronide
M6G	Morphine-6-glucuronide
Mb	Megabase
β -ME	β -Mercaptoethanol
MEM	Minimum Essential Medium
mfe	Minimum folding energy
miR/ miRNA	microRNA;
miRISC	miRNA induced silencing complex
miR-neg	Negative control miRNA
miRNA-seq	miRNA-sequencing
MRE	miRNA response element
mRNA	Messenger RNA
MRP	Multidrug resistance protein
MSKCC	Memorial Sloan-Kettering Cancer Center
4-MU	4-methylumbelliferone
NAT	N-acetyltransferase
NCBI	National Center for Biotechnology Information
NGS	Next generation sequencing
NR	Nuclear receptor
Nrf	Nuclear factor erythroid 2-related factor
NST	Nucleotide sugar transporter
nt	Nucleotide
OAT	Organic anion transporter
Oct-1	Octamer transcription factor 1
OD	Optical density
PABPC	Polyadenylate-binding protein
PAN	Poly(A) nuclease; Poly(A) specific ribonuclease subunit
PAGE	Polyacrylamide gel electrophoresis
PAPSS	3'-phosphoadenosine-5'-phosphosulfate synthases
PBS	Phosphate buffered saline
PCa	Prostate Cancer

PCR	Polymerase chain reaction
PLB	Passive lysis buffer
PPAR	Peroxisome proliferator-activated receptor
PRAD	Prostate adenocarcinoma
pre-miRNA	Precursor miRNAs
pri-miRNA	Primary miRNA
PSA	Prostate-specific antigen
PSMB	Proteasome subunit beta
RBP	RNA-binding protein
RIPA	Radioimmunoprecipitation assay
RISC	RNA induced silencing complex
RNA	Ribonucleic acid
rRNA	Ribosomal ribonucleic acid
RNAseq	RNA sequencing
RNP	Ribonucleoprotein
RNU6-2	U6 small nuclear-2 RNA
RT-qPCR	Quantitative real-time polymerase chain reaction
RPMI	Roswell Park Memorial Institute
S.D.	Standard deviation
SDS	Sodium dodecyl sulphate
S.E.M	Standard error of mean
siRNA	Small interfering RNA
SNP	Single nucleotide polymorphism
Sp1	Specificity protein 1
SULT	Sulfotransferase
TAE	Tris-acetate EDTA electrophoresis buffer
TBE	Tris-borate-EDTA buffer
TBS	Tris-buffered saline
TCGA	The Cancer Genome Atlas
TCPOBOP	1,4-bis[2-(3,5-dichloropyridyloxy)]benzene
TE	Tris-EDTA buffer
TEA	Triethylamine
TIA	T-cell internal antigen
TIAR	TIA-1-related protein
TLC	Thin layer chromatography

Tris	Tris[hydroxymethyl]aminomethane
TSS	Transcription start site
TTP	Tristetraprolin
TPMT	Thiopurine S-methyl transferases
UDP	Uridine diphosphate
UDPGA	UDP-glucuronic acid
UGT	UDP glucuronosyltransferases
USF	Upstream stimulating factor
UTR	Untranslated region
UV	Ultra violet
UBE2W	Ubiquitin conjugating enzyme E2 W
WT	Wild type

CHAPTER 1

REVIEW OF THE LITERATURE

1.1 Biotransformation of small lipophilic molecules

As all organisms are exposed constantly to various potentially hazardous chemicals including drugs, pollutants, dietary components and carcinogens, it remains a challenge for organisms to render these chemicals biologically harmless. Higher organisms have developed versatile and sophisticated immune systems in addition to the obvious physical barriers against a variety of molecular threats from the environment. However, the immune defences are directed against large molecules or particles and do not recognize smaller, simpler chemicals, which may accumulate to toxic levels in the body (Armstrong, 1987). In order to overcome this challenge, organisms possess biotransformation enzymes that can regulate these chemical xenobiotics. Given their critical roles in xenobiotic metabolism, they are also referred to as drug metabolising or detoxification enzymes (Gregory, 2004). However, it is important to note that these same enzymes can biotransform many chemicals produced endogenously in the body, including those that act as effector ligands such as steroids (Nebert, 1994). Moreover, these enzymes could regulate the biological activities and intracellular levels of diverse exogenous and endogenous molecules by acting cooperatively.

Biotransformation is classified into two groups termed phase I and phase II reactions (Kebamo et al., 2015, Kang et al., 2010, Jancova et al., 2010). The enzymes

involved in phase I reactions are known as functionalization (or phase I) enzymes whereas the enzymes involved in phase II reactions are known as conjugation (or phase II) enzymes. Phase I enzymes are involved in catalysing the unmasking or interchanging of an existing functional group or addition of a new functional group (usually polar) to its substrate via oxidation or reduction reactions and making it amenable to conjugation (Kebamo et al., 2015). Such reactions include N- and S-oxidation, N- and O-dealkylation, aliphatic and aromatic hydroxylation, and deamination (Jancova et al., 2010). The resultant molecules are generally less biologically active compared to their parent molecules; however, in some instances, the metabolites do maintain substantial biological activity and could lead to toxicity and carcinogenesis by interacting with cellular macromolecules (Miller and Miller, 1981).

The superfamily of cytochrome P450 (CYP) enzymes represent the largest group of phase I enzymes and account for more than 80% of phase I metabolism. The human CYP superfamily consists of 57 functional genes (and 58 non-coding pseudogenes) and they are known to be involved in the metabolism of more than 90% of all drugs (Ingelman-Sundberg et al., 2007, Zhou et al., 2009). Other non-CYP Phase I enzymes include monoamine oxidase, xanthine oxidase, flavin monooxygenase, alcohol dehydrogenase, aldehyde dehydrogenase, aldehyde oxidase and amine oxidases (Bachmann, 2009, Evans and Relling, 1999).

Phase II enzymes catalyse the conjugation of an additional polar moiety to the exposed functional group of the parent substrate and the resulting conjugated product is more hydrophilic and could be readily excreted from the body in urine, faeces, or bile (Jancova et al., 2010, Bock et al., 1987). In these phase II reactions, the

functional groups of the substrates that conjugate with polar moieties are formed during phase I reactions. In instances where substrates contain appropriate functional groups, direct conjugation may occur (Kebamo et al., 2015). The excretion of these conjugated products from the cell, is achieved via an export pathway which is often referred to as phase III of the biotransformation process. This involves the efflux of conjugates by a range of active transport proteins known as the multidrug resistance proteins (MRP) (Konig et al., 1999). The superfamily of UDP-glucuronosyltransferases (UGTs) represent the majority of phase II enzymes and they are responsible for the phase II metabolism of approximately 40 to 70% of clinical drugs (Wells et al., 2004). Other enzyme families that are responsible for phase II metabolism include the sulfotransferases (SULTs), N-acetyltransferases (NATs), glutathione-S-transferases (GSTs), thiopurine S-methyl transferases (TPMT) and catechol O-methyl transferases (COMT) (Jancova et al., 2010). Phase II metabolism typically renders the substrate biologically inactive or at least reduces its potency. In some instances, phase I and phase II reactions/ processes are not necessarily sequential as some substrates could be already relatively polar and be excreted without conjugation and some substrates could already contain appropriate functional groups and enter the phase II pathway directly (Tephly and Burchell, 1990). Nevertheless, the action of both phase I and phase II enzymes are needed for the cell to mount an effective and comprehensive metabolism/detoxification response to excess levels of xenobiotics and endogenous compounds.

1.2 Glucuronidation

Glucuronidation is defined as the covalent attachment of glucuronic acid to lipophilic chemicals and serves as one of the major biotransformation pathways for the inactivation and elimination of a diverse range of xenobiotics and endogenous compounds. The glucuronidation process was initially observed as early as 1855 but a better understanding of the process emerged after the landmark discovery of the co-factor UDP-glucuronic acid (UDPGA) in 1953 (Dutton, 1980, Dutton and Storey, 1953). This biosynthetic reaction involves the transfer of glucuronic acid from UDPGA to a suitable functional group on a substrate resulting in a β -D-glucopyranosiduronic acid (glucuronide). In addition to the formation of the glucuronide, uridine diphosphate (UDP) is produced as illustrated in Figure 1.1. This process follows an acid-base second order nucleophilic substitution (S_N2) mechanism resulting in the inversion of the α -configuration of the C1 atom of the glucuronic acid and forming a respective conjugate with a β -D configuration (Miners and Mackenzie, 1991, Radomska-Pandya et al., 1999, Tukey and Strassburg, 2000, Rowland et al., 2013, Jancova et al., 2010). The glucuronidation reaction is catalyzed by the superfamily of UGT enzymes and the functional groups known to be conjugated by UGTs include phenols, aliphatic alcohols, carboxylic acids, primary, secondary, and tertiary amines, thiols and nucleophilic carbon atoms (e.g., phenylbutazone) (Miners and Mackenzie, 1991, Tukey and Strassburg, 2000, Rowland et al., 2013, Fisher et al., 2001). As glucuronidated products are usually biologically inactive, more water-soluble and are able to be readily excreted from the body, this process is considered as a major detoxification and elimination mechanism. However, in some instances, glucuronidated products are pharmacologically more active than the parent compound (Ohno et al., 2008). For example, the minor metabolite of morphine

glucuronidation, morphine-6-glucuronide is more active (and shows significantly higher analgesic effects) than the parent compound morphine itself (Osborne et al., 1992, Osborne et al., 1988).

Removed due to copyright restriction

Figure 1.1: Glucuronidation reaction.

The UGT catalysed glucuronidation reaction involves the conjugation of glucuronic acid from UDPGA to a lipophilic substrate (R-OH) [The figure was obtained from (Rowland et al., 2013)].

Glucuronidation is involved in the metabolism of numerous xenobiotic compounds including therapeutic drugs, environmental pollutants, toxins, dietary substances and carcinogens as well as endogenous compounds such as steroid hormones, thyroid hormones, retinoids, fat-soluble vitamins, bile acids, bilirubin, and fatty acids (Miners et al., 2004, Kiang et al., 2005, Burchell et al., 1995, Court, 2005, Radomska-Pandya et al., 1999, Tukey and Strassburg, 2000). The glucuronidation of these diverse range of xenobiotics and endogenous compounds is due to the

existence of a large multigene UGT family wherein members generally show distinct but overlapping substrate and inhibitor specificities and thus functions (Miners et al., 2004, Miners et al., 2006, Miners et al., 2010, Court, 2005, Rowland et al., 2013). The level of UGT expression and activity in individuals varies considerably according to factors including species, race, age, xenobiotic exposure, as well as genetic determinants including genetic polymorphisms (Miners and Mackenzie, 1991, Guillemette et al., 2014). These factors could affect the response of an individual to a wide range of drugs, other xenobiotics and endogenous molecules, leading to an increase in disease susceptibility and other pharmacological and toxicological implications.

1.3 UDP-glucuronosyltransferases

1.3.1 The UGT multi-gene Family - Nomenclature and Genomic organization

The UGTs are divided into four families, UGT1, UGT2, UGT3 and UGT8 based on their amino acid sequence. Genes within a family show more than 50% sequence homology, while there is less than 50% homology across families. This large multi-gene family is found in all animal species and the functions of individual family members have been studied in species as diverse as human, mouse, rabbit, rat, monkey, guinea-pig, dog and cow (Meech and Mackenzie, 1997a, Mackenzie et al., 2005). At present, a total of 117 mammalian UGTs have been identified, 22 of which are functional human UGTs. Figure 1.2 illustrates the relationships between human UGT family members.

Removed due to copyright restriction

Figure 1.2: Phylogenetic tree of human UGT members

This figure represents relationships between amino acid sequences of human UGT enzymes (sequence homology is indicated as percentage value). Pseudogenes are not shown in this dendrogram. [The figure was obtained from (Meech et al., 2019)].

1.3.2 Human UGT1 family

The human UGT1 family contains nine functional UGT isoforms namely UGT1A1, UGT1A3, UGT1A4, UGT1A5, UGT1A6, UGT1A7, UGT1A8, UGT1A9, and UGT1A10 along with four pseudogenes UGT1A2p, UGT1A11p, UGT1A12p and UGT1A13p (Gong et al., 2001, Mackenzie et al., 2005). The pseudogenes contain multiple mutations and stop codons that prevent transcription or the production of an active enzyme (Radomska-Pandya et al., 1999). The 9 functional isoforms of this

family are encoded by a single gene locus which spans over 200 kb on chromosome 2q37. The UGT1 gene locus contains 9 unique first exons (exon 1) and four downstream shared exons (exons 2-5) thus giving rise to the 9 functional UGT1A isoforms (Figure 1.3). Each UGT1 isoform contains one of the unique first exons fused to the common exons 2-5 (Gong et al., 2001, Mackenzie et al., 2005, Meech and Mackenzie, 1997a). Recent identification of an additional 3' exon, named 5b located 1091 bp downstream of exon 4, led to the discovery of 9 truncated protein products (referred to as UGT1A isoforms 2 or i2s) (Lévesque et al., 2007). These newly discovered isoforms contain exon 5b instead of the classic exon 5a due to alternative splicing and they function as inhibitors of functional full-length UGT1A enzymes. These truncated UGT1A mRNA variants have been demonstrated in the liver, kidney, colon, oesophagus and small intestine (Lévesque et al., 2007).

As the unique first exons of functional UGT1A mRNAs encode the amino-terminal half of the isoform, and exons 2-5a encode the carboxyl-terminal half of the isoform, each UGT protein contains a unique amino-terminal domain and a carboxyl-terminal domain that is identical to all other UGT1A proteins. In addition, the 5th exon (exon 5a and 5b) contains the 3' untranslated region (3' UTR). As all functional UGT1 isoforms share exon 5a, their 3'UTRs are identical (Guillemette et al., 2014, Radomska-Pandya et al., 1999). The amino-terminal domain which shares 37-90% sequence homology between UGT1A members, determines substrate specificity whereby each member has a distinct, but overlapping range of substrates (Meech and Mackenzie, 1997a). These family members are transcribed by individual promoters upstream of their first exon (Mackenzie et al., 2005), giving them different tissue-specific expression patterns.

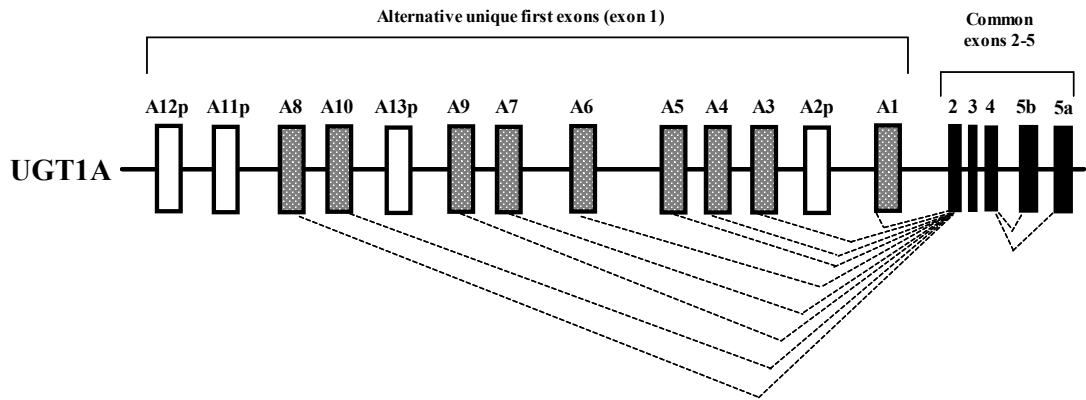


Figure 1.3: The UGT1A family gene locus

Alternate UGT1A unique first exons can fuse with common exons 2-4 and alternative 3' exon 5a or 5b. First exons of the functional UGT1A isoforms are shown in grey and first exons that give rise to pseudogenes are shown in white. Common exons 2-5a/b are shown in black. Alternative splicing of exons are shown with dotted lines [Adapted from (Mackenzie et al., 2005) and (Guillemette et al., 2014)].

1.3.3 Human UGT2 family

The human UGT2 family is divided into two subfamilies, UGT2A and UGT2B. These two subfamilies share approximately 70% sequence homology. The UGT2A subfamily members include three functional UGTs, UGT2A1, UGT2A2 and UGT2A3, while the UGT2B subfamily members include seven functional UGTs, UGT2B4, UGT2B7, UGT2B10, UGT2B11, UGT2B15, UGT2B17, and UGT2B28, along with five pseudogenes UGT2B24p, UGT2B25p, UGT2B26p, UGT2B27p, and UGT2B29p (Mackenzie et al., 2005, Radomska-Pandya et al., 1999). The UGT2 family shares approximately 40% sequence homology with the UGT1 family (Figure 1.2). The UGT2 family is encoded by a gene cluster on chromosome 4q13 (Turgeon et al., 2000). Figure 1.4 illustrates the genomic organization of the UGT2 gene locus. Similar to the UGT1A family, both UGT2A1 and UGT2A2 contain an alternatively spliced unique first exon and five common exons (exons 2-6). Thus, they contain

different amino-terminal domains and an identical carboxyl-terminal domain. However, UGT2A3 contains 6 unique exons that are not shared with the other two UGT2A members (Mackenzie et al., 2005, Sneitz et al., 2009). Similar to UGT2A3, each of the seven UGT2B genes contain 6 unique exons. The exons are conserved in length whereas the intronic regions are variable in length. In addition, exons 2-6 show high sequence homology between UGT2B genes, as well as with the shared exons 2-5 of the UGT1 genes (Radomska-Pandya et al., 1999). All of the UGT2B genes along with UGT2A3, are transcribed by individual promoters (Mackenzie et al., 2005, Turgeon et al., 2000). Furthermore, the tissue specific pattern of UGT2B gene expression is influenced by unique regulatory regions that share significant sequence homology (discussed in detail in section 1.4)

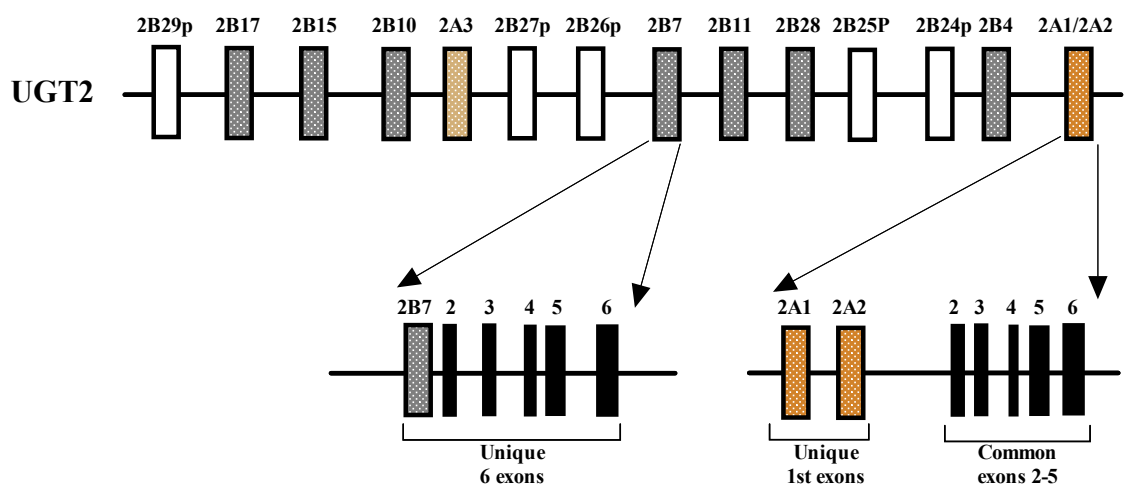


Figure 1.4: The UGT2 family gene locus

UGT2A genes, UGT2B functional genes and UGT2B pseudogenes are shown in orange, grey and white, respectively. UGT2A1 and UGT2A2 genes are encoded by an alternatively spliced unique first exon fused to shared exons 2-5 (shown in black). Each UGT2B gene and UGT2A3 are encoded by 6 unique exons of variable length. The 6 exons of the UGT2B7 gene are illustrated as an example [Adapted from (Mackenzie et al., 2005, Mackenzie et al., 2003)].

1.3.4 Human UGT8 and UGT3 families

The human UGT8 family consists of a single gene, initially named as UDP-galactose ceramide galactosyl transferase. It is encoded by a locus containing five exons, located on chromosome 4q26 (Mackenzie et al., 2005) and shares 33% sequence homology with the UGT1 and UGT2 families. UGT8 is not involved in drug metabolism and it does not use UDPGA as its sugar-donor cofactor. Its primary role is the synthesis of galactosyl-ceramide (by conjugating galactose from the sugar donor UDP-galactose to the 1-hydroxyl moiety of ceramide), which is an important step in the synthesis of glycosphingolipids and cerebroside that are found in the myelin sheath of the central and peripheral nervous system. Recently, our laboratory has found that not only ceramides, but also bile acids are substrates of UGT8 (Meech et al., 2015).

The recently identified human UGT3 family consists of two members, UGT3A1 and UGT3A2. Each of the UGT3 enzymes is encoded by seven exons located on chromosome 5p13.2 and shares approximately 32% sequence homology with UGT1, UGT2 and UGT8 families (Mackenzie et al., 2005, Mackenzie et al., 2011, Mackenzie et al., 2008, Meech and Mackenzie, 2010). In contrast to the UGT1 and UGT2 families, the UGT3 family utilizes sugar donors other than UDPGA. UDP-N-acetylglucosamine is utilized by UGT3A1 while UDP-glucose and UDP-xylose is utilized by UGT3A2 (Mackenzie et al., 2008, Mackenzie et al., 2011). UGT3A1 was found to be involved in bile acid and estrogen metabolism and UGT3A2 to be involved in the metabolism of classic UGT substrates including 4-methylumbelliferone, 1-hydroxypyrene, estrogens and bioflavones (Meech and Mackenzie, 2010).

1.4 Structure, localization and function of UGTs

The UDP glucuronosyltransferases (UGT) that carry out glucuronidation are found in the endoplasmic reticulum (ER) of cells (Burchell et al., 1989, Radomska-Pandya et al., 1999, Bossuyt and Blanckaert, 1997) where they protect against chemical insults and regulate signaling processes mediated by chemical ligands. The complement of UGTs within a cell determines its capacity to resist chemical insults and controls endogenous responses such as steroid driven growth. The UGT protein contains an N-terminal variable region/domain and a C-terminal conserved region/domain. The N-terminal variable region is encoded by exon 1 of UGT1A genes or exons 1 and 2 of UGT2 genes and determines substrate specificity as it comprises the substrate binding domain (Figure 1.5). It also contains an amino terminal signal peptide which is cleaved after localization of the UGT in the ER, generating a mature protein of approximately 505 amino acids. A non-spanning membrane-association domain is also speculated to be present in the variable N-terminal region. The C-terminal region of UGT enzymes show high sequence similarity among UGT1A and UGT2 family members and is identical among functional UGT1A family members. It comprises a UDPGA co-substrate binding domain that includes the so-called 'UGT signature sequence', a hydrophobic transmembrane spanning domain, and a dilysine motif that is involved in ER-localization (Figure 1.5). The majority of the UGT enzyme resides on the luminal side of the ER membrane; only the distal C-terminal part of the protein comprising approximately 20 amino acids including the dilysine motif, resides on the cytosolic side (Guillemette et al., 2014, Mackenzie et al., 1997). The co-substrate UDPGA is transported from the cytosol to the lumen of the ER by members of the nucleotide

sugar transporter (NSTs) family (Hauser et al., 1988, Muraoka et al., 2007). Glucuronides formed in the ER are transported out of the cell by multi-drug resistance proteins (MDRs) and organic anion transporters (OATs)(Cui et al., 2001, Hirohashi et al., 1999, Keppler et al., 1997, Muraoka et al., 2007, Jedlitschky et al., 1997). UGTs are known to form dimers and it has been suggested that these might act as channels to influx UDPGA and efflux the glucuronide and by-products (discussed further below, Figure 1.5). Physical interactions between the UGTs and transporters are also proposed but not confirmed.

Dimerization can be observed with UGTs in their native form. They are predicted to form homodimers as well as heterodimers with different UGT isoforms (Fremont et al., 2005, Meech and Mackenzie, 1997b, Operana and Tukey, 2007). The formation of dimers was first detected in studies with the rat UGT2B1 enzyme and appeared to involve the amino terminal domain (Meech and Mackenzie, 1997b). Heterodimerisation of UGTs has been postulated to alter the rate of glucuronidation and the breadth of substrates metabolised by co-expressed UGT enzymes. For example, UGT1A1 which exclusively glucuronidates bilirubin shows an increase in its maximal enzymatic rate (V_{max}) when co-expressed with either UGT1A4 or UGT1A6 (Fujiwara et al., 2007). Dimerization may also be involved in the transportation of UDPGA to the ER lumen from the cytosol (discussed further below). In addition, mutant and truncated UGTs, such as the naturally occurring UGT1A-i2 proteins, may form inactive dimers with functional UGTs and reduce their glucuronidation activity (Yuan et al., 2016, Ikushiro et al., 1997, Ghosh et al., 2001). Interactions of UGTs may also occur with other biotransformation enzymes such as cytochrome P450. Interaction of UGT with CYPs and other microsomal proteins may influence the catalytic activity of UGT and facilitate a more concerted

biotransformation process (Taura et al., 2004, Taura et al., 2000, Fujiwara and Itoh, 2014).

Removed due to copyright restriction

Figure 1.5: Structure of the UDP-glucuronosyltransferase

(A) Functional domains of the UGT protein. The N-terminal variable domain contains a substrate binding domain, a signal peptide and a putative non-spanning membrane-anchoring domain. The C-terminal half contains the UDPGA-binding domain, a UGT signature sequence, the transmembrane region, and a cytosolic dilysine motif. (B) The glucuronidation reaction by a UGT enzyme located in the ER. The majority of the UGT is located in the ER lumen, with only a 20 amino acid positively charged tail existing on the cytoplasmic side. The co-substrate UDPGA is actively transported into the ER lumen where the conjugation of the lipophilic substrate occurs. The substrates that already contain appropriate functional groups (R-OH) are directly conjugated whereas the other substrates (R) are conjugated after the addition of a functional group by phase I enzymes such as cytochrome P450. The glucuronide (R-G) formed is actively transported out of the lumen for elimination [Figure obtained from (Guillemette et al., 2014)].

1.5 Substrates of UGTs

The substrates of human UGT family members are diverse and span a broad range of substrate classes. These include various endogenous compounds such as steroid hormones, bile acids, fatty acids, retinoids and exogenous compounds including various drugs, environmental toxins and dietary chemicals/carcinogens. Table 1.1 illustrates some of the important substrate classes of the UGT isoforms [reviewed in (Hu et al., 2014b)]. It is important to notice the overlapping substrate specificity between several UGT isoforms.

Table 1.1: Selected substrates of UGT1A and UGT2B families

UGT	Substrate	Reference
UGT1A1	Billirubin Estrogens Retinoic acids Flavonoids N-hydroxy-PHIP (a food-borne carcinogen) SN-38 (the active metabolite of irinotecan) Thyroid hormones	Bosma et al., 1994 Lepine et al., 2004 Rowbotham et al., 2010 Hagenauer et al., 2001; Wu et al., 2011 Malfatti & Felton, 2001 Hanioka et al., 2001; Iyer et al., 1998 Findlay et al. (2000)
UGT1A3	Bile acids (e.g. Chenodeoxycholic acid) Estrogens Vitamin D metabolites Hydroxylated benzo(a)pyrene Amines Statins Non-steroidal anti-inflammatory drugs Angiotensin receptor antagonists Flavonoids	Trottier et al., 2006 Lepine et al., 2004 Kasai et al., 2005; Wang et al., 2014 Mojarrabi et al., 1996 Green et al., 1998 Prueksaritanont et al., 2002a Kuehl et al., 2005 Alonen et al., 2008 Chen et al., 2008b; Xie et al., 2011
UGT1A4	Progestins Dihydrotestosterone and trans-androsterone 25-hydroxyvitamin D3	Green & Tephly, 1996 Ehmer et al., 2004; Green & Tephly, 1996; Zhou et al., 2010b Wang et al., 2014

	Therapeutic drugs (i.e. Amitriptyline, ketotifen, diphenhydramine, imipramine, trifluorperazine, clozapine, hydroxymidazolam, tamoxifen and 4-hydroxytamoxifen olanzapine Nicotine	Court, 2005; Green & Tephly, 1996; Kaivosaaari et al., 2011, Mori et al., 2005 Seo et al., 2010, Sun et al., 2006, Haslemo et al., 2012; Kassahun et al., 1997 Tricker, 2003
UGT1A5	1-hydroxypyrene 4-methylumbelliferone	Finel et al., 2005 Finel et al., 2005
UGT1A6	4-methylumbelliferone Serotonin Arylamines Benzo(a)pyrene metabolites Menadione (vitamin k3) metabolites Aspirin	Harding et al., 1988 Krishnaswamy et al., 2003 Orzechowski et al., 1994 Bock & Kohle, 2005 Nishiyama et al., 2008 Chan et al., 2005; Hutt et al., 1986
UGT1A7	Flavonols NGF1586 (a neutrophil growth factor) Triclocarban (an antibacterial agent) Menadione metabolites 13- <i>cis</i> retinoic acid (13cisRA) SN-38 Tobacco carcinogens benzo(a)pyrene (BaP) and 4-(methylnitrosamino)- 1-(3-pyridyl)-1-butanone (NNAL)	Niemeyer & Brodbelt, 2013; Wu et al., 2011 Siller et al., 2011 Schebb et al., 2012 Nishiyama et al., 2008 Rowbotham et al., 2010 Ciotti et al., 1999 Lacko et al., 2009; Zheng et al., 2001
UGT1A8	Estrogens Dihydrotestosterone Flavonoids and coumarins Primary amines (e.g. 4-aminobiphenyl) Thyroxine Raloxifene Bicalutamide Hydroxylated warfarin metabolites Morphine Mycophenolic acid 13- <i>cis</i> -retinoic acids N-hydroxy-PhIP	Lepine et al., 2004 Murai et al., 2006 Cheng et al., 1998a Cheng et al., 1998a Yamanaka et al., 2007 Sun et al., 2013 Grosse et al., 2013 Zielinska et al., 2008 Ohno et al., 2008 Bernard & Guillemette, 2004 Rowbotham et al., 2010 Nowell et al. (1999)
UGT1A9	Ethanol Thyroid hormones Benzo(a)pyrene metabolites	Al Saabi et al., 2013 Findlay et al., 2000 Dellinger et al 2006

	<p>mycophenolic acid <i>N</i>-hydroxy-PhIP NNAL Non-steroidal anti-inflammatory drugs</p>	<p>Bernard & Guillemette, 2004 Nowell 1999 Ren et al., 2000 Gaganis et al., 2007; Mano et al., 2007a</p>
UGT1A10	<p>Flavonoids Estrogens Aldosterone Mycophenolic acid PhIP, <i>N</i>-OH-PhIP Benzo(a)pyrene metabolites Valproic acid Thyroxine Menadione raloxifene</p> <p>Anti-tumor agents C-1305 (dimethylaminopropylamino-8-hydroxytriazoloacridinone) and C-311 (5-Diethylaminoethylamino-8-hydroxyimidazoacridinone)</p>	<p>Boersma et al., 2002, Lee et al., 2007; Lewinsky et al., 2005; Wu et al., 2011 Lepine et al., 2004; Sneitz et al., 2013 Knights et al., 2009 Mojarrabi & Mackenzie, 1997 Dellinger et al., 2007 Dellinger et al., 2006 Argikar & Rimmel, 2009 Yamanaka et al., 2007 Nishiyama et al., 2008 Kemp et al., 2002</p> <p>Fedejko-Kap et al., 2012; Pawlowska et al., 2013</p>
UGT2B4	<p>Bile acids (i.e. hyodeoxycholic acid and hyocholic acid) Fatty acids Phenol derivatives Catecholestrogens (e.g. 2-OH-estrone and 4-OH-estradiol) Androgen metabolites (i.e. androsterone and androstane-3α,17β-diol) Codeine Hydroxymidazolam Lorazepam (a hypnosedative-anxiolytic agent) Deoxynivalenol (a mycotoxin) Eslicarbazepine (an antiepileptic agent) Carvedilol (a β-adrenoceptor blocker)</p>	<p>Barbier et al., 2009; Pillot et al., 1993; Radomska et al., 1993; Ritter et al., 1992a Turgeon et al. (2003b) Levesque et al., 1999 Lepine et al., 2004; Levesque et al., 1999 Levesque et al., 1999; Turgeon et al., 2001 Raungrut et al., 2010 Seo et al., 2010 Uchaipichat et al., 2013 Maul et al., 2014 Loureiro et al., 2011 Ohno et al., 2004</p>

UGT2B7	Fatty acids (i.e. linoleic acid and its oxidative derivatives 13- HODE and 13-OXO)	Jude et al., 2001
	Dietary fatty acids (i.e. phytanic acid and docosahexaenoic acid)	Little et al., 2002; Turgeon et al. (2003b)
	Bile acids (i.e. DCA, LCA, HCA and HDCA)	Barbier et al., 2009; Gall et al., 1999
	Estrogens (e.g. estradiol and estriol) and catecholestrogens (e.g. 4-OH-estrone and 4-OH-estradiol)	Cheng et al., 1998b; Gall et al., 1999; Lepine et al., 2004; Turgeon et al., 2001
	Androgens and their metabolites (e.g. androsterone and androstane-3 α ,17 β -diol)	Gall et al., 1999; Turgeon et al., 2001
	Mineralocorticoid and glucocorticoid hormones and their metabolites	Girard et al., 2003; Knights et al., 2009
	Retinoic acids	Czernik et al., 2000
	Hydroxyestradiol	Iyer et al., 2003
	Deoxynivalenol (a mycotoxin)	Maul et al., 2014
	Trans-3'-hydroxycotinine (a major metabolite of nicotine)	Yamanaka et al., 2005
	Carbinol (a metabolite of letrozole)	Precht et al., 2013
	Morphine	Coffman et al., 1997
	Epirubicin	Innocenti et al., 2001
	Valproic acid	Argikar & Rimmel, 2009
	Gemfibrozil	Mano et al., 2007c
	Non-steroidal anti-inflammatory drugs	Gaganis et al., 2007; Jin et al., 1993a,b; Mano et al., 2007b
	3-OH-benzodiazepines	Jin et al., 1993a
	Chloramphenicol	Chen et al., 2010b
	Mycophenolic acid	Picard et al., 2005
	Lorcaserin (a weight management agent)	Sadeque et al., 2012
Haloperidol (an antipsychotic agent)	Kato et al., 2012	
Ornidazole	Du et al., 2013	
Ethanol	Al Saabi et al., 2013	
Lorazepam	Uchaipichat et al., 2013	
Codeine	Raungrut et al., 2010	
Carvedilol	Ohno et al., 2004	
3'-azido-3'-deoxythymidine (AZT)	Barbier et al., 2000	
Efavirenz (EFV)	Belanger et al., 2009	
UGT2B10	Fatty acids Nicotine	Turgeon et al. (2003b) Kaivosari et al. (2007)
UGT2B11	Fatty acids	Turgeon et al. (2003b)

UGT2B15	<p>Androgens (e.g. testosterone, dihydrotestosterone and androstane-3α,17β-diol), Estrogens, phenolic compounds, Flavonoids and coumarins and anthraquinones</p> <p>oxazepam (i.e. S-oxazepam)</p> <p>rofecoxib</p> <p>3,4-methylenedioxymethamphetamine (MDMA; a recreational drug)</p> <p>dabigatran (a thrombin inhibitor)</p> <p>bisphenol A</p> <p>sipoglitazar (a novel PPAR agonist with anti-diabetic activity)</p> <p><i>cis</i>-4-OH-tamoxifen</p> <p>ezetimibe</p> <p>lorazepam</p> <p>3-OH-desloratadine</p> <p>phenytoin (an anticonvulsant)</p> <p>acetaminophen</p> <p>19-norandrosterone</p> <p>lorcaserin</p>	<p>(Chen et al., 1993; Green et al., 1994; Levesque et al., 1997; Schwab & Skopp, 2014; Turgeon et al., 2001).</p> <p>Court et al., 2002; He et al., 2009)</p> <p>Zhang et al., 2003</p> <p>Schwaninger et al., 2009; Shoda et al., 2009</p> <p>Ebner et al., 2010</p> <p>Hanioka et al., 2008b</p> <p>Nishihara et al., 2013; Stringer et al., 2013</p> <p>Nishiyama et al., 2002</p> <p>Ghosal et al., 2004a</p> <p>Chung et al., 2005</p> <p>Ghosal et al., 2004b</p> <p>Nakajima et al., 2007</p> <p>Court et al., 2001; Mutlib et al., 2006</p> <p>Strahm et al., 2013</p> <p>Sadeque et al., 2012</p>
UGT2B17	<p>androgens (testosterone and dihydrotestosterone) and their metabolites (e.g. androsterone and androstane 3α,17β-diol</p> <p>flavonoids, coumarins and anthraquinones</p> <p>trans-3'-hydroxy-cotinine (a major metabolite of nicotine)</p> <p>4-hydroxy-3-methoxymethamphetamine (HMMA)</p> <p>Therapeutic drugs and/or their metabolites; Diclofenac</p> <p>Vorinostat (an oral histone deacetylase inhibitor)</p> <p>17-dihydroexemestane</p> <p>eslicarbazepine</p> <p>edaravone</p> <p>gemfibrozil</p>	<p>Beaulieu et al., 1996; Turgeon et al., 2001</p> <p>Turgeon et al., 2003a</p> <p>Chen et al., 2010a, 2012a</p> <p>Schwaninger et al., 2009</p> <p>Zhang et al., 2012</p> <p>Balliet et al., 2009; Kang et al., 2010</p> <p>Sun et al., 2010b</p> <p>Loureiro et al., 2011</p> <p>Ma et al., 2012</p> <p>Mano et al., 2007c</p>
UGT2B28	<p>Bile acids</p> <p>Eugenol</p>	<p>Levesque et al. (2001)</p> <p>Levesque et al. (2001)</p>

	Androgens (5 β -androstane 3 α ,17 β -diol, estradiol, androsterone, testosterone)	Levesque et al. (2001)
	4-methylumbelliferone	Levesque et al. (2001)

1.6 Tissue specific expression of UGTs

UGTs are expressed in a wide range of tissues and cell types in the human body and each UGT has its own unique tissue expression profile. Liver is considered to be the primary organ of phase I and phase II metabolism (Dutton, 1980). It has been found that the expression of UGTs, is higher in liver compared to other organs (Izukawa et al., 2009, Ohno and Nakajin, 2009, Court et al., 2012). Several studies have used real-time PCR to obtain quantitative data for UGT expression in human tissues including liver. Data from 3 separate studies [Izukawa et al., 2009, Ohno and Nakajin, 2009 and Court et al., 2012 (n=66)] are summarized in Figure 1.6. All UGT2B isoforms and UGT1A isoforms except for UGT1A5, UGT1A7, UGT1A8 and UGT1A10 are expressed abundantly in the liver (Izukawa et al., 2009, Ohno and Nakajin, 2009, Mackenzie et al., 2003, Miners et al., 2004, Zhang et al., 2005, Guillemette et al., 2014) (Figure 1.6). Furthermore, UGT2B members are generally more abundant than UGT1A members and UGT2B4 is the most abundant isoform seen in human liver followed by UGT2B15, UGT2B10 and UGT2B7 (Rowland et al., 2013, Izukawa et al., 2009, Ohno and Nakajin, 2009, Court et al., 2012). However, there are discrepancies between data on the relative expression of UGTs in the liver due to various factors. For instance, a study by Congiu et al suggests UGT2B4 and UGT2B7 are the predominantly expressed UGT forms in the liver (Congiu et al., 2002).

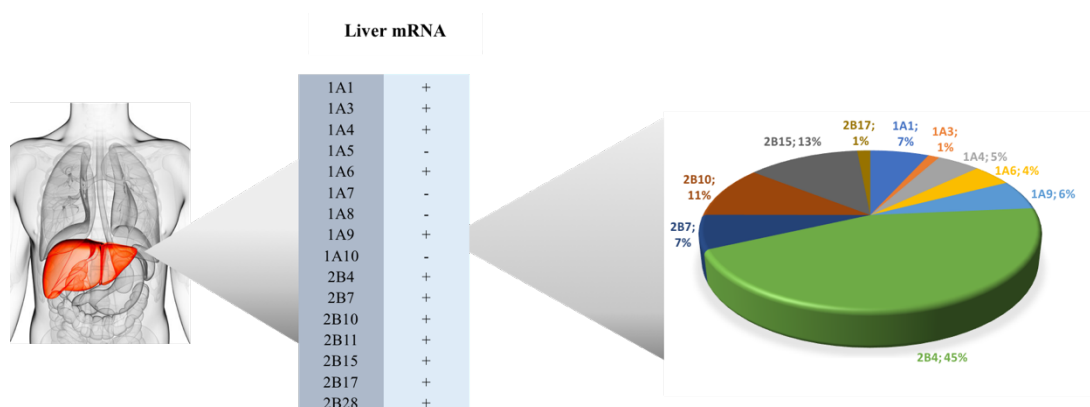


Figure 1.6: UGT expression in liver

Hepatic expression of all UG1A and UGT2B family members at the mRNA level are shown in the table. (+) indicates the presence of the UGT mRNA transcript and (-) indicates the absence of the UGT mRNA transcript. Their relative expression percentages are shown in the pie chart. Data are generated by summarizing quantitative data from 3 different studies; Izukawa et al., 2009; Ohno and Nakajin, 2009; Court et al., 2012 (n=66). [Adapted from (Rowland et al., 2013)].

Given its vast array and abundance of UGTs, liver is recognised as the major site of glucuronidation in the body. Extrahepatic expression of UGTs has become of increasing interest over the last 2 decades (Strassburg et al., 1997, Strassburg et al., 1998). Increasing evidence now indicates that numerous other organs make a significant contribution towards overall glucuronidation capacity (Guillemette, 2003). Kidney, lung, brain, gastrointestinal tract including oesophagus, stomach, small intestine, and colon, and steroidogenic tissues including prostate, breast, and testis, and skin are some of the known extrahepatic tissues that express UGTs. Steroidogenic tissues and the gastrointestinal tract are particularly significant locations of extra-hepatic glucuronidation activity [reviewed in (Tukey and Strassburg, 2001); (Belanger et al., 2003) respectively]. Table 1.2 shows a summary of quantitative UGT expression data in various extra-hepatic tissues from several studies and reviews in the literature. Intestine and colon are the two main locations in

the gastrointestinal tract which show significant glucuronidation activities for all UGT1As and most of UGT2Bs (Ohno and Nakajin, 2009). Among these, UGT1A1, UGT1A8, UGT1A10, UGT2B7, UGT2B15 and UGT2B17 are abundantly expressed in both the intestine and colon (Wu et al., 2011). The functions of UGTs in steroidogenic tissues, especially UGT2B15 and UGT2B17 which are the main focus of this study, will be discussed further in Section 1.7. The two other UGT isoforms of interest in this study; UGT2B4 and UGT2B7 are expressed extrahepatically at low levels in organs including small intestine, kidney, lung, breast, testes and thyroid, compared to the liver. In addition, UGT2B4 is also expressed in the prostate, skin, brain, heart and trachea whereas UGT2B7 is expressed in the stomach, uterus, pancreas, thymus and placenta.

It should be noted that there are discrepant reports about the presence/absence of some UGTs in some tissues/organs as indicated in Table 1.2. The expression of UGT2B15 and UGT2B17 in a panel of human tissues was analysed and reported in Chapter 3 and such discrepancy was seen in the presented data as well. For example, even though UGT2B15 was not detected in the ovary and UGT2B17 was not detected in the oesophagus and bladder according to some of the studies compiled here, we were able to detect UGT2B15 in the ovary at a very low level and UGT2B17 in the oesophagus and bladder at a moderate and a low level, respectively. In addition, UGT2B15 was not detected in brain tissue samples in this study, in contrast to some previous reports. Sample variation, differing sensitivities of detection mechanisms, ethnic or polymorphic diversity between individuals may underlie these discrepancies. It is also important to note that mRNA levels do not always correlate to protein levels (e.g. Izukawa et al 2009) and thus, further studies

on evaluating UGT protein levels in these tissues are required for more accurate conclusions.

Table 1.2: Distribution of UGT mRNAs in human tissues

		Tissue																						
		Prostate	Breast	Testis	Skin	Oesophagus	Stomach	Small Intestine	Colon	Kidney	Lung	Brain	Cerebellum	Thyroid	Thymus	Ovary	Placenta	Cervix	Heart	Trachea	Bladder	Spleen	Uterus	Pancreas
UGT mRNA	1A1	+	+	+	-	-	+	+	+	+	-	+	-	+/-	+/-	-	+/-	-	-	+/-	-	-	+	-
	1A3	ND	-	+/-	ND	-	+	+	+	+	+/-	+	-	+/-	+/-	-	-	-	-	+/-	-	-	+	-
	1A4	ND	-	+/-	ND	-	+	+	+	+	-	+	-	+/-	+/-	-	+/-	-	-	+/-	+	-	+	+
	1A5	ND	-	+	ND	+	+	+	+	+	-	+/-	-	-	+	-	-	+	-	+	+	-	+	-
	1A6	ND	-	+	ND	-	+	+	+	+	+/-	-	-	+/-	+/-	-	+/-	-	-	+	-	+/-	+	-
	1A7	ND	-	+/-	ND	+	+	+	+	+	-	+	-	+/-	+/-	-	+/-	+	-	+	+	-	-	-
	1A8	ND	+/-	+/-	ND	+	-	+	+	+	-	+	-	-	+/-	-	-	-	-	+	+	-	-	-
	1A9	+	+	+	+	+	-	+	+	+	-	+	-	+/-	+/-	-	+/-	-	-	+/-	-	-	-	-
	1A10	ND	-	+/-	ND	+	+	+	+	+	-	+	-	-	+/-	-	+/-	-	-	+	-	-	-	-
	2B4	+	+	+	+	+	-	+	+	+	+	+	-	-	+	-	-	-	+/-	+/-	-	-	-	-
	2B7	-	+	+/-	ND	+	+	+	+	+	+	-	-	-	+/-	-	+/-	-	-	-	-	-	+	+
	2B10	+	+	+	ND	+	-	-	-	+	+	+	-	-	-	-	-	-	-	-	-	-	-	-
	2B11	+	+	+/-	+	-	-	+	-	+	+	+/-	+/-	+/-	-	-	-	-	-	-	-	-	-	+
	2B15	+	+	+	+	+	+	+	+	+	+	+	-	+/-	-	-	-	-	-	+	-	-	-	+
	2B17	+	+	+	+	-	+	+	+	+	+	+/-	+/-	+/-	+	+	+/-	+	-	+	-	+	+	+
	2B28	-	+	-	-	-	-	-	-	-	-	+	-	-	-	-	-	ND	ND	-	+	-	-	-

This table shows a summary of tissue-specific patterns of expression of UGT mRNAs quantified using RT-PCR (Court et al., 2012, Nakamura et al., 2008, Ohno and Nakajin, 2009) and compiled data from (Gregory, 2004, Gardner-Stephen, 2008) and Dr. Siti Mubarakah (Mubarakah, 2018). (+) indicates the presence of the UGT mRNA transcript, (-) indicates the absence of the UGT mRNA transcript, (+/-) indicates either polymorphic UGT mRNA transcript or discrepancies between studies and ND indicates that the tissue has not been tested for the expression of the UGT mRNA transcript (ND=not determined).

1.7 UGTs in steroid target tissues and steroid glucuronidation

Steroid hormone glucuronidation is essential for the inactivation and removal of biologically active endogenous compounds such as androgens, estrogens, progestins, corticoids, vitamins and bile acids from the body (Tukey and Strassburg, 2000). In general, the transformation that these compounds undergo via glucuronidation is one of only a few irreversible transformations and is thus considered to be extremely important for signal termination (Meech et al., 2019). Steroid hormone metabolism plays a major role in hormone-dependent cancer risk and progression and therefore, an understanding of the function of UGTs in steroid target tissues such as prostate and breast is vital. In this introduction, the primary focus will be on the prostate. The role of UGTs in prostate cancer risk and progression will be discussed further in sections 1.7.1 and 1.8.1.

The gonads and adrenal glands are the primary sites of steroid hormone production in mammals. Once synthesised in the gonads, steroid hormones are delivered to target tissues via the circulatory system. These steroid hormones stimulate the growth and function of their target tissues including prostate, breast and skin (Gregory, 2004). Once the steroids are secreted into the circulatory system, it was initially thought that their glucuronidation was primarily occurring in the liver (Rittmaster et al., 1993). However, later evidence suggested that glucuronidation also occurs locally within steroid target tissues including prostate, breast, testis and skin (Belanger et al., 1998).

UGT2B family members are primarily known to be involved in steroid glucuronidation in both liver and peripheral steroid target tissues in humans. Among

them UGT2B15, UGT2B17 and UGT2B7 are the androgen metabolizing UGTs with the highest catalytic efficiency (Turgeon et al., 2001). UGT2B4 and UGT2B28 have been shown to glucuronidate androgens to a limited extent and the remaining two UGT2B family members UGT2B10 and UGT2B11 are known to be inactive towards steroid hormones (Levesque et al., 2001, Turgeon et al., 2001).

In terms of estrogen glucuronidation, UGT2B7 is the UGT2B family member that metabolizes the widest range of estrogens including the most potent estrogen 17 β -estradiol and its catechol estrogen metabolites. Most of the other UGT2B members only glucuronidate estrogens to a modest extent (Ritter et al., 1990, Gall et al., 1999). UGT2B17 has also been reported to be involved in estrogen metabolism as it glucuronidates 17 β -estradiol modestly (Itaaho et al., 2008, Williams et al., 2002). UGT1A family members have been shown to be inactive towards androgens but significantly involved in estrogen glucuronidation. UGT1A1, UGT1A3, UGT1A7, UGT1A8, UGT1A10 glucuronidate 17 β -estradiol with UGT1A1, UGT1A8 and UGT1A10 being the most active UGT1A members. In addition, UGT2A1, UGT2A2, UGT3A1 and UGT3A2 also show modest catalytic activity towards 17 β -estradiol (Itaaho et al., 2008, Lépine et al., 2004, Vergara et al., 2017, Meech et al., 2012).

1.7.1 Androgen glucuronidation in the prostate

In the prostate, androgens modulate prostate tissue growth via regulating the expression of several genes and controlling the production of secretory proteins including prostate-specific antigen (PSA) and various other proteins involved in growth regulatory processes and other cellular functions (Carson and Rittmaster,

2003). Therefore, androgen signaling is vital for normal prostate development and its function.

The sex steroid hormone, testosterone is produced at a significant level by the testes in human males and at a very low level in female ovaries. Once secreted from the testes, testosterone is circulated to androgen sensitive tissues such as the prostate. Apart from the gonads, both male and female adrenal glands also produce the androgens; dehydroepiandrosterone (DHEA), DHEA sulphate (DHEA-S) and androstenedione in large amounts (Barbier and Belanger, 2008). Even though these adrenal steroids lack biological activity, they can be converted into biologically active testosterone locally in the prostate. Testosterone can be converted further into dihydrotestosterone (DHT) and its metabolites (Barbier and Belanger, 2008) which act primarily through binding to the androgen receptor (AR) to activate target gene transcription and affect cellular processes in these tissues. DHT is a more potent AR agonist as its affinity towards the AR is 5-10 fold higher than that of testosterone (Belanger et al., 2003, Meech et al., 2019). By the action of a series of phase I enzymes 3α , 3β and 17β -hydroxysteroid dehydrogenase (3α -HSD, 3β -HSD and 17β -HSD), DHT can be converted into phase I metabolites; 5α -androstane- $3\alpha,17\beta$ -diol (3α -DIOL), 5α -androstane- $3\beta,17\beta$ -diol (3β -DIOL) and androsterone (ADT), all of which are inactive as AR agonists (Figure 1.7). Both 3α -DIOL and ADT can be converted back to DHT in the prostate while 3β -DIOL can act as a weak estrogen (Belanger et al., 2003, Meech et al., 2019). These compounds can be irreversibly converted into glucuronide products that are biologically inactive, unable to undergo metabolic inter-conversions and easily excreted. Thus, glucuronidation of androgens in the prostate, modulates androgen levels and AR signaling.

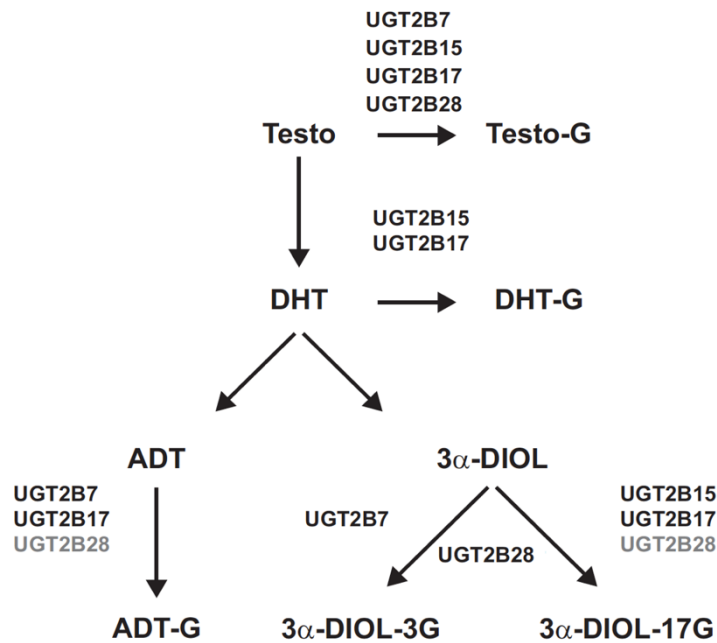


Figure 1.7: UGT2B enzymes involved in androgen metabolism

Testosterone is converted into DHT by steroid 5α-reductase in androgen target tissues such as the prostate and DHT can be further converted into several metabolites including ADT, 3α-DIOL and 3β-DIOL (not shown) by aldoketo reductases. Both UGT2B15 and UGT2B17 glucuronidate testosterone, DHT, 3α-DIOL, forming testosterone glucuronide (Testo-G), DHT-glucuronide (DHT-G), and 3α-DIOL-17-glucuronide (3α-DIOL-17G) respectively at varying efficiencies. In addition, UGT2B7 also glucuronidates testosterone and ADT, forming Testo-G and ADT-glucuronide (ADT-G). UGT2B28 glucuronidates testosterone, ADT and 3α-DIOL at a much lower efficiency as well (shown in lighter font). [Adapted from (Meech et al., 2019)].

As UGT2B15 and UGT2B17 metabolize the active androgen testosterone and its most active metabolite DHT, these UGTs are two of the major factors that govern androgen levels and androgen signaling in the prostate (Turgeon et al., 2001, Chouinard et al., 2007). Of particular importance, despite their sequence similarity (95%), the specificity and affinity of UGT2B15 and UGT2B17 towards androgens are different (Beaulieu et al., 1996, Turgeon et al., 2001). UGT2B17 conjugates the 17β-hydroxy position of DHT at a higher efficiency compared to UGT2B15.

Testosterone is also glucuronidated at a higher efficiency by UGT2B17 compared to UGT2B15. However, both enzymes conjugate the metabolite of DHT, 3 α -DIOL, at the 17 β -hydroxy position, at high but similar efficiencies (Beaulieu et al., 1996, Belanger et al., 2003, Turgeon et al., 2001). As previously mentioned, UGT2B7 also glucuronidates testosterone, ADT and 3 α -DIOL; however, its absence in the prostate suggests that UGT2B15 and UGT2B17 are more important in androgen metabolism in this organ. Additionally, the highest circulating 3 α -DIOL-glucuronide in both normal men and women is the 17 β -glucuronide (3 α -DIOL-17G), and it is the major 3 α -DIOL metabolite derived from DHT as well (Rittmaster et al., 1988). Therefore, UGT2B15 and UGT2B17 are the predominant 3 α -DIOL-conjugating enzymes. In addition, UGT2B17 conjugates another metabolite of DHT, ADT at the 3 α -hydroxy position with moderate efficiency and is believed to be the major ADT conjugating enzyme (Belanger et al., 2003, Turgeon et al., 2001). The order of preference of UGT2B17 activity towards androgen substrates is DHT>3 α -DIOL>testosterone>ADT (Meech et al., 2019). UGT2B28 was shown to be expressed in the prostate as well and in vitro studies have shown its capacity to glucuronidate testosterone, ADT, and 3 α -DIOL. However, when compared to UGT2B15 and UGT2B17, the relative androgen glucuronidation activity of UGT2B28 is extremely low (Meech et al., 2019, Levesque et al., 2001, Grant et al., 2017). Thus, UGT2B17 and UGT2B15 remain primary determinants of androgen levels in the prostate.

Removed due to copyright restriction

Figure 1.8: Localization of UGT2B15 and UGT2B17 in prostate tissue by immunohistochemistry

UGT2B17 is detected specifically in the basal epithelial cells of the alveoli (shown by arrowheads) whereas UGT2B15 is detected in the epithelial luminal cells (shown by arrows). L, alveolar lumen [Figure obtained from (Barbier and Belanger, 2008)].

In addition to differences in substrate specificity, UGT2B15 and UGT2B17 are expressed in different cell types of the prostate. As shown in Figure 1.8, UGT2B17 is expressed in basal epithelial alveoli cells whereas UGT2B15 is expressed in the epithelial luminal cells of the prostate (Belanger et al., 2003). Basal epithelial alveoli cells are where circulating androgens and testosterone from the testis or adrenal gland come in first contact with the prostate (Figure 1.9). Phase I enzymes 3α -HSD, 3β -HSD and 17β -HSD are found within the basal cells which can convert testosterone and adrenal androgens into DHT and other androgen metabolites (Belanger et al., 2003). DHT can be metabolized further into ADT, 3α -DIOL and 3β -DIOL in the basal cells as well. As basal cells express little or no AR, DHT must diffuse into the luminal cells, which constitute the largest fraction of the prostate, to

exert its function as a high affinity ligand for AR. Circulating testosterone can also diffuse into luminal cells where it is converted to DHT (Mostaghel, 2013). UGT2B17 glucuronidates both testosterone and DHT in basal cells which may prevent the accumulation of DHT in luminal cells. UGT2B15 is expressed in luminal cells where it primarily glucuronidates DHT to promote clearance (Barbier et al., 2000).

Removed due to copyright restriction

Figure 1.9: Androgen metabolism in the prostate

Testosterone produced in testes and adrenal androgens are metabolized by phase I enzymes into DHT and other androgen metabolites. DHT and these metabolites including ADT and 3 α -DIOL can be glucuronidated by UGT2B17 present in the basal cells and secreted back into the circulation. DHT diffuses into luminal cells where it binds to AR and modulates AR signaling. DHT is glucuronidated by UGT2B15 present in the luminal cells. [Figure obtained from (Belanger et al., 2003)].

Notably, UGT2B15 and UGT2B17 are negatively regulated by androgens via the AR signaling pathway in prostate cells, allowing androgens to inhibit their UGT2B15/17-dependent inactivation and modulate their own signaling activity through a feedback

regulatory loop (Chouinard et al., 2008), details of which, are discussed further in sections 1.8 and 1.9.

1.8 UGTs in Carcinogenesis: Impact on cancer risk and Drug metabolism

As UGTs are important enzymes that can conjugate various carcinogens including both exogenous compounds such as environmental toxins as well as cancer promoting endogenous compounds such as steroid hormones, alterations in their expression may affect their metabolic capabilities, and contribute to potentially altering an individual's exposure to carcinogenic chemicals. Consequently, this may influence the risk of cancer development and progression (Guillemette, 2003, Mackenzie et al., 2000, Nagar and Remmel, 2006). Genetic variability including polymorphisms (including in the coding region and promoter elements) of the UGTs have been identified by a large number of studies as risk factors for various cancers. Increased risk of cancer is associated with decreased glucuronidation activity in these studies. Hu et al have comprehensively reviewed these genetic variations in UGTs that are associated with cancer risk (Hu et al., 2016a). However, altered expression of UGTs in cancer is less investigated. Table 1.3 contains compelling examples of UGTs reported to be linked to cancer risk, progression or clinical outcome.

Table 1.3: UGTs reported to be associated with certain types of cancers

Type of Cancer	UGTs reported to be associated with cancer risk and/or progression
Breast Cancer	UGT1A1, UGT1A6, UGT1A7, UGT2B4, UGT2B15, UGT2B17
Endometrial Cancer	UGT1A1, UGT1A6, UGT2B17
Prostate Cancer	UGT2B15 and UGT2B17, UGT2B28
Liver Cancer	UGT1A7, UGT1A1, UGT1A9, UGT1A6
Lung Cancer	UGT2B4, UGT2B7, UGT2B10, UGT2B17, UGT1A1, UGT1A4, UGT1A6, UGT1A7, UGT1A9
Head and Neck Cancers	UGTA1, UGT1A7, UGT1A10
Colorectal Cancers	UGT1A1, UGT1A3, UGT1A4, UGT1A6, UGT1A7, UGT1A9, UGT2B7, UGT2B15, UGT2B17
Colon Cancer	UGT1A7
Esophageal Cancer	UGT1A8, UGT2B4
Bladder Cancer	UGT1A7, UGT2B7, UGT1A9, UGT1A6, UGT1A10, UGT1A

Data summarised from (Meech et al., 2019).

1.8.1 Involvement of UGT2B15 and UGT2B17 in Prostate cancer

The Prostate Cancer Foundation of Australia (www.prostate.org.au) lists prostate cancer as the most commonly diagnosed cancer in Australian men and approximately 1.1 million men were diagnosed with prostate cancer (PCa) worldwide in 2012 (Taitt, 2018). It is the 5th leading cause of death from cancer accounting for about 3500 deaths per year in Australia (www.prostate.org.au) and 307,000 deaths per year worldwide (Ferlay et al., 2015). As androgens play a major role in the growth,

differentiation and development of prostate cells, excessive androgen action may contribute towards prostate cancer development and progression (Heinlein and Chang, 2004, Belanger et al., 2003). During initial stages of prostate cancer, androgen deprivation therapy (inhibition of testosterone synthesis and/ or AR inhibition) would be a typical treatment option. However, after a few years of androgen deprivation therapy the cancer can evolve into a more aggressive and often metastatic type which is androgen-independent, and hence castrate resistant (CRPC). Often with CRPC, AR amplification/overexpression is seen. With this cancer-type, AR inhibition could still be therapeutically beneficial; however, chemotherapy is most commonly suggested (Meech et al., 2019).

As previously mentioned, testosterone and DHT are the 2 main androgens that are involved in prostate cancer development and progression (Mazaris and Tsiotras, 2013). Therefore, inactivation of these androgens by glucuronidation is extremely important, especially in a prostate cancer setting. UGT2B15 and UGT2B17 are considered to be the primary contributors of androgen glucuronidation due to their capacity to efficiently glucuronidate androgens and the presence of the large amount of circulating ADT and 3 α -DIOL glucuronides in the body. UGT2B7 could be a significant contributor to androgen glucuronidation as it can glucuronidate testosterone, 3 α -DIOL and ADT. However, its absence in the prostate where high levels of androgens such as ADT and 3 α -DIOL are synthesized and its low affinity towards ADT suggest otherwise. Hence, a tight regulation of UGT2B15 and UGT2B17 both at the transcriptional level and post-transcriptional level is of utmost importance for intra-prostatic androgen homeostasis, as any disruptions of this regulation may impact on the risk of developing androgen-sensitive prostate diseases, such as prostate cancer.

As genetic variations including polymorphisms in genes may influence the risk of developing prostate cancer, several studies have investigated multiple polymorphisms in both UGT2B15 and UGT2B17 and their association with prostate cancer risk. Several groups have investigated the UGT2B17 deletion/insertion (del/ins) polymorphism with conflicting results (Gallagher et al., 2007, Karypidis et al., 2008, Park et al., 2007, Olsson et al., 2008, Vidal et al., 2013, Hu et al., 2016a). Regardless of the contradictory results shown in these studies, it is important to note that carriers of the UGT2B17-del allele (a deletion that removes the UGT2B17 gene) have shown a higher prostate cancer risk, according to two independent meta-analysis studies (Cai et al., 2012, Kpoghomou et al., 2013). Carriers of the UGT2B17-del allele showed lower UGT2B17 expression in the prostate (Karypidis et al., 2008) and lower activity in liver microsomes compared to UGT2B17-Ins allele (Lazarus et al., 2005). Patients with UGT2B17 deletions (both null or heterozygous) showed significantly lower androgen glucuronide levels (Nadeau et al., 2011), which presumably indicates increased androgen exposure and an altered androgen metabolism. Therefore, increased levels of unconjugated active androgens in the prostate and/or systemically due to lower expression of UGT2B17, could be the reason for this higher risk in prostate cancer (Meech et al., 2019). A recent study by Habibi et al 2017, also shows a link between UGT2B17 deletion and the risk of benign prostatic hyperplasia (BPH) (Habibi et al., 2017).

The single nucleotide polymorphism (SNP) where the aspartic acid (D, or nucleotide G) to tyrosine (Y, or nucleotide T) substitution found in codon 85 of the *UGT2B15* gene (*UGT2B15^{D85Y}*, rs1902023), has been associated with altered prostate cancer risk in both in vitro studies and epidemiological studies (Zhong et al., 2017, Vidal et al., 2013, Karypidis et al., 2008). Both D85 and Y85 variants of

UGT2B15 show similar affinity towards DHT; however, UGT2B15 D85 variant has a two-fold decrease in enzyme activity (V_{\max}) compared to that of the UGT2B15 Y85 variant (Levesque et al., 1997). Therefore, the association of UGT2B15 D85 variant with higher risk of prostate cancer may be due to its lower clearance of DHT in the prostate (Vidal et al., 2013). Furthermore, the UGT2B15 D85 allele was significantly more prevalent in prostate cancer patients and was associated with a three-fold increased risk of prostate cancer compared to controls (MacLeod et al., 2000, Park et al., 2004). However, another study shows no such association between the UGT2B15 genotype and prostate cancer (Gsur et al., 2002). The association of both UGT2B variants (UGT2B17-deletion and UGT2B15 D85) with prostate cancer risk, has been evaluated as well. The presence of UGT2B15 D85 in combination with the UGT2B17-deletion was shown to increase the risk of prostate cancer further (Habibi et al., 2017). Discrepancies in these polymorphism and cancer risk evaluation studies could possibly be due to variable sample sizes and genetic heterogeneity of the study populations (Karypidis et al., 2008).

In addition to the *UGT2B15 D85Y* SNP, there have been reports of 6 other SNPs including: rs9994887, rs13112099, rs7686914 and rs7696472 which are located in the UGT2B15 promoter, rs4148269 which is present in the UGT2B15 coding region, and rs3100 which is located in the UGT2B15 3'UTR. These SNPs were associated with higher risk of prostate cancer according to a case-control study conducted on both Caucasians and African Americans which included 233 prostate cancer patients and 342 controls (Vidal et al., 2013).

In addition to genetic variations, the association between prostate cancer progression and the expression of UGT2B15 and UGT2B17 has also been investigated by several

groups. In general, functional analyses performed in prostate cancer cell lines support a role for UGT2B15 and UGT2B17 in reducing androgen levels (Meech et al., 2019). Small interfering RNA (siRNA)-mediated knockdown studies performed in the human androgen-dependent cancer cell line LNCaP, have shown that the reduction of UGT2B15 and UGT2B17 expression results in an increase of DHT in the culture media and increased response to DHT, which was determined by expression of several AR-target genes. UGT2B15/17-deficient LNCaP cells also showed an increase in proliferation rate in response to DHT compared to control cells, further validating the impact of glucuronidation on androgen signaling/response in target tissues (Chouinard et al., 2007). Furthermore, another study performed in the same cell line with AR antagonists shows that knockdown of UGT2B15 and UGT2B17 significantly reduced the anti-proliferative effects of bicalutamide (Grosse et al., 2013) suggesting that induction of UGT2B15/17 is an important component in initial androgen deprivation therapy (Gauthier-Landry et al., 2015). These data are in line with the role of UGT2B15 and UGT2B17 in androgen regulation in prostate cells and suggest that the induction of UGT expression may reduce androgen/AR-driven prostate cancer growth (Meech et al., 2019).

Studies conducted to investigate the alteration of UGT2B15 and UGT2B17 expression in prostate cancer cells, identified that AR is involved in the negative regulation of UGT2B15/17 expression (Bao et al., 2008, Grosse et al., 2013, Gauthier-Landry et al., 2015). Chromatin immunoprecipitation studies confirmed the binding of AR to the UGT2B15/UGT2B17 gene promoters (Bao et al., 2008); moreover, the use of synthetic AR agonists R1881 and antagonists (Chouinard et al., 2006), flutamide and bicalutamide (Bao et al., 2008, Grosse et al., 2013) confirmed the contribution of AR in UGT2B15/17 gene regulation. Therefore, as previously

mentioned, AR modulates its own signaling via a feedback regulatory loop in prostate cancer cells. As negative regulation of UGT2B15 and UGT2B17 leads to reduced glucuronidation and accumulation of androgens, this AR-mediated downregulation of UGT2B15 and UGT2B17 might be a part of the complex prostate cancer cell transformation process (Gauthier-Landry et al., 2015).

Surprisingly, some studies have reported high UGT2B17 and/or UGT2B15 expression levels in androgen-independent prostate tumors (Li et al., 2016, Montgomery et al., 2008, Stanbrough et al., 2006), which are further discussed below. A study conducted by Paquet et al has reported an increase in UGT2B17 protein levels in prostate tumors when compared to benign prostatic hyperplasia (BPH). Furthermore, UGT2B17 protein levels were increased 5-fold in metastatic tumors compared to benign tumors. In contrast, a decrease in UGT2B15 protein levels was reported in naive and CRPC tumors compared to BPH (Paquet et al., 2012), although increased UGT2B15 expression in androgen-independent prostate cancer has been reported in another study (Stanbrough et al., 2006). In the study conducted by Paquet et al, neither protein nor mRNA levels of UGT2B15 or UGT2B17 were significantly associated with Gleason score stratification. However a later study by Li et al reported different findings (Li et al., 2016). According to the latter study, higher UGT2B17 protein levels in prostate tumors were associated with higher Gleason score as well as higher risk of metastasis and CRPC progression. In addition, androgen-independent prostate cancer cell lines have shown increased UGT2B17 expression and activity compared to androgen-dependent prostate cancer cell lines. After prolonged androgen deprivation, UGT2B17 has also been shown to increase cancer cell proliferation/growth, invasion as well as xenograft progression to CRPC (Li et al., 2016). Increased expression of UGT2B17 has been reported in

castrate-resistant metastasis compared to primary prostate tumors as well (Montgomery et al., 2008) Overall, data from these studies suggest that UGT2B17 may be associated with androgen-independent prostate cancer growth leading to CRPC. One possible mechanism by which UGT2B17 promotes CRPC progression in the androgen-independent cancer setting could be via its involvement in c-Src kinase mediated regulation of AR signaling (Li et al., 2016). In the study conducted by Li et al, gene microarray analysis showed that UGT2B17 promotes ligand-independent transcriptional activity of AR at genes associated with cell mitosis. UGT2B17 was also shown to physically interact with c-Src kinase. c-Src kinase acts downstream of the EGF/IGF-1 signaling pathway to activate AR in a ligand independent manner (in the absence of androgens) by phosphorylating AR at Tyr-534 (Guo et al., 2006, Yang et al., 2015, Li et al., 2016). Moreover, elevated levels of c-Src kinase activity has been reported in CRPC and reduced levels of c-Src kinase is involved with prostate tumor regression (Li et al., 2016). In fact, currently c-Src kinase inhibitors are being tested for treatment of advanced prostate cancer in phase III clinical trials (Tatarov et al., 2009). Therefore, UGT2B17 may be playing a major role in CRPC progression by activating c-Src kinase and modulating ligand-independent AR activity via indirectly stimulating AR phosphorylation and thus in turn activating mitosis in cancer cells.

In conclusion, although there is no precisely defined model for how UGT2B15 and UGT2B17 function in the prostate cancer setting, studies suggest that they're involved in protecting against androgen-driven hyperproliferation and development of prostate cancer by reducing growth stimulatory androgen levels. Furthermore, in advanced prostate cancers with androgen independence, overexpression of UGT2B17 (which may occur due to loss of androgen-mediated repression), might

lead to increased androgen-independent cancer growth via signaling pathways that are not yet fully understood (Meech et al., 2019).

It is important to note that ethnicity appears to play a role in prostate cancer risk as different ethnic groups differ in the risk of developing prostate cancer. The order of incidence of prostate cancer from high to low is African-American>Caucasian>Asian. In the Asian population, the plasma levels of the glucuronidated testosterone metabolites such as ADT-G and 3 α -DIOL-3G were lower (in Japanese vs US African-American and Caucasian and in Chinese males vs Caucasian males) (Ross et al., 1992, Lookingbill et al., 1991) and this lower androgen load may contribute to the lower incidence of prostate cancer. However, environmental and lifestyle factors may contribute towards 10-15% of these aforementioned racial differences as well (Whittemore et al., 1995). Other factors such as gender, genetic variation, pregnancy, xenobiotic exposure and health status could influence the rate of glucuronidation (Gardner-Stephen, 2008) and hence may also have an effect on the risk of cancer.

1.9 Transcriptional regulation of UGTs

The mechanisms by which UGT expression and activity is regulated, have been investigated intensively over the last two decades by many research groups. Such studies show that the regulation of UGT expression could occur at multiple levels including the pre-transcriptional, transcriptional, post-transcriptional and post-translational levels [reviewed in (Hu et al., 2014b)]. Mechanisms of UGT regulation at the pre-transcriptional level include DNA methylation and histone modification at promoters and enhancers (Belanger et al., 2010, Oda et al., 2013, Oda et al., 2014,

Gagnon et al., 2006, Yasar et al., 2013). The typical transcriptional regulation of UGT genes is mediated by a combination of constitutively active and ligand-activated transcription factors (Mackenzie et al., 2010, Hu et al., 2014b). Mechanisms of post-transcriptional UGT regulation include alternative mRNA splicing and miRNA-mediated regulation of UGT mRNA stability and/or protein translation, which will be discussed extensively in this thesis. Post-translational regulation includes UGT modification via phosphorylation and alterations of UGT activities via oligomerization (Mitra et al., 2011, Guillemette et al., 2010, Basu et al., 2008, Basu et al., 2003, Basu et al., 2005). This section will focus on transcriptional regulation of UGTs, which is the most investigated type of UGT regulation among the aforementioned. Also, emphasis will be given to the transcriptional regulation of UGT2B family members UGT2B4, UGT2B7, UGT2B15 and UGT2B17 as the bulk of this thesis involves investigating post-transcriptional regulation mechanisms of these UGTs.

Typically, after a series of pre-transcriptional events including chromatin remodeling and histone modifications, transcription of a gene is initiated with binding of transcriptional activators to promoter and enhancer regions, eventually leading to the recruitment of RNA polymerase II and its accessory factors (which are also known as the general transcription machinery), to specific DNA sequences within the core promoter (Smale and Kadonaga, 2003). Regulatory promoters are located up to several hundred base pairs upstream of the transcription start site (TSS) whereas enhancer regions are more distal and may be located up or downstream of the TSS. Both regions contain binding sites that are specifically recognized by transcription factors. It has been reported that all UGT genes contain their own unique regulatory promoter region that controls transcription (Mackenzie et al., 2005). Core promoters

are generally in close proximity to the transcription start site (typically ~ 35 base pairs upstream) and contain several sequence motifs including a TATA box, initiator (Inr) region, transcription factor II (TFII)B recognition element (BRE), and the downstream core promoter element (DPE). Either some, none or all of these sequence motifs may be present in a particular core promoter (Smale and Kadonaga, 2003) and the UGT family shows such variation in sequence motifs in different UGT genes. These sequence motifs play individual roles in either stabilizing or directly binding to proteins composing the transcriptional machinery. The transcription factors bound to regulatory promoter and enhancer regions along with general transcription machinery bound to sequence motifs on the core promoter, enables combinatorial gene regulation leading to diverse gene expression patterns (Smale, 2001, Gregory, 2004). These transcription factors control both constitutive and inducible UGT expression which are the two major aspects of UGT transcriptional regulation that are of interest.

1.9.1 Regulation of tissue-specific constitutive expression of UGTs

As previously discussed in section 1.6 in detail, UGTs show tissue-specific expression patterns. In addition, inter-individual variations in UGT expression have been reported in various tissues in several studies. The main tissue-specific transcription factors that are known to regulate constitutive UGT expression include the intestine-specific caudal-related homeodomain protein 2 (Cdx2) that controls expression of UGT1A8, UGT1A10 and UGT2B7 (Gregory et al., 2004, Gregory et al., 2006) and the liver-enriched hepatocyte nuclear factors (HNF)1 α and (HNF)4 α that control several hepatic UGTs (Gardner-Stephen and Mackenzie, 2008). In addition to tissue-specific transcription factors, there are transcription

factors that may be expressed ubiquitously, or in a limited number of cell types and that may work often in concert with tissue-specific factors. These include the Forkhead box protein A1 (FOXA1) (Hu and Mackenzie, 2010, Hu et al., 2010), the activator protein 1 (AP-1) (e.g., Fra-2 and c-Jun) (Hu and Mackenzie, 2009, Hu et al., 2014a), the specificity protein 1 (Sp1) (Chen et al., 2009), the upstream stimulating factors (USF1 and USF2) (Belanger et al., 2010) and the tumor suppressor protein p53 (Hu et al., 2014c, Hu et al., 2015). These transcription factors may further influence the tissue-specific expression of UGTs (constitutive expression) and may also control inducible expression of some UGTs (which will be discussed later in section 1.9.2).

The regulation of constitutive expression of UGT2B4 is not well studied and constitutively active transcriptional regulators that bind to this gene have not been identified. However, a single study showed increased mRNA levels of UGT2B4 in HepG2 cells when sulfotransferase (SULT) activity was inhibited in the cells via knockdown of 3'-phosphoadenosine-5'-phosphosulfate synthases (PAPSS) 1 and 2 as well as knockdown of SULT2A1 (which catalyzes bile acid sulfonation). Although the study was unable to identify the underlying mechanism behind this regulation, data suggests knockdown of PAPSS results in an increase of UGT2B4 transcription and its mRNA stability (Barrett et al., 2015). The constitutive expression of UGT2B7 is reported to be regulated by HNF1 α when bound to an HNF1 α binding site in its proximal promoter (Toide et al., 2002, Ramirez et al., 2008). The capacity of HNF1 α to activate the UGT2B7 promoter is enhanced by the ubiquitous transcription factor, octamer transcription factor 1 (Oct-1). This enhancement is most likely achieved through the direct interaction of Oct-1 with HNF1 α (Ishii et al., 2000), rather than

direct binding to the promoter itself. A previous study in our laboratory by Gregory et al. (2006) shows that the UGT2B7 proximal promoter contains 2 Cdx2 sites and that Cdx2 and HNF1 α could synergistically activate the UGT2B7 promoter when bound to their respective sites (Gregory et al., 2006). The UGT2B7 promoter also contains several SNPs that alter certain binding sites of proteins including AP-1 (Hu et al., 2014a).

The constitutive expression of both UGT2B15 and UGT2B17 has been shown to be regulated by FOXA1 binding to a cognate site in the proximal promoters of both these UGT genes (Hu et al., 2010, Hu and Mackenzie, 2010). In prostate cancer cell lines LNCaP and VCaP (but not in breast MCF7 or liver HepG2), a reported SNP [with a minor allele frequency (MAF) of 0.33] within the FOXA1 binding site of the UGT2B17 proximal promoter reduced its basal promoter activity (Hu et al., 2010). Thus, polymorphisms present in the promoter may in fact affect its capacity to glucuronidate androgens in the prostate.

1.9.2 Regulation of inducible expression of UGTs

The inducible expression of UGTs involves a variety of ligand-activated transcription factors, prominently the nuclear receptor (NR) superfamily. Table 1.4 summarizes these nuclear receptors, their ligands and their target UGTs [obtained from (Hu et al., 2014b)]. The control of inducible expression of UGT2B members; 2B4, 2B7, 2B15 and 2B17 are explained in detail below.

The Farnesoid X receptor (FXR) ligand chenodeoxycholic acid (CDCA) induces the expression of UGT2B4 by interacting with FXR monomer which binds to a bile acid response element (BARE) within the proximal promoter (Barbier et al., 2003b). In

addition, peroxisome proliferator-activated receptor α (PPAR α) and PPAR agonists (e.g., fenofibric acid or Wy14643) were shown to induce the expression of UGT2B4 via binding to the PPAR response element, direct repeat-1 (DR1) present within the promoter (Barbier et al., 2003a). Notably, despite the overlap between BARE and DRI elements, FXR and PPAR α activators show an additive effect on UGT2B4 induction (Barbier et al., 2003b).

FXR and constitutive androstane receptor (CAR) are two ligand-dependent transcription factors that could repress the expression of UGT2B7. The FXR ligand LCA and the CAR agonist 1,4-bis[2-(3,5-dichloropyridyloxy)]benzene (TCPOBOP), have been shown to mediate this repression in Caco2 cells and HepG2 cells (along with mouse studies) respectively. LCA-activated FXR binds directly to a cognate element in the proximal promoter to mediate repression whereas TCPOBOP-activated CAR indirectly mediates repression via inhibiting the binding of HNF4 α to the promoter (Lu et al., 2005, Yueh et al., 2011). Anticancer drugs including epirubicin, doxorubicin, temozolomide and vemurafenib are also inducers of UGT2B7 expression (Dellinger et al., 2012). Importantly, epirubicin is primarily glucuronidated by UGT2B7 and thus induction of UGT2B7 causes its own inactivation in a negative feedback loop. Epirubicin exerts its effects on UGT2B7 via recruitment of p53 to the proximal promoter p53 response element (Hu et al., 2014b, Meech et al., 2019).

Table 1.4: Nuclear receptors, their ligands and their target UGTs

Receptors	Ligands	Target UGTs
ER α	17-beta estradiol Tamoxifen	1A4, 2B15, 2B17
AR	Testosterone Dihydrotestosterone R1881 Flutamide	1A1, 1A3, 2B10, 2B11 2B15, 2B17, 2B28
GR	Cortisone Dexamethasone	1A1
AhR	3-Methylcholanthrene Benzo[a]pyrene Bilirubin TCCD 12-HETE	1A1, 1A3, 1A4, 1A6, 1A7 1A8, 1A10, 2B4
CAR	TCPOBOP 3 α ,5 α -androst-enol 3 α ,5 α -androstanol Artemisinin	1A1, 2B7
FXR	Chenodeoxycholic acid Cholic acid Deoxycholic acid Z-Guggulsterone	1A3, 2B4, 2B7
LXR	24(S)-Hydroxycholesterol 24(S),25-Epoxycholesterol	1A3
Nrf2	Bilirubin α -Naphthoflavone tert-Buthylhydroquinone Oltipraz	1A1, 1A6, 1A7, 1A8 1A10, 2B7
PPAR α	Clofibric acid Gemfobrozil Bezafirate GW 7647 20-HETE 11,12-EET	1A3, 1A6, 1A9, 2B4
PPAR γ	Ciglitazone Troglitazone 15-Deoxy-D12, 14-prostaglandin J2 GW 9662	1A9
PXR	Rifampicin Litocholic acid Hyperforin	1A1
VDR	25-Hydroxyvitamin D3 1,25-Dihydroxyvitamin D3	2B15, 2B17

[obtained from (Hu et al., 2014b)]

Both UGT2B15 and UGT2B17 inducible expression involves steroid hormones. These genes contain highly conserved proximal promoters with conserved ‘estrogen response units’ (ERU) that mediate activation via 17 β -estradiol. The ERU contains an imperfect estrogen response element (ERE), two ERE half-sites, and two AP-1 binding sites and is located next to a FOXA1 binding site. 17 β -estradiol mediates this activation of UGT2B15 via recruiting ER α , Fra-2 and c-Jun to the ERU (Hu and Mackenzie, 2009). FOXA1 is a major transcription factor which is involved in both androgen- and estrogen-mediated regulation of the UGT2B15 and UGT2B17 promoters via the recruitment of AR and ER to the adjacent AR and ER binding sites (Hu et al., 2014b). Recent work in our laboratory has also found that AR binds to a site designated the ‘3’ ERE half site’ within the ERU in breast cancer cells and mediates UGT2B15 and UGT2B17 induction (Hu et al., 2016b). As mentioned previously, this negative regulation of UGT2B15 and UGT2B17 by AR, allows androgens to inhibit their UGT2B15/17-dependent inactivation and modulate their own signaling activity through a feedback regulatory loop (Chouinard et al., 2008). Furthermore, our laboratory has recently shown that ERU is involved in both UGT2B15 and UGT2B17 induction in breast cancer cells. The anti-cancer drug tamoxifen and its active metabolites 4-hydroxytamoxifen and endoxifen induce UGT2B15 while exemestane and its active metabolite 17-hydroexemestane induce UGT2B17 by acting as ER ligands and AR ligands respectively (Chanawong et al., 2015, Chanawong et al., 2017). As the active tamoxifen and exemestane metabolites are glucuronidated by UGT2B15 and UGT2B17 respectively, this regulation facilitates their clearance potentially leading to drug resistance.

In contrast to breast cancer, in prostate cancer cells (LNCaP), UGT2B15 and UGT2B17 are repressed by androgens, DHT (natural) and R1881 (synthetic AR agonist), by mechanisms which remain unknown (Chouinard et al., 2006). Although the exact Androgen Response Element (ARE) sequence hasn't been identified, AR in fact binds to the proximal promoters of UGT2B15 and UGT2B17 as shown by chromatin immunoprecipitation (ChIP) assays (Bao et al., 2008). Other compounds that have been shown to repress UGT2B15 and/or UGT2B17 include activators of FXR (CDCA and GW4064), calcitriol (active metabolite of vitamin D), cytokines and growth factors [summarized in (Meech et al., 2019)].

As discussed in this section, transcriptional regulation of UGTs has been investigated extensively for the last few decades. However, the mechanisms controlling UGT mRNA stability at the post-transcriptional level remain poorly characterized. MicroRNAs have been identified as one of the major post-transcriptional regulators of gene expression (Filipowicz et al., 2008) and will be further discussed in section 1.10.

1.10 microRNAs

1.10.1 Overview of miRNA

MicroRNAs are a family of 21-25-nucleotide long, endogenous, evolutionarily conserved small RNAs (Shukla et al., 2011, He and Hannon, 2004). They belong to the class of non-coding RNAs (ncRNA) which consists of several RNA classes that can be divided into 2 types; housekeeping ncRNAs and regulatory ncRNAs. Housekeeping ncRNAs include ribosomal RNAs (rRNA), transfer RNA (tRNA), small nuclear RNAs (snRNA), small nucleolar RNAs (snoRNA), telomerase RNA (TERC), tRNA-derived fragments (tRF) and tRNA halves (tiRNA). Regulatory ncRNAs include miRNAs, small interfering RNAs (siRNA), piwi-interacting RNAs (piRNA), enhancer RNA (eRNA), long non-coding RNAs (lncRNAs) and circular RNAs (circRNA) (Hombach and Kretz, 2016, Zhang et al., 2019). MiRNAs are one of the most thoroughly investigated ncRNA classes and are thought to be one of the most abundant gene classes due to their widespread expression in vertebrates, flies, worms and plants, and even in viruses [(Ha and Kim, 2014), www.miRbase.org].

Recent investigations have led to the finding of microRNAs as post-transcriptional regulators of gene expression in various cellular processes (Filipowicz et al., 2008). They have been linked to cell differentiation, cell fate determination, organ development, physiology as well as pathology and disease (Ambros, 2004, Kosik, 2010, Bizuayehu and Babiak, 2014, Christodoulou et al., 2010, Grimson et al., 2008). The first miRNA, *lin-4* was discovered in 1993 while screening for post-embryonic developmental genes in the nematode *Caenorhabditis elegans* (Lee et al., 1993, Wightman et al., 1993). In recent years, powerful bioinformatics tools and deep

sequencing experiments have facilitated the discovery of a vast number of microRNA genes in many organisms including humans (Gomes et al., 2013). Several miRNA databases including miRBase (Kozomara and Griffiths-Jones, 2011), ZooMir (Li et al., 2010), miRNEST (Szczesniak and Makalowska, 2014) and miRMaid (Jacobsen et al., 2010) have catalogued miRNAs in many different species. Since the discovery of the first miRNA over 25 years ago, over 2500 mature miRNAs have been identified in humans (www.miRBase.org).

MiRNAs are initially expressed as long stem-loop structures termed primary microRNAs and then processed into precursor miRNAs which are transported into the cytoplasm, where they are cleaved into double-stranded mature miRNAs. One strand of the mature miRNA is then incorporated into RNA induced silencing complex (RISC), and guides the RISC to recognize complementary target mRNAs (discussed further in section 1.10.2) (Shukla et al., 2011, Satoh and Tabunoki, 2011, He and Hannon, 2004). These non-protein coding small RNAs contain unique seed sequences (nucleotides 2-8) which determines their specificity towards target genes. They are known to repress target gene expression by binding mainly to 3'UTRs, although they also bind to coding regions and 5'UTRs of transcripts, and inhibiting protein translation and/or enhancing mRNA degradation (Grimson et al., 2007, Hu and Coller, 2012). At least 60% of mammalian protein coding genes have been estimated to be regulated by microRNAs (Friedman et al., 2009, Lewis et al., 2003).

1.10.2 Biogenesis of miRNAs

MiRNA genes are located throughout the genome. Most miRNA genes are transcribed as individual transcripts whereas some miRNAs are located in clusters

that can be transcribed as single polycistronic transcripts containing multiple miRNAs (Lagos-Quintana et al., 2001, Lau et al., 2001, Lee and Ambros, 2001, Lee et al., 2002, Macfarlane and Murphy, 2010). It is also important to note that recent evidence shows independent transcription and regulation of individual miRNAs within the same genomic cluster (Song and Wang, 2008). MiRNAs within a genomic cluster can be either related or different to each other (Lagos-Quintana et al., 2001, Lau et al., 2001). Mammalian miRNAs are frequently found within inter-genic regions and introns of protein-coding or non-protein coding genes (Rodriguez et al., 2004, Macfarlane and Murphy, 2010). Previously, as the function of these regions were unknown, they were classified as 'junk DNA'. However, with the discovery of miRNA genes in these regions, it is now known that they are of importance (Macfarlane and Murphy, 2010). MicroRNAs are less frequently found within exons of long non-protein-coding transcripts and anti-sense transcripts (Rodriguez et al., 2004, Lagos-Quintana et al., 2003, Macfarlane and Murphy, 2010).

In the canonical miRNA biogenesis pathway, miRNA genes are transcribed by RNA polymerase II into primary miRNAs (pri-miRNAs) which are several kilobases long and typically contain a hairpin stem of approximately 33 base pairs, a terminal loop and two single-stranded flanking segments that are critical for further processing (Han et al., 2006, Winter et al., 2009, Zeng and Cullen, 2005). Typically, most pri-miRNAs undergo 5' m7G capping and polyadenylation at the 3' end, in a similar manner to protein coding mRNAs (Cai et al., 2004, Lee et al., 2004). Even though, the characterization of miRNA promoters is not yet investigated in depth, several studies have shown that they are similar to protein coding gene promoters (Hammond, 2015).

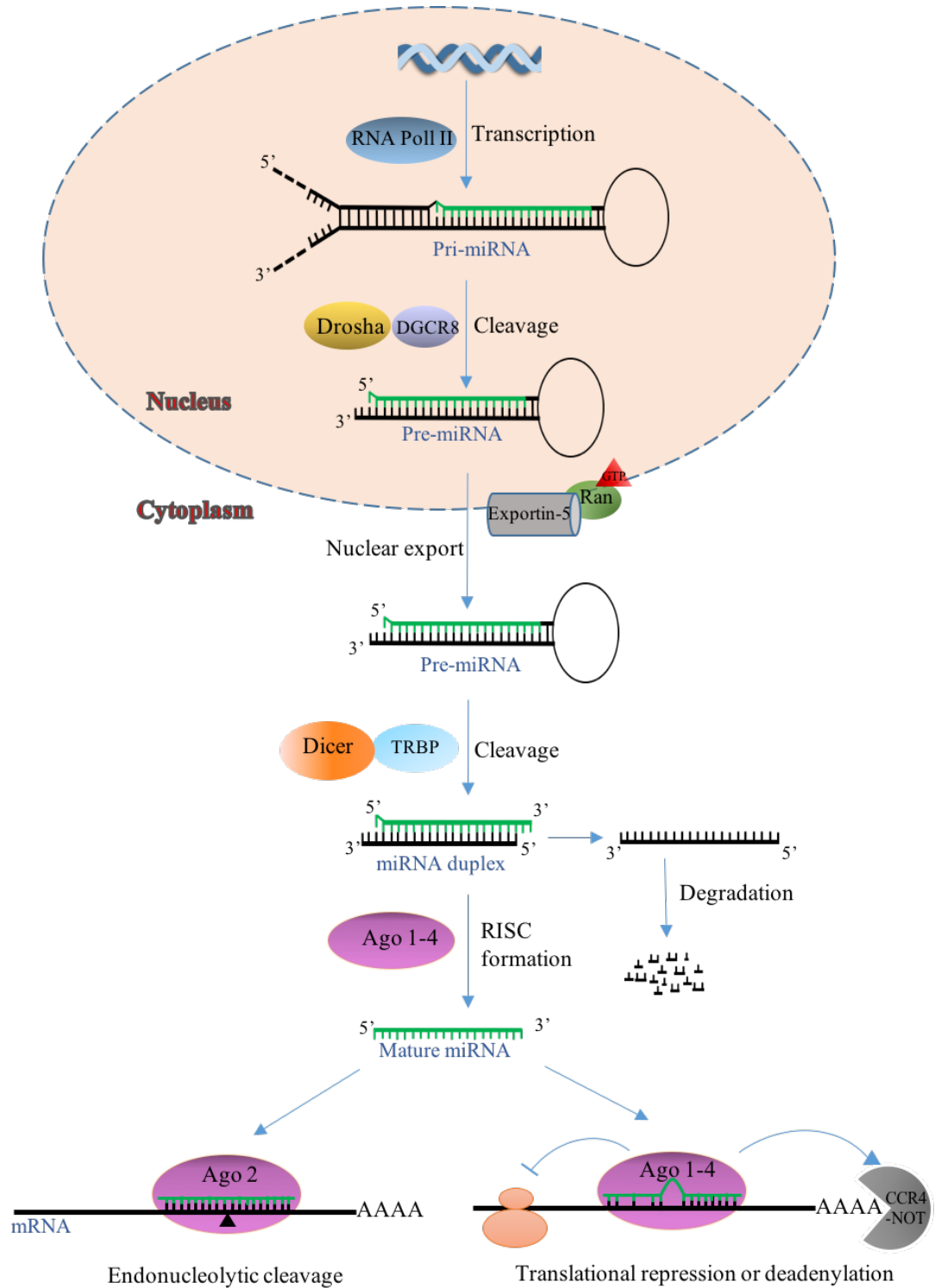


Figure 1.10: The canonical pathway of miRNA biogenesis

MiRNAs are initially transcribed as stem-loop structures termed pri-miRNAs from miRNAs genes by RNA polymerase II. A pri-miRNA is then processed into a pre-miRNA by RNase III enzyme Dorsha and DGCR8. The Ran-GTP dependent transporter Exportin-5 transports the pre-miRNA into the cytoplasm, where it is cleaved into a double-stranded miRNA duplex by the RNase III enzyme Dicer with the associated TRBP protein. One strand of the miRNA duplex (mature miRNA) is

then incorporated into RISC, where it guides the RISC to recognize complementary target mRNAs leading to endonucleolytic cleavage, translational repression and/ or deadenylation whereas the passenger strand of the miRNA duplex gets degraded [Figure adapted from (Winter et al., 2009)].

A pri-miRNA undergoes two sequential cleavages before becoming a mature miRNA. The initial cleavage step occurs in the nucleus during or subsequent to transcription of pri-miRNA, by the RNase III enzyme Drosha. The double stranded RNA-binding protein DGCR8 (DiGeorge syndrome critical region 8; also known as Pasha in *Drosophila* and *C. elegans*) is associated with Drosha and required for pri-miRNA cleavage. Drosha contains two tandem RNase-III domains, a dsRNA binding domain and an amino-terminal segment. The two RNase domains of Drosha catalyse the cleavage of the 3' and 5' flanking sequences of the pri-miRNA, while DGCR8 stably interacts with the pri-miRNA directly and help determine the specific cleavage site. This process generates a precursor miRNA (pre-miRNA) of approximately 70 base pairs, which consists an imperfect stem-loop structure (He and Hannon, 2004, Esquela-Kerscher and Slack, 2006, Chu and Rana, 2007, Winter et al., 2009). It has been demonstrated that the efficiency of pri-miRNA processing by Drosha depends on the size of the terminal loop, the stem structure and the flanking nucleotides of the Drosha cleavage site (Lee et al., 2003, He and Hannon, 2004, Zeng and Cullen, 2005). The Ran GTP dependent transporter, Exportin-5 transports the pre-miRNA into the cytoplasm, where it undergoes the second cleavage step. The RNase III enzyme Dicer with the associated TRBP protein (transactivation-response RNA binding protein), cleaves the terminal loop of the pre-miRNA releasing the double-stranded miRNA duplex (miRNA:miRNA*). This miRNA duplex contains both the mature miRNA strand and a passenger strand (miRNA*) and is approximately 22

nucleotides long with two nucleotide overhanging at each 3' end (Hutvagner et al., 2001, Grishok et al., 2001, Kim, 2005, Ketting et al., 2001, He and Hannon, 2004, Hammond, 2015, Winter et al., 2009). Of note, the length of the duplex may vary among miRNAs possibly as a result of mismatches and bulges on the pre-miRNA stem (He and Hannon, 2004). One strand of the duplex (the mature strand) is subsequently incorporated stably into miRNA induced silencing complex (miRISC). The main protein component of the miRISC complex is Argonaute (Ago). In humans, 4 family members of Ago proteins (Ago 1-4) have been identified, all of which can be associated with miRNAs (Meister and Tuschl, 2004). Once the mature miRNA strand is loaded into the miRISC complex, the passenger strand gets removed by one of several possible mechanisms. If the miRNA duplex displays high complementarity in the central region of the hairpin stem, the passenger strand can be cleaved by Ago2 and the removal of it is facilitated by the component 3 promoter of RISC (C3PO) nuclease complex, in a similar manner to the siRNA pathway (Liu et al., 2009, Matranga et al., 2005, Shin, 2008, Winter et al., 2009, Ye et al., 2011b). Despite the sequence similarity in the Ago proteins, only Ago2 possess the endonuclease activity to cleave the passenger strand. In addition, most miRNA duplexes contain central mismatches which prevent splicing. Therefore, duplex strand unwinding is more common than the cleavage of passenger strand in the miRNA pathway (Chu and Rana, 2007, Ha and Kim, 2014). Several helicases such as RNA helicase A (RHA) (Robb and Rana, 2007), human MOV10 (Meister et al., 2005), RCK/p54 (Chu and Rana, 2006), p68 (also known as DDX5) (Salzman et al., 2007), p72 (also known as DDX17), and Gemin3/4 have been linked to this activity in humans. However, a universal helicase that is responsible for duplex unwinding is not yet reported (Winter et al., 2009).

The mature miRNA strand selection during the Ago loading step mainly depends on the thermodynamic stability of the base pairs at the two ends of the duplex (Khvorova et al., 2003, Schwarz et al., 2003, Ha and Kim, 2014, Winter et al., 2009). The strand with a relatively unstable base pair at its 5' end of the duplex is typically selected to be loaded into RISC (Khvorova et al., 2003). Additionally, the strand with a U at the nucleotide position 1 is favoured by Ago proteins as well (Ha and Kim, 2014). However, as strand selection is not a strict mechanism, the passenger strand can also be loaded in to miRISC at varying frequencies. Moreover, recent next generation sequencing (NGS) investigations have led to the finding of a small fraction of passenger strand of essentially all miRNA families being loaded into the RISC complex. Therefore, the strand from the 5' end of the stem-loop is termed "5p" and the 3' end is termed "3p" rather than termed mature miRNA/miRNA* strands (Hammond, 2015, Yang et al., 2011). It has also been shown that both strands transcribed from the same hairpin can be functional at the same time in the same cell (Almeida et al., 2012). Furthermore, some miRNAs show alternative strand selection ('arm switching') depending on cell/tissue type or biological state (Ohanian et al., 2013, Chiang et al., 2010, Ha and Kim, 2014, Hammond, 2015). For instance, miR-142-5p is dominantly expressed in ovaries, brain and testes, whereas in the embryonic and newborn tissue samples, miR-142-3p is the dominant isoform (Chiang et al., 2010).

In contrast, some miRNAs are generated through non-canonical pathways. These include the mirtron class of miRNAs. They are produced from introns by splicing machinery and lariat debranching enzyme where the resulting pre-miRNAs could bypass the Drosha-DGCR8 recognition and cleavage step and get processed by Dicer (Curtis et al., 2012, Okamura et al., 2007, Ruby et al., 2007, Hammond, 2015).

There is also Dicer-independent miRNA biogenesis reported where the pre-miRNA generated after Drosha cleavage, binds directly to Ago2 instead of Dicer (Cheloufi et al., 2010, Yang and Lai, 2010, Cifuentes et al., 2010).

1.10.3 miRNA Target Recognition and Function

Once the mature miRNA binds to Ago in the RISC, it guides the RISC to recognize complementary target mRNAs. The corresponding region of the mRNA that pairs to the miRNA, is known as the miRNA response element (MRE). miRNAs contain unique seed sequences (nucleotides 2-7 from the 5' terminus) which is a key determinant of their specificity towards target genes. The corresponding 6-nt region (in the MRE) of the target mRNA which makes direct contact with the miRNA seed sequence is called the 'seed site'. The canonical seed sequence binds to the target mRNA in perfect Watson-Crick complementation and this seed pairing is known to be sufficient for effective repression of target gene expression (Brennecke et al., 2005, Friedman et al., 2009, Grimson et al., 2007, Brodersen and Voinnet, 2009, Saito and Sætrom, 2010). In addition to canonical seed pairing, non-canonical target sites have been reported as well. These will be discussed further in Chapter 4 (Discussion). Along with seed pairing, most miRNAs bind to their target mRNAs with mismatches and bulges (Carthew and Sontheimer, 2009). A single miRNA may potentially regulate multiple mRNA transcripts due to sequence similarities in the genome. Nevertheless, a single mRNA can be regulated by more than one miRNA (either multiple copies of a single miRNA or several different miRNAs) in a combinatorial way (Duskova et al., 2013, Dluzen and Lazarus, 2015, Brennecke et al., 2005, Mukherji et al., 2011, Saito and Sætrom, 2010). In addition, having

multiple binding sites for the same miRNA in the target mRNA causes a higher degree of repression (Doench et al., 2003).

miRNAs are known to repress target gene expression predominantly by guiding the RISC to bind mainly to 3'UTRs and thereby reducing overall protein expression (Grimson et al., 2007, Hu and Collier, 2012). This reduction of protein expression could occur via translational repression and/or mRNA degradation (Chu and Rana, 2007, Dluzen and Lazarus, 2015, Filipowicz et al., 2008). The degree of miRNA-mRNA complementarity plays a pivotal role in determining the possible regulatory mechanism (Carthew and Sontheimer, 2009). The presence of perfect complementarity of miRNA:MRE leads to the cleavage of target mRNA by the endonuclease activity of Ago2 (Liu et al., 2004, Doench et al., 2003, Xu et al., 2014). However the majority of animal miRNA:mRNA interactions show imperfect complementary (Jonas and Izaurralde, 2015) with mismatches and bulges (Carthew and Sontheimer, 2009), thus preventing Ago2-catalysed cleavage. The lack of perfect complementarity leads to translational repression and/or mRNA decay. However, the mechanisms by which miRNAs repress translation are still not completely understood and remain a matter of debate (Carthew and Sontheimer, 2009). There is evidence that the repression may occur at translation initiation where Argonaute of the miRISC competes with eukaryotic initiation factor 4E (eIF4E) and cap binding proteins for binding to the 5'-terminal 7-methylguanosine (m⁷G) cap of mRNA (Filipowicz et al., 2008, Kiriakidou et al., 2007, Mathonnet et al., 2007, Valinezhad Orang et al., 2014). Another possible mechanism of translation repression is by obstructing the assembly of 80S ribosome complex. In this model, human Ago2 of miRISC recruits eukaryotic initiation factor 6 (eIF6) which binds to the 60S ribosomal subunit which in turns prevents it from joining the 40S subunit

(Chendrimada et al., 2007, Wang et al., 2008, Chu and Rana, 2007). The miRISC may repress translation at post-initiation steps as well. Inhibition of ribosome elongation by competing with elongation factors, premature drop-off of ribosomes leading to premature termination and degradation of nascent polypeptides by proteolytic enzymes are some of the post-initiation regulation models proposed (Petersen et al., 2006, Valinezhad Orang et al., 2014, Morozova et al., 2012, Nottrott et al., 2006, Fabian et al., 2010)

Degradation of mRNA occurs mainly due to deadenylation, decapping and eventual decay rather than endonucleolytic cleavage by Ago2 (O'Brien et al., 2018, Carthew and Sontheimer, 2009). In this pathway, initially the silencing miRISC complex is formed with the interaction of Ago of the RISC complex with GW182 family proteins (Behm-Ansmant et al., 2006, O'Brien et al., 2018). GW182 interacts with polyadenylate-binding protein (PABPC), followed by the recruitment of other effector proteins such as poly(A) nuclease (PAN) deadenylation complexes; PAN2-PAN3 and carbon catabolite repressor protein 4 (CCR4)-NOT. Deadenylation is initiated by the PAN2-PAN3 complex and completed by the CCR4-NOT complex (Jonas and Izaurralde, 2015). Subsequently, mRNA is decapped by the decapping protein 1 and 2 (DCP1 and 2) complex along with associated co-factors (Behm-Ansmant et al., 2006) leading to eventual 5'-3' degradation of the target mRNA by cytoplasmic exoribonuclease 1 (XRN1) (Braun et al., 2012). Furthermore, the recruitment of CCR4-NOT by GW182 is involved in translation repression via the recruitment of RNA helicase DEAD-box ATPase DDX6 which is a known translation inhibitor (Mathys et al., 2014, Gebert and MacRae, 2019).

The majority of miRNA related studies show that miRNAs modulate expression by specifically binding to 3'UTRs of their target mRNAs. Nevertheless, interaction of miRNAs with other mRNA regions including 5'UTRs, coding regions and gene promoter regions have been detected. Depending on the binding region, miRNAs have been shown to repress gene expression, activate translation or even regulate transcription (O'Brien et al., 2018, Xu et al., 2014). The interaction of miRNAs with 5' UTRs has been shown to have both repression and activation effects (Tsai et al., 2009, Zhang et al., 2018), while the interaction with coding regions has been shown to repress gene expression (Brummer and Hausser, 2014, Duursma et al., 2008, Forman et al., 2008). Of note, upregulation of gene expression is also reported in several studies by miRNAs that bind to 3'UTRs (Valinezhad Orang et al., 2014). Interestingly, induction of transcription has also been seen due to miRNAs interacting with genomic promoter regions (Dharap et al., 2013). The function of miRNAs is dependent on several factors including the abundance of miRNAs and their cognate mRNAs, the affinity of miRNA:mRNA interactions, cell type, cell condition, subcellular location as well as the availability of various factors and elements including miRISC components (O'Brien et al., 2018, Valinezhad Orang et al., 2014).

miRNA can act as a genetic 'switch' or a 'fine tuner' of gene expression (Mukherji et al., 2011). In both instances, the concentration of miRNA as well as the target mRNA have an impact on target protein outcome. When miRNAs are thought to act as genetic switches, the targets are essentially inactive or reduced to an inconsequential level following miRNA-mediated repression (i.e. switched off). Thus, to overcome the miRNA mediated repression, high mRNA levels may be needed within the cell (Dluzen and Lazarus, 2015). In animals, miRNAs are most

commonly seen as fine-tuners of protein expression where they help maintain protein expression of target genes at a desirable level. Under certain conditions where miRNAs are targeting highly expressed mRNA, the effect can be subtle, whereas in low-expressing mRNA targets, the effect can be dramatic (Dluzen and Lazarus, 2015, Mukherji et al., 2011). The role of the fine-tuner miRNA is to precisely set a limit on target mRNA and/or protein levels. Either as a switch or a fine-tuner, miRNA mediated regulation is known to be essential for various biological pathways.

1.10.4 miRNA target prediction

As miRNAs bind to their targets with Watson-Crick complementarity, it is feasible to think that bioinformatic target prediction should be straightforward. However, the miRNA seed sequence which is a major determinant of target binding, is only 6 nucleotides long and thus, could lead to many false negative predictions (Hammond, 2015). Therefore, additional parameters are considered by *in silico* target prediction algorithms for more reliable predictions (Ekimler and Sahin, 2014). As miRNA binding sites are most commonly found in 3'UTR regions, the majority of these programs predict target sites only within 3'UTRs. Some of the other parameters include evolutionary conservation among species, compensatory pairing outside the seed region, flanking sequence determinants, folding free-energy (ΔG) of the miRNA:mRNA duplex, accessibility of target site within the 3'UTR and abundance of binding sites (Lewis et al., 2003, Saito and Sætrum, 2010, Ekimler and Sahin, 2014, Hammond, 2015). TargetScan, miRanda, PicTar, DIANA-microT, PITA, RNAhybrid, RNA22, miRTar, microTar, miRTarget, TargetMiner and SVMicO are some of the most popular web-based bioinformatic algorithms that use several

parameters to predict miRNA targets (Table 1.5). A prediction ‘score’ is created weighing various criteria by these bioinformatic algorithms to identify true positives.

Table 1.5: miRNA target prediction tools

Algorithm	Web link	References
TargetScan	http://www.targetscan.org/	(Lewis et al., 2005, Grimson et al., 2007, Friedman et al., 2009)
miRanda-mirSVR	http://www.microrna.org/microrna/getGeneForm.do	(Betel et al., 2010)
PicTar	http://pictar.mdc-berlin.de/	(Krek et al., 2005)
DIANA-microT	http://www.microrna.gr/microT-CDS	(Paraskevopoulou et al., 2013)
PITA	http://genie.weizmann.ac.il/pubs/mir07/mir07_prediction.html	(Kertesz et al., 2007)
RNAhybrid	http://bibiserv.techfak.uni-bielefeld.de/rnahybrid/	(Rehmsmeier et al., 2004)
RNA22	https://cm.jefferson.edu/rna22/	(Miranda et al., 2006)
miRTar	mirtar.mbc.nctu.edu.tw/	(Hsu et al., 2011)
microTar	http://tiger.dbs.nus.edu.sg/microtar/	(Thadani and Tammi, 2006)
miRTarget	http://www.mirdb.org/index.html	(Liu and Wang, 2019), (Wong and Wang, 2015)
TargetMiner	https://www.isical.ac.in/~bioinfo_miu/targetminer20.htm	(Bandyopadhyay and Mitra, 2009)
SVMicrO	http://compgenomics.utsa.edu/svmicro.html	(Liu et al., 2010)

TargetScan and RNAhybrid are the two prediction algorithms used in this study for miRNA target prediction. TargetScan which is the first human miRNA target prediction tool (Lewis et al., 2005), uses seed matching and conservation as its two

major features. TargetScan classifies predicted miRNA target sites based on their pairing with the miRNA seed region, into four types [(Lewis et al., 2005), Figure 1.11]. These are known as 8mer (a pairing to the 2-7 nt miRNA seed and nucleotide 8 plus A at nucleotide 1), 7mer-m8 (a pairing to the 2-7 nt miRNA seed and nucleotide 8), 7mer-A1 (a pairing to the 2-7 nt miRNA seed plus an A at nucleotide 1) and 6mer (a pairing to the 2-7 nt miRNA seed only). Studies have shown the following hierarchy of miRNA site targeting efficacy: 8mer > 7mer-8m > 7mer-A1 > 6mer (Grimson et al., 2007, Nielsen et al., 2007). TargetScan predicts targets by searching the presence of ‘conserved’ seed match types. Poorly conserved sites are also predicted as an option. The predicted targets are ranked either by predicted efficacy of targeting (Context ++ scores of the sites) or the probability of conserved targeting (P_{CT}) (Agarwal et al., 2015, Friedman et al., 2009). TargetScan also identifies sites with 3’ end compensation pairing (at positions 13-16) where mismatches in the seed site is present as well as centered sites (Friedman et al., 2009, Shin et al., 2010). The context++ score is generated by summing the contribution of several features including site type, supplementary pairing, local AU content, target site abundance, seed pairing stability and P_{CT} (Agarwal et al., 2015). This tool allows a target search by miRNA name or gene name without the requirement of a sequence input or the need for the adjustment of advanced settings, which makes it easy to use (Peterson et al., 2014).

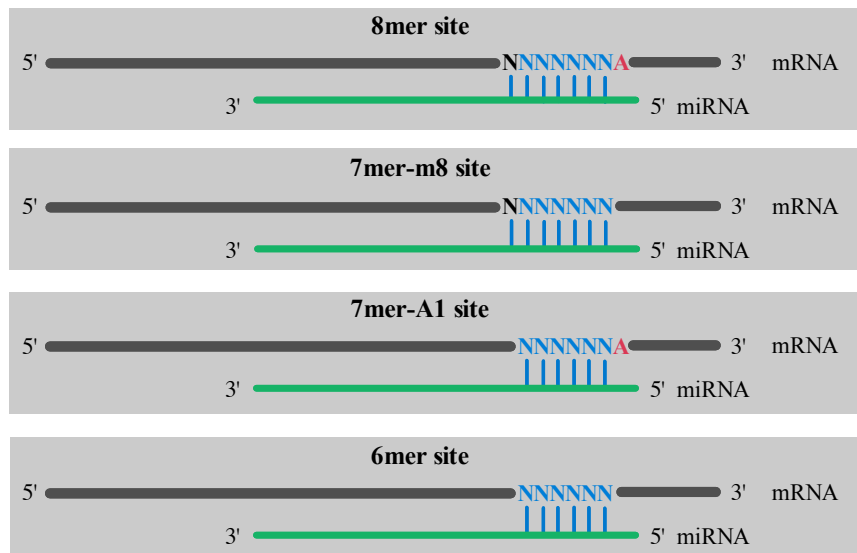


Figure 1.11: Canonical miRNA:mRNA interactions

Shown are the main four types of canonical miRNA interactions in target mRNAs (8mer, 7mer-m8, 7mer-A1 and 6mer) according to TargetScan (www.targets.van.org). mRNA is shown in grey and miRNA is shown in green. Seed binding sites of the mRNAs are highlighted in blue.

RNAhybrid calculates the free energy between the miRNA and mRNA duplex and finds the energetically most favourable hybridization sites using a dynamic programming algorithm (Rehmsmeier et al., 2004). This program allows the user to specify a miRNA sequence and a target mRNA sequence (in FASTA format) for target site prediction. It also offers advanced settings including specification of hits per target, helix constraints, maximal internal loop size, maximal bulge loop size and maximum free energy cutoff (Peterson et al., 2014). Therefore, these settings provide an option for the user to impose several restrictions to narrow down the predictions. In addition to evaluation of the thermodynamic properties of miRNA:mRNA interactions, target site abundance is also considered by RNAhybrid and a *p*-value is assigned for each interaction based on the number of binding sites within the 3' UTR sequence (Peterson et al., 2014). Even though these in silico programs may not

produce all experimentally derived possibilities, they can be a good starting point for miRNA analysis before experimental validation.

1.10.5 Regulation of drug metabolising enzymes (DMEs) by miRNAs

UGTs are involved in removing cancer causing chemicals as well as controlling steroid driven growth. With several UGTs, the correlation between mRNA and protein levels are very weak. Therefore, elucidating post-transcriptional regulatory mechanisms that affect UGT protein output and the enzymatic response to endogenous and exogenous compounds is important as that will ultimately determine their effect on cancer risk and progression. Moreover, an individual's response to environmental or endogenous cancer risk factors (e.g. excess steroid hormone action) as well as drug response and toxicity, may vary widely from one individual to another. Within the complex regulatory mechanisms of UGT expression and activity, miRNAs are considered likely to play an important role in this inter-individual variation.

Inter-individual variability in drug response and toxicity may be due genetic variants (including SNPs, copy number variants), environmental stimuli, individual's health condition, drug-drug interactions as well as epigenetic regulation of DME expression by methylation, post-translational histone modification or non-coding RNAs (Koturbash et al., 2015). Thus, inter-individual variability in DME expression is critical in terms of improving drug efficacy and reducing adverse outcomes. A number of studies have examined the link between genetic variation and DME expression and subsequent drug response. Genetic variations do not fully account for inter-individual variability in drug response. Therefore, investigating epigenetic

factors such as involvement of miRNAs in gene regulation could be a new avenue in assessing inter-individual variability in DME gene expression (Koturbash et al., 2015). To date, only a handful of studies have focused on miRNA-mediated regulation of DME expression (Dluzen and Lazarus, 2015). Regulation of both phase I and phase II DMEs by miRNAs have been reported (Table 1.6). Amongst these, the majority of studies have focused on the phase I DMEs, CYP450 enzymes, and only a few studies show miRNA mediated regulation of UGTs (Table 1.6 and recent study data on miRNAs involved in UGT2B15, UGT2B17 and UGT2B7 expression are discussed in Chapter 7). In addition, at the commencement of this study, there were no published studies on miRNA regulation on UGTs. Thus, it was considered of critical importance to investigate the functional effects of miRNAs on UGT expression and activity.

Table 1.6: List of miRNAs reported to regulate DME expression

Enzyme Family	Enzyme	miRNA	Reference
Cytochrome P450s (CYP450s)	CYP1A1	miR-892a	(Choi et al., 2012)
	CYP1A2	miR-132-5p	(Chen et al., 2017)
	CYP1B1	miR-27b	(Tsuchiya et al., 2006)
		miR-187-5p	(Mao et al., 2016)
		miR-200c	(Chang et al., 2015)
	CYP2C8	miR-103, miR-107	(Zhang et al., 2012a)
	CYP2C9	miR-130b, miR-128-3p	(Rieger et al., 2015) (Yu et al., 2015a)
	CYP2C19	miR-29a-3p	(Yu et al., 2015b)
	CYP2E1	miR-378	(Mohri et al., 2010)
		miR-570	(Nakano et al., 2015)
miR-212, miR-132		(Shukla et al., 2013)	
miR-552		(Miao et al., 2016)	
CYP2J2	Let-7b	(Chen et al., 2012)	
CYP3A4	miR-27b	(Pan et al., 2009)	

1.10 Project overview and Experimental Aims

Although the growth of a tissue or organ is finely regulated, a single cell, either a somatic or a stem cell, may begin to grow aberrantly to form a tumour. This aberrant growth is often initiated by a chemical carcinogen which mutates DNA, and is driven by an abnormal response to growth factors. For example, a breast tumour may be initiated by mutations induced by various genotoxic stressor including mutagenic estrogen metabolites, and then induced to proliferate by the excessive action of steroid hormones. Hence, mechanisms that eliminate chemical carcinogens and moderate steroid hormone action are important targets for therapeutic intervention in cancer. UGT-mediated glucuronidation is a major process for the inactivation and elimination of numerous cancer-causing chemicals and steroid hormones and also regulates multiple signaling processes mediated by chemical ligands (Mackenzie et al., 2005). The complement of UGTs within a cell, determines its capacity to resist chemical carcinogenesis and control steroid driven growth. In support of a role for UGTs in preventing cancer initiation and growth, several studies have shown that UGT expression is down-regulated in cancer cells compared to corresponding normal cells. Hence, an understanding of cellular mechanism that control UGT expression may provide new avenues for assessing cancer risk and controlling cancer growth.

The expression of a specific gene is generally controlled at both the transcriptional level to control mRNA synthesis and the post-transcriptional level to control mRNA stability. It appears that both the synthesis and stability of UGT mRNAs are tightly regulated in humans. Indeed, our studies on transcriptional regulation of UGTs over the last decade have identified a large number of transcription factors that govern

tissue-specific expression of human UGTs in the liver, gastrointestinal tract, breast and prostate. In contrast, the mechanisms controlling UGT mRNA stability at the post-transcriptional level remain poorly characterized. By binding to target sequences in mRNA 3'-untranslated regions (3'-UTRs), microRNAs represent one of the major factors that control mRNA stability. Preliminary bioinformatic analyses reveal that the 3'-UTRs of human UGTs have many target sequences for microRNAs. Furthermore, preliminary studies and recent evidence from the literature suggest that microRNAs may directly and/or indirectly impact UGT expression, especially in the cancer setting.

Characterization of microRNAs that regulate UGTs could have significant benefit by providing novel therapeutic targets to increase UGT expression, thereby reducing exposure to cancer-causing chemicals and excess steroid hormone action. This is a novel approach to preventing and/or controlling cancer.

Project Aims:

1. To define the microRNAs that control levels of the major steroid metabolizing enzymes UGT2B15 and UGT2B17 in commonly used human prostate cancer cell lines (e.g. LNCaP).
2. To define the microRNAs that control levels of UGT2B4 and UGT2B7 in commonly used human liver cancer cell lines (e.g. HepG2).
3. To evaluate the potential clinical relevance of findings in cell lines by examining the association between levels of UGT mRNAs and their regulatory microRNAs in clinical tissue samples.

CHAPTER 2

MATERIALS AND METHODS

2.1 Materials

2.1.1 Chemicals and Reagents

Table 2.1: Reagent used in experimental procedures

Reagent	Supplier
<i>Buffer Chemicals</i>	
Acetic acid	Ajax Finechem, Seven Hills, NSW
Acetonitrile	Merck KGaA, Darmstadt, Germany
Boric acid	Fluka Analytical (Honeywell), Morris Plains, NJ, USA
Bovine serum albumin (BSA) solution (100 mg/ml)	New England Biolabs, Beverly, MA
Bromophenol blue	Sigma Chemical Co, St Louis, MO
β -Mercaptoethanol (β -ME)	BDH Laboratory Supplies, Poole, UK
CaCl ₂ .2H ₂ O	Ajax Finechem, Seven Hills, NSW
Chloroform	Chem Supply, Gillman, SA, Australia
Dimethyl sulfoxide (DMSO)	Merck KGaA, Darmstadt, Germany
Dithiothreitol (DTT)	Sigma-Aldrich, St Louis, MO
Ethanol	Sigma-Aldrich, St Louis, MO
Ethylenediaminetetra-acetic acid, di-sodium salt (EDTA)	Biochemicals, Gympie, NSW, Australia
Glycerol	Amresco, Solon, OH

Glycine	Amresco, Solon, OH
HCl	VWR International, Radnor, PA, USA
Igepal CA-630	Sigma-Aldrich, St Louis, MO
Isopropanol	Chem-Supply, Gillman, SA, Australia
KCl	Amresco, Solon, OH
KH ₂ PO ₄	Amresco, Solon, OH
KOAc (Potassium Acetate)	Fison Scientific Equipemt, Glasgow, UK
Methanol	RCI Labscan, Bangkok, Thailand
MgCl ₂ .6H ₂ O	Amresco, Solon, OH
MnCl ₂ .4H ₂ O	Astral Scientific, Taren Point, NSW, Australia
Na ₂ HPO ₄	Ajax Finechem, Seven Hills, NSW
NaCl	Biochemicals, Gymea, NSW, Australia
Nonidet P-40	Fluka Analytical (Honeywell), Morris Plains, NJ, USA
1-Octanesulfonic acid	Sigma-Aldrich, St Louis, MO
Proteinase K	New England Biolabs, Beverly, MA
Sodium dodecyl sulphate (SDS)	A.G. Scientific, San Diego, CA, USA
Triethylamine (TEA)	Sigma-Aldrich, St Louis, MO
Tris[hydroxymethyl]aminomethane (Tris)	Astral Scientific, Taren Point, NSW, Australia
<i><u>Mammalian Tissue Culture</u></i>	
Dulbecco's modified Eagle's medium (DMEM)	Gibco/Life Technologies (Thermofisher Scientific), Grand Island, NY
Fetal bovine serum	Bovogen Biologicals Pty Ltd, VIC, Australia

5% dextran-coated charcoal-stripped fetal bovine serum	Sigma-Aldrich, St Louis, MO
MEM non-essential amino acids	Gibco/Life Technologies (Thermofisher Scientific), Grand Island, NY
MEM sodium pyruvate	Gibco/Life Technologies (Thermofisher Scientific), Grand Island, NY
Roswell Park Memorial Institute (RPMI) 1640 medium	Gibco/Life Technologies (Thermofisher Scientific), Grand Island, NY
Phenol-red free RPMI 1640 medium	Gibco/Life Technologies (Thermofisher Scientific), Grand Island, NY
Tissue culture flasks and plates	Nunc, Roskilde, Denmark
Trypsin-EDTA	Life Technologies (Thermofisher Scientific) Grand Island, NY
Trypan blue	Sigma-Aldrich, St Louis, MO
<i><u>Transfection and Reporter Gene Assays</u></i>	
Dual-luciferase™ Reporter Assay System	Promega, Madison, WI
Lipofectamine™ 2000	Invitrogen (Life Technologies/Thermofisher Scientific), Grand Island, NY
<i><u>Bacterial Culture</u></i>	
Agar	Amresco, Solon, OH
Ampicillin	Aspen Pharmacare, KwaZulu-Natal, South Africa
Kanamycin	Sigma-Aldrich, St Louis, MO
Luria Broth (LB) EZMix™	Amresco, Solon, OH
<i><u>DNA Detection, Purification and Site-directed mutagenesis</u></i>	
100bp/1kb DNA ladder	New England Biolabs

30% Acrylamide/Bis solution 19:1	Bio-Rad, Hercules, CA, USA
Agarose	Astral Scientific, Taren Point, NSW, Australia
Adenosine 5'-triphosphate (ATP)	Invitrogen, Grand Island, NY
Elution Buffer (EB)	Qiagen, Hilden, Germany
E. coli poly (A) polymerase and reaction buffer	New England Biolabs, Beverly, MA
Calf intestinal phosphatase (CIP)	New England Biolabs, Beverly, MA
Dpn I	New England Biolabs, Beverly, MA
Ethidium bromide	Amresco, Solon, OH
NEB Buffer 2	New England Biolabs, Beverly, MA
Restriction enzymes and buffers	New England Biolabs, Beverly, MA
QIAGEN Plasmid Midiprep kit	Qiagen, Hilden, Germany
QIAprep Spin Miniprep kit	Qiagen, Hilden, Germany
QIAquick Gel Extraction kit	Qiagen, Hilden, Germany
QIAquick PCR Purification kit	Qiagen, Hilden, Germany
Quick Ligation kit	New England Biolabs, Beverly, MA
Quick-Change site-directed mutagenesis kit	Stratagene, La Jolla, CA
Sybr Green	Promega, Madison, WI
 <i><u>RNA, miRNA Purification and cDNA Synthesis</u></i>	
Amplification grade DNase I and reaction buffer	Invitrogen (Life Technologies/Thermofisher Scientific)
miRNeasy mini kit	Qiagen, Hilden, Germany
RNeasy Midi kit	Qiagen, Hilden, Germany
RNeasy mini kit	Qiagen, Hilden, Germany

RNA ^{later} ® stabilisation solution	Ambion/Life Technologies Australia Pty Ltd, Melbourne, Victoria
SuperScript™ FirstStrand Synthesis System for RT-PCR	Invitrogen (Life Technologies/ThermoFisher Scientific)
RnaseOUT™ Recombinant Ribonuclease Inhibitor	Invitrogen (Life Technologies/ThermoFisher Scientific)
Taqman® miRNA reverse transcription kit	Applied Biosystems, USA
ThermoPol® buffer	New England Biolabs, Beverly, MA
Trizol	Life Technologies (Thermo Fisher Scientific, VIC, Australia)
 <i><u>Polymerase Chain Reaction (PCR) and qRT-PCR</u></i>	
Deoxynucleotide-triphosphate mix (dNTP)	Astral Scientific, Taren Point, NSW, Australia
Go-Taq qPCR master mix	Promega, Madison, WI
PfuTurbo™ DNA polymerase	Stratagene, La Jolla, CA
Phusion hot-start high fidelity DNA polymerase	New England Biolabs, Beverly, MA
QuantiTect SYBR Green PCR Kit	Qiagen, Hilden, Germany
Random hexamers	Invitrogen (ThermoFisher Scientific), Carlsbad, USA
Taq polymerase	New England Biolabs, Beverly, MA
TaqMan® MicroRNA Assays	Thermo Fisher Scientific, VIC, Australia
 <i><u>Western blot and Antibody construction</u></i>	
40% Acrylamide/Bis solution (29:1)	Bio-Rad, Hercules, CA, USA
Bio-Rad Protein Assay Reagent	Bio-Rad, Hercules, CA, USA
cComplete™ protease inhibitor cocktail	Roche Diagnostics, Mannheim, Germany
Horseshoe Peroxidase (HRP) substrate	ThermoFisher Scientific, MA, USA

SuperSignal® West Pico Chemiluminescent substrate	ThermoFisher Scientific, MA, USA
Skim milk powder	Fonterra Brands, NZ
Slide-A-Lyzer® dialysis cassettes	Pierce Biotechnology, MA, USA
N,N,N',N'-Tetramethyl-1-,2- diaminomethane (Temed)	Sigma-Aldrich, St Louis, MO
Trans-Blot nitrocellulose membrane (0.45 µm)	Bio-Rad, Hercules, CA, USA
Tween 20	Astral Scientific, Taren Point, NSW, Australia
Unstained protein standard (broad range 10-200kDa)	New England Biolabs, Beverly, MA
 <i><u>Glucuronidation Assay</u></i>	
¹⁴ C Testosterone	NEN, Boston, MA
¹⁴ C UDP-glucuronic acid	PerkinElmer, Boston, MA
17β-estradiol	Sigma-Aldrich, St Louis, MO
2-hydroxyestradiol	Sigma-Aldrich, St Louis, MO
4-hydroxyestradiol	Sigma-Aldrich, St Louis, MO
4-Methylumbelliferone (4-MU)	Sigma-Aldrich, St. Louis, MO
70% perchloric acid	Chem-Supply, Gillman, SA, Australia
8-hydroxyquinoline	Sigma-Aldrich, St Louis, MO
Androsterone	Sigma-Aldrich, St Louis, MO
Kodak storage phosphor screen	Amersham Biosciences, Piscataway, NJ
Morphine	GlaxoSmithKline, Brentford, UK
Morphine-3-glucuronide	Sigma-Aldrich, St Louis, MO
Morphine-6-glucuronide	Salford Ultrafine Chemicals , Manchester, UK
4-MU glucuronide	Sigma-Aldrich, St. Louis, MO

Phenolphthalein	Sigma-Aldrich, St Louis, MO
Silica gel thin layer chromatography plates	Uniplate; Analtech, Newark, DE
UDP-glucuronic acid	Sigma-Aldrich, St. Louis, MO
UGT2B15, UGT2B17, UGT2B4, UGT2B7, UGT2B10 supersomes	In Vitro Technologies, Noble Park North, VIC, Australia

2.1.2 General Buffers

1 x Phosphate buffered saline (PBS): 137 mM NaCl, 2.7 mM KCl, 10 mM Na₂HPO₄ and 2 mM KH₂PO₄, pH 7.4

1 x Tris-acetate EDTA electrophoresis buffer (TAE): 40 mM Tris pH 8, 20 mM acetic acid, 1 mM EDTA

0.5 x Tris-borate EDTA electrophoresis buffer (TBE): 40 mM Tris pH 8.3, 1 mM EDTA, 45 mM boric acid

1 x SDS-PAGE running buffer: 25 mM Tris pH 8.3, 192 mM glycine, 0.1% SDS

1 x SDS-PAGE transfer buffer: 25 mM Tris pH 8.3, 192 mM glycine, 20% methanol

1 x Tris-buffered saline (TBS): 50 mM Tris pH 7.4, 150 mM NaCl

1 x SDS loading sample buffer (Laemmli buffer): 50 mM Tris-HCL pH 6.8, 10% SDS, 30% glycerol, 5% β-mercaptoethanol, 0.02% bromophenol blue

2.1.3 Oligonucleotides

Oligonucleotides were purchased either from Sigma-Aldrich Australia (Merck KGaA, Darmstadt, Germany) or GeneWorks (Hindmarsh, SA, Australia). All primers were of standard purification quality (desalted), except the primers used for site directed mutagenesis, which were PAGE-purified. The sequences of all oligonucleotides are listed within the relevant Chapters.

2.1.4 miRNA mimics and Human Tissue Total RNA

Synthetic mimics corresponding to hsa-miR-376c, hsa-miR-331-5p, hsa-miR-222, hsa-miR-105, hsa-miR-525, hsa-miR-375-3p, hsa-miR-382, hsa-miR-376a, hsa-miR-376b, hsa-miR-125b, hsa-miR-21, hsa-miR-147, hsa-miR-1289, hsa-miR-3911, hsa-miR-409, hsa-miR-450b-5p, hsa-miR-489, hsa-miR-494, hsa-miR548x, hsa-miR-656, hsa-miR-3664-3p, hsa-miR-1266-5p, hsa-miR-4483, hsa-miR-4317, hsa-miR-216b-5p, hsa-miR-135a-5p, hsa-miR-410-3p, hsa-miR-489-3p, hsa-miR-4691-5p, hsa-miR-101-3p, hsa-miR-3160, hsa-miR-3679-5p and a negative control miRNA (miR-neg) were purchased from Shanghai GenePharma (Shanghai, China).

Synthetic miRNA inhibitor of hsa-miR-3664-3p and a negative control were purchased from Ambion/Applied Biosystems (Foster City, CA).

Total RNA samples from a panel of human tissues were purchased from Thermofisher (Ambion FirstChoice Human Total RNA Survey Panel, Waltham, MA).

The normal human liver tissues were previously reported (Hu et al., 2014a).

Three total RNA samples of normal prostate tissues were purchased from (AMBION, Dallas, TX) and Applied Biosystems (Foster City, CA) (RNA pooled from three Caucasian males; catalogue number AM6000), Life Technologies (Carlsbad, CA) (RNA from Caucasian male), and Clontech (Mountain View, CA) (RNA pooled from 12 Caucasian males), which were termed as prostate tissue 1, 2, and 3, respectively.

2.1.5 Eukaryotic and prokaryotic cell lines

The human prostate cancer cell lines LNCaP, VCaP, PC3 and Du145, the liver cancer cell lines HepG2 and HuH7, the human embryonic kidney HEK293T cell line and the breast cancer cell lines MCF7, ZR75, MDA-MB-453, MFM223 and T47D were purchased from American Type Culture Collection (ATCC; Manassas, Virginia, USA). The DH5 α *Escherichia coli* (*E. coli*) strain was also originally purchased from the ATCC.

2.1.6 Luciferase Reporter and Expression Vectors

Three luciferase expression vectors [pGL3-promoter vector, pGL3 basic vector and pRL-null (expressing *Renilla* luciferase) vector] were purchased from Promega (Madison, WI). The pET28a expression vector used to generate anti-UGT2B15/UGT2B17 antibody was purchased from Novagen (Madison, WI).

2.1.7 Antibodies

Anti-actin and anti-Calnexin antibodies were purchased from Sigma-Aldrich (St. Louis, MO). The horseradish peroxidase-conjugated donkey anti-rabbit secondary antibody was purchased from NeoMarkers (Fremont, CA). The anti-UGT2B7 antibody used in Western blotting was developed in our laboratory as previously

reported (Hu et al., 2014c). An antibody that recognized both UGT2B15 and UGT2B17 proteins was developed in this study as described in section 2.2.6.3.

2.2 Methods

2.2.1 Cell Culture

All tissue culture was performed using aseptic technique in class I biological safety cabinets to ensure sterility. Cells were maintained in a standard cell culture incubator at 37°C and 5% CO₂. The human prostate cancer cell lines, liver cancer cell lines and the HEK293T cell line were maintained in complete DMEM (Invitrogen) supplemented with 10% (v/v) fetal bovine serum with 1% (v/v) MEM non-essential amino acids (Gibco/ Life Technologies, Grand Island, NY). The VCaP cell line was maintained in DMEM with the above supplements and 1nM DHT. The human breast cancer cell lines were maintained in RPMI 1640 medium (Gibco/ Life Technologies, Grand Island, NY) supplemented with 5% (v/v) fetal bovine serum. Mycoplasma screening of all cell lines were performed by Mrs. Anne Rogers at regular intervals.

Sub-culturing of cells was carried out routinely at 80-90% confluence. Cells were firstly washed with PBS and incubated with 0.05% trypsin at 37°C to aid detachment from the culture flask and immediately diluted into flasks containing pre-warmed fresh medium. As HepG2 cells tend to form clumps after re-suspension with medium, the cells were passed through a sterile stepper syringe (Nichiryo, Tokyo, Japan) before re-plating. Incubation with trypsin was not needed for HEK293T cells as pipetting itself was adequate to detach the cells from the flasks. Cells were maintained in culture up to a maximum of 20 passages. Cells required for later use were preserved in liquid nitrogen by centrifuging for 5 minutes at 1,500 rpm and re-

suspending the pellets in fetal bovine serum containing 10% dimethylsulfoxide (DMSO). For re-culturing of frozen cell stocks, initially the cells were thawed in a 37°C water bath and then transferred into a 10 ml tube with fresh culture medium and centrifuged to remove DMSO. The cells were washed in 1 x PBS, resuspended in fresh culture medium and placed into a T75 flask.

2.2.2 Transient Transfection

All transfections were performed using Lipofectamine 2000 (Invitrogen) according to the manufacturer's protocol. For LNCaP transfections, firstly cells were plated in phenol-red free RPMI 1640 (Invitrogen, Carlsbad, CA) supplemented with 5% dextran-coated charcoal-stripped FBS. After 32h, cells were plated into 6-well plates at approximately 1×10^6 cells per well and grown overnight (16h) at 37°C in 5% CO₂ before transient transfection with miR mimics. Transfections were performed when cells reached 60 to 70% confluence. Synthetic miR mimics and miR-neg control were obtained from Shanghai GenePharma Pty Ltd (Shanghai, China). Cells were harvested 24h after transfection for RNA analysis and 72h after transfection for protein analysis and glucuronidation assays.

For transfections, DU145 cells were plated at approximately 2.5×10^4 cells per well, HEK293T at approximately 5×10^4 cell per well, HepG2, HuH7 and VCaP cells at approximately 1×10^5 cells per well in 96-well plates and grown at 37°C/5% CO₂ for 5hr before co-transfection with 100ng of each luciferase construct, 0.8ng of RL-null vector, 4.5 pmol miR-mimics or miR-neg (30nM final concentration) and 0.4µl of Lipofectamine2000 (Invitrogen) per well. LNCaP cells were plated in 96-well plates at approximately 1.25×10^5 cells per well, 16h before cotransfection with 100ng of plasmid, 0.8ng of pRL-null vector and 4.5 pmol miR-mimics or miR-neg (30nM

final concentration). Cells were grown at 37°C/5% CO₂, harvested 24h post transfection and subjected to luciferase assays.

2.2.3 Extraction of RNA

2.2.3.1 Extraction of RNA from monolayer cells

In the initial experiments, RNA was extracted by the RNeasy mini kit, according to the manufacturer's protocol. Cells which were grown in 6-well culture plates were harvested 24 hours post transfection for RNA, unless otherwise specified. Briefly, the cells were washed once with PBS and harvested in 350µL of RLT buffer containing 1% (v/v) β-mercaptoethanol. The lysate was transferred into 1.5ml microcentrifuge tube and homogenized using a syringe and a 21-gauge (G) needle (BD PrecisionGlide™ needle, Becton Dickinson Medical Pte Limited, Singapore). An equal amount of 70% ethanol was added to the lysate before transferring to a spin column placed in a 2 ml collection tube. The tubes were centrifuged at 10000 x g for 15 seconds and the flow through was discarded. A 700 µl aliquot of buffer RW1 was added and the sample centrifuged at 10000 x g for a further 15 seconds. The spin column was washed twice with 500 µl of Buffer RPE and centrifuged for 15 seconds and then a further 2 minutes. RNA was eluted from the spin column by adding 30 µl RNase free H₂O and centrifuging for 1 minute at 10,000 rpm. All RNA samples were stored at -20°C .

2.2.3.2 Extraction of total RNA, including small RNAs from monolayer cells

In the initial experiments, total RNA was extracted using the miRNeasy mini kit (QIAGEN, Clifton Hill, VIC, Australia) according to the manufacturer's protocol. Cells were grown in 6-well Nunc™ Cell-Culture Treated Multidishes (Thermo Scientific, Massachusetts, United States) and 700 µl of QIAzol lysis reagent was

added directly to the each well after aspiration of culture medium. The culture dish was then placed on a rocker for 5 minutes at room temperature and the lysate was mixed by pipetting and transferred into a microcentrifuge tube. A 140 μ l aliquot of chloroform was added to the tube and the contents mixed vigorously for 15 seconds and incubated at room temperature for 2 minutes. The sample was then centrifuged at 12000 x g for 15 minutes at 4°C and the upper aqueous phase was transferred into a new microcentrifuge tube, followed by the addition of 525 μ l of 100% ethanol. After mixing thoroughly, the sample was transferred into an RNeasy mini spin column in a collection tube and centrifuged at 8000 x g for 15 seconds at room temperature. The flow-through was discarded and the column was washed twice with 500 μ l of buffer RPE (centrifuged at 8000 x g for 15 seconds and 2 minutes respectively). The column was then transferred into a new 1.5 ml tube and 45 μ l of RNase-free water was added directly onto the column which was then centrifuged at 8000 x g for 1 minute to elute the total RNA.

In later experimental studies, TRIzol reagent (Life Technologies, Victoria, Australia) was used to extract total RNA from monolayer cells, according to the manufacturer's protocol. Briefly, the cells were washed with PBS and harvested in 1ml TRIzol solution. The cell lysates were then homogenized by pipetting and transferred into 1.5ml microcentrifuge tubes. An aliquot of 200 μ l of chloroform was added to each sample. After shaking vigorously for 15s and a 2-minute incubation at room temperature, samples were centrifuged at 12,000 x g for 15 minutes at 4°C. The RNA containing aqueous phase was removed and placed into a new sterile tube. To precipitate the RNA, 0.5 mL of 100% isopropanol was added and the sample incubated for 10 minutes at room temperature. The samples were centrifuged at

12,000 x g for 10 minutes at 4°C and the RNA pellet was washed with 1 ml of 75% ethanol and centrifuged for a further 5 minutes. The pellet was then air dried and resuspended in 30 µl of RNase-free H₂O and incubated in a heat block for 10 minutes at 55–60°C. All RNA samples were stored at -20°C.

2.2.3.2 Extraction of total RNA from human tissues

Human liver tissues from Caucasian donors were obtained from the liver bank of the Department of Clinical Pharmacology of Flinders Medical Centre, Flinders University of South Australia, Australia. Genomic DNA and human liver microsomes were prepared from the liver tissues as described previously (Bhasker et al., 2000). Approval for the use of human liver tissues for pharmacogenetic and pharmacokinetic studies was granted by Flinders Medical Centre Research Ethics Committee. A hundred milligrams of each tissue (≤ 0.5 cm in any single dimension) was excised and placed in 5-10 volumes of RNAlater® Stabilization Solution (AMBION, Life Technologies Australia Pty Ltd, Melbourne, Victoria) and kept on ice for up to 2 hours for the solution to penetrate the tissue. The excess RNAlater solution was removed and the tissue pieces were further sliced on a petri dish into smaller pieces using a sterile blade and transferred into a 1.5 ml microcentrifuge tube. Hundred microliters of TRIzol reagent were added to the tissue pieces and homogenized using a UV sterilized micro-pestle. A final volume of 1 ml TRIzol reagent was added to each sample and RNA was extracted from these samples using the same protocol as described above for monolayer cells.

2.2.3 Quantification of mRNA

2.2.3.1 Reverse transcription polymerase chain reaction (RT-PCR) of mRNA

RNA (2 µg) extracted either by RNeasy mini kit, miRNeasy mini kit or TRIzol reagent was first treated with one unit amplification grade DNase I (Invitrogen) in 1 x DNase I reaction buffer containing 20 mM Tris-HCl (pH 8.4), 2 mM MgCl₂ and 50 mM KCl (Invitrogen) for 15 minutes at room temperature. DNase I was inactivated by the addition of EDTA to a final concentration of 2.5 mM and incubating at 65°C for 15 minutes. DNase I treated RNA was transcribed into cDNA using the SuperScript III First-Strand Synthesis System (Invitrogen). One microgram of DNase I treated RNA was added to a 10 µl reaction mixture containing 1 mM dNTPs and 5 ng/µl random hexamers and incubated at 65°C for 5 minutes. After cooling on ice, the reaction volume was brought up to 20 µl by the addition of 1 x First-Strand buffer (containing 50 mM Tris-HCl (pH 8.3), 75 mM KCl, 3 mM MgCl₂), 5 mM DTT, RNaseOUT™ Recombinant Ribonuclease Inhibitor (40 units/ µl) and 0.25 µl SuperScript® III Reverse Transcriptase (50 units). The reaction mixture was incubated at 25°C for 10 minutes, then at 50°C for 50 minutes for the reverse-transcription of RNA. The reaction was then inactivated by heating at 75°C for 15 minutes. Synthesized cDNA was diluted up to 100 µl in nuclease-free water and stored at -20°C.

2.2.3.2 Quantification of mRNA by quantitative real-time polymerase chain reaction (qPCR)

UGT mRNA, GAPDH mRNA, β-actin mRNA and 18S ribosomal RNA (rRNA) levels present in RNA extracted from the human monolayer cells, human prostate tissues or human liver tissues were quantified using real-time qPCR following reverse transcription. Real-time qPCR was performed using a Corbett Rotor-Gene

3000 (Corbett Research, NSW, Australia) in a 20 μ l reaction mixture containing 3 μ l of cDNA (20-40 ng), 10 μ l of 2 x GoTaq® qPCR Master Mix (Promega, Madison, WI), and a pair of mRNA-specific forward and reverse primers (at a final concentration of 500 nM each). The details of the specific primers used are listed in the corresponding Chapters. The PCR reaction was initially incubated at 95°C for 15 minutes (activation step), followed by 40 cycles of 95°C for 10 seconds (denaturation phase), 58°C for 20 seconds (annealing phase), and 72°C for 25 seconds (extension phase); and a melt curve was produced by a temperature ramp from 72°C and 95°C with 5 second, 1°C steps. Data was acquired during the 72°C extension phase of each cycle and analysed using the Rotor-Gene 6 software (Corbett Life Science) with $2^{-\Delta\Delta CT}$ method (Livak and Schmittgen, 2001) unless otherwise specified.

2.2.4 Reverse Transcription and quantification of mature and primary miRNAs

2.2.4.1 Reverse Transcription of mature miRNA

Reverse transcription PCR was performed using either a BioRad iCycler (BioRad) or a PCR Palm Cycler (Corbett Research). In the initial experiments, Taqman® microRNA reverse transcription kit (Applied Biosystems, USA) was used to produce cDNA for quantification of miRNA according to manufacturer's protocol. First, 10 ng of RNA in a volume of 5 μ l was added to a master mix containing 0.15 μ l of dNTP mix, 1 μ l of Multiscribe™ RT enzyme (50U/ μ l), 1.5 μ l of 10x RT buffer, 0.19 μ l RNase inhibitor (20U/ μ l), 4.16 μ l of nuclease free water. Second, 3 μ l of the specific RT primers for each microRNA were added to the appropriate tubes bringing the final volume to 15 μ l and the reaction mixture then incubated on ice for 5 minutes [The details of the specific primers used are listed in the corresponding

Chapters and details on primer designing is explained in (Balcells et al., 2011)]. The PCR cycling parameters were: 16°C for 30 minutes; 42°C for 30 minutes and 85°C for 5 minutes.

Reverse transcription of miRNAs, U6 small nuclear-2 RNA (termed RNU6-2), U44, U48 was performed as recently reported by Balcells et al. (2011) as well. Briefly, 1 µg of total RNA containing miRNA was treated with DNase I (one unit) in 1 x DNase I reaction buffer for 15 minutes at room temperature. EDTA to 2.5 mM was added to the reaction and heated at 65°C for 15 minutes for the inactivation of DNase I. Three hundred micrograms of DNase I treated total RNA was then polyadenylated using poly(A) polymerase (New England Biolabs, Ipswich, MA) to generate a poly(A) tail at the 3'-termini of the miRNAs. The reaction consisted of 300 ng of RNA, 1 µl of 10 x poly(A) polymerase buffer, 25 µM of ATP, 0.25 µl of RNaseOUT and 0.5 µl of 1:5 diluted *E.coli* poly (A) polymerase in a total volume of 10 µl which was incubated at 37°C for 30 minutes. Polyadenylated RNA was then subjected to reverse transcription PCR to synthesise cDNA. Firstly, 1 µl of 10 mM dNTP (consisting of dATP, dCTP, dGTP and dTTP) and 1 µl of Oligo Universal Primer (GeneWorks) were added to the polyadenylated RNA sample and incubated at 65°C for 5 minutes. The reaction volume was increased up to 20 µl by the addition of 1 x First-Strand buffer (Invitrogen), 5 mM DTT, RNaseOUT™ Recombinant Ribonuclease Inhibitor (40 units/ µl) and 0.25 µl SuperScript® III Reverse Transcriptase (50 units). The reaction mixture was incubated at 25°C for 10 minutes, then at 50°C for 50 minutes, followed by 75°C for 15 minutes. Synthesized cDNA was diluted up to 100 µl in nuclease-free water and stored at -20°C.

2.2.4.2 Quantitative RT-PCR of mature miRNA

Real-time qPCR for the quantification of cDNA synthesized from polyadenylated RNA, was performed using a Corbett Rotor-Gene 3000 (Corbett Research, Mortlake, NSW, Australia). The 15 µl PCR reaction mixture contained 2 µl of cDNA (~40 ng), 7.5 µl of 2 x GoTaq® qPCR Master Mix, and a pair of miRNA-specific forward and reverse primers (at a final concentration of 600 nM each, the miRNA-specific primers used are listed in corresponding Chapters.). The primers were designed according to the method published by (Balcells et al., 2011). The PCR reaction was initially incubated at 95°C for 10 minutes, followed by 40 cycles of 95°C for 10 seconds and 60°C for 40 seconds. At the end of the 40th cycle, the temperature was ramped from 60 to 94°C to produce a melting curve. The expression level of miRNA was analysed using the Rotor-Gene 6 software (Corbett Life Science) and presented relative to that (set as a value of 1) of a housekeeping miRNA using the $2^{-\Delta\Delta CT}$ method (Livak and Schmittgen, 2001).

2.2.4.3 Quantitative RT-PCR of primary miRNA

Primary miRNA (termed pri-miR) 376c and RNU6-2 was quantified in 18 human prostate tissue cDNA [(which were kindly provided to us by Professor Wayne Tilley (Adelaide University, South Australia)] by performing quantitative real-time PCR using a RotorGene 3000 (Corbett Research). The reaction mixture contained a total of 20 µl in volume, with 3 µl of cDNA sample, 10 µl of GoTaqPCR master mix and pri-miR-specific forward and reverse primers at a final concentration of 500 nM each (The pri-miR-specific primers used for qRT-PCR are listed in Chapter 3). The primers were designed according to the method published by (Balcells et al., 2011). The PCR cycling conditions were; incubation at 95°C for 5 minutes, followed by 40

cycles of 95°C for 10 seconds, 57°C for 15 seconds, and 72°C for 20 seconds. At the end of the 40th cycle, the temperature was ramped from 55 to 95°C to produce a melting curve. The expression level of pri- miR-376c was presented relative to that of RNU6-2 using the $2^{-\Delta\Delta CT}$ method as mentioned above.

2.2.5 Site directed mutagenesis

2.2.5.1 Polyacrylamide Gel (PAGE) purification of oligonucleotides for site directed mutagenesis

Some oligonucleotides used for site directed mutagenesis were only subjected to the standard desalting purification procedure when purchased. These oligonucleotides were PAGE-purified in our laboratory before used in mutagenesis studies. Complementary F and R oligonucleotides containing the mutation were dissolved in nuclease free water at 100 μ M concentration and then annealed together in a 50 μ l reaction containing 20 μ l of each oligonucleotide and 1x NEBuffer 2 (10 mM Tris-HCl, 50 mM NaCl, 10 mM MgCl₂ and 1 mM DTT, pH 7.9) by heating for 5 mins at 99°C and slow cooling for 2 hours back to room temperature. After adding SYBR Green 1:50000 dilution, the sample was electrophoresed on a 10% Acrylamide/Bis (19:1) gel for 40mins at 80V in 0.5 x TBE buffer. The DNA fragments were excised from the gel under UV and crushed by passing the gel through a sterile tube containing holes created by a 21-G needle by centrifugation. DNA was then eluted in 400 μ l 1x NEB buffer 2 by rotation overnight at 4°C. The DNA was precipitated at -20°C for 20 minutes using two volumes of cold 100% ethanol. The DNA was then pelleted by centrifuging at 13,000 rpm for 15 minutes. The DNA pellet was washed with 1 ml 70% ethanol and further centrifuged for 5mins, air dried and resuspended in 45 μ l of EB buffer.

2.2.5.2 DNA Site directed mutagenesis

Mutations or deletions for a single nucleotide or multiple nucleotides in pGL3 luciferase construct containing 3'UTRs of UGTs were generated via PCR using the QuikChange™ site directed mutagenesis kit (Stratagene, La Jolla, CA). The overlapping mutagenic primers were designed according to the manufacturer's protocol and PAGE-purified as mentioned above. Briefly, the primer pairs were complementary and contained the desired mutation or deletion in the middle with 10-15 bases of correct sequence on both sides. The primers were 35-45 bases in length and possessed melting temperatures of $\geq 78^{\circ}\text{C}$, a minimum GC content of 40% and one or more C or G terminating residues. The complete list of primers are provided in the relevant Chapters. Briefly, the 50 μl PCR reaction contained 5 μl of 10x *PfuTurbo* reaction buffer, 125 ng of each primer, 1 μl of *PfuTurbo*™ DNA polymerase (2.5 Units/ μl), 1 μl of 10mM dNTP and 50 ng of wild-type luciferase construct. PCR amplification conditions were 95°C for 3 minutes initially followed by 18 cycles of 95°C for 30 seconds, 55°C for 1 minute, 68°C for 13 minutes and a final 15 minutes at 68°C . Seven microliters of the resultant amplicons were analysed using Agarose gel electrophoresis and 10 Units of *DpnI* were added to the remaining PCR product and incubated at 37°C for 1 hour to eliminate the wildtype luciferase constructs seeded as PCR templates as described above. For transformation, 1.5 μl of the *Dpn I*-digested PCR product was added to 50 μl competent DH5 α *E. coli* cells as described in Section 2.2.10 The mutated constructs were confirmed by DNA sequencing.

2.2.6 Western Blotting

2.2.6.1 Preparation of lysates

Mammalian cells in 6-well plates were scraped off in 800 μ l of cold 1 x PBS in two successive washes and cell pellets were collected by centrifugation at 6000 rpm for 5 minutes. The pellets were resuspended in 80 μ l (LNCaP, 160 μ l for HepG2) of cold RIPA buffer (Radioimmunoprecipitation assay buffer) containing 50 mM Tris-HCl, pH 8.0, 1% Igepal CA-630, 150 mM sodium chloride, 0.5% sodium deoxycholate, 0.1% sodium dodecyl sulphate and 1 x cOmplete™ protease inhibitor cocktail. The cells were homogenized to facilitate lysis by passing through a BD Ultra-Fine 1ml insulin syringe 10 times on ice, and the supernatant containing the proteins was separated from the remaining cell debris by centrifugation for 10 minutes at 10,000 rpm at 4°C. The protein concentrations of the lysates were determined using the Bradford Protein Assay (Bio-Rad, Hercules, CA) as per manufacturer's instructions, before storage at -80°C. Briefly, 2 μ l of lysate was added to 100 μ l 1 x BioRad Protein Assay reagent (1:50 dilution of lysate), incubated for 30 minutes and the absorbance was measured at 595 nm in a plate reader (DTX 880 Multimode Detector; Beckman Coulter). Protein concentration was estimated by comparison to a BSA standard curve of known concentrations (0, 0.1, 0.2, 0.4, 0.6 and 1 mg/ml).

2.2.6.2 Polyacrylamide gel electrophoresis (PAGE)

Aliquots of each lysate (25 μ g, unless otherwise specified) or 5 μ g recombinant human UGT2B15, UGT2B17, UGT2B4, UGT2B7 and UGT2B10 proteins expressed in baculovirus-infected insect cells (Supersomes from In vitro Technologies, VIC, Australia) were heated at 95°C for 5 minutes with 1 x SDS-PAGE sample loading buffer. Proteins (of the sample lysates) along with unstained protein standards (broad range, 10-200kDa, NEB) which were used as size markers, were separated by

electrophoresis on a SDS-PAGE gel (4% stacking gel, 10% separation gel) at room temperature: at 80 V through stacking gel for 20 minutes and 150 V through separating gel for 60 – 80 minutes (until the tracking gel reach the bottom), using Mini-Protean II Cell equipment (BioRad). After separation, proteins were transferred on to Trans-blot nitrocellulose membrane (Bio-Rad) in a Mini Trans-Blot Cell apparatus at 25 V overnight at 4°C. The membrane was washed in 1 x TBST (TBS + 0.2% Tween-20) and incubated in blocking buffer containing 1 x TBST containing 5% (w/v) skim milk powder, for 90 minutes at room temperature. After rinsing the blocking buffer with 1 x TBST, the membrane was first probed with the primary antibody (1:1000 dilution unless otherwise specified, anti-UGT2B15/UGT2B17 antibody in 1:2500 dilution) in 1% blocking buffer (unless otherwise specified) for 2 hours, washed 3 times with 1 x TBST for 10 minutes each, followed by the incubation with horseradish peroxidase-conjugated donkey anti-rabbit secondary antibody (NeoMarkers) in 1:2000 dilution in 1% blocking buffer for 90 minutes. After probing, the membrane was washed 3 times with 1 x TBST for 10 minutes per wash. All probing steps were performed at room temperature. Immuno-signals were visualized with SuperSignal®West Pico Chemiluminescent substrate (Thermo Scientific) and HRP substrate (1:50,000 dilution, Thermo Scientific) using an ImageQuant LAS4000 luminescent image analyzer (GE Healthcare Life Sciences, Piscataway, NJ). For normalizing the quantity of proteins loaded in each well, membranes were re-probed either with an anti-actin antibody (Sigma-Aldrich) or anti-calnexin antibody (Sigma-Aldrich) and re-imaged. Band intensity was quantified using Multi Gauge Version 3.0 image software (FUJIFILM, Tokyo, Japan).

2.2.6.3 Development of an antibody specific for UGT2B15 and UGT2B17, and Western Blotting

The UGT2B17 coding sequence between amino acids 84 and 167 was amplified from LNCaP cDNA using the forward, TAGAGGATCCACTAAAAATGATTTGGAAGATT and reverse, GGTCCTCGAGTATGTTAAGTAGCTCAGCCA primers and Phusion hot-start high-fidelity DNA polymerase, and subsequently cloned into the BamHI and XhoI sites of the pET28a expression vector (Novagen, Madison, WI). The corresponding peptide attached with a 6-histidine tag at the carboxyl terminus was then generated following transformation of the resultant vector into *Escherichia coli* BL21 (DE3) cells. Rabbits were immunized with this peptide and an antibody was obtained through the antibody development facilities of South Australian Health and Medical Research Institute (Gilles Plains, Adelaide, Australia).

The antibody was tested for cross-reactivity with recombinant human UGT2B15, UGT2B17, UGT2B4, UGT2B7 and UGT2B10 proteins expressed in baculovirus-infected insect cells (Supersomes from In vitro Technologies, VIC, Australia). Aliquots of 5 µg of the aforementioned recombinant human proteins were subjected to SDS-polyacrylamide gel electrophoresis on 12% acrylamide gels followed by transfer onto nitrocellulose membranes. Membranes were first probed with the constructed antibody as described above, followed by the horseradish peroxidase-conjugated donkey anti-rabbit antibody. Immuno-signals were visualized as mentioned above (in section 2.2.6.2). As shown in Figure. 2.1, this antibody recognized both UGT2B15 and UGT2B17 (the latter more robustly) but did not cross-react with three other UGT2B enzymes, (i.e. 2B4, 2B7, and 2B10) and hence is designated, anti-UGT2B15/2B17 antibody.

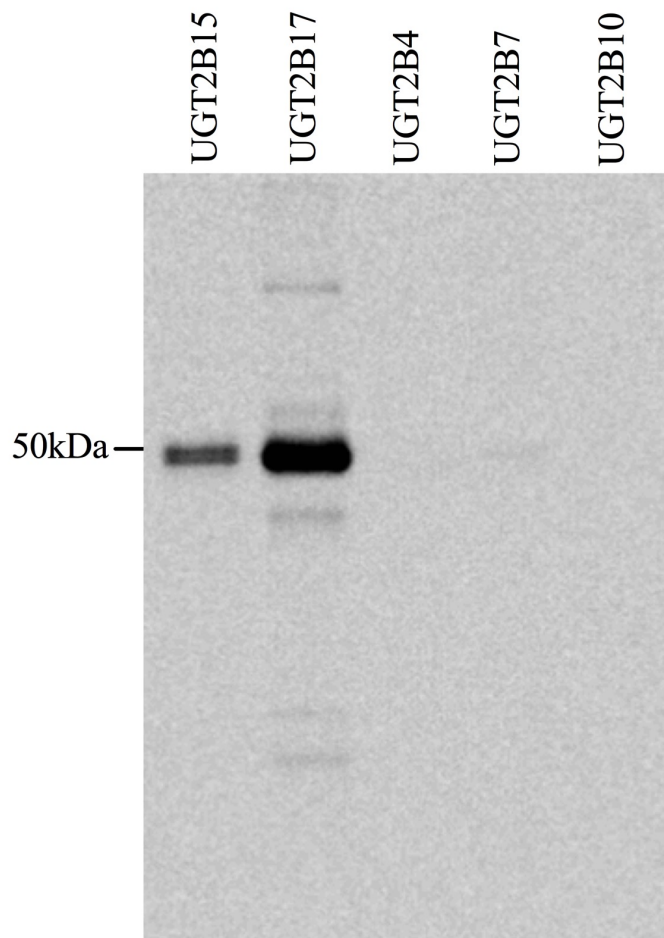


Figure 2.1: Specificity of the UGT2B15/2B17 antibody

Recombinant UGT supersomes containing UGT2B4, UGT2B7, UGT2B10, UGT2B15, and UGT2B17 (5ug each) were subjected to Western Blotting using the anti-UGT2B15/2B17 antibody. Shown are the immune-signals of a representative experiment.

2.2.7 Bacterial culture

All bacteria were grown at 37°C under appropriate antibiotic selection (100 µg/ml ampicillin or 30 µg/ml kanamycin) either in LB liquid broth with vigorous shaking (225 rpm) in an Innova 4330 Refrigerated Incubator Shaker (New Brunswick Scientific) or on LB plates solidified with 15 g/L agar in a Shimadem (Scientific

Equipment Manufacturers) incubator. Bacterial stocks for long term storage were prepared in LB broth containing 17.5% glycerol and kept at -80°C.

2.2.8 Restriction digests

All restriction enzymes used in this study were purchased from New England Biolabs and the digests were performed according to manufacturer's recommendations. Digests were performed in a total of 50 µl reaction volume with 1-3 µg vector/insert DNA (including PCR products), 2 µl restriction enzyme (20Units), 1x appropriate NEB reaction buffer in nuclease-free water. DNA was digested at 37°C for 1 hour, unless otherwise stated. The digested DNA fragments were subsequently purified either using the QIAquick PCR purification kit or by gel extraction kit and eluted in EB buffer (Qiagen).

To prevent self-ligation, vectors that have been digested with a single restriction enzyme were treated with calf intestinal alkaline phosphatase (CIP) in a 50 µl total reaction volume containing 10-15 Units of CIP and 1xCutSmart buffer (NEB) at 37°C for 1 hour and proceeded with ligation.

2.2.9 Ligations and transformations

Ligations were conducted with NEB Quick ligation kit according to the manufacturer's instructions. Briefly, 20 µl-reactions were prepared with 20-100 ng purified and digested plasmid DNA, a 3 to 10-fold molar excess of insert DNA (digested PCR product), 1 µl Quick DNA ligase and 1xQuick Ligase buffer (66 mM Tris-HCl, 10 mM MgCl₂, 1 mM DTT, 1 mM ATP and 7.5% polyethylene glycol 6000, pH 7.6) and incubated for 10 minutes at 25°C (room temperature). The

reactions were chilled on ice before use in transformation (the ligation products can be stored at -20°C until ready for transformation).

Transformations were performed using chemically competent DH5α *E. coli* cells (competent cell preparation is described in section 2.2.10). The competent cells were initially thawed gently on ice for approximately 10 minutes before the addition of 2 μl of ligation product. The cells were then mixed gently and incubated on ice for 30 minutes, followed by a heat shock of 42°C incubation for 45 seconds to facilitate the uptake of ligated DNA. Subsequently, the cells were immediately placed on ice for a further 2 minutes. One milliliter of LB (without any antibiotic) was added to the shocked cells and placed in a shaking incubator at 37°C for 1 hour to allow for the cells to recover, before being plated on LB agar plates with appropriate antibiotic (approximately 150 μl of recovered cells). Agar plates were then incubated at 37°C overnight (>16h). Colonies were then screened for appropriate insert by PCR followed by gel-electrophoresis and restriction digest and sequencing of miniprep DNA.

2.2.10 Preparation of competent cells

To prepare competent cells, DH5α *E. coli* was inoculated in 5 ml of LB (without antibiotics) and grown overnight in a 37°C shaking incubator. 1 ml of the DH5α overnight culture was then inoculated in to 100 ml of LB broth and incubated at 37°C until the culture density reached an OD₅₉₅ of 0.25-0.3 in a shaking incubator. The culture was then pelleted by centrifugation at 3000 x g for 10 minutes at 4°C, using a Sigma 4K15 centrifuge (Quantum Scientific). The pellet was resuspended in 32 mL of ice-cold CCMB80 buffer (10 mM KOAc pH 7, 80 mM CaCl₂·2H₂O, 20 mM MnCl₂·4H₂O, 10 mM MgCl₂·6H₂O, 10% glycerol, pH 6.4) and left on ice for 20

minutes. After a second centrifugation of 10 minutes, the cell pellets were resuspended in 4ml of ice-cold CCMB80 buffer, aliquoted (50 μ l, 100 μ l and 200 μ l) and stored at -80°C.

2.2.11 Plasmid preparations

QIAprep Spin Miniprep Kit (QIAGEN) was used to isolate the plasmid DNA from small scale bacterial cultures (1-5 ml) according to the manufacturer's instructions. Briefly, the bacterial culture was pelleted by centrifugation at 5100 xg for 10 minutes at 4°C in a Sigma 4K15 centrifuge and resuspended in 250 μ l Buffer P1. The cells were then lysed with 250 μ l Buffer P2, and all genomic DNA and bacterial proteins present were precipitated by addition of 350 μ l Buffer N3. The precipitate was pelleted by centrifugation at 13,000 rpm for 10 minutes in a microcentrifuge and the supernatant was applied onto a QIAprep spin column and centrifuges for 30-60s. The column was then washed with buffer 0.75ml of Buffer PE and centrifuged further for 1 min to remove any residual wash buffer. Finally, the plasmid DNA bound to the column was eluted in 40 μ l Buffer EB by brief centrifugation for 1 minute.

QIAGEN Plasmid Midiprep kit was used for isolation of plasmid DNA from large scale bacterial cultures, according to the manufacturer's instructions. Briefly, 50 ml overnight bacterial cultures were pelleted by centrifugation at 5100 x g for 15 minutes at 4°C in a Sigma 4K15 centrifuge, resuspended in 4 ml Buffer P1 and incubated for 5 minutes at room temperature for lysis to occur. Pre-chilled Buffer P3 (4 ml) was added to the bacterial lysate, mixed vigorously and incubated on ice for 15 minutes. The precipitate was pelleted by centrifugation at 20000 x g for 30 minutes at 4°C in a JM20 rotor/Beckman J2-21M/E ultracentrifuge or at 5100 x g for 40 minutes at 4°C in a Sigma 4K15 centrifuge. The supernatant containing the

plasmid DNA was applied to a QIAGEN-tip 100 (QIAGEN) pre-equilibrated with 4 ml Buffer QBT and allow to enter the resin by gravity flow. The QIAGEN-tip was washed twice with 10 ml Buffer QC and plasmid DNA was eluted in 5 ml Buffer QF. 3.5 ml Isopropyl alcohol was added to precipitate the eluted DNA, and centrifugated at 5100g for 30 minutes at 4⁰C. The pelleted DNA was carefully washed with 2 ml 70% ethanol, centrifuged further for 15 minutes at 4⁰C and air dried for 1 hour before resuspension in 300 µl Buffer EB.

2.2.12 Quantification of RNA/ DNA

The concentration and purity of DNA and RNA samples were measured by spectrophotometry using a GeneQuant II (Pharmacia Biotech (GE Healthcare), Buckinghamshire, England). The samples were prepared by 1:50 dilution of DNA or RNA in nuclease free water to a total volume of 100 µl and optical absorbance was measured at 260 nm and DNA/RNA to protein ration (purity) at 260 nm versus 280 nm. Absorbance readings were given as 1 unit = 50 µg/ml double strand DNA or 40 µg/ml single strand RNA. Therefore, the concentration of DNA was calculated at Absorbance x 50 x 50 (dilution factor), and for Absorbance x 40 x 50 for RNA.

2.2.13 Agarose Gel electrophoresis

To analyse the purity and size of DNA fragments and plasmids from culture preparations, PCR amplification or restriction digests, agarose gel electrophoresis was used. Agarose gels (1.5%) were made in TAE buffer and ethidium bromide was added to a final concentration of 0.01 µg/ml. The samples were diluted in dye containing glycerol prior to loading them on to the gel along with 100 bp or 1 kb standard DNA ladders (NEB) which were used as size markers. Electrophoresis was then performed at 80-120V in a Bio-Rad Mini-Sub Gel GT electrophoresis system

and the gel was visualized in a Gene Genius Bio Imaging system (SynGene, Cambridge, England) using GeneSnap version 6.04 software (SynGene).

2.2.14 DNA Purification

QIAquick PCR purification kit was used to purify all DNA products generated either by PCR or restriction digests according to the manufacturer's instructions.

2.2.15 Sequencing

Following either a miniprep or midiprep, DNA was sequenced for confirmation of cloning. All sequencing was performed by the DNA Sequencing Core Facility (Department of Haematology and Genetic Pathology, Flinders University) using Big Dye Terminator Cycle Sequencing Version 3.1 chemistry and an ABI 3130 Genetic Analyser sequencer (both from Applied Biosystems). Sequencing data was analysed using Vector NTi software (Informax, North Bethesda, MD).

2.2.16 Luciferase Assays

Cells were plated in 96-well plates and transfected in triplicate with the internal control pRL-null vector (5 ng in each well), a luciferase reporter (100 ng in each well), and mimics of one miRNA at 30 nM, as indicated in the relevant result Chapters. 24 hours post-transfection cells were washed with 1xPBS (137 mM NaCl, 2.7 mM KCl, 10 mM Na₂HPO₄, 2 mM KH₂PO₄) and lysed in 30 µl in 1x lysis buffer (Promega) on a rocking platform for 15 minutes. Lysates were assayed for firefly (promoter) and Renilla (internal control) luciferase activities using 20 µl of lysate with the Dual-Luciferase Reporter Assay System and a Packard TopCount luminescence and scintillation counter (PerkinElmer Life and Analytical Sciences, Waltham, MA) as per the manufacturers' instructions. Firefly luciferase activity was

first normalized to Renilla activity and the reporter activity was then presented relative to that of the control pGL3-promoter vector (set at a value of 100%).

2.2.17 Glucuronidation Assays

2.2.17.1 4-Methylumbelliferone Glucuronidation Assays

LNCaP cells were serum starved for 48h and then transfected with miRNA mimics (miR-331-5p or miR-neg) at 30 nM. Whole cell lysates were prepared after 72h post-transfection and protein concentrations of the lysates were determined. Two-hundred μ l reactions of each sample containing 100 mM potassium phosphate pH 7.4, 4 mM MgCl₂, 400 μ M 4-MU, 225 μ g lysate and 5 mM UDP-glucuronic acid were incubated for 2 hours at 37°C in a shaking water bath. After the addition of 2 μ l of 70% perchloric acid, samples were kept on ice for a minimum of 10 minutes and centrifuged at 5000g for 10 minutes at 4°C. Sixty μ l of the supernatant fraction was analysed by high-performance liquid chromatography using an Agilent 1100 series instrument (Agilent Technologies, Sydney, Australia) as previously described (Uchaipichat et al., 2004). Concentrations of 4-MU-glucuronide in samples were quantified using a standard curve of 4-MU glucuronide prepared over the concentration ranges of 0.5 to 10 μ M. Human UGT2B15 and UGT2B17 supersomes (In Vitro Technologies) were used to determine their selectivity towards 4-MU.

2.2.18 Statistical analysis

Statistical analyses of all data were performed using GraphPad Prism 6 software (GraphPad Inc., La Jolla, CA), with two-tailed independent t test. Correlation analysis on comparison studies were conducted by Spearman correlation (specific details are mentioned in relevant Chapters). A P value of 0.05 was considered statistically significant.

CHAPTER 3

REGULATION OF UGT2B15 AND UGT2B17 EXPRESSION BY MICRORNAS

Published in part as: Wijayakumara DD, Hu DG, Meech R, McKinnon RA and Mackenzie PI (2015), 'Regulation of Human UGT2B15 and UGT2B17 by miR-376c in Prostate Cancer Cell Lines'. *Journal of Pharmacology and Experimental Therapeutics*, 354(3):417-25.

Reproduced with permission of the American Society for Pharmacology and Experimental Therapeutics. All rights reserved.

3.1 Introduction

The primary site of glucuronidation, where metabolism and systemic clearance of endogenous and exogenous lipophilic compounds occurs, is the liver and therefore, most UGTs are expressed in this organ. However, UGTs are also found in extra-hepatic tissues including prostate, breast, small intestine, colon, kidney and lung. They play an important role in inactivating certain endogenous and exogenous biologically active molecules in these organs and contribute towards overall intratissular homeostasis (Nishimura and Naito, 2006, Nakamura et al., 2008, Izukawa et al., 2009, Ohno and Nakajin, 2009, Court, 2010, Court et al., 2012, Schaefer et al., 2012). For instance, in the prostate, androgens modulate normal development and function via regulating the expression of multiple genes involved in growth regulatory processes and other cellular functions (Carson and Rittmaster, 2003). However, excessive growth-promoting androgen activity may contribute

towards prostate cancer development and progression (Heinlein and Chang, 2004). As previously described, UGT2B15 and UGT2B17 metabolize active androgens such as testosterone and DHT, and can hence control androgen signaling in the prostate (Turgeon et al., 2001, Chouinard et al., 2007).

Both UGT2B15 and UGT2B17 share extremely similar sequences with 95% overlap; however, they show varying affinity and specificity towards androgens (Beaulieu et al., 1996, Turgeon et al., 2001). DHT and testosterone are conjugated by UGT2B17 at a higher efficiency compared to UGT2B15, while they conjugate the major DHT metabolite 3 α -DIOL at high but similar efficiencies (Beaulieu et al., 1996, Belanger et al., 2003, Turgeon et al., 2001). 3 α -DIOL-glucuronide is the highest circulating glucuronide metabolite of DHT in humans (both men and women) (Rittmaster et al., 1988). In addition, UGT2B17 is believed to be the major ADT conjugating enzyme (Belanger et al., 2003, Turgeon et al., 2001). Thus, UGT2B17 and UGT2B15 are the main determinants of active androgen levels.

As mentioned previously, these UGTs are expressed in different cell types of the prostate; UGT2B17 is expressed in basal alveoli cells whereas UGT2B15 is expressed in the luminal cells (Belanger et al., 2003). In basal cells, circulating androgens and testosterone are metabolized by phase I enzymes into DHT and other metabolites. DHT and its metabolites including ADT and 3 α -DIOL can be glucuronidated by UGT2B17 in these cells and secreted back into circulation. DHT then diffuses into luminal cells where it exerts its function as a high affinity ligand for the androgen receptor and modulate AR signaling. UGT2B15 is specifically expressed in luminal cells of the prostate, where it metabolizes DHT to regulate its intracellular concentration and prevent accumulation (Barbier et al., 2000).

Because of these important functions of UGT2B15 and UGT2B17 in controlling androgen homeostasis, and potential impact on androgen-sensitive prostate diseases such as prostate cancer, their regulation both at the transcriptional level and post-transcriptional level is of utmost importance to understand. Various compounds including androgens have been reported to regulate UGT2B15 and UGT2B17 at the transcriptional level in AR-positive prostate cancer cell lines (Guillemette et al., 1996, Guillemette et al., 1997, Levesque et al., 1998, Chouinard et al., 2006, Bao et al., 2008, Kaeding et al., 2008a, Kaeding et al., 2008b). The downregulation of UGT2B15 and UGT2B17 by androgens generates a positive feedback loop to enhance androgen activity (Chouinard et al., 2008). To date, the regulation of these two UGTs at the post-transcriptional level remains unexplored.

As microRNAs have been recently found to be post-transcriptional regulators of gene expression (Filipowicz et al., 2008) via targeting mainly 3'UTRs and inhibiting protein translation and /or promoting mRNA degradation (Grimson et al., 2007, Hu and Coller, 2012), we investigated their regulation of UGT2B15 and UGT2B17 expression. As mentioned previously, miRNAs contain unique seed sequences (nucleotides 2-8 from the 5' end) which determine their specificity towards target genes. Several bioinformatic programs (mentioned in Chapter 1) have been created to predict putative microRNA target sites in the human genome; using some of these programs, we identified predicted microRNAs target sites in the 3'UTRs of UGT2B15 and UGT2B17. This chapter presents an extensive functional validation of these sites, and represents the first evidence for direct regulation of endogenous UGT2B15 and UGT2B17 by miRNA-3'UTR interactions in prostate cancer cells.

3.2 Materials and Methods

3.2.1 Luciferase Reporter Construction

The 3'UTR of UGT2B15 mRNA (NM_001076.3) is 513-base pair (bp) in length and the 3'UTR of UGT2B17 mRNA (NM_001077.3) is 463-bp in length. In order to generate a reporter construct containing the 3'UTR of UGT2B15 (pGL3/2B15/UTR), the 454 bp region between the stop codon (TAG) and the poly(A) tail of the 2B15 3'UTR was initially amplified from human genomic DNA (Roche Diagnostic, Indianapolis, IN) by Phusion hot-start high-fidelity DNA polymerase (Thermo Fisher Scientific, Pittsburgh, PA). The amplified region was then cloned into the pGL3-promoter vector at the XbaI restriction site which is located downstream of the luciferase coding sequence. Similarly, to generate a construct containing the 2B17 3'UTR (pGL3/2B17/UTR), the 431 bp region between the stop codon and the poly(A) tail was amplified and cloned into the pGL3-promoter vector at the XbaI restriction site. For cloning, a common forward primer (UGT2B15/17_3UTR_F) and two UGT2B15-specific (UGT2B15_3UTR_R) and UGT2B17-specific (UGT2B17_3UTR_R) reverse primers were used. The primer sequences are listed in Table 3.1.

Using the pGL3/2B15/UTR construct as a template and the QuickChange site-directed mutagenesis kit (Stratagene, La Jolla, CA), the miR-376c seed binding site (5'-UCUAUGUC-3'), which is complementary to the miR-376c seed sequence (3'-AGAUACAA-5'), was changed to 5'-CGGUUGUC-3', producing the mutated construct pGL3/2B15/UTR/miR-376c/MT. In the pGL3/2B17/UTR construct, the miR-376c seed site (5'-UCUAUGUC-3') that is complementary to the miR-376c seed sequence (3'-AGAUACAA-5') was mutated to 5'-CGACUGUC-3' to make the

mutated construct pGL3/2B17/UTR/miR-376c/MT. Similarly, the miR-376b seed binding site in UGT2B15 3'UTR (5'-CUAUGA-3') which is complementary to the miR-376b seed sequence (3'-GAUACU-5'), was changed to 5'-CUUCGU-3' in the pGL3/2B15/UTR construct producing the mutated construct pGL3/2B15/UTR/miR-376b/MT. The miR-222 seed binding site in the UGT2B15 3'UTR (5'-AUGUAGC-3'), which is complementary to the miR-222 seed sequence (3'-UACAUCG-5'), was also mutated to 5'-AUGCUAG-3' in the wild type pGL3/2B15/UTR construct to generate the mutated construct pGL3/2B15/UTR/miR-222/MT. The identities of all constructs were confirmed by DNA sequencing. The sequences of the primers used for mutagenesis are given in Table 3.1.

3.2.2 Glucuronidation Assays

LNCaP cells were transfected with miRNA mimics (miR-376c or miRneg) at 30 nM. Seventy-two hours later, whole cell lysates were prepared in TE buffer (10 mM Tris-HCl and 1 mM EDTA, pH 7.6) and protein concentrations of the lysates were determined using the Bradford protein assay, according to the manufacturer's protocol (Bio-Rad, Hercules, CA). For testosterone glucuronidation assays, duplicate 100- μ l reactions of each sample containing 100 mM potassium phosphate, pH 7.5, 4mM MgCl₂, 1440pM [¹⁴C] testosterone (NEN, Boston, MA), 25 μ g lysate protein, and 2 mM UDP-glucuronic acid (Sigma-Aldrich, St. Louis, MO) were incubated at 37°C in a shaking water bath for 2 hours. Reactions were terminated by the addition of 300 μ l of chloroform. The reaction mixture was vortexed vigorously to help partition unreacted testosterone into the chloroform phase and then centrifuged at 11,000g for 5 minutes. One third of the aqueous phase (66 μ l) from each sample was combined with an equal volume of 100% ethanol and centrifuged at 11,000g for 3

minutes. Sixty microliters of the supernatant of each sample was spotted onto silica gel thin layer chromatography plates (Uniplate; Analtech, Newark, DE) and chromatographed for 1 hour in a solvent of chloroform/methanol/water/acetic acid (65:25:4:2). The plates were placed on Kodak storage phosphor screens (Amersham Biosciences, Piscataway, NJ) for 72 hours and then imaged using the Typhoon 9000 Imager (GE Healthcare, Giles, UK). Band intensity was measured using ImageQuant version 5.2 (GE Healthcare).

For all other glucuronidation assays, 100- μ l reactions were prepared containing 100 mM potassium phosphate, pH 7.5, 4 mM MgCl₂, 200 μ M substrate (androsterone, 17 β -estradiol, phenolphthalein, 2-hydroxyestradiol, 4-hydroxyestradiol, 8-hydroxyquinoline or 4-methylumbelliferone), 25 μ g cell lysate protein, 200 μ M UDP-glucuronic acid (Sigma-Aldrich), and 319 pmol of [¹⁴C]UDP-glucuronic acid (PerkinElmer, Boston, MA) and incubated at 37°C in a shaking water bath for 2 hours. Reactions were terminated by the addition of 200 μ l of ethanol. The reaction mixture was vortexed and then centrifuged at 11,000g for 3 minutes. Aliquots of 100 μ l from each reaction were spotted onto silica gel thin layer chromatography plates and chromatographed for 1 hour as described above. The dried plates were then imaged and quantified as described above. To demonstrate UGT2B15 and UGT2B17 substrate specificity, 25 μ g of recombinant UGT2B15 and UGT2B17 supersomes were used as controls in the assays (In Vitro Technologies, Noble Park North, VIC, Australia).

Details on 4-Methylumbelliferone (4-MU) glucuronidation assays, are mentioned in Chapter 2, section 2.2.17.1.

3.2.3 Statistical Analysis

Statistical analysis of all data was performed using GraphPad Prism 6 software (La Jolla, CA, USA), with a two-tailed Student's independent t-test. Correlation between UGT2B15 and UGT2B17 mRNA versus miR-376c expression in human tissues were analysed using one-tailed Spearman correlation. P-values <0.05 were considered statistically significant.

Table 3.1: Primers used in this study for mutagenesis, cloning and qPCR (5'–3')

Primer	Sequence (5' - 3')
<i>Cloning</i>	
UGT2B15/17_3UTR_F	CCGCTCTAGATTATATCAAAAAGCCTGAAGT
UGT2B15_3UTR_R	CCGGTCTAGAGACACTTTATTTTCAGATCC
UGT2B17_3'UTR_R	CCGCTCTAGAGAAGATTTTCATTGGCAAAT
<i>Site-directed mutagenesis</i>	
2B15_miR376c_MT_F	CTTTAGCTGAATTATCGGTTGTCAATGATTTTTAAGC
2B15_miR376c_MT_R	GCTTAAAAATCATTGACAACCGATAATTCAGCTAAAG
2B17_miR376c_MT_F	CTTTAGTTGGAATTATCGACTGTCAATGATTTTTAAGC
2B17_miR376c_MT_R	GCTTAAAAATCATTGACAGTCGATAATTCCTAACTAAAG
2B15_miR376b_MT_F	CAATGATTTTTAAGCTCGTGAAAATACAATGGGGGGAAG
2B15_miR376b_MT_R	CTTCCCCCATTGTATTTTCACGAGCTTAAAAATCATTG
2B15_miR222_MT_F	GCACATGTATACATATGCTAGTAACCTGCACGTTGTGC
2B15_miR222_MT_R	GCACAACGTGCAGGTTACTAGCATATGTATACATGTGC
<i>miRNA-specific qPCR</i>	
hsa-miR-376c_F	CGCAGAACATAGAGGAAATTCC
hsa-miR-376c_R	GGTCCAGTTTTTTTTTTTTTTTCGT
RNU6-2_F	CGCAAGGATGACACGCAA
RNU6-2_R	CAGGTCCAGTTTTTTTTTTTTTTTAAAAATAT

<i>Primary miRNA-specific qPCR</i>	
pri-miR-376c_F	GGTATTTAAAAGGTGGATATTCCTTCTATG
pri-miR-376c_R	GATACTGAAAACGTGGAATTTCTCTATG
RNU6-2_F	CGCAAGGATGACACGCA
RNU6-2_R	AAAAATATGGAACGCTTCAC

3.3 Results

3.3.1 3'UTRs of UGT2B15 and UGT2B17 contain putative miRNA target sites

The bioinformatics analysis program, TargetScan (version 6.2) which uses parameters such as seed pairing, probability of conserved targeting and local AU content was used to predict miRNA target sites in UGT2B15 and UGT2B17 3'UTRs (Friedman et al., 2009, Grimson et al., 2007, Lewis et al., 2005). With this program, 7 putative miRNA target sites were identified in the 3'UTR of UGT2B15. These were miR-105, miR-222, miR-331-5p, miR-21, miR-376b, miR-376c and miR-382. Except for miR-105, miR-222 and miR-331-5p, the remaining microRNAs also had predicted target sites in the 3'UTR of UGT2B17 (Figure 3.1). Moreover, miR-382 had two separate target sites in the UGT2B15 3'UTR (Figure 3.1). A study performed by Shi *et al* using microarray analysis showed that miR-125b mimics reduced the expression of UGT2B15, UGT2B17 and UGT2B28 mRNA levels in LNCaP cells by 2.15, 2.73 and 2.29 fold respectively (Shi et al., 2007), suggesting that both UGT2B15 and UGT2B17 may contain target sites for miR-125b. Furthermore, a previous bioinformatic investigation in our laboratory predicted that miR-525 may bind to the coding regions of both UGT2B15 and UGT2B17. Along

with these 9 miRNAs, the effects of miR-375-3p which was available in the laboratory, were tested on the expression of both UGT2B15 and UGT2B17.

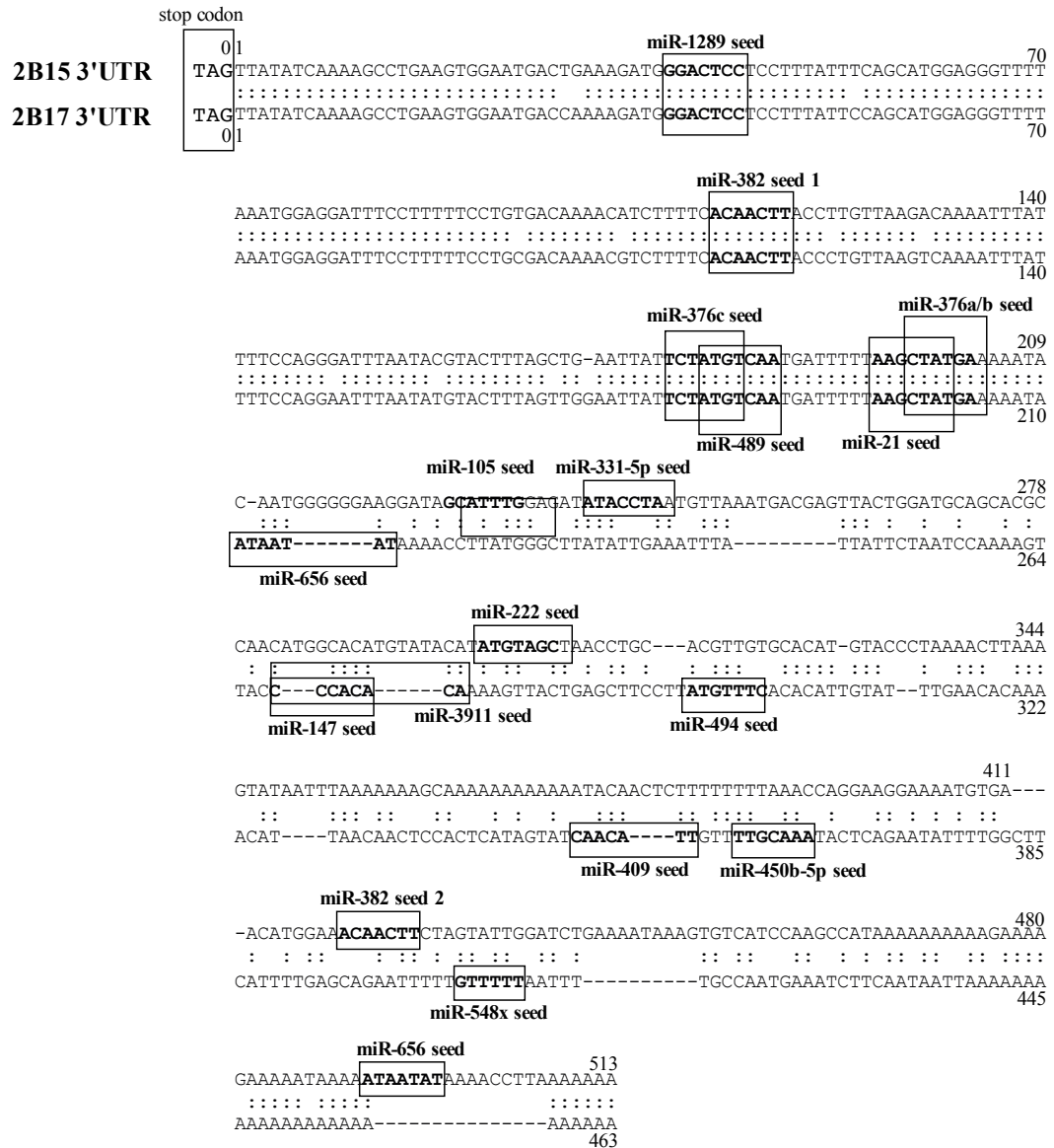
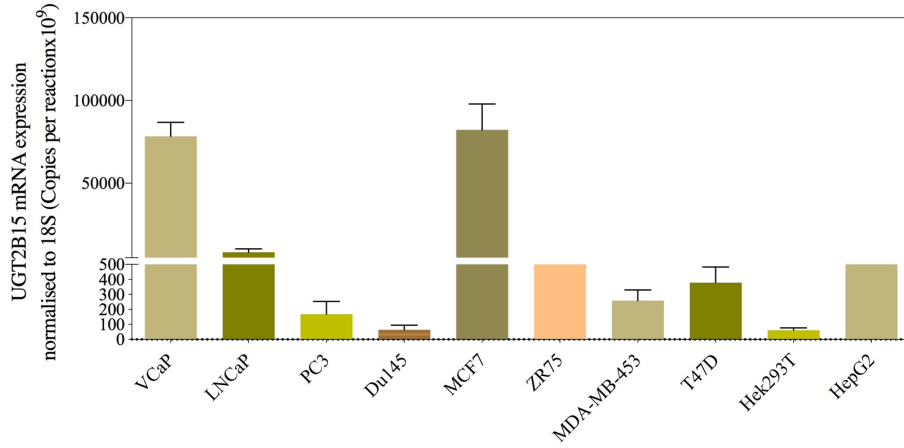


Figure 3.1: The 3'UTRs of both UGT2B15 and UGT2B17 mRNAs contain putative miRNA binding sites

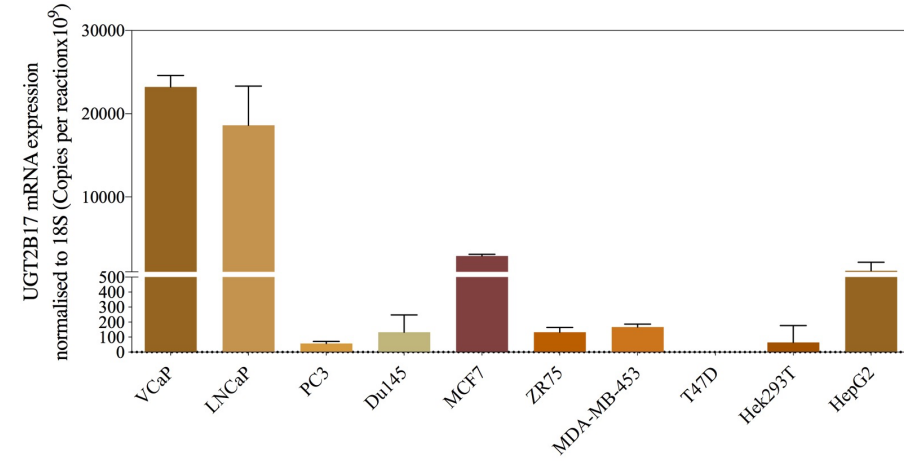
Shown are predicted miRNA seed pairing sites (boxed and in bold) in the 3'UTRs of UGT2B15 and/ or UGT2B17. The 3'UTRs of the two UGTs are aligned and nucleotide sequences are numbered relative to the stop codon (TAG with G positioned as 0).

To identify suitable cell lines for analysis, the expression profiles of UGT2B15, UGT2B17 and selected miRNAs were measured in commonly used cancer cell lines using RT-qPCR (Figure 3.2). The expression of the selected 10 miRNAs in these cell lines were measured using the Taqman™ MicroRNA Assays. The cell lines chosen were the prostate cancer cell lines LNCaP, VCaP, PC3 and Du145, the breast cancer cell lines MCF7, ZR75, MDA-MB-453 and T47D, the kidney cell line HEK293T and the hepatic cancer cell line HepG2. Both LNCaP and VCaP cells expressed the highest level of UGT2B15 and UGT2B17 among the prostate cancer cell lines (Figure 3.2 A, B). MiR-125b, miR-222 and miR-21 were the only miRNAs expressed in these cell lines (Figure 3.2 C).

A



B



C

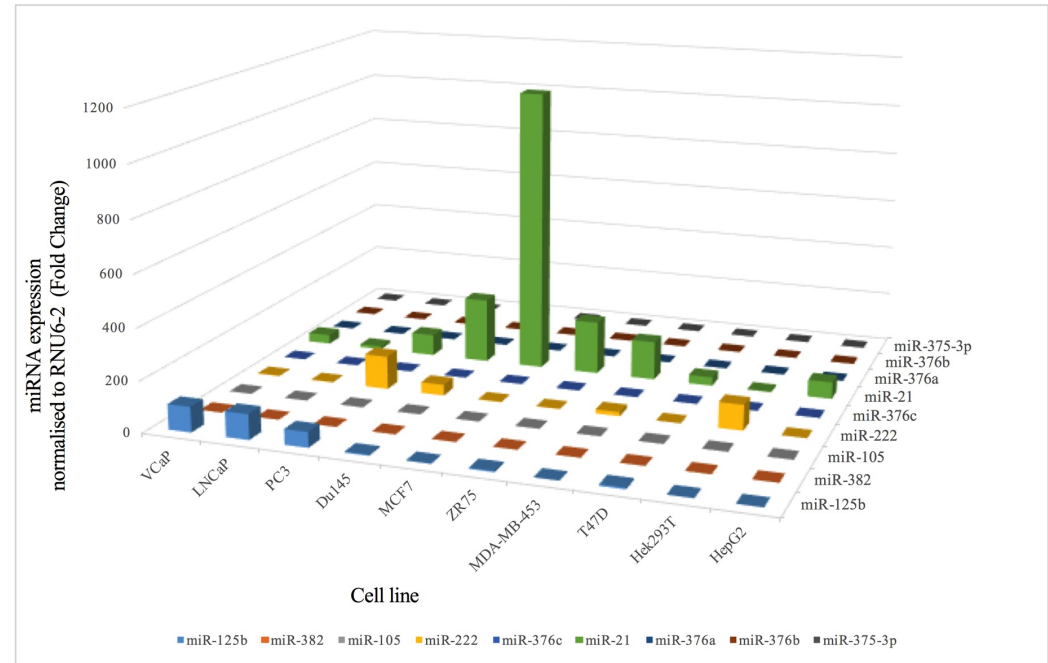


Figure 3.2: Expression patterns of UGT2B15, UGT2B17 and predicted miRNAs in ten cell lines

Shown are the expression of UGT2B15 (A), UGT2B17 (B) and nine predicted miRNAs (C) in ten human cell lines. Total RNA was extracted from the cells and then subjected to quantitative real-time RT-qPCR for measuring target gene mRNA levels. UGT2B15 and UGT2B17 mRNA levels were normalized to 18S rRNA levels presented as copy number per reaction. The miR-376c levels were normalized to RNU6-2 and presented relative to the miR-125b expression in Hek293T cells (set at a value of 1). Data shown are from a representative experiment performed in triplicate, the error bar representing \pm S.D.

In order to investigate the potential direct regulation of UGT2B15 and UGT2B17 mRNAs by these microRNAs in vitro, the 3'UTR of either UGT2B15 or UGT2B17 was cloned into the pGL3 promoter luciferase vector, downstream of the luciferase gene as described in Materials and Methods. Co-transfection of miRNA mimics with the luciferase constructs was performed in Du145 cells as an initial screening. These cells showed low expression of the selected miRNAs and hence were predicted to have low background activity. As shown in Figure 3.3, the luciferase results showed that those miRs that only targeted the UGT2B15 3'UTR, miR-105, miR-222 and miR-331-5p, significantly reduced the UGT2B15 3'UTR containing reporter activity (pGL3/2B15/UTR) by 58% ($p < 0.0005$), 20% ($p < 0.005$) and 77% ($p < 0.0005$). The activity of the UGT2B17 3'UTR-containing reporter (pGL3/2B17/UTR) was not significantly affected by the transfection of miR-222 or miR-331-5p, but there was a 31% reduction ($p < 0.05$) seen in its activity with miR-105 mimics. As miR-105 had no predicted target site in the UGT2B17 3'UTR this might represent an indirect effect of this miRNA, or a technical artefact. The results also showed that miR-21, miR-375-3p, miR-376b and miR-376c significantly reduced activities of both pGL3/2B15/UTR and pGL3/2B17/UTR reporters. The reduction of pGL3/2B15/UTR reporter with miR-21, miR-375-3p, miR-376b and miR-376c were 25% ($p < 0.05$), 31% ($p < 0.05$), 46% ($p < 0.005$) and 69% ($p < 0.0005$) respectively. The reduction of the pGL3/2B17/UTR reporter with miR-21, miR-375-3p, miR-376b and

miR-376c were 23% ($p<0.05$), 28% ($p<0.005$), 20% ($p<0.005$) and 73% ($p<0.0005$) respectively. However, in HEK293T cells and LNCaP cells, the activity of pGL3/2B17/UTR reporter was not affected by either miR-376b (Figure 3.7 B) or miR-21. As UGT2B15 or UGT2B17 3'UTRs do not contain predicted target sites for miR-375-3p, the reduction of activity seen could be an indirect effect or a technical artefact. MiR-125b, miR-382 and miR-525 did not affect either of the reporter activities confirming that there are no functional target sites of the miRNAs in UGT2B15 or UGT2B17 3'UTRs (Figure 3.3). This was expected for miR-525 as the target site was predicted to be in the coding regions of both UGT2B15 and UGT2B17 (Figure 3.12).

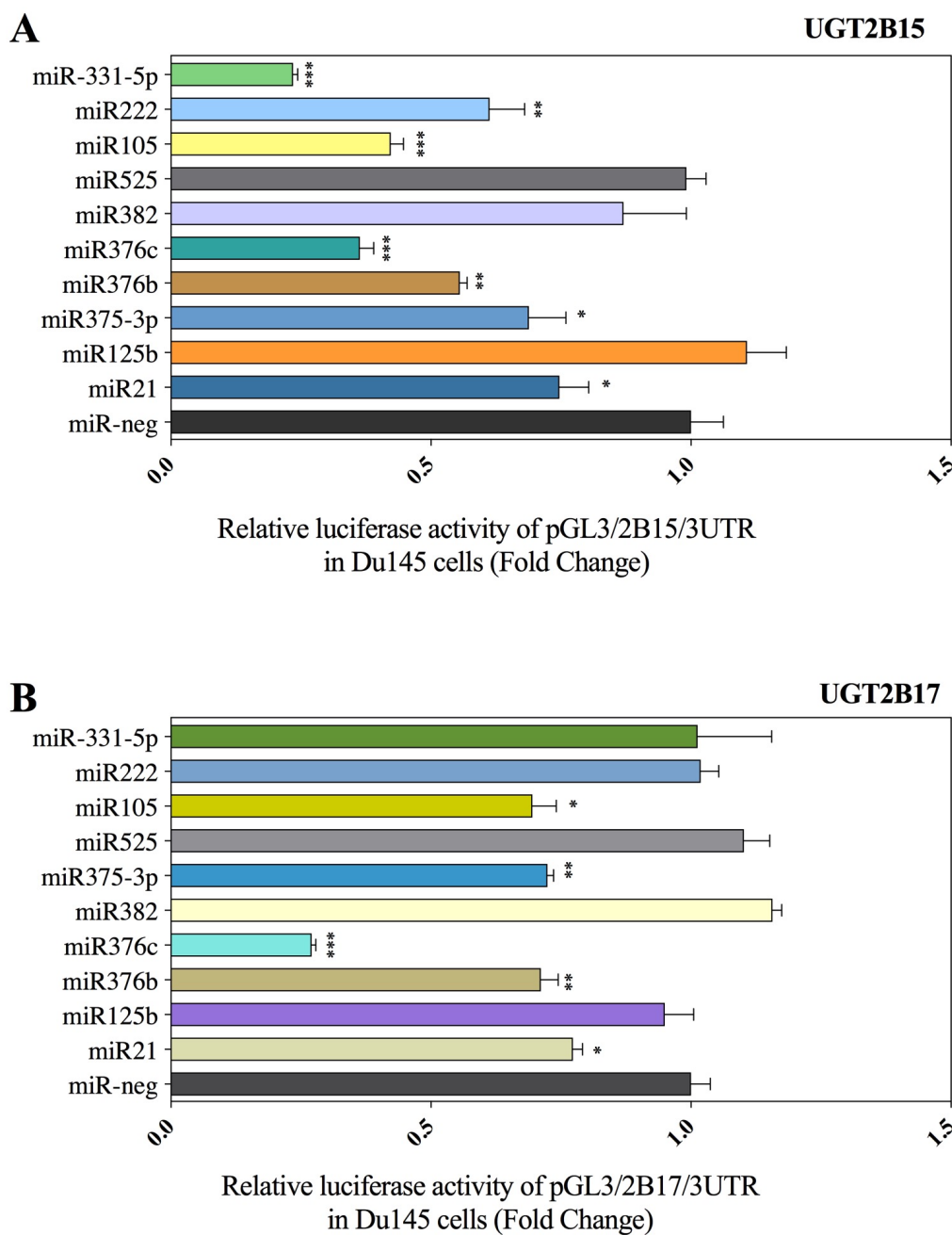


Figure 3.3: MiRNAs target 3'UTRs of UGT2B15 and/or UGT2B17 in Du145 cells

Shown are the luciferase reporter activities measured in Du145 cells co-transfected with the UGT2B15 3'UTR containing reporter, pGL3/2B15/UTR (A) or the UGT2B17 3'UTR containing reporter, pGL3/2B17/UTR (B) along with miRNA mimics or miR-neg control. The activities of the reporter constructs were first normalized to the activity of the pRL-null vector and then presented relative to those of the empty pGL3-promoter vector (set at a value of 1). Data shown are mean \pm S.D. from a representative experiment performed in quadruplicate. *** $P < 0.0001$, ** $p < 0.005$, * $p < 0.05$.

A further 10 miRNA target sites in the UGT2B17 3'UTR were identified using TargetScan. The miRNAs were miR-147, miR-1289, miR-376a, miR-3911, miR-409, miR-450b-5p, miR489, miR-494, miR-548x and miR-656. Of these miRNAs, miR-1289, miR-376a, miR-489 and miR-656 also contained target sites in the UGT2B15 3'UTR (Figure 3.1). However, the putative target site for miR-656 in the UGT2B15 3'UTR was different to its target site in the UGT2B17 3'UTR (Figure 3.1). As shown in Figure 3.4 A, in Du145 cells, miR-147, miR-1289, miR-450b-5p, miR-494, miR-548x and miR-656 reduced the activity of the UGT2B17 3'UTR containing reporter. MiR-656 also reduced the activity of the UGT2B15 3'UTR containing reporter. The miR-376a seed site is the same as the miR-376b seed site (Figure 3.1) and these miRNAs are highly conserved in sequence with only a 4-nucleotide difference at the 3' end. Despite their similarity in sequence and predicted binding by bioinformatics programs, miR-376a did not alter the activity of either UGT2B15 or UGT2B17 containing reporters. However, the reduction of luciferase activity seen in Du145 cells with the latter 10 miRNAs were not replicable either in LNCaP cells or HEK293T cells (Figure 3.4). Therefore, we decided not to continue work on these miRNAs and focus only on miR-376c, miR-376b, miR-222 and miR-331-5p. This Chapter describes studies with miR-376c, miR-376b and miR-222, and studies with miR-331-5p will be described in detail in Chapter 4.

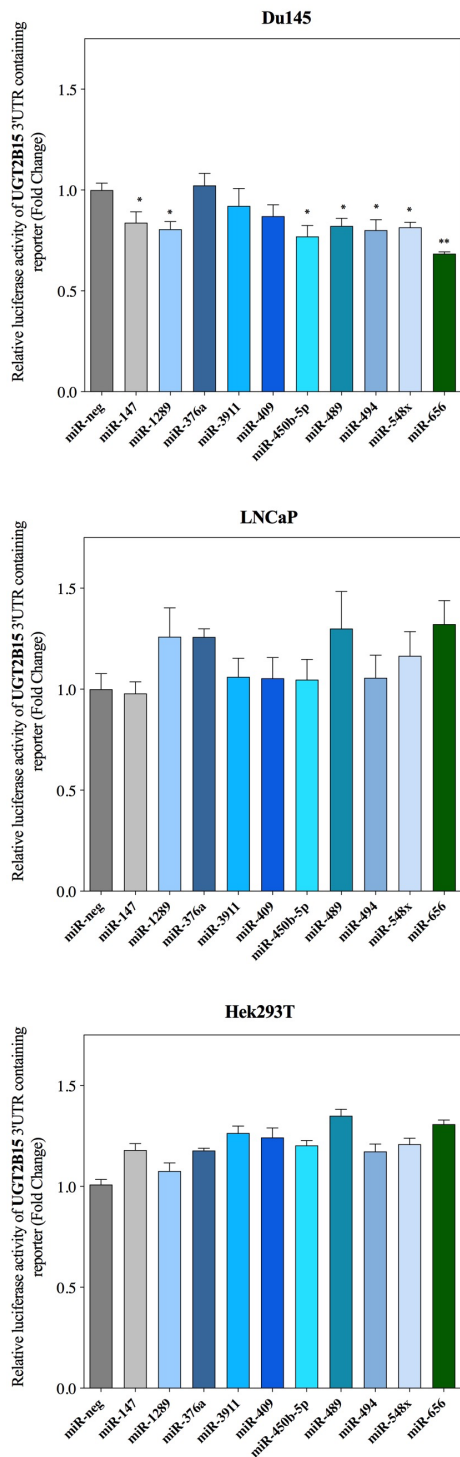
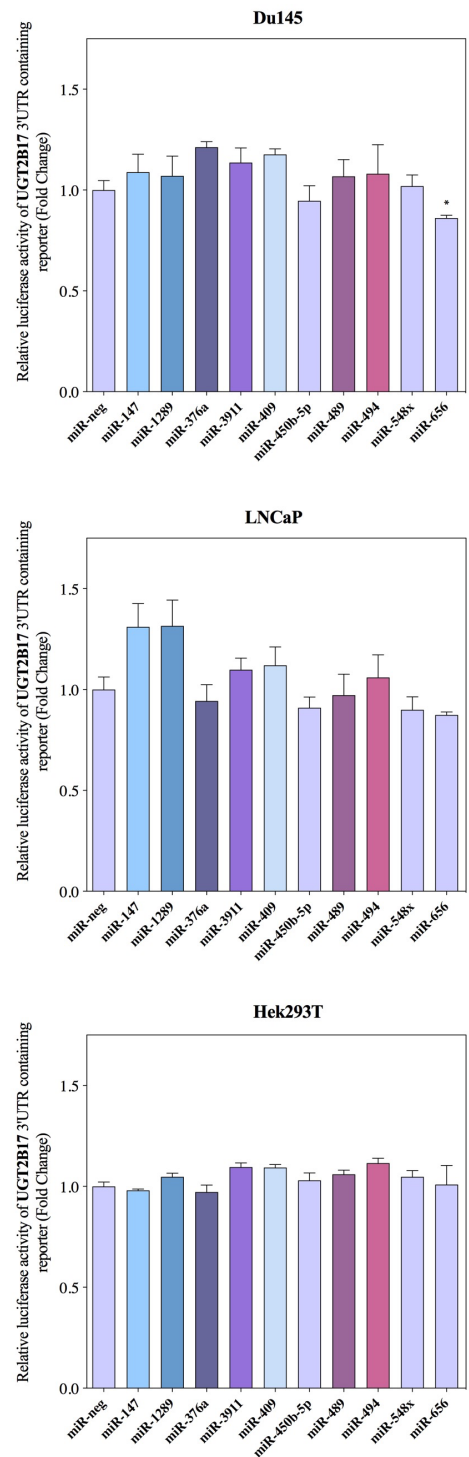
A**B**

Figure 3.4: Investigation of new miRNAs that target the 3'UTR of UGT2B17 in Du145, LNCaP and HEK293T cells

Shown are the luciferase reporter activities measured in either Du145, LNCaP or Hek293T cells co-transfected with the UGT2B15 3'UTR containing reporter, pGL3/2B15/UTR (A) or the UGT2B17 3'UTR containing reporter, pGL3/2B17/UTR (B) along with miRNA mimics or miR-neg control. The activities of the reporter

constructs were first normalized to the activity of the pRL-null vector and then presented relative to those of the empty pGL3-promoter vector (set at a value of 1). Data shown are mean \pm S.D. from a representative experiment performed in quadruplicate. ** $p < 0.005$, * $p < 0.05$.

TargetScan classifies predicted miRNA target sites based on their pairing with miRNA seed regions, into four types as described in Chapter 1 (section 1.10.4) (Lewis et al., 2005). According to this classification, the miR-376c target sites in both UGT2B15 and UGT2B17 3'UTRs are 7mer-m8 sites. In addition to seed pairing, miR-376c shows supplementary pairing at nucleotides 12-15 in the UGT2B15 target site and at nucleotides 12-18 in the UGT2B17 target site, and typically supplementary pairing is known to augment the efficacy of microRNA targeting (Grimson et al., 2007). Moreover, the miR-376c target sites in both UGT2B15 and UGT2B17 3'UTRs are highly conserved in sequence and position, with only a C/U mismatch at position 19 and a G deletion at position 17 in the UGT2B15 miR-376c target site (Figure 3.5). Furthermore, both target sites are conserved between humans and chimpanzees according to TargetScan. As shown in Figure 3.5, miR-376b target sites in UGT2B15 and UGT2B17 are also highly conserved in position and identical in sequence with supplementary 3' pairing at nucleotides 11-16. Both sites are 7mer-A1 sites conserved between humans, chimpanzees and rhesus. The miR-222 target site is a 7mer-m8 site which is conserved between humans and chimpanzees. This binding site also contains additional supplementary 3' pairing at nucleotides 14-16 (Figure 3.5).

and Methods, four contiguous bases within the predicted miR-376c seed site sequences were mutated to abolish miRNA seed pairing (Figure 3.6). The wild-type and mutated constructs were transfected along with miRNA-mimics (miR-neg or miR-376c) into LNCaP cells and 24h post-transfection the luciferase activity of each reporter construct was measured. MiR-376c mimics significantly reduced the luciferase activity of the construct carrying the wild-type 3'UTR of UGT2B15 (pGL3/2B15/UTR) by 46% and the wild-type 3'UTR of UGT2B17 (pGL3/2B17/UTR) by 43% in LNCaP cells (Figure 3.6). This reduction was completely abrogated in the two miR-376c site-mutated constructs (pGL3/2B15/UTR/miR-376c/MT and pGL3/2B17/UTR/miR-376c/MT) confirming the direct binding of miR-376c to the 3'UTRs of both UGT2B15 and UGT2B17. These experimental results were confirmed in a second prostate cancer cell line Du145 (Figure 3.7 A, B) as well. In Du145 cells, miR-376c mimics reduced the pGL3/2B15/UTR and pGL3/2B17/UTR reporter activities by 62% and 65% respectively and mutations in the miR-376c seed sites completely abrogated these effects. Therefore, these results demonstrate the functionality of the predicted miR-376c sites in a prostate cancer cellular context.

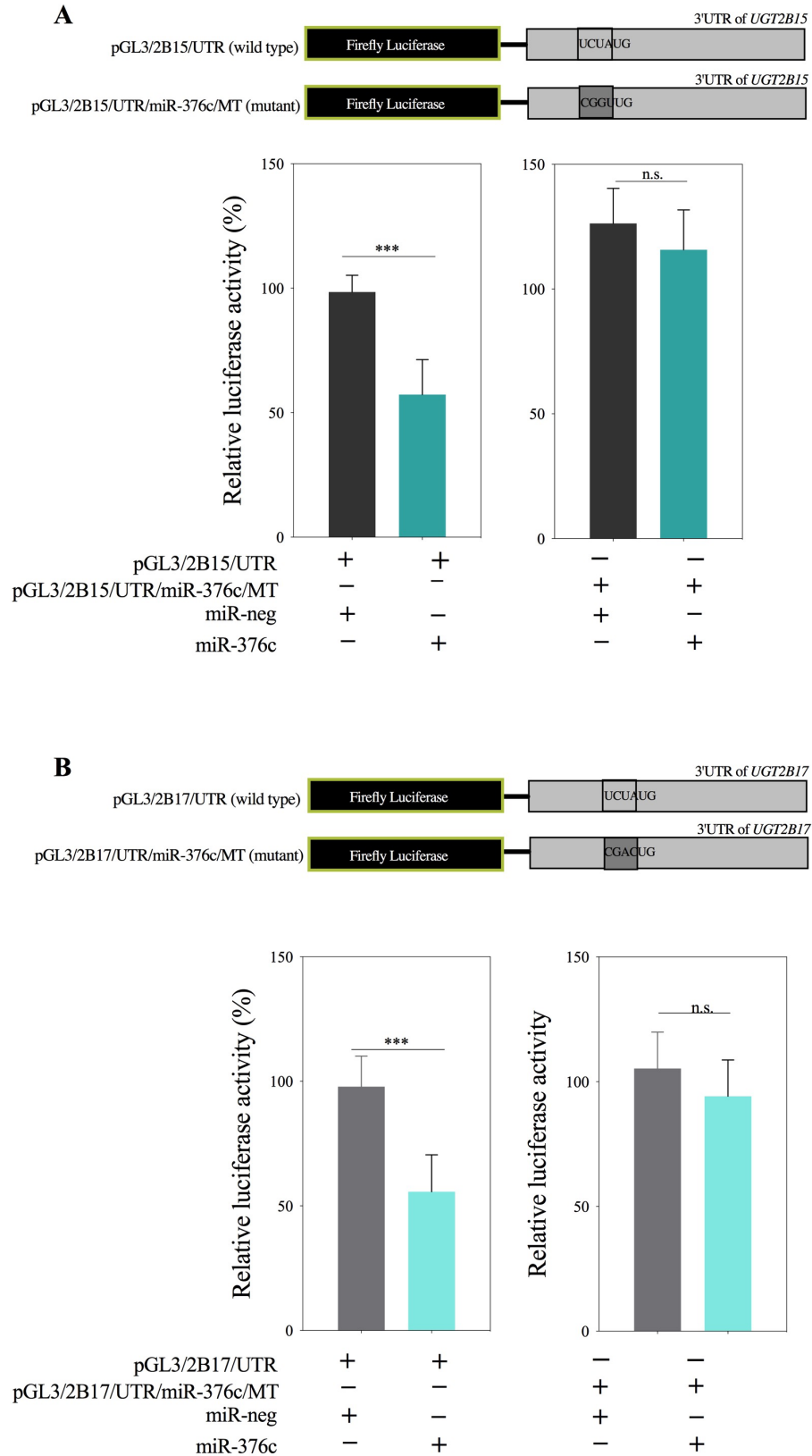


Figure 3.6: MiR-376c mimics reduce the activity of the pGL3-reporter construct carrying the UGT2B15 or UGT2B17 3'UTR via their binding to the predicted miR-376c site in prostate cancer LNCaP cells

(A) Measured luciferase reporter activity in LNCaP cells co-transfected with wild-type or mutant 2B15 3'UTR containing reporters along with miR-neg or miR-376c mimics. (B) Measured luciferase reporter activity in LNCaP cells co-transfected with wild-type or mutant 2B17 3'UTR containing reporters along with miR-neg or miR-376c mimics. The activities of the reporter constructs were first normalized to the activity of the pRL-null vector and then presented relative to those of the empty pGL3-promoter vector (set at a value of 100%). Data shown are mean \pm S.E.M. from two independent experiments performed in quadruplicate. ***P , 0.0001. ns, not statistically significant. Schematic representation of firefly luciferase reporter constructs containing either the wild-type pGL3/2B15/UTR reporter or wild-type pGL3/2B17/UTR reporter or the mutated pGL3/2B15/UTR/miR-376c/MT or mutated pGL3/2B17/UTR/miR-376c/MT at the predicted miR-376c seed binding site is shown above corresponding graphs. Mutated four nucleotides in the seed binding site are boxed and highlighted.

These experiments were repeated in the liver cancer HepG2 and embryonic kidney HEK293T cell lines with similar results. In HepG2 cells, both wild-type reporters showed a 68% reduction in activity with miR-376c mimics, which was significantly abrogated with the two mutant reporters (Figure 3.7 C and D). The reduction seen in the wild-type reporters in HEK293T cells with miR-376c mimics was 48-56% and this reduction was also completely abrogated in the mutant reporters as shown in Figure 3.7 E and F. Thus, these data suggest the functionality of the UGT2B15 and UGT2B17 miR-376c target sites, in not only prostate cancer cells but also in other cellular contexts. Overall, these results provide evidence that the UGT2B15 and UGT2B17 3'UTRs are in fact direct targets of miR-376c.

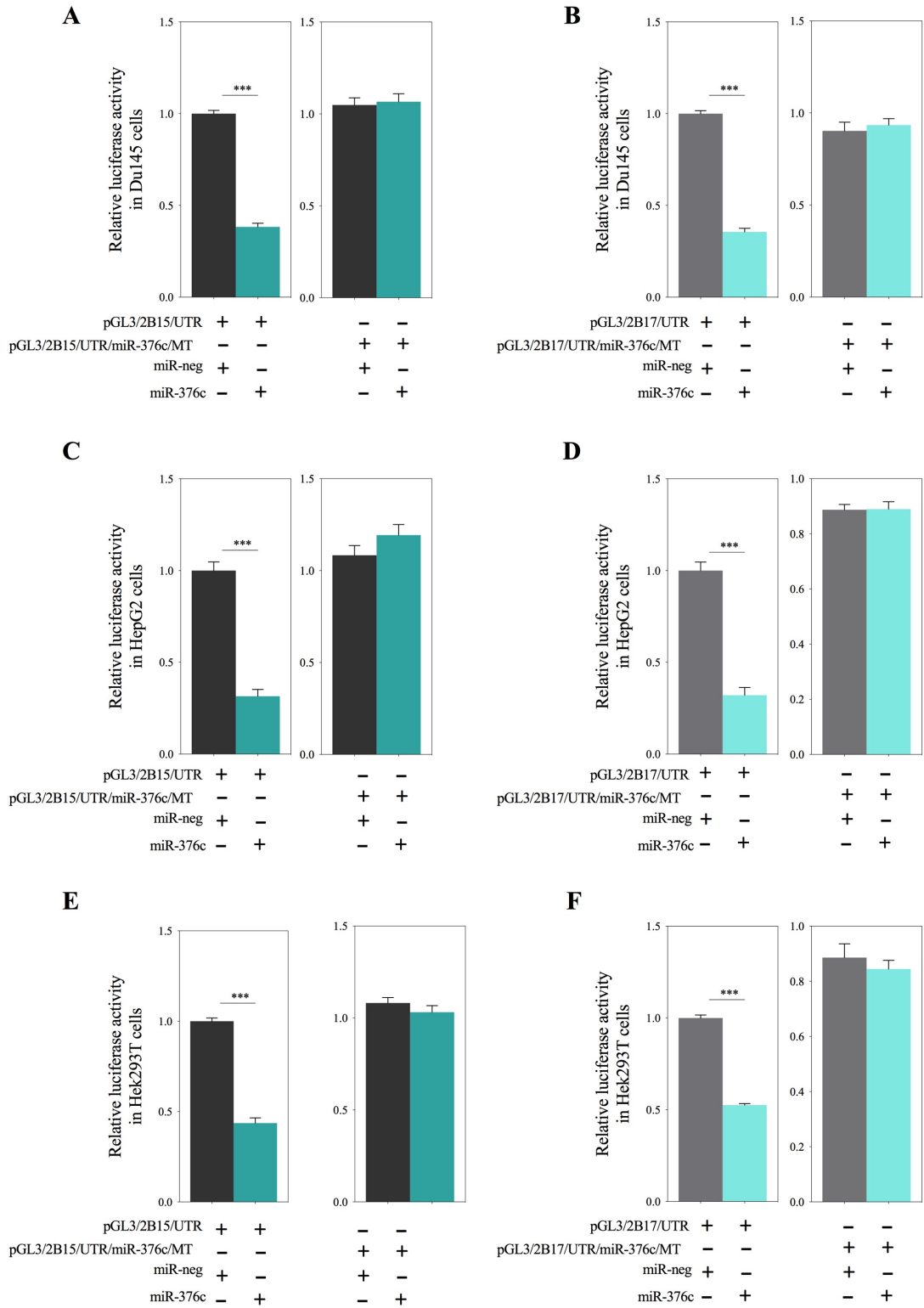


Figure 3.7: MiR-376c mimics reduce the activity of the luciferase reporter containing the UGT2B15 or UGT2B17 3'-UTR via their binding to the predicted miR- 376c site in prostate cancer Du145, liver HepG2 and kidney HEK293T cells

Luciferase reporter assays were performed in Du145 (A, B), HepG2 (C, D) and Hek293T (E, F) cells co-transfected with miR-neg or miR-376c and the wild type or mutant reporter constructs containing UGT2B15 3'-UTR (A, C, E) and UGT2B17 3'-UTR (B, D, F). The activities of the reporter constructs were first normalized to the activity of the pRL-null vector and then presented relative to those of the empty pGL3-promoter vector (set at a value of 1). The reporter constructs are described in Fig. 7A and B. Data shown are means \pm S.E.M. from at least two independent experiments performed in quadruplicate. ***P < 0.0001.

To investigate the effects of miR-376b on UGT2B15 and UGT2B17 expression, four contiguous bases within the predicted miR-376b seed site sequences were mutated in the UGT2B15 and UGT2B17 3'UTR reporters (Figure 3.6). The wild-type and mutated constructs were transfected along with miRNA-mimics (miR-neg or miR-376b) into LNCaP cells and 24h post-transfection the luciferase activity of each reporter construct was measured. As shown in Figure 3.8 A, miR-376b mimics significantly reduced the luciferase activity of the wild-type pGL3/2B15/UTR reporter by 38% in LNCaP cells. This reduction was significantly abrogated in the miR-376b site-mutated construct (pGL3/2B15/UTR/miR-376b/MT). In Du145 cells, a significant 41% reduction was seen in the luciferase activity of the wild-type pGL3/2B15/UTR reporter which was consistent with the previous data in Figure 3.3 A. Similar to the results seen with LNCaP cells, this reduction was completely abrogated in the mutant pGL3/2B15/UTR/miR-376b/MT reporter. Similar results were also seen in HEK293T cells (Figure 3.8 A). These data support the direct binding of miR-376b to its seed site in the 3'UTR of UGT2B15. As shown in Figure 3.8 B (n=4) and also in Figure 3.3 B (n=1), in Du145 cells, miR-376b mimics reduced the activity of the pGL3/2B17/UTR reporter by 16%. However, such reduction was not seen in either LNCaP cell line or Hek293T cell line, suggesting the predicted miR-376b in the 3'UTR of UGT2B17 may not be functional.

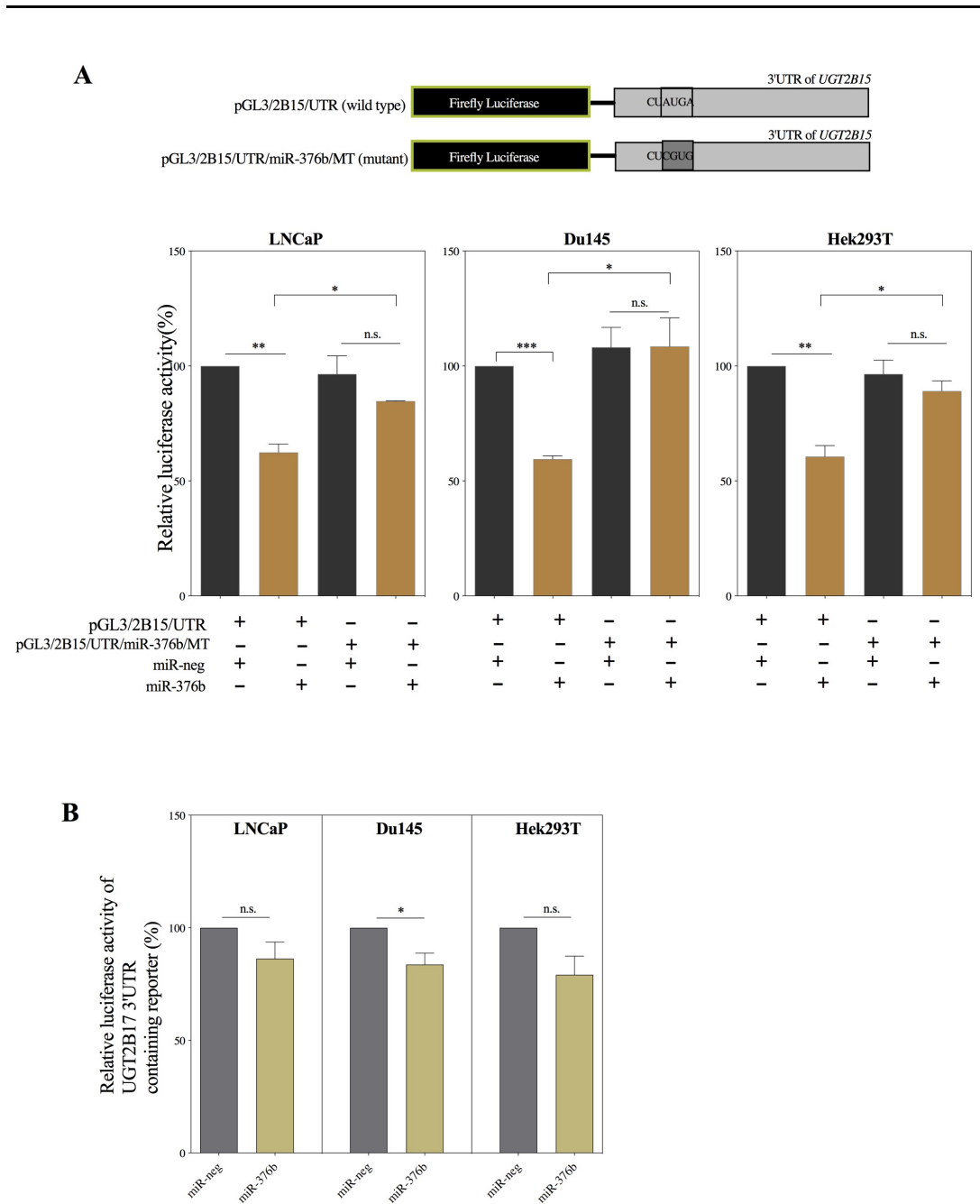


Figure 3.8: MiR-376b mimics reduce the activity of the pGL3-promoter construct carrying the UGT2B15 3'-UTR via binding to its predicted miR-376b site in prostate cancer LNCaP, Du145 and kidney HEK293T cells

(A) Measured luciferase reporter activity in cells co-transfected with wild-type or mutant 2B15 3'UTR containing reporters along with miR-neg or miR-376b mimics. Schematic representation of firefly luciferase reporter constructs containing either the wild-type UGT2B15 3'UTR (pGL3/2B15/UTR reporter) or that mutated at the predicted miR-376b seed binding site (pGL3/2B15/UTR/miR-376b/MT reporter) is shown above the graph. The four mutated nucleotides in the seed binding site are boxed and highlighted. (B) Measured luciferase reporter activity in cells co-transfected with wild-type 2B17 3'UTR containing reporters along with miR-neg or miR-376b mimics. The activities of the reporter constructs were first normalized to the activity of the pRL-null vector and then presented relative to those of the empty

pGL3-promoter vector (set at a value of 100%). Data shown are mean \pm S.E.M. from two or three independent experiments performed in quadruplicate. **P<0.005, *p<0.05, ns, not statistically significant.

To investigate the effects of miR-222 on UGT2B15 expression, four contiguous bases within the predicted miR-222 seed site sequence were mutated in the UGT2B15 3'UTR reporters to abolish seed pairing (Figure 3.9). Transfection experiments were performed in LNCaP, Du145 and HEK293T cells with wild-type and mutated constructs along with miRNA-mimics (miR-neg or miR-222). The luciferase activity of each reporter construct was measured at 24h post-transfection. MiR-222 significantly reduced the luciferase activity of the wild-type pGL3/2B15/UTR by 22%, 53% and 21% in LNCaP, Du145 and HEK293T cells respectively. The mutation in the miR-222 seed side significantly abrogated the miR-mediated reduction in the cell lines (Figure 3.9 A), supporting the idea that miR-222 directly targets the UGT2B15 3'UTR. As expected, miR-222 had no effect on the activity of pGL3/2B17/UTR in all three cell lines (Figure 3.9B).

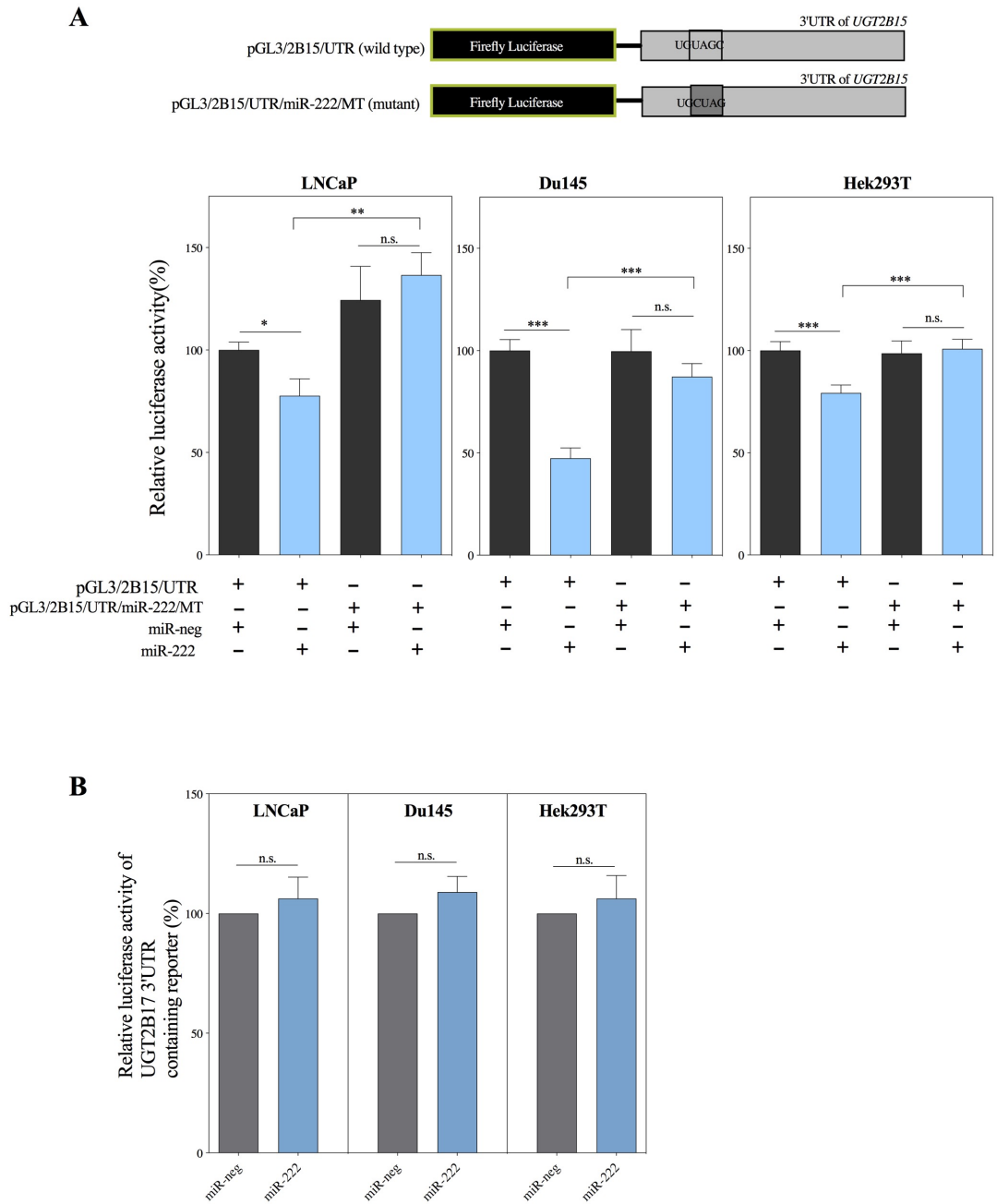


Figure 3.9: MiR-222 mimics reduce the activity of the pGL3-promoter construct carrying the UGT2B15 3'-UTR via binding to its predicted miR-222 site in prostate cancer LNCaP, Du145 and kidney HEK293T cells

(A) Measured luciferase reporter activity in cells co-transfected with wild-type or mutant 2B15 3'UTR containing reporters along with miR-neg or miR-222 mimics. Schematic representation of firefly luciferase reporter constructs containing either the wild-type pGL3/2B15/UTR reporter or the mutated pGL3/2B15/UTR/miR-222/MT at the predicted miR-222 seed binding site is shown above the graph. Mutated four nucleotides in the seed binding site are boxed and highlighted. (B) Measured luciferase reporter activity in cells co-transfected with wild-type 2B17 3'UTR containing reporters along with miR-neg or miR-222 mimics. The activities of the reporter constructs were first normalized to the activity of the pRL-null vector and

then presented relative to those of the empty pGL3-promoter vector (set at a value of 100%). Data shown are mean \pm S.D. from a representative experiment performed in quadruplicate. **P<0.005, *p<0.05, ns, not statistically significant.

3.3.3 MiR-376c reduces both UGT2B15 and UGT2B17 mRNA and protein levels in LNCaP cells.

RT-qPCR analysis showed high UGT2B15 and UGT2B17 mRNA levels and low miR-376c levels in the LNCaP cell line (Figure 3.2). Hence this line was used to investigate the potential negative regulation of endogenous UGT2B15 and UGT2B17 mRNA levels by miR-376c in an androgen receptor-positive prostate cancer cell context.

LNCaP cells were transfected with miRNA mimics (miR-376c or miR-neg) and RT-qPCR was used to quantify UGT2B15 and UGT2B17 mRNA levels. As expected, transfection of miR-376c mimics resulted in a significant down-regulation of both UGT2B15 and UGT2B17 mRNA expression in LNCaP cells by 55% (p<0.0005) and 63% (p<0.0005) respectively (Figure 3.10 A, B). This suggests that miR-376c negatively regulates these two UGTs, likely through targeting the predicted miR-376c site in their 3'UTRs. The mRNA levels of glyceraldehyde-3-phosphate dehydrogenase (GAPDH) were not altered by miR-376c (Figure 3.10 C).

In order to investigate the negative regulation by miR-376c on UGT2B15 and UGT2B17 protein levels, an antibody was developed that recognized both UGT2B15 and UGT2B17 proteins (Chapter 2; section 2.2.6.3). This antibody did not cross-react with the other three UGT2B enzymes UGT2B4, UGT2B7 or UGT2B10 as shown in Chapter 2. Western blotting with the newly developed antibody showed that

endogenous UGT2B15 and/or UGT2B17 protein levels were significantly reduced in miR-376c mimic-transfected cells as compared with miR-neg-transfected cells (Figure 3.10 D).

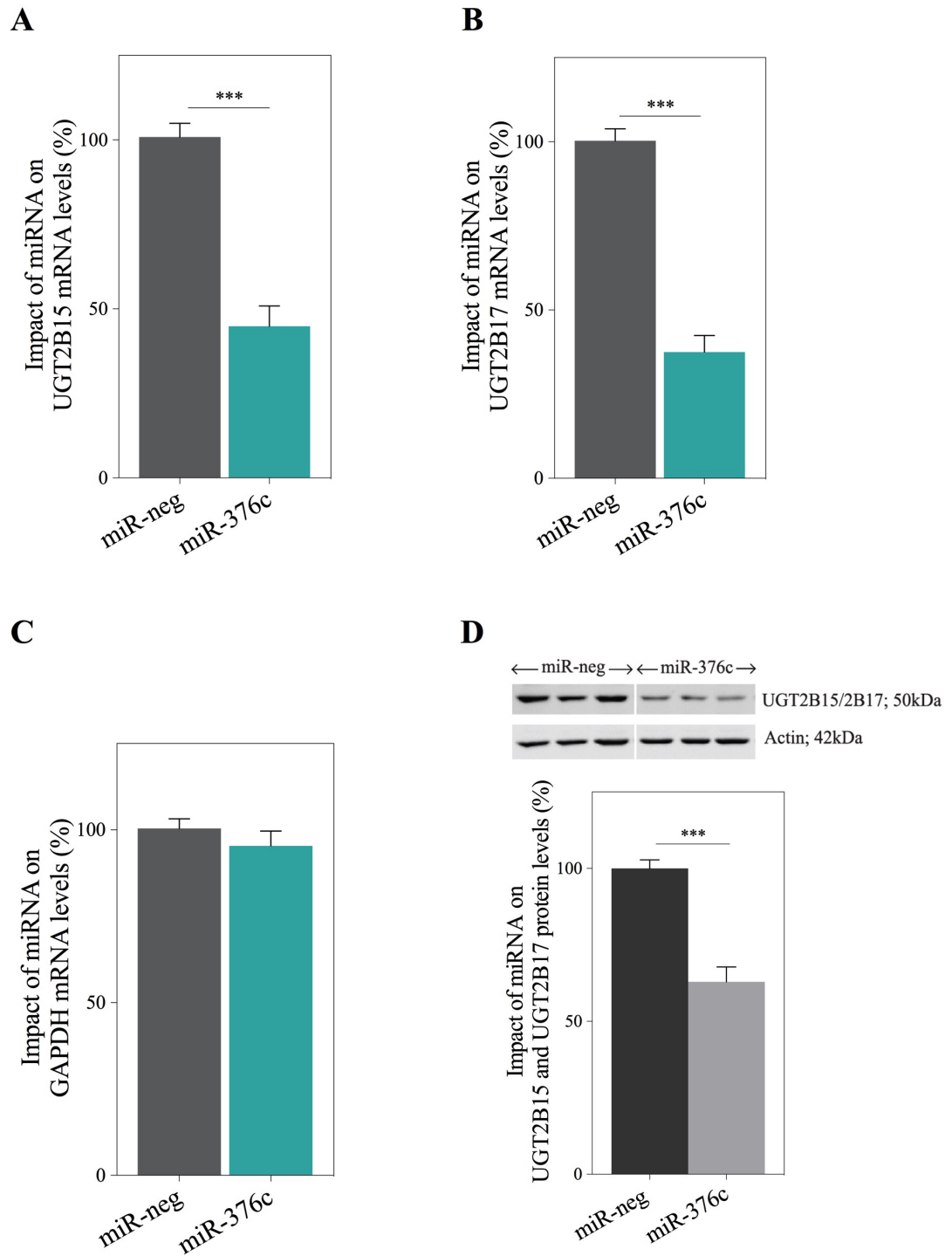


Figure 3.10: miR-376c mimics reduce the mRNA and protein levels of UGT2B15 and UGT2B17 in LNCaP cells

Cells were transfected with miR-neg or miR-376c mimics and total RNA was harvested 24 hours later and then subjected to RT-qPCR for measuring the mRNA levels of target genes, including UGT2B15, UGT2B17, GAPDH and β -actin. After being normalized to the β -actin mRNA levels, the mRNA levels of UGT2B15 (A), UGT2B17 (B), or GAPDH (C) in cells transfected with miR-376c are presented relative to those in the respective miR-neg-transfected cells (set at a value of 100%). Data shown are mean \pm S.E.M. from three independent experiments performed in triplicate. ***P $<$ 0.0001. (D) Cells were transfected with miR-neg or miR-376c mimics and harvested 72 hours later for Western blotting using anti-UGT2B15/2B17 antibody and anti-actin. Quantification of reduction in UGT2B15 and UGT2B17 protein levels relative to actin levels in LNCaP cells transfected with miR-376c are presented relative to those in the respective miR-neg-transfected cells (set at a value of 100%). Data shown are the immune signals of a representative experiment performed in triplicate (top) and the means \pm S.E.M. from two independent experiments performed in triplicate (bottom). ***P $<$ 0.0004.

3.3.4 MiR-376b and miR-222 reduce UGT2B15 mRNA levels whereas miR-525 reduces both UGT2B15 and UGT2B17 mRNA levels in LNCaP cells

Potential negative regulation of endogenous UGT2B15 and/or UGT2B17 mRNAs by miR-376b and miR-222 was tested in the LNCaP cell line. Consistent with the luciferase data, there was a significant downregulation of UGT2B15 mRNA levels in miR-376b and miR-222 mimic transfected cells as compared to miR-neg-transfected cells (Figure 3.11 A, C). There was no significant alteration in UGT2B17 mRNA levels with these miR-mimics (Figure 3.11 B, D).

The possible regulation of endogenous UGT2B15 and UGT2B17 mRNAs by miR-525 was examined in LNCaP cells. Both UGT2B15 and UGT2B17 contain miR-525 target sites in their coding regions as shown in Figure 3.12A. As shown in Figure 3.12 B and C, both UGT2B15 and UGT2B17 mRNA levels were significantly reduced in miR-525 mimic-transfected cells as compared to miR-neg-transfected cells, suggesting a negative regulation of these two UGTs by miR-525, possibly through targeting the predicted miR-525 site in their coding regions.

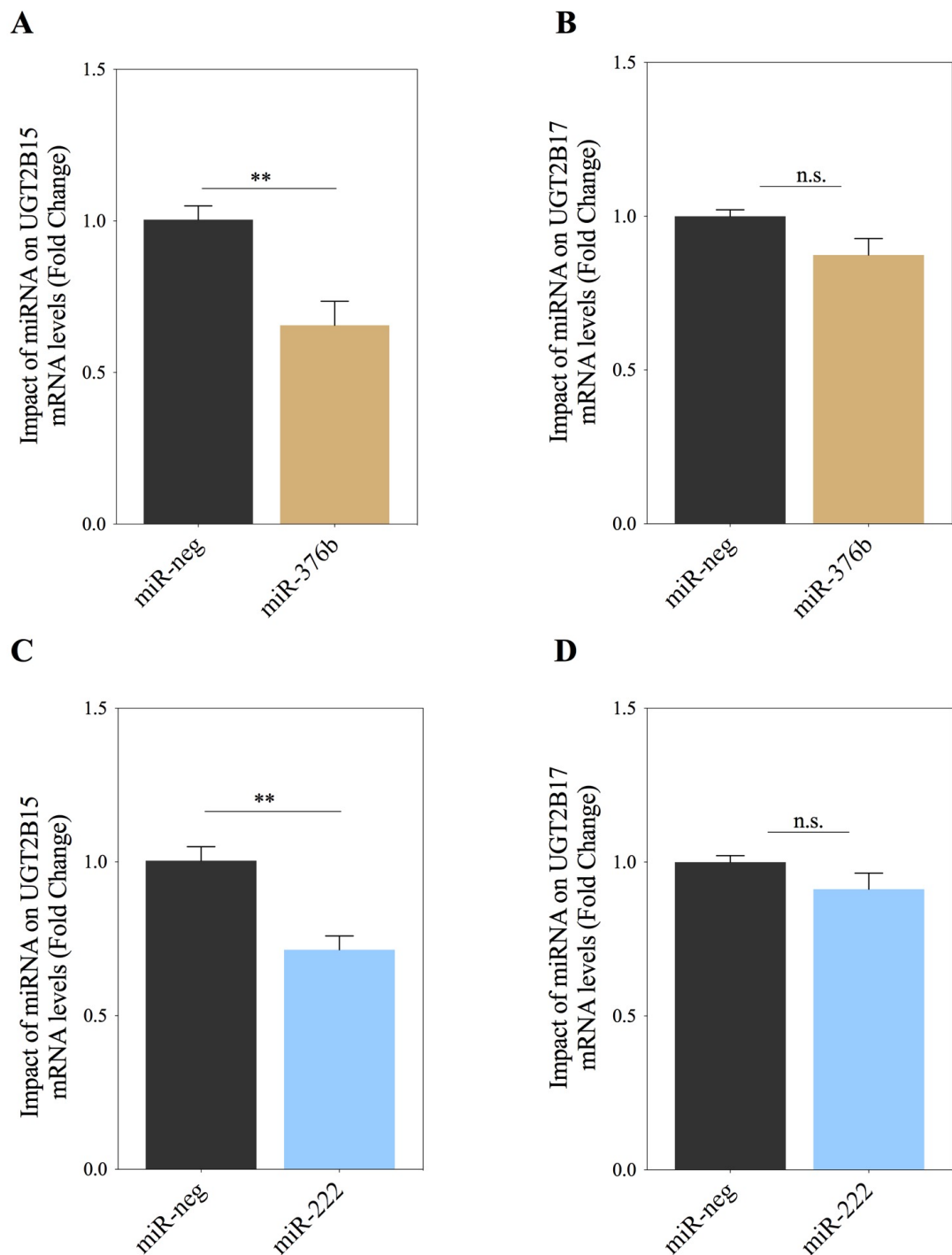
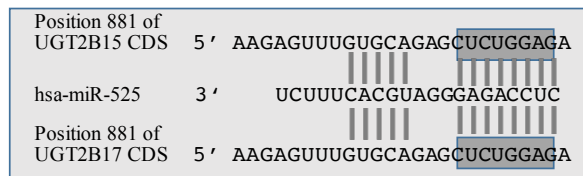


Figure 3.11: miR-376b and miR-222 mimics reduce UGT2B15 mRNA levels in LNCaP cells

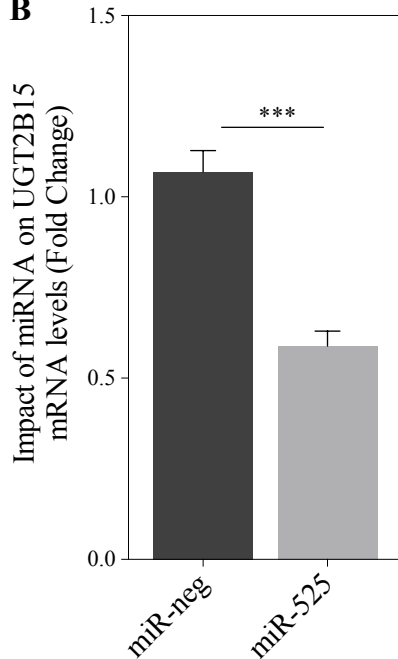
Cells were transfected with miR-neg or mimics of miR-376b or miR-222 and total RNA was harvested 24 hours later and then subjected to RT-qPCR for measuring the mRNA levels of UGT2B15, UGT2B17 and β -actin. After being normalized to β -

actin, the mRNA levels of UGT2B15 (A, C) or UGT2B17 (B, D) in cells transfected with miR-376b or miR-222 are presented relative to those in the respective miR-neg-transfected cells (set at a value of 1). Data shown are mean \pm S.E.M. from three independent experiments performed in triplicate. **P, 0.005.

A



B



C

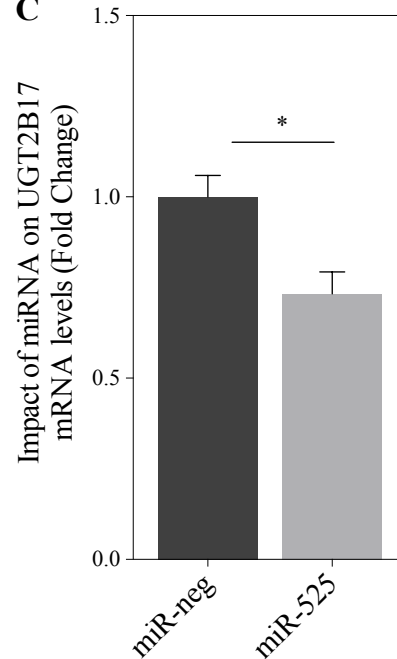


Figure 3.12: MiR-525 reduces the mRNA levels of UGT2B15 and UGT2B17 via possible binding to target sites in the coding regions of the two UGTs

(A) Shown are Watson-Crick pairing between the miRNA seed and its respective predicted binding sites in the UGT2B15 and UGT2B17 coding regions. The seed binding site of the mRNAs are boxed and highlighted in grey. LNCaP cells were transfected with miR-neg or miR-525 mimics and total RNA was harvested 24 hours later and then subjected to RT-qPCR for measuring the mRNA levels of UGT2B15, UGT2B17, and β -actin. After being normalized to β -actin, the mRNA levels of UGT2B15 (B) and UGT2B17 (C) in cells transfected with miR-525 are presented relative to those in the respective miR-neg-transfected cells (set at a value of 1). Data shown are mean \pm S.E.M. from three independent experiments performed in triplicate. ***P < 0.0005, **p < 0.005.

3.3.5 MiR-376c reduces glucuronidation activities of both UGT2B15 and UGT2B17 in LNCaP cells

To define the effects of miRNA-mediated UGT2B15 and UGT2B17 inhibition on cellular glucuronidation capacity, a radioactive thin layer chromatography (TLC) based glucuronidation assay was performed using lysates from miR-mimic-transfected LNCaP cells. Testosterone is a substrate of both UGT2B15 and UGT2B17 (Turgeon et al., 2001). Consistent with the gene expression data, miR-376c mimics significantly reduced the capacity of LNCaP cells to glucuronidate testosterone (Figure 3.13). However, the capacity to glucuronidate testosterone was little affected by either miR-376b or miR-222 in LNCaP cells. These miRNAs only targeted UGT2B15, hence their impact on testosterone glucuronidation may be masked by the 10-fold higher capacity of UGT2B17 to glucuronidate testosterone as compared to UGT2B15 (Turgeon et al., 2001).

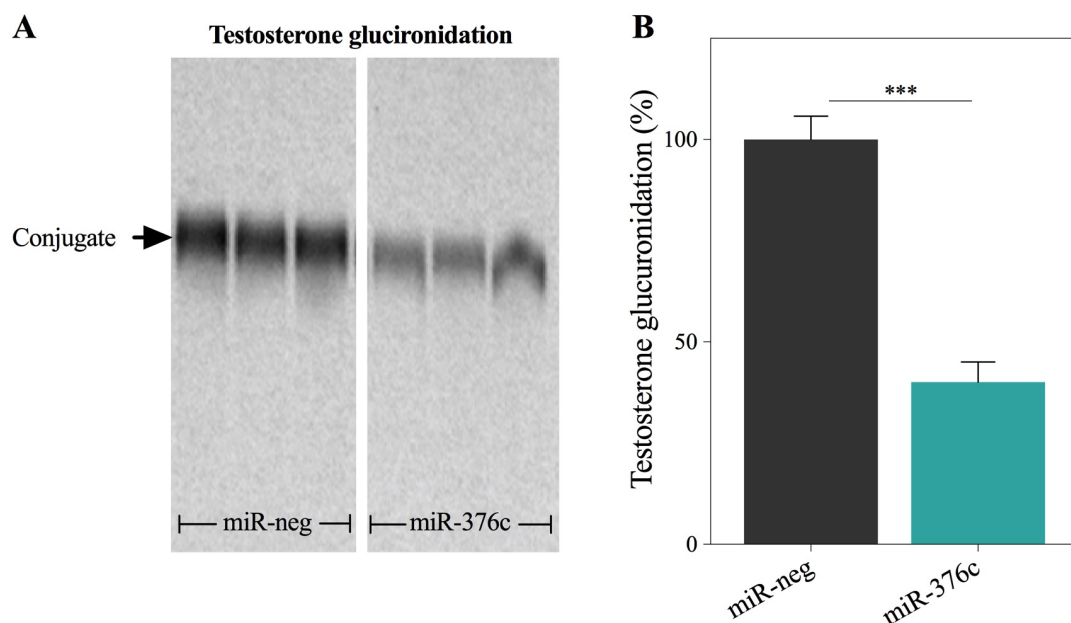


Figure 3.13: MiR-376c mimics reduce the testosterone glucuronidating activity of UGT2B15 and UGT2B17 in prostate cancer LNCaP cells

(A) Cells were cultured in stripped serum containing medium for 48 hours before transfection with miR-neg or miR-376c mimics and then harvested 72h post-transfection. Glucuronidation assays were performed using 25ug of whole cell lysates and C¹⁴ labelled testosterone. After thin layer chromatography separation, the glucuronidated testosterone was quantified using ImageQuant. (B) Quantification of reduction in UGT2B15/2B17 glucuronidation activity in LNCaP cells transfected with miR-376c, compared to miR-neg transfected cells (set at a value of 100%). Data are means \pm S.E.M. from three separate experiments each consisting of triplicates, ***P<0.0001.

In order to confirm specific downregulation of UGT2B15 and UGT2B17 by miR-376c, specific substrates of UGT2B15 and UGT2B17 were sought. Androsterone is glucuronidated by both UGT2B17 and UGT2B7 (Turgeon et al., 2001) and 17 β -estradiol is glucuronidated by UGT2B17, UGT2B7, UGT1A3, UGT1A4, UGT1A8, UGT1A10 and UGT2A1 (Itaaho et al., 2008). However, as LNCaP cells do not express UGT2B7 or any of the UGT1A family enzymes, these substrates could be used for determining the specific glucuronidation activity of UGT2B17. To confirm the predicted specificity of UGT2B17 for androsterone and 17 β -estradiol, activity assays were performed using recombinant UGT2B15 or UGT2B17 expressing supersomes. As shown in Figure 3.14 A, androsterone glucuronidation was detected with recombinant UGT2B17 supersomes. However, 17 β -estradiol glucuronide formation was not detected. Therefore, to confirm the specific downregulation of UGT2B17 activity by miR-376c, the androsterone glucuronidation capacity of miR-376c- or neg-miR-transfected LNCaP cell lysates was measured. As expected, androsterone glucuronidation was significantly reduced by miR-376c (Figure 3.15 A).

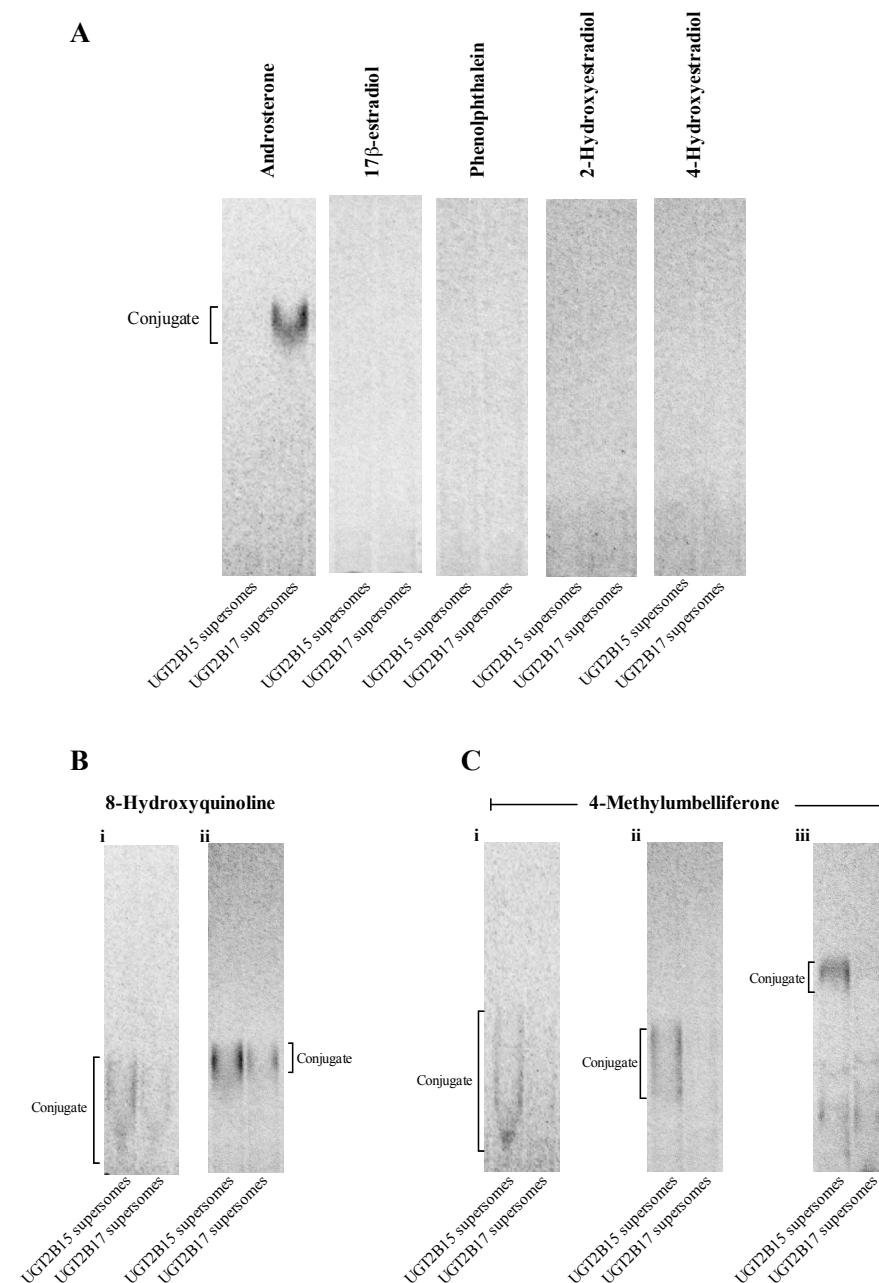


Figure 3.14: Androsterone is a specific substrate of UGT2B17

(A) Glucuronidation assays were performed using 25ug of UGT2B15 and UGT2B17 supersomes and androsterone, 17 β -estradiol, phenolphthalein, 2-hydroxyestradiol or 4-hydroxy estradiol. After thin layer chromatography separation, the glucuronidated substrates (conjugate) was quantified using ImageQuant. (B) Glucuronidation assays were performed using 25ug of UGT2B15 and UGT2B17 supersomes and 8-hydroxyquinoline. (i) Fresh solvent and (ii) solvent prepared 48 hours before was used for liquid chromatography separation and the glucuronidated substrates were then quantified using ImageQuant. (C) Glucuronidation assays were performed using 25ug of UGT2B15 and UGT2B17 supersomes and 4-MU. (i) Fresh solvent, (ii) solvent was prepared 48 hours before thin layer chromatography and (iii) solvent of

butanol/acetone/acetic acid/water (7:7:2:4) was used for chromatography separation and the glucuronidated substrates were then quantified using ImageQuant.

Phenolphthalein, 2-hydroxyestradiol, 4-hydroxyestradiol, 8-hydroxyquinoline and 4-methylumbelliferone (4-MU) are reported to be glucuronidated by UGT2B15 (Green et al., 1994, Turgeon et al., 2001). To determine whether any of these represent specific substrates for UGT2B15 (versus UGT2B17) in LNCaP cells, glucuronidation assays were performed using supersomes. As shown in Figure 3.14 A, there was no detectable glucuronidation of phenolphthalein, 2-hydroxyestradiol and 4-hydroxyestradiol by UGT2B15 or UGT2B17 supersomes. In the 8-hydroxyquinoline activity assay, a smeared glucuronide band was detected with both UGT2B15 and UGT2B17 supersomes (Figure 3.14 Bi). After optimizing the chromatography solvent, glucuronide bands were detectable after incubation with both UGTs, showing that 8-hydroxyquinoline is a substrate of both UGT2B15 and UGT2B17 (Figure 3.14 B ii). The 4-MU glucuronidation assay showed promising results once the chromatography solvent was optimized (Figure 3.14 C). Because an efficient high-performance liquid chromatography (HPLC) assay for 4-MU glucuronidation was available in-house (as detailed in Materials and Methods), this method was substituted for the TLC-based assay in the subsequent studies. The HPLC assays showed that UGT2B15 has an approximately 20-fold higher activity for 4-MU than UGT2B17. As expected, the glucuronidation of 4-MU was significantly reduced by miR-376c (Figure 3.15 B). The contribution of other UGTs to the glucuronidation of 4-MU was considered negligible as only UGT2B15 and UGT2B17 are expressed to any significant extent in LNCaP cells. Any reduction of 4-MU glucuronidation by miR-376b or miR-222 was not assessed due to time constraints and the focus on the more robust regulatory effects of miR-376c.

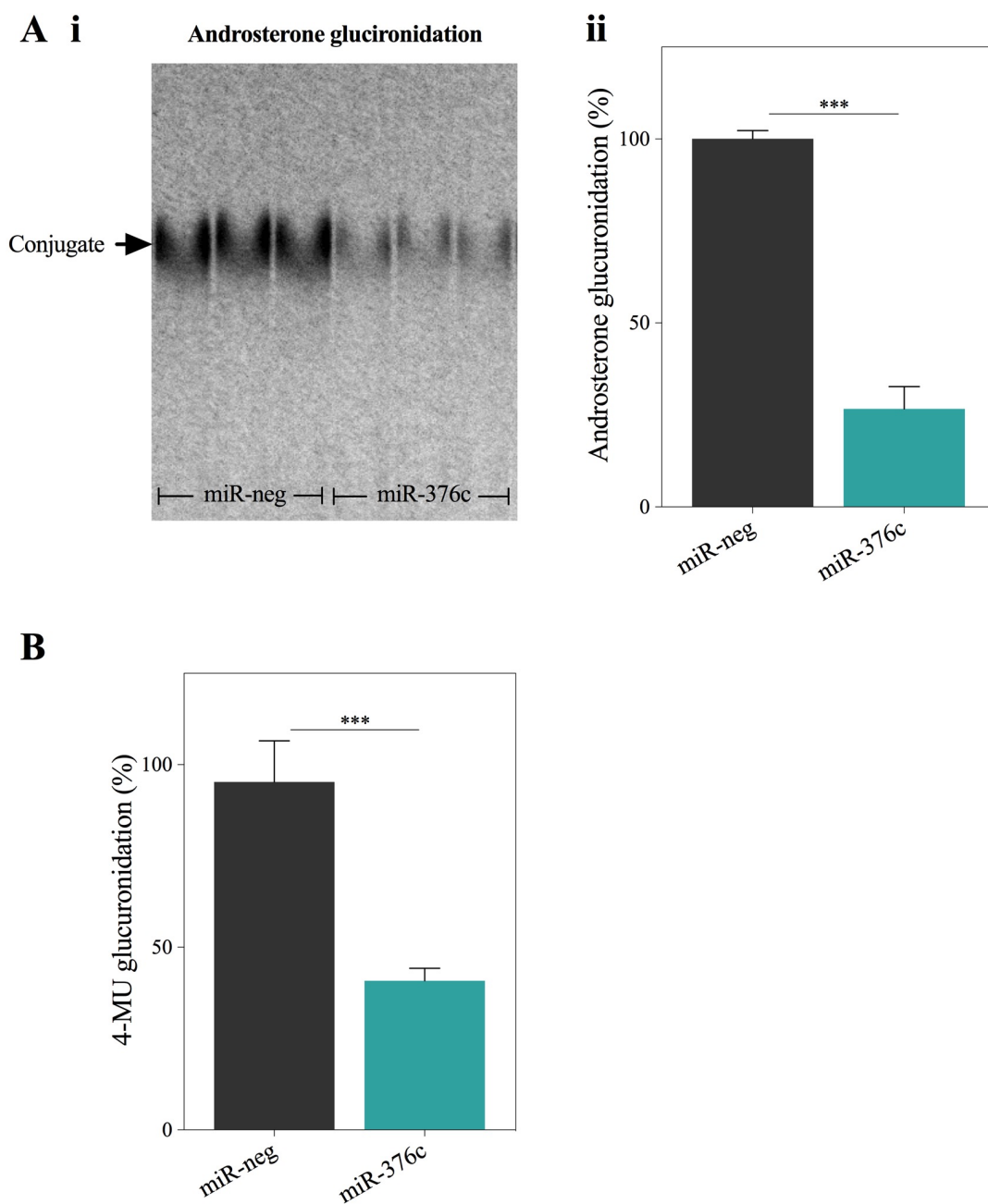


Figure 3.15: MiR-376c mimics reduce the androsterone glucuronidating activity of UGT2B17 and 4-MU glucuronidation activity of UGT2B15 in prostate cancer LNCaP cells

(Ai) Cells were transfected with miR-neg or miR-376c mimics and then harvested 72h post-transfection. Glucuronidation assays were performed using 25ug of whole cell lysates and androsterone as the substrate. After thin layer chromatography separation, the glucuronidated androsterone was quantified using ImageQuant. (Aii) Quantification of reduction in UGT2B17 glucuronidation enzymatic activity in LNCaP cells transfected with miR-376c, compared to miR-neg transfected cells (set at a value of 100%). Data are means \pm S.E.M. from three separate experiments each consisting of triplicates, *** $P < 0.0001$. (B) 4-MU glucuronidation activity in LNCaP cells transfected with miR-376c mimics or miR-neg. Cells were harvested 72 hours

post-transfection and glucuronidation assays were performed with 225ug of lysate using HPLC. The reduction in UGT2B15 glucuronidation enzymatic activity in LNCaP cells transfected with miR-376c is presented compared to that of miR-neg transfected cells (set at a value of 100%). Data are means \pm S.E.M. from two separate experiments each consisting of triplicates, ***P<0.0001.

3.3.6 UGT2B15 and UGT2B17 mRNA levels are inversely correlated to the levels of miR-376c in human tissues.

The expression levels of UGT2B15 and UGT2B17 were obtained by RT-qPCR, from 17 different normal human tissue RNA pools. Each pool of human total RNA was derived from at least three tissue donors. These data revealed that UGT2B15 was predominantly expressed in the liver, followed by colon, small intestine and prostate (Figure 3.16 A). Trachea, esophagus, cervix, thyroid, ovary and thymus expressed UGT2B15 at very low levels and the UGT2B15 expression in all the other tissues was barely detectable. Extremely high expression of UGT2B17 was detected in the colon and the small intestine in comparison to other tissues. UGT2B17 was also well expressed in the liver, but only low levels were detected in the esophagus, kidney, cervix, trachea, thymus, brain, prostate, ovary, thyroid and bladder (Figure 3.16 B).

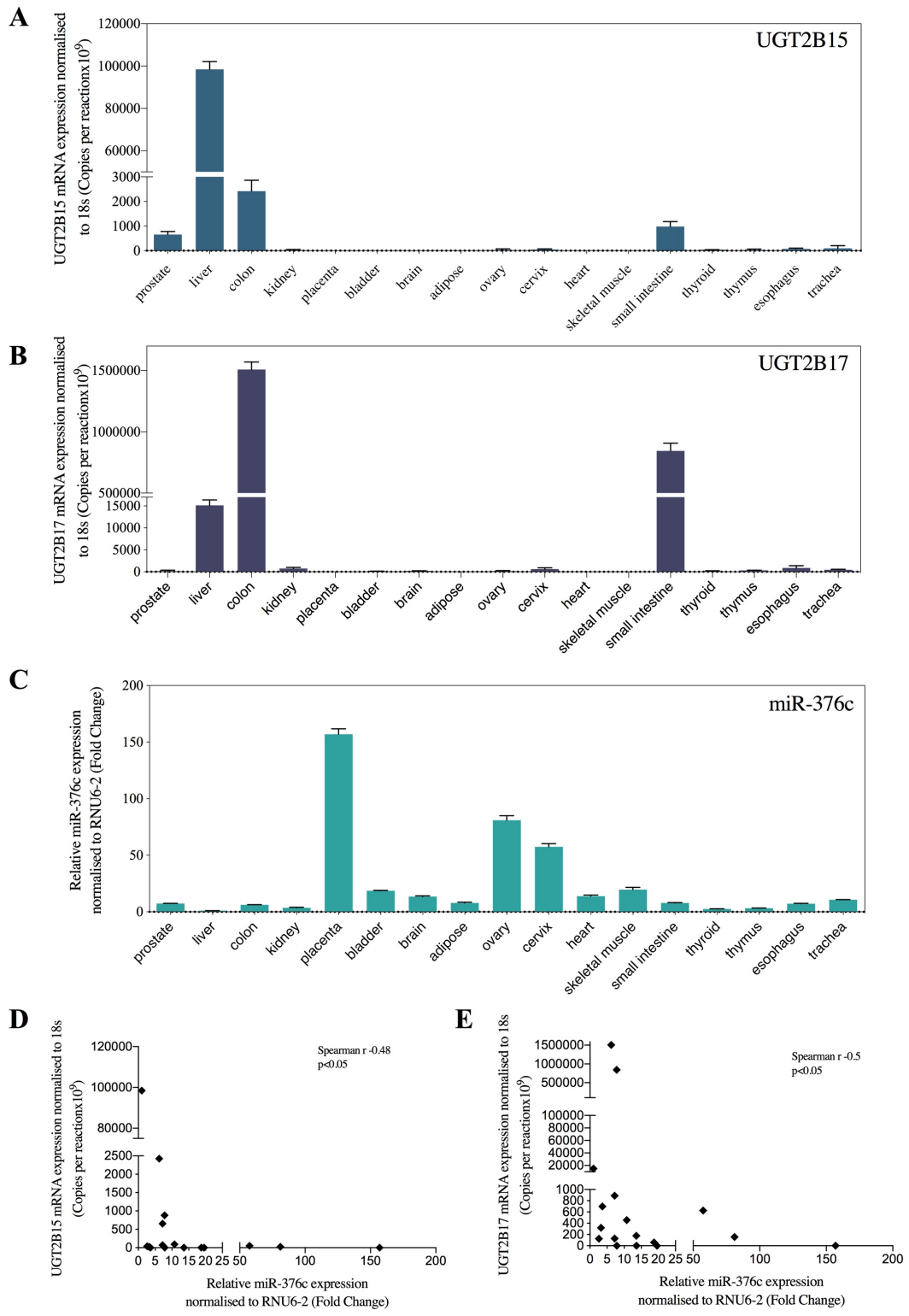


Figure 3.16: Negative correlation between UGT2B15 and UGT2B17 mRNA levels versus miR-376c in human tissues

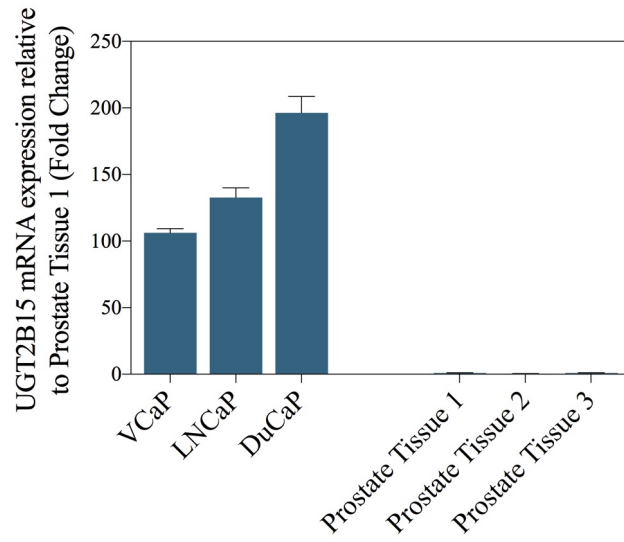
Shown are the expression of UGT2B15 mRNA (A), UGT2B17 mRNA (B), miR-376c (C) in human tissues. A human total RNA survey panel was subjected to RT-qPCR for measuring target gene mRNA levels and miRNA levels. After

normalization with 18S, the UGT2B15 and UGT2B17 mRNA levels were presented as copy numbers per reaction. MiR-376c expression is normalized to RNU6-2 snRNA and presented relative to that of liver (set at a value of 1). Data shown are from a representative experiment performed in triplicate, the error bar representing \pm S.D. (D) Expression of UGT2B15 mRNA versus miR-376c and (E) UGT2B17 mRNA versus miR-376c in human tissues. Data were examined using the Spearman correlation method. Each dot (\blacklozenge) represents the value of an independent tissue sample. $p < 0.05$.

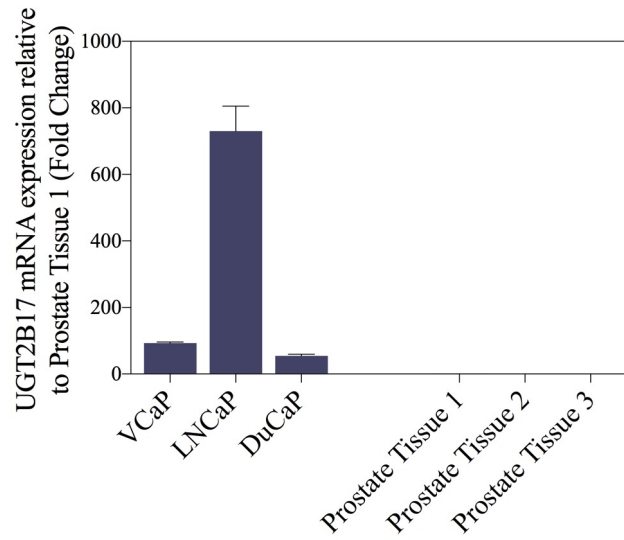
Quantitative real time PCR revealed that miR-376c expression levels in normal human tissue samples were extremely high compared to their expression levels in cancer cell lines. MiR-376c was abundantly detected in the placenta followed by ovary and cervix. MiR-376c had the lowest expression levels in the liver where UGT2B15 and UGT2B17 are expressed at high levels (Figure 3.16 C). As determined by Spearman's correlation test, there was a significant negative correlation between miR-376c expression versus UGT2B15 mRNA expression (Spearman $r = -0.48$; $p < 0.05$; Figure 3.16 D) in the human tissues. In addition, a significant negative correlation was obtained between miR-376c expression versus UGT2B17 mRNA expression as well (Spearman $r = -0.5006$; $p < 0.05$; Figure 3.16 E).

3.3.7 UGT2B15 and UGT2B17 mRNA levels are inversely correlated with the levels of miR-376c in prostate cell lines and tissues.

A



B



C

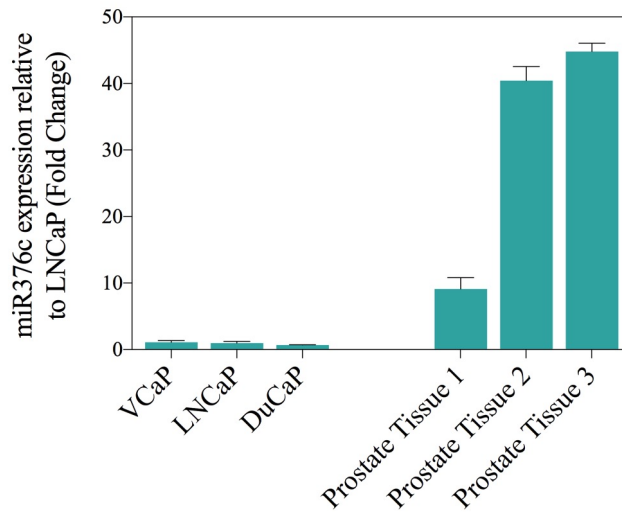


Figure 3.17: Negative correlation between UGT2B15 and UGT2B17 mRNA levels versus miR-376c in androgen receptor–positive prostate cancer cell lines as compared with normal prostate tissues

Shown are the expression of UGT2B15 (A), UGT2B17 (B) mRNA, and miR-376c (C) in prostate cancer cells and normal prostate tissues. The expression levels of UGT2B15, UGT2B17 and miR-376c were quantified by qRT-PCR. UGT2B15 and UGT2B17 mRNA levels were normalized to 18S RNA levels and presented relative to those in Prostate Tissue Sample 1 (set at a value of 1). The miR-376c levels were normalized to RNU6-2 and presented relative to that in LNCaP cells (set at a value of 1). Data shown are mean + 1 S.E.M. from two independent experiments performed in triplicate.

UGT2B15 and UGT2B17 are highly expressed in normal and cancerous prostate tissues (Barbier and Belanger, 2008). These two UGTs are also highly expressed in androgen receptor-positive prostate cancer cell lines such as LNCaP and VCaP, whereas no expression is seen in androgen receptor-negative prostate cancer cell lines such as PC3 and Du145 (Bao et al., 2008, Chouinard et al., 2007, Hu and Mackenzie, 2010, Hu et al., 2010). UGT2B15, UGT2B17 and miR-376c expression levels were measured in three androgen receptor–positive prostate cancer cell lines: LNCaP, VCaP, and DuCaP and three normal pooled prostate RNA samples from different commercial sources using RT-qPCR. As shown in Figure 3.17, prostate cancer cell lines expressed high levels of UGT2B15 and UGT2B17 and low levels of miR-376c compared to normal prostate tissues and vice versa. This inverse correlation between levels of the UGTs and miR-376c suggests a negative regulation of UGT2B15 and UGT2B17 by miR-376c in androgen receptor-positive prostate cancer cell lines.

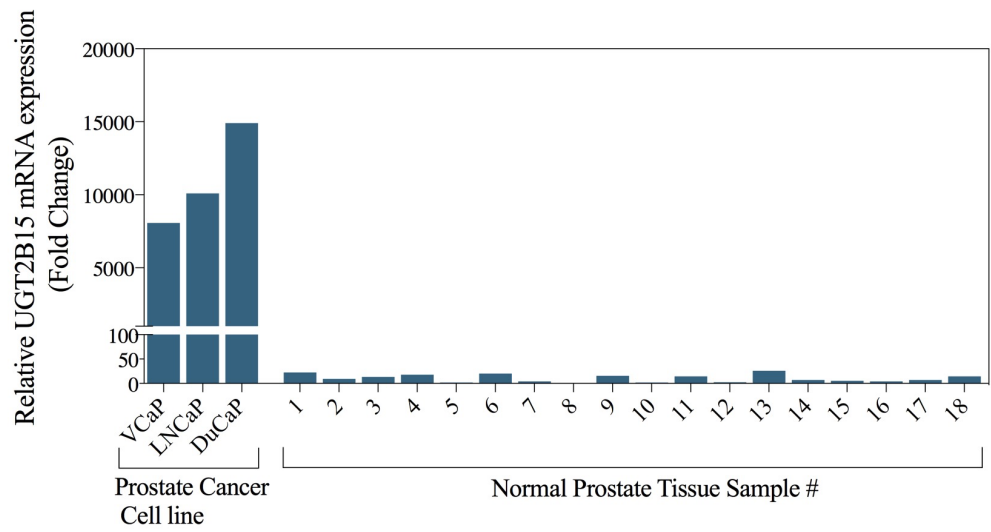
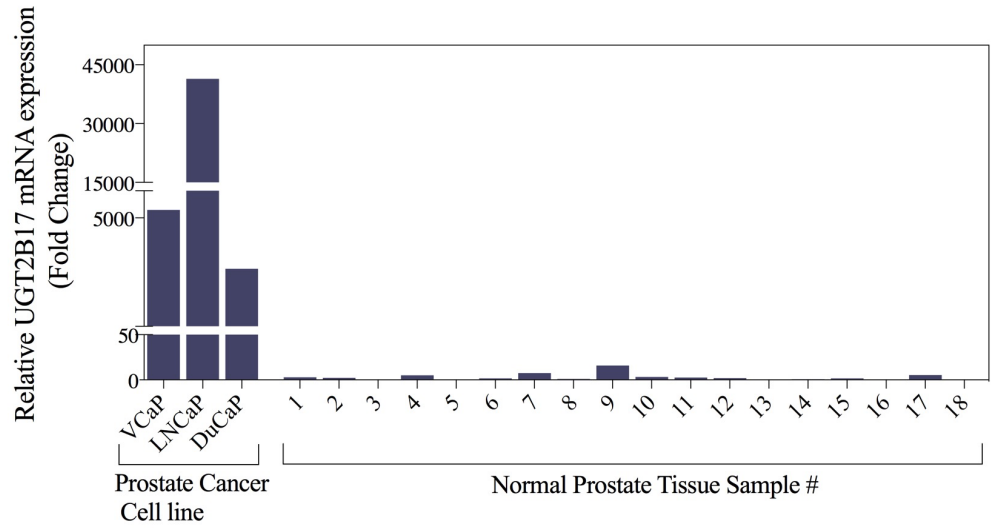
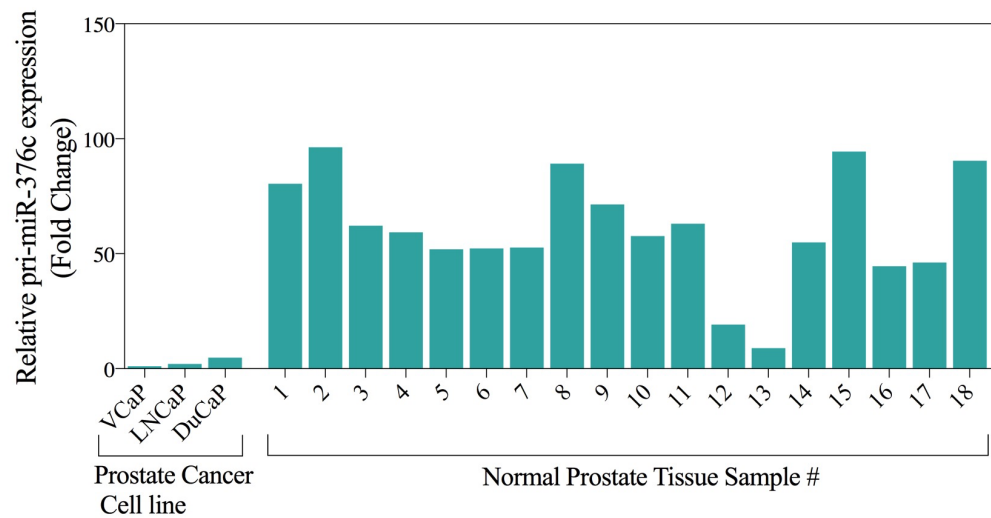
A**B****C**

Figure 3.18: Negative correlation between UGT2B15 and UGT2B17 expression versus pri-miR-376c expression in androgen receptor positive prostate cancer cell lines as compared to 18 normal prostate tissue samples

The expression levels of UGT2B15 (A), UGT2B17 (B) and pri-miR-376c (C) were quantified by qRT-PCR. UGT2B15 and UGT2B17 mRNA levels were normalized to 18S rRNA levels and presented relative to those in the lowest expressing prostate tissue sample #8 (set at a value of 1). Pri-miR-376c levels were normalised to pri-RNU6-2 and presented relative to that in VCaP cells (set at a value of 1).

cDNAs from 18 normal human prostate samples were kindly provided to us by Professor Wayne Tilley (Adelaide University, South Australia). Levels of UGT2B15 and UGT2B17 mRNAs and the primary miR-376c transcript (pri-miR-376c) were measured in these samples. Levels of the pri-miR-376c were also measured in three prostate cancer cell lines (VCaP, LNCaP, and DuCaP). Similar to the data shown in Figure 3.17, an inverse correlation was observed between pri-miR-376c and the two UGTs in the cancer cell lines as compared with normal prostate tissues (Figure 3.18).

3.3.8 UGT2B15/ UGT2B17 mRNA levels show an inverse relationship to miR-376c levels in normal prostate, primary tumour and metastatic prostate cancer tissues.

To further investigate the relationship between UGT2B15, UGT2B17 and miR-376c in human normal prostatic tissues, primary prostate tumour tissues and metastatic prostate tumour tissues, publicly available expression data from the Memorial Sloan-Kettering Cancer Center (MSKCC) Prostate Oncogenome Project was analysed using cbiportal (www.cbiportal.org). This prostatic RNA expression data was generated by Taylor et al. (Taylor et al., 2010) and includes 29 normal prostate, 131 primary tumour and 19 metastatic prostate tumour RNA samples from a total of 179

patients. The mature miRNA expression patterns from 141 out of 179 patients were also available, with 27 normal prostate, 99 primary tumour and 14 metastatic prostate tumour miRNA samples represented (Taylor et al., 2010).

The UGT2B15 and UGT2B17 mRNAs could not be distinguished from each other within this particular dataset due to their high sequence similarity as described in Margailan et al (Margailan et al., 2016); hence a UGT2B15/UGT2B17 combined expression value was obtained for each sample. As shown in Figure 3.19 A, UGT2B15/UGT2B17 mRNA was significantly upregulated in metastatic prostate tumours compared to normal prostate tissues ($p < 0.05$) as well as primary/localized prostate tumours ($p < 0.05$). In contrast, the expression of miR-376c was significantly reduced in both metastatic prostate tumours ($p < 0.0005$) and primary prostate tumours ($p < 0.0005$) as compared to normal prostate tissues. There was a significant reduction in miR-376c levels in metastatic prostate tumours as compared to primary prostate tumours ($p < 0.0005$) as well (Figure 3.19 B). In addition, as shown in Figure 3.19 C, a significant negative correlation between UGT2B15/UGT2B17 mRNA and miR-376c was observed among metastatic prostate tumour tissues (spearman $r = -0.7473$, $p < 0.005$).

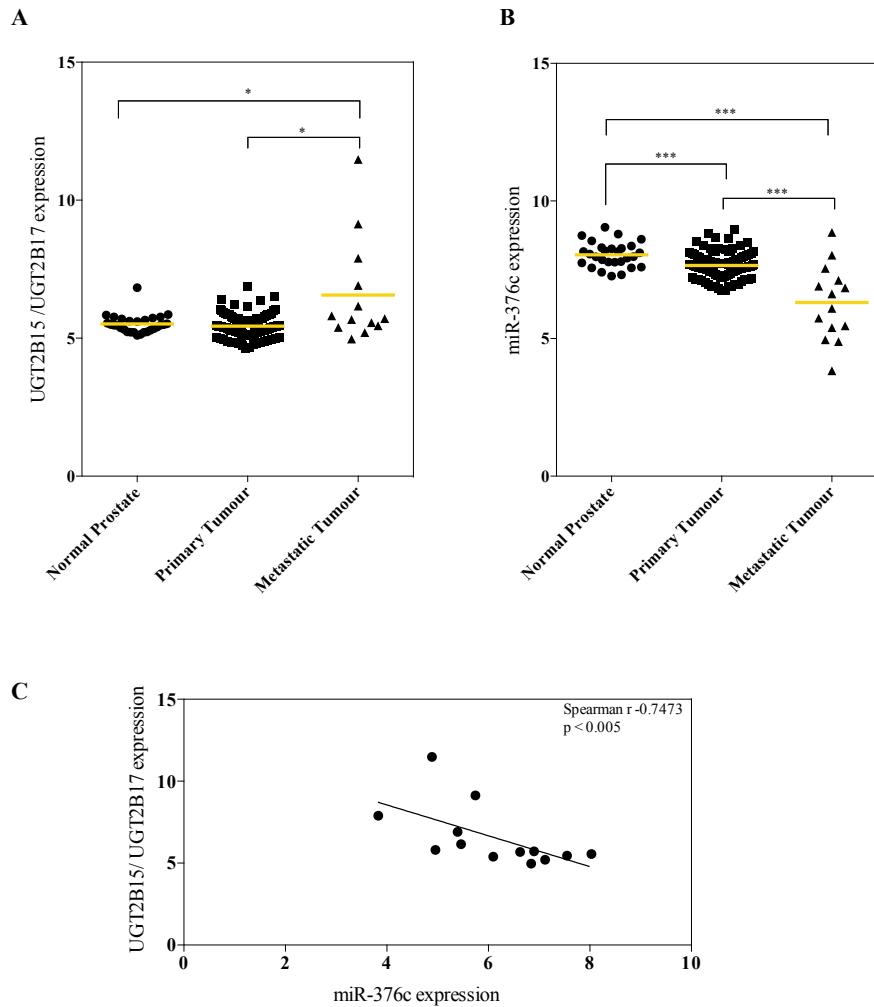


Figure 3.19: Relationship between miR-376c versus UGT2B15 and UGT2B17 normal prostate tissues, primary prostate tumours and metastatic prostate tumours

Analysis of UGT2B15 and UGT2B17 mRNA (A) and miR-376c expression (B) in a total of 179 normal, primary tumour and metastatic prostate tumour tissues. Data was obtained from MSKCC database using cbiportal (www.cbiportal.org), from a study performed by Taylor et al (Taylor et al., 2010). Mean expression levels of either UGT2B15 and UGT2B17 or miR-376c in prostatic tissues (yellow lines) were compared to each prostatic classification group using a 2-tailed Student's t-test. *** $P < 0.0005$, * $p < 0.05$. (C) Negative correlation between UGT2B15 and UGT2B17 expression versus miR-376c expression in 14 metastatic prostate tumour tissues. Data were examined using the Spearman correlation method. Each symbol represents the value of an independent tissue sample. $p < 0.05$.

As miR-376b and miR-222 also target UGT2B15, the relationship between UGT2B15/UGT2B17 and the levels of these two miRNAs in prostate tissues was

also examined. However, miR-376b showed no significant difference in expression between normal, primary tumour and metastatic prostate tumours. Interestingly, miR-222 showed a similar pattern to miR-376c in these tissues. As shown in Figure 3.20, miR-222 levels were significantly reduced in primary prostate tumours ($p < 0.0001$) and metastatic prostate tumours ($p < 0.0001$) as compared to normal prostate tissues. The metastatic tumours showed a further reduction in miR-222 as compared to primary tumours ($p < 0.0001$).

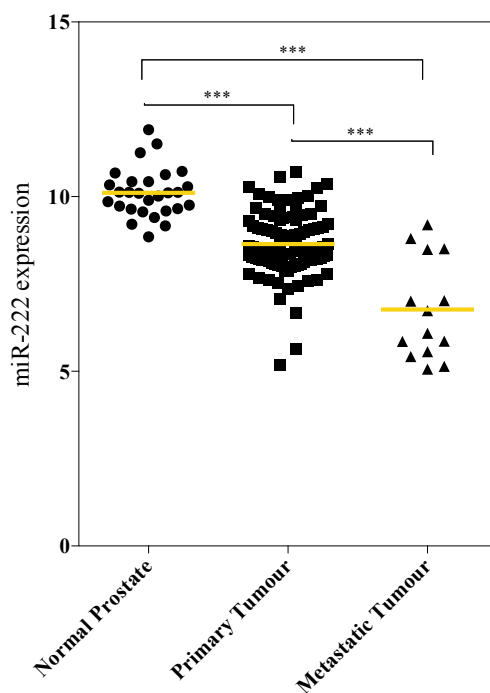


Figure 3.20: Relationship between miR-222 levels in normal prostate tissues, primary prostate tumours and metastatic prostate tumours

Analysis of miR-222 expression in a total of 141 normal, primary tumour and metastatic prostate tumour tissues from a study performed by Taylor et al (Taylor et al., 2010). Mean expression levels of miR-222 in all normal, primary tumour and metastatic tissues (yellow lines) were compared to each other using a 2-tailed Student's t-test. *** $P < 0.0005$. Each symbol represents the value of an independent tissue sample.

3.4 Discussion

Given the importance of UGT2B15 and UGT2B17 in inactivating testosterone and DHT and their expression in the prostate, fine control of their intraprostatic expression and enzymatic activity becomes essential for the maintenance of androgen signaling homeostasis and activity in the prostate (Chouinard et al., 2007, Chouinard et al., 2008, Turgeon et al., 2001). Both UGT2B15 and UGT2B17 are highly expressed in AR positive prostate cancer cell lines (Figure 3.17 and (Chouinard et al., 2006, Hu et al., 2010), and previous studies have extensively examined their transcriptional regulation in these contexts (Guillemette et al., 1997, Levesque et al., 1998, Guillemette et al., 1996, Chouinard et al., 2006, Bao et al., 2008, Kaeding et al., 2008a, Kaeding et al., 2008b). However, prior to this study, the post-transcriptional regulation of UGT2B15 and UGT2B17 in prostate cancer cells had not been explored. The data presented here shows that UGT2B15 and/or UGT2B17 expression is regulated at the post-transcriptional level via miRNAs including miR-376c, miR-376b, miR-222 and possibly miR-525.

The sequence identity between UGT2B15 and UGT2B17 mRNAs is approximately 95% and their 3'UTRs have similar lengths (513 bp and 463 bp for UGT2B15 and UGT2B17, respectively). They exhibit high homology in the 210-bp region at the 5'-end of their 3'UTRs but diverge considerably in the 3'-region (Figure 3.1). This sequence similarity and divergence may allow regulation of both UGTs by common miRNAs with target sites in the conserved part of their 3'-UTR sequences but might also permit their differential regulation by miRNAs with target sites in the divergent regions. Indeed, in this study miR-376c was found to negatively regulate both UGT2B15 and UGT2B17 via a miR-376c target site that is highly conserved in both

position and sequence within the conserved region of the 3'-UTR sequences (Figure 3.6). As previously mentioned, this miR-376c target site is classified as a 7mer-8m site and there is only a C/U mismatch at position 19 between the two sites and a G-deletion at position 17 in the UGT2B15 miR-376c target site. Negative regulation of UGT2B15 but not UGT2B17 by miR-222 through a 7mer-m8 target site was also shown. This site is present in the region of the UGT2B15 3'-UTR that differs from the UGT2B17 3'-UTR sequence (Figure 3.6). Interestingly, miR-376b negatively regulated only UGT2B15 and not UGT2B17, even though the miR-376b target site is identical in sequence and located at a similar position within the conserved region of the UGT2B15 and UGT2B17 3'-UTRs (Figure 3.6). Thermodynamic properties of the miRNA:mRNA duplex formation and accessibility of the RISC complex to the target site, play a major role in miRNA binding to its target mRNA, and this can be influenced by secondary structures in the target mRNA (Hofacker, 2007). It is possible that the secondary structure of the UGT2B17 3'UTR is unfavourable for effective miR-376b binding or recruitment of the RISC.

MiRNAs regulate target gene expression at the post-transcriptional level by mRNA degradation and/or translational inhibition (Hu and Coller, 2012). The present study showed that miRNAs can reduce UGT2B15 and/or UGT2B17 mRNA levels, indicating their capacity to promote mRNA degradation. This could contribute to the observed miR-376c-mediated reduction in UGT2B17 protein levels; however, direct translational inhibitory effects of these miRNAs on UGT2B15 and/or UGT2B17 remain to be investigated in future studies.

The miR-376c cluster on human chromosome 14 (human 14q32.31), encodes four pri-miRNAs (miR-376a1, miR-376a2, miR-376b and miR-376c previously known as

miR-368). The miR-376 cluster pri-miRNA complex is processed further into 5 mature miRNAs; miR-376a, miR-376a*, miR-376a2-5p, miR-376b, and miR-376c with high sequence similarity (Kawahara et al., 2007, Baker and Delles, 2013, Choudhury et al., 2012). In this study the regulation of UGT2B15 and UGT2B17 by miR-376a, miR-376b and miR-376c was investigated. Despite the same miR-cluster origin and their sequence similarities, all three miRNAs differed in their effects on their targets. MiR-376c targeted the 3'UTRs of both UGT2B15 and UGT2B17, miR-376a did not target either UGT, and miR-376b targeted only UGT2B15. The miR-376a and miR-376b predicted target sites in UGT2B15 and UGT2B17 were the same (Figure 3.1), suggesting that miRNA activity is controlled by factors other than just target site recognition, these may include RNA secondary structure as discussed above.

Several human genes have been shown to be direct targets of miR-376c, including growth factor receptor-bound protein 2 (GRB2) in intrahepatic cholangiocarcinoma cells (Iwaki et al., 2013), activin receptor-like kinase 7 and 5 (ALK7 and ALK5) in ovarian cancer cells (Ye et al., 2011a), transforming growth factor-alpha (TGFA) in osteosarcoma cancer cells (Jin et al., 2013) and insulin growth factor 1 receptor (IGF1R) in melanoma cell lines (Zehavi et al., 2012). The present study reveals UGT2B15 and UGT2B17 as novel targets of miR-376c in prostate cancer cells. Several studies have reported an upregulation of miR-376c in a subset of acute myeloid leukemias (Dixon-McIver et al., 2008), plasma of breast cancer patients (Cuk et al., 2013a, Cuk et al., 2013b) and sera of gastric cancer patients (Song et al., 2012), suggesting its role as an oncogenic microRNA which can be used as a potential biomarker for detection of the aforementioned cancers. Although, miR-376c was upregulated in plasma of breast cancer patients, it was also reported that

the expression of miR-376c is downregulated in malignant breast tissue compared to benign breast tissue (Cuk et al., 2013a). Several studies have reported differences in microRNA expression patterns in the tissue and circulation of cancer patients but the cause of this remains unknown (Cuk et al., 2013a, Roth et al., 2010, van Schooneveld et al., 2012).

MiR-376b has been reported to be a regulator of hypoxia-inducible factor 1 α (HIF1 α) in HUVEC cells (Li et al., 2014) and ATG4C and Beclin-1 (BECN1) autophagy protein in MCF7 and Huh7 cells (Korkmaz et al., 2012). The present study identified miR-376b as a direct regulator of UGT2B15 in prostate cancer cells; how this UGT may fit into a larger regulatory network controlled by miR-376b in this context remains to be determined.

MiR-221 and miR-222 are encoded in tandem from a gene cluster on the short arm of chromosome X and their expression is presumably controlled by shared regulatory mechanism (Galardi et al., 2007). These two miRNAs have identical seed sequences and theoretically target the same site. In this study, miR-222 regulated UGT2B15; however, miR-221 was not studied. To date, cumulative evidence shows that these two miRNAs are amongst the most frequently overexpressed miRNAs in a variety of human tumours, including glioblastoma (Ciafre et al., 2005), melanoma (Felicetti et al., 2008), hepatocellular carcinoma (Gramantieri et al., 2008), thyroid papillary carcinoma (Visone et al., 2007), kidney and bladder cancers (Gottardo et al., 2007), gastric cancer (Kim et al., 2009), pancreatic cancer (Lee et al., 2007) and ovarian cancer (Dahiya et al., 2008). More interestingly, it appears that these two miRNAs are downregulated in prostate cancer (Spahn et al., 2010, Porkka et al., 2007, Ambs

et al., 2008, Tong et al., 2009). Thus further investigation of the role of UGT2B15 in the regulatory network controlled by miR-222 in prostate would be of interest.

MiR-525 is encoded from the C19MC gene cluster located at 19q13.42 in chromosome 19 (Miura et al., 2015). Studies have demonstrated that miR-525 regulates A Disintegrin And Metalloprotease with Thrombospondin type I repeats-13 (ADAMTS13) in a model of cell ischemia (Zhao et al., 2015), vasoactive intestinal peptide (VIP) receptor type 1 (VPAC1) in primary monocytes and the U937 cell line (Cocco et al., 2010) and phosphatidylinositol-4,5-Bisphosphate 3-Kinase Catalytic Subunit Alpha (PIK3CA) in colorectal cancer cells (Arcaroli et al., 2012). This miRNA is also downregulated in colon tumours compared to normal colon (Mullany et al., 2015). The present study showed that miR-525 reduces both UGT2B15 and UGT2B17 mRNA levels in LNCaP cells. Further studies are needed to determine whether these two UGTs are a direct target of miR-525. In addition to miR-376c, miR-376b, miR-222 and miR-525, the UGT2B15 and UGT2B17 3'-UTRs contain putative binding sites for several other miRNAs. However, mimics for these miRNAs (miR-147, miR-1289, miR-376a, miR-3911, miR-450b-5p, miR-489, miR-548x, miR-656, miR-125b, miR-382, miR-21, miR-105, miR-409, miR-494 and miR-375-3p) had no consistent impact on mRNA levels of UGT2B15 or UGT2B17 or the activity of the UGT2B15 or UGT2B17 3'-UTR luciferase reporter constructs in LNCaP or Du145 cells. It is possible however, that the activities of these miRNAs are cell context dependent, and it may be useful to screen some of these miRNAs in other cell lines. Such cell type dependence of miRNA activity could be due to the presence of other miRNAs or proteins that can bind to the 3'UTR.

Deregulation of miRNA expression is widely seen in prostate cancers (Ozen et al., 2008). In the present study miR-376c was downregulated in prostate cancer cell lines as compared to normal prostate tissues (Figure 3.17). Moreover, there was a negative correlation between the two UGTs and pri-miR-376c expression in androgen receptor positive prostate cancer cell lines as compared to 18 normal prostate tissue samples (Figure 3.18). Lower levels of miR-376c in metastatic cell lines as compared with normal prostatic epithelial cells has also been reported previously (Formosa et al., 2014). Analysis of the MSKCC prostate cancer database (Taylor et al., 2010) showed that the expression patterns of miR-376c and UGT2B15/UGT2B17 are inversely correlated in normal prostate, primary tumours and metastatic tumours (Figure 3.19). MiR-376c is downregulated in primary tumours compared to normal prostate tissues and levels are further reduced in metastatic prostate tumour tissues whereas UGT2B15/UGT2B17 was elevated in metastatic tumours compared to both normal prostate tissues and primary tumours. Furthermore, a significant inverse correlation between miR-376c and UGT2B15/UGT2B17 expression was observed in a set of metastatic prostate tumour tissues. Consistent with these findings, other published studies have reported that miR-376c is downregulated in prostate cancer tissues (especially in advanced metastatic and invasive tumours) as compared to normal prostate tissues (Srivastava et al., 2013, Formosa et al., 2014). In addition, other studies have reported that UGT2B15 and/or UGT2B17 are upregulated in metastatic androgen-independent prostate cancer as compared to primary prostate cancer (Montgomery et al., 2008, Stanbrough et al., 2006, Hornberg et al., 2011, Zhang et al., 2011, Mitsiades et al., 2012) and raise the possibility that high UGT2B15/UGT2B17 expression could be associated with tumor aggressiveness. Combined with these reports, our findings suggest that miR-376c downregulation

might enhance the expression of UGT2B15 and UGT2B17 in prostate cancer in vivo and may partly contribute to their upregulation in metastatic prostate tumours.

MiR-222 shows a similar expression pattern to miR-376c in normal prostate, primary tumour and metastatic tumours (Figure 3.20). Consistent with our data, a recent study shows that both miR-221 and miR-222 are downregulated in prostate cancer tissues and castrate-resistant prostate cancer tissues and that they are involved in prostate cancer progression (Goto et al., 2015). As miR-222 directly targets UGT2B15, downregulation of miR-222 in turn might partially lead to upregulation of UGT2B15 levels in the prostate cancer tissues.

In summary, the present study demonstrates UGT2B15 is a direct target of miR-376c, miR-376b and miR-222 and UGT2B17 is a direct of miR-376c. This provides the first evidence for post-transcriptional regulation of UGT2B15 and UGT2B17 by miRNAs in prostate cancer cells. Altered expression of miRNAs especially miR-376c in the prostate, may have a role in fine-tuning intraprostatic androgen signalling homeostasis and activity through modulating the androgen glucuronidation pathway and hence, may impact on the risk of developing prostate cancer as well as possibly influencing cancer progression to the metastasis stage.

CHAPTER 4

REGULATION OF *UGT2B15* EXPRESSION BY MIR-331-5P

Published as: Wijayakumara DD, Mackenzie PI, McKinnon RA, Hu DG, Meech R (2018), 'Regulation of UDP-Glucuronosyltransferase 2B15 by miR-331-5p in Prostate Cancer Cells Involves Canonical and Noncanonical Target Sites'. *Journal of Pharmacology and Experimental Therapeutics*, 365(1):48-59.

Reproduced with permission of the American Society for Pharmacology and Experimental Therapeutics. All rights reserved.

4.1 Introduction

As detailed in Chapter 1, androgen/AR signaling is vital for normal prostate development and function; however, excessive androgen signaling contributes to prostate carcinogenesis (Kaarbo et al., 2007). UGT2B15 and UGT2B17 are expressed in the prostate and also in the liver where they inactivate various androgens. The regulation of these UGTs in these contexts is therefore relevant to the control of both local and systemic androgen levels, which can impact on prostate cancer development (Chouinard et al., 2007, Heinlein and Chang, 2004, Turgeon et al., 2001).

This Chapter extends on studies shown in Chapter 3, and demonstrates that miR-331-5p is a regulator of UGT2B15 that may be relevant to its control in both prostate and liver contexts. The data presented here reveal that miR-331-5p targets UGT2B15 by

binding to 2 sites in the 3'UTR that include a canonical site with perfect Watson-crick seed pairing and a non-canonical site with imperfect pairing at the 3' end of miR-331-5p. The expression of UGT2B15 and miR-331-5p were inversely correlated in a panel of human tissues including liver, and also in a liver cancer data set, but not in a prostate cancer data set. Intriguingly, UGT2B17 was not regulated by miR-331-5p despite the high sequence similarity between UGT2B15 and UGT2B17. Thus miR-331-5p is a differential regulator of these UGTs.

4.2 Methods

4.2.1 Luciferase plasmid Construction

pGL3/2B15/UTR and pGL3/2B17/UTR luciferase reporter plasmids were generated as previously described in Chapter 3. Using the pGL3/2B15/UTR (wild-type) construct as a template and the QuickChange site-directed mutagenesis kit (Stratagene, La Jolla, CA), the miR-331-5p seed sequence (5'-AUACCUA-3') was changed to 5'-CGCAACA-3' or completely deleted, producing the mutated construct pGL3/2B15/UTR/miR-331-5p/MT1 and pGL3/2B15/UTR/miR331-5p/delMT respectively (Figure 4.6 A).

Eight additional pGL3-promoter derived luciferase reporter constructs containing different segments of 2B15 3'UTR were constructed for this study in order to define the second miR-331-5p binding site (Figure 4.6 A). Different segments of UGT2B15 3'UTR were amplified using pGL3/2B15/UTR as the template and Phusion hot start high-fidelity DNA polymerase (Thermo Fisher Scientific) and cloned into the XbaI site of the pGL3 promoter vector, generating 8 constructs named pGL3/2B15/UTR(1-75) (75bp in length), pGL3/2B15/UTR(1-150) (150bp in length),

pGL3/2B15/UTR(1-225) (225bp in length), pGL3/2B15/UTR(1-314) (314bp in length), pGL3/2B15/UTR(1-384) (384bp in length), pGL3/2B15/UTR(244-314) (71bp in length), pGL3/2B15/UTR(244-384) (141bp in length) and pGL3/2B15/UTR(244-454) (211bp in length). The constructs were named relative to the nucleotide G (set as position 0) of the stop codon TAG of UGT2B15 mRNA (NM_001076.3).

As shown in Figure 4.6 B, mutations of the 2B15/1-150 construct, which contains the UGT2B15 3'UTR between nucleotides +1 and +150, were created at site A (MT1 and MT2) and site B (MT3) which were predicted by RNAhybrid (Kruger and Rehmsmeier, 2006) as putative miR-331-5p target sites and also at three other positions as negative controls (MT4, MT5, and MT6). The sequences of the six mutants were changed from 5'-TCCTG-3' to 5'-AGAAC-3' in MT1, 5'-TACCT-3' to 5'-GTAGC-3' in MT2, 5'-CCAGG-3' to 5'-AGCGA-3' in MT3, 5'-ATTTA-3' to 5'-CGAGC-3' in MT4, 5'-CAAAA-3' to 5'-AGCGC-3' in MT5, 5'-TTTCA-3' to 5'-CAGAG-3' in MT6. To investigate the cooperativity of the two miR-331-5p sites, the first site (site 1) and the second site (site 2) were mutated separately (MT A, MT B, MT D) and simultaneously (MT C, MT E) using the pGL3/2B15/UTR reporter construct as the template (Figure 4.7 A). The identities of all constructs were confirmed by DNA sequencing. The sequences of the primers used for mutagenesis are given in Table 4.1.

4.2.2 Analyses of Prostate Adenocarcinoma (PRAD) and Hepatocellular Carcinoma Data Sets.

RNA-seq and miRNA-seq data from The Cancer Genome Atlas (TCGA) liver hepatocellular carcinoma (LIHC) and Prostate adenocarcinoma (PRAD) datasets

were downloaded from the TCGA data portal (<https://gdc-portal.nci.nih.gov/>) by Dr. Shashi Marri (Flinders genomics Facility, Flinders University. The RNA expression level of the LIHC (371 tissues) and PRAD (498 tissues) RNA-seq datasets were represented in the form of high-throughput sequencing counts. Genes (protein coding and noncoding) with a mean of less than 10 counts were discarded; the counts of the remaining genes were normalized using the upper quantile normalization method (<https://gdc-portal.nci.nih.gov/>).

4.2.3 Statistical Analysis

Statistical analysis of all data was performed using GraphPad Prism 6 software (La Jolla, CA, USA), with a two-tailed Student's independent t-test. Correlation analyses between the expression levels of UGT and miRNA gene sets were conducted using the Spearman rank method and plots were drawn using the R statistical package (<https://cran.r-project.org/>; R Foundation for Statistical Computing, Vienna, Austria). Correlations between UGT2B15 and UGT2B17 mRNA versus miR-331-5p expression in human tissues were analysed using one-tailed Spearman correlation. p-values <0.05 were considered statistically significant.

Table 4.1: Primers used in this study for mutagenesis, cloning and qPCR (5'–3')

Primer	Sequence (5' - 3')
<i>Site directed mutagenesis</i> 2B15_miR331-5p_F or MT_A_F 2B15_miR331-5p_R or MT_A_R	GATAGCATTGGAGATCGCAACAATGTTAAATGACGA TCGTCATTTAACATTGTTGCGATCTCCAAATGCTATC
2B15_miR-331-5p/delMT_F 2B15_miR-331-5p/delMT_R	GGGGAAGGATAGCATTGGAGATATGTTAAATGACGAGT ACTCGTCATTTAACATATCTCCAAATGCTATCCTTCCCC
MT_B_F and MT_C_F MT_B_R and MT_C_R	GACAAAATTTATTTAGCGAGATTTAATACGTAC GTACGTATTAATCTCGCTAAAATAAATTTTGTC

MT D_F and MT E_F MT D_F and MT E_R	TTTTCCAGGGATTACGCAGTACTTTAGCTGGAA TTCCAGCTAAAGTACTGCGTAAATCCCTGGAAAA
MT1_F MT1_R	GAGGATTTCTTTTAGACTTGACAAAACATCTTTTC GAAAAGATGTTTTGTCAAGTCTAAAAGGAAATCCTC
MT2_F MT2_R	CATCTTTTCACAACGTAGCTGTAAAGACAAAATT AATTTTGTCTTAACAGCTACAGTTGTGAAAAGATG
MT3_F MT3_R	GACAAAATTTATTTTAGCTAGATCTAGAGTCGGGGC GCCCCGACTCTAGATCTCGCTAAAATAAATTTTGTCT
MT4_F MT4_R	CCTTGTTAAGACAAACGAGCTTTTCCAGGGATCTAG CTAGATCCCTGGAAAAGCTCGTTTGTCTTAACAAGG
MT5_F MT5_R	TCCTTTTCTGTGAAGCGCCATCTTTTCACAAC GTTGTGAAAAGATGGCGCTTCACAGGAAAAAGGA
MT6_F MT6_R	TGTGACAAAACATCTCAGAGCACTTACCTTGTTAAG CTTAACAAGGTAAGTTGCTCTGAGATGTTTTGTCACA
<u>Cloning</u> 2B15/3UTR_F1 2B15/3UTR (1-75)_R 2B15/3UTR (1-150)_R 2B15/3UTR (1-225)_R 2B15/3UTR (1-314)_R 2B15/3UTR (1-384)_R 2B15/3UTR_F2 2B15/3UTR (244-318)_R 2B15/3UTR (244-384)_R 2B15/3UTR (244-454)_R	CCGCTCTAGATTATATCAAAAAGCCTGAAGT CCGCTCTAGACATTTAAAACCCTCCATGCT CCGCTCTAGATCCCTGGAAAATAAATTTTG CCGCTCTAGAATCCTTCCCCCATTGTATT CCGCTCTAGAGCAGGTTAGCTACATATGTA CCGCTCTAGAAAGAGTTGTATTTTTTTTTTT CCGCTCTAGAAATGTTAAATGACGAGTTAC CCGCTCTAGAGCAGGTTAGCTACATATGTA CCGCTCTAGAAAGAGTTGTATTTTTTTTTTT CCGGTCTAGAGACACTTTATTTTCAGATCC
<u>RT-qPCR</u> miR331-5p_qPCR_F miR-331-5p_qPC_R	GCAGCTAGGTATGGTCCCA CCAGTTTTTTTTTTTTTTGGATCCC

4.3 Results

4.3.1 The 3'UTR of UGT2B15 contains a putative canonical target site for miR-331-5p

Bioinformatic analysis of UGT2B15 3'-UTR by TargetScan (release 7.0: August 2015) was used to identify putative miRNA target sites. A miR-331-5p target site was the top ranked hit based on the context score percentile given by program (Figure 4.1). The miRNA-331-5p target site at nucleotides 224-249 of the UGT2B15 3'UTR, is classified as a 8mer site (a pairing to the 2–7 nt miRNA seed and nucleotide 8 plus an A at nucleotide 1, mentioned in Chapter 3, Figure 4.5) (Lewis et al., 2005) and has a context score percentile of 98% (Grimson et al., 2007). As this site matches perfectly to miR-331-5p at nucleotides 2–7 (seed pairing) and nucleotides 13–15 (3'-pairing), it is considered a canonical miR-331-5p target site (Grimson et al., 2007, Lewis et al., 2005). There was no miR-331-5p target site predicted in the 3'UTR of UGT2B17 using the TargetScan program. At the time that this study commenced, this canonical miR-331-5p binding site in UGT2B15 had not been reported; however, recently identified in a study by Margaillan *et al* (Margaillan et al., 2016). However, Margaillan *et al* only examined the site using 3'UTR luciferase reporter assays. In the present study, the ability of miR-331-5p to regulate endogenous UGT2B15 expression at mRNA, protein, and activity levels was assessed.

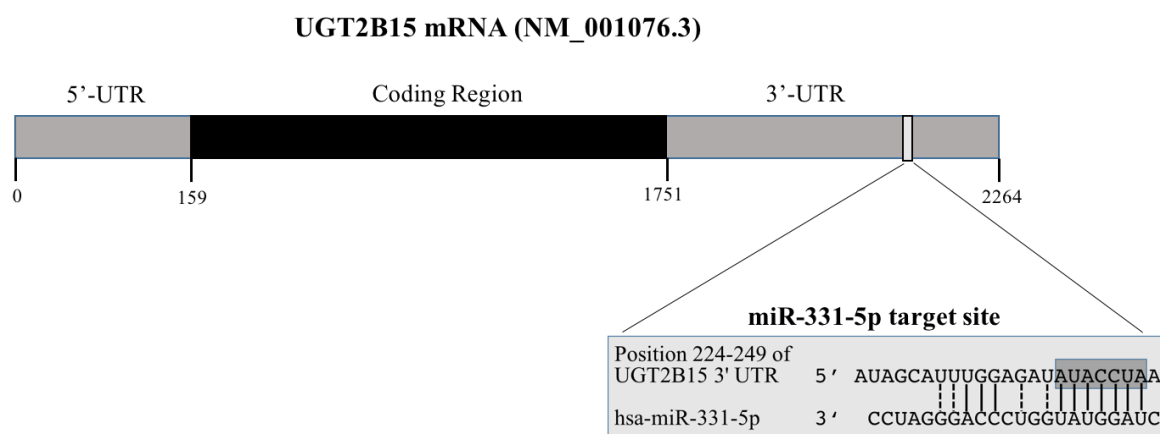


Figure 4.1: The putative miR-331-5p binding site in the 3'-UTR of UGT2B15 mRNA

Shown is the predicted pairing between miR-331-5p and its target site in the UGT2B15 3'-UTR. The seed binding site is highlighted. The nucleotides of the miR-binding site are numbered relative to the stop codon (TAG with G positioned as -1) of UGT2B15 mRNA (NM_001076.3).

4.3.2 MiR-331-5p down-regulates UGT2B15 mRNA and glucuronidation activity in human Prostate Cancer cells

The expression levels of UGT2B15 and miR-331-5p were measured in the prostate cancer cell lines LNCaP and Du145, the kidney cell line HEK293T and the hepatic cancer cell line HepG2. Among these cell lines, LNCaP cells expressed the highest level of UGT2B15 and lowest level of miR-331-5p (Figure 4.2 A, B). Therefore, transfection experiments to investigate the regulation of UGT2B15 by this miRNA, were performed in LNCaP cells. As expected, transfection of miR-331-5p mimics into LNCaP cells resulted in a significant down-regulation of UGT2B15 mRNA as compared with miR-neg-transfected cells (Figure 4.2 C), supporting a negative regulation of endogenous UGT2B15 by miR-331-5p. UGT2B17 mRNA levels (Figure 4.2 D) and control GAPDH mRNA levels (Figure 4.2 E) were not significantly altered by miR-331-5p.

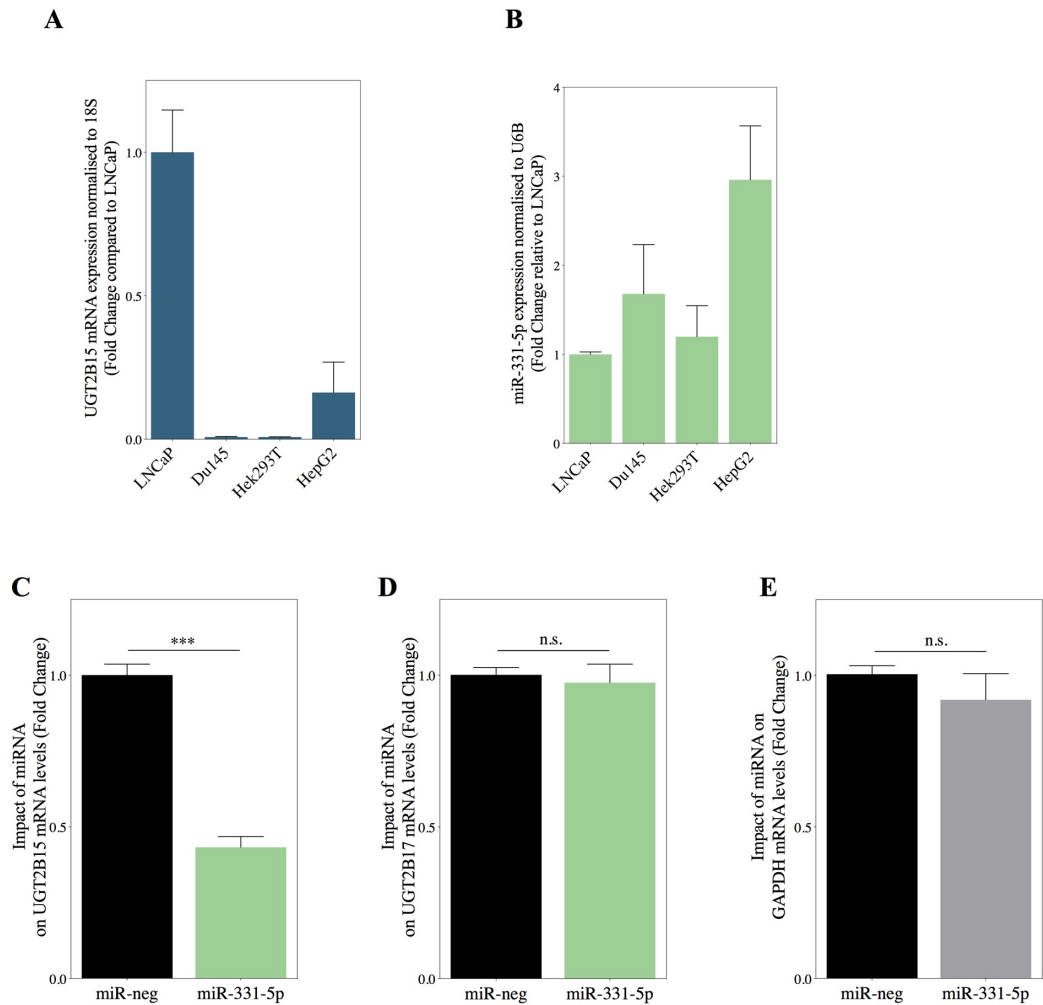


Figure 4.2: miR-331-5p reduces UGT2B15 mRNA levels in LNCaP cells

Expression of UGT2B15 (A) and miR-331-5p (B) in LNCaP, Du145, HEK293T and HepG2 cells. UGT2B15 mRNA expression is normalised to 18S rRNA and presented relative to that of LNCaP cells (set at a value of 1). MiR-331-5p expression is normalised to RNU6-2 and presented relative to that of LNCaP cells (set at a value of 1). Impact of miR-331-5p on UGT2B15 mRNA (C) UGT2B17 mRNA (D) or GAPDH mRNA (E) in LNCaP cells. Cells were transfected with miR-331-5p or miR-neg at 30nM in triplicate and total RNA was extracted from the cells and then subjected to quantitative real-time RT-qPCR for measuring target gene mRNA levels. After being normalized to the β -actin mRNA levels, the mRNA levels of genes of interest, were presented relative to those in the respective miR-neg-transfected cells (set at a value of 1). Data shown are mean \pm S.E.M. from two or three independent experiments performed in triplicate. ***P, 0.001.

As detailed in Chapter 2 (section 2.2.6.3), an anti-rabbit antibody that could recognize both UGT2B15 and UGT2B17 proteins was generated; this antibody

showed greater sensitivity for recognition of UGT2B17 than UGT2B15. The antibody was used in Western blotting in an attempt to measure the effects of miR-331-5p on UGT2B15 protein levels. However, no significant reduction in UGT2B15/2B17 protein levels was observed after overexpression of miR-331-5p (Figure 4.3 B). This may be due to the higher level of UGT2B17 than UGT2B15 expression in LNCaP cells (Chapter 3 Figure 3.2) and greater recognition of UGT2B17 protein by the antibody. No other UGT2B15 specific antibodies were known to be available; hence any effect of miR-331-5p on UGT2B15 protein levels could not be verified using Western blotting.

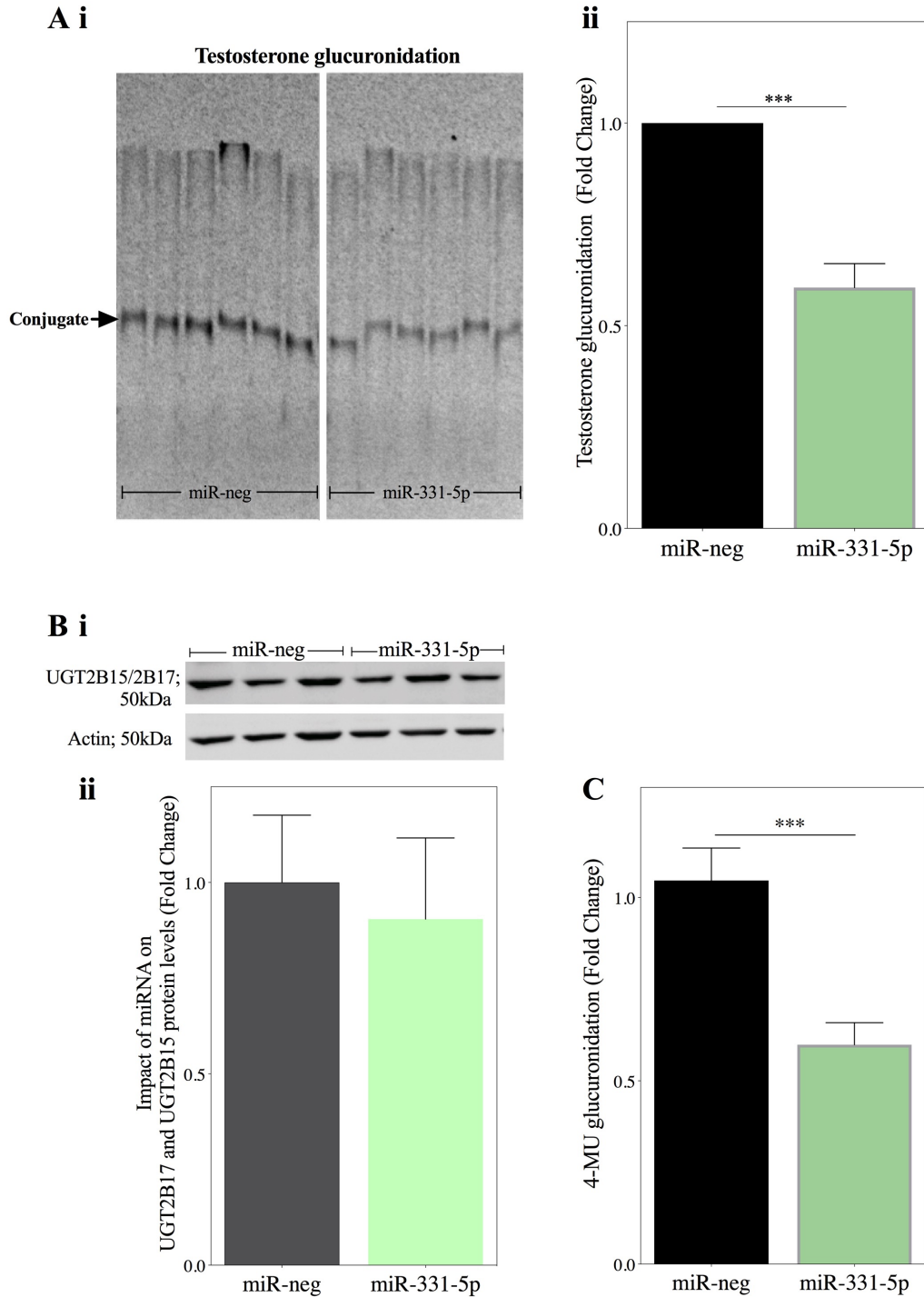


Figure 4.3: miR-331-5p reduces UGT2B15 enzymatic activity in LNCaP cells

(A i) Testosterone glucuronidation in LNCaP cells transfected with miR-neg and miR-331-5p (ii) Quantification of reduction in UGT2B15/2B17 glucuronidation enzymatic activity in LNCaP cells transfected with miR-331-5p, compared to miR-neg transfected cells (set at a value of 1). LNCaP cells were cultured in stripped serum containing medium for 48 before transfection and cells were harvested 72h post-transfection. Glucuronidation assays were performed using 25ug of whole cell lysates and C^{14} labelled Testosterone. After thin layer chromatography separation, the

glucuronidated testosterone was quantified using ImageQuant. Data are means \pm SEM from four separate experiments each consisting of triplicates. *** $p < 0.0005$. (B) Protein expression levels of UGT2B17/2B15 in LNCaP cells transfected with miR-neg and miR-331-5p. LNCaP cells were cultured in stripped serum containing medium for 48 before the transfection and then cells were harvested 72h post-transfection. Western blotting was performed with anti-UGT2B17 antibody. Quantification of reduction in UGT2B17 protein levels relative to β -actin levels in LNCaP cells transfected with miR-331-5p, compared to miR-neg transfected cells (set at a value of 1). Data shown are the immune signals of a representative experiment performed in triplicate (i) and the means \pm S.E.M. from three independent experiments performed in triplicate (ii). (C) 4-MU glucuronidation activity in LNCaP cells transfected with miR-331-5p mimics measured by HPLC is presented relative to those in miR-neg-transfected cells (set as a value of 1). Data are means \pm SEM from three separate experiments each consisting of triplicates, *** $p \leq 0.0009$.

To determine whether miR-331-5p alters UGT2B15 or UGT2B17 activity, lysates from LNCaP cells transfected with miR-331-5p or neg-miR—were used in testosterone glucuronidation assays. Testosterone is a substrate of both UGT2B15 and UGT2B17. Testosterone glucuronidation activity was significantly reduced by miR-331-5p (Figure 4.3 A). As 4-MU had been shown to act as a UGT2B15 specific substrate in LNCaP cells (see Chapter 3, section 3.3.5), 4-MU glucuronidation activity was also measured in the lysates. As expected, miR-331-5p reduced the glucuronidation of 4-MU by 53% (Figure 4.3 C). As LNCaP cells express only UGT2B15 and UGT2B17 at high levels, the contribution of other UGTs to the glucuronidation of testosterone and 4-MU was considered negligible.

4.3.3 MiR-331-5p directly binds to the 3'UTR of UGT2B15

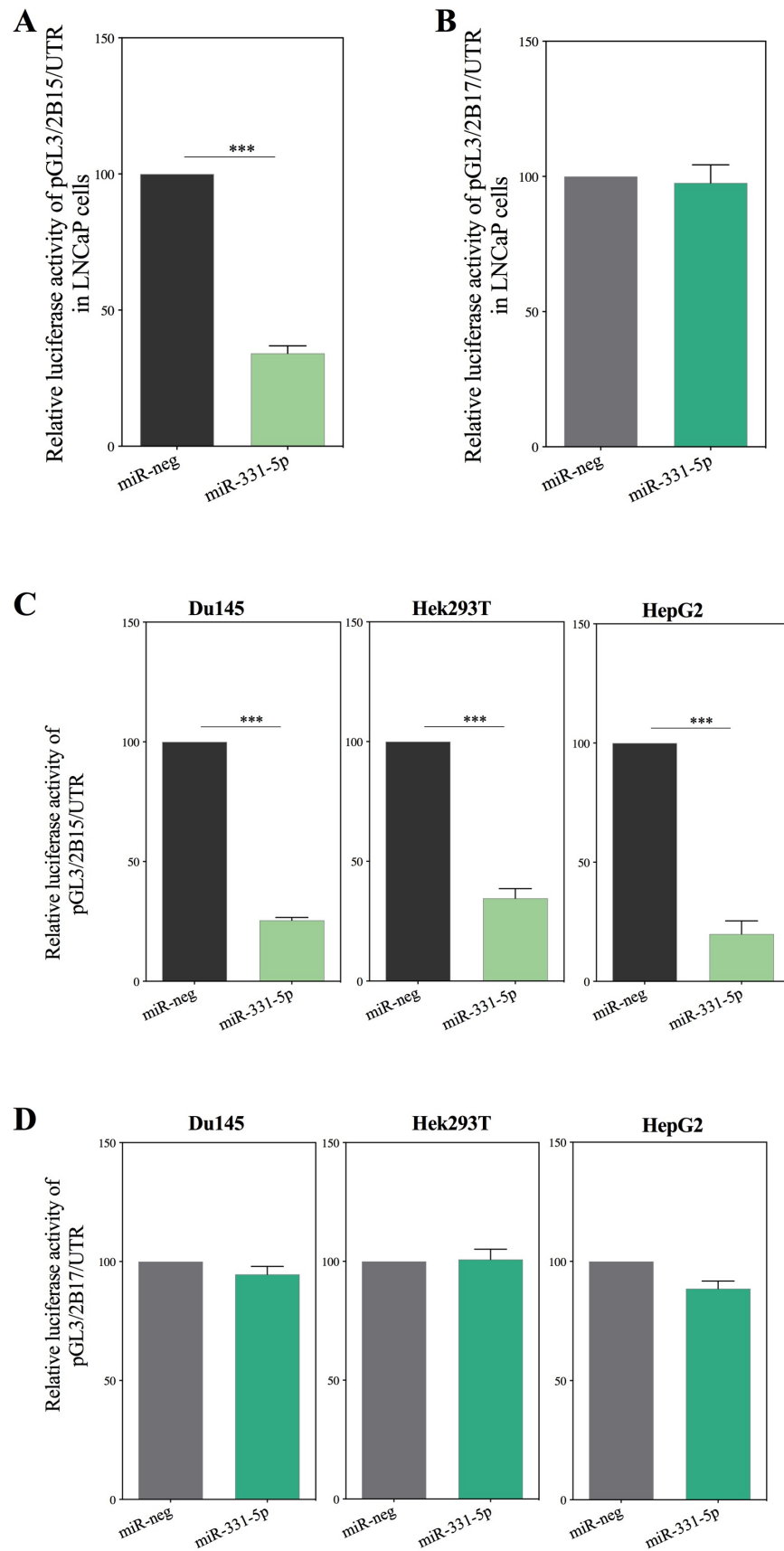
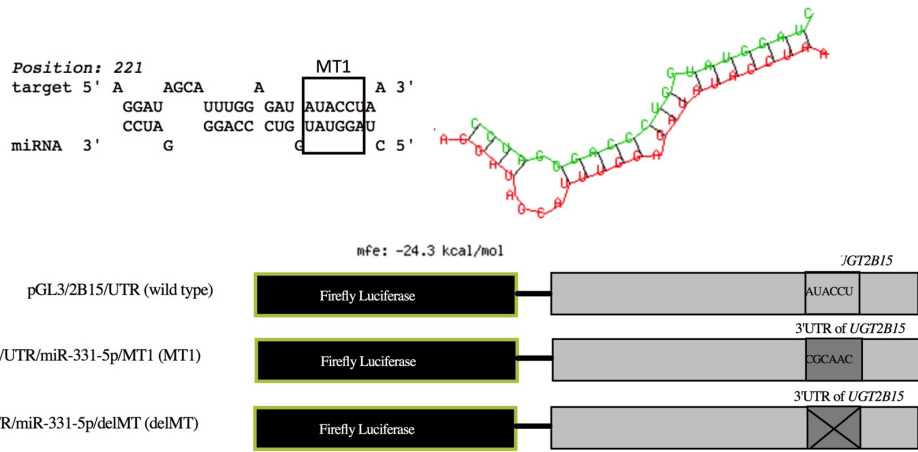


Figure 4.4: miR-331-5p mimics reduce the activity of a luciferase reporter containing the UGT2B15 3'UTR in LNCaP, Du145, HEK293T and HepG2 cells

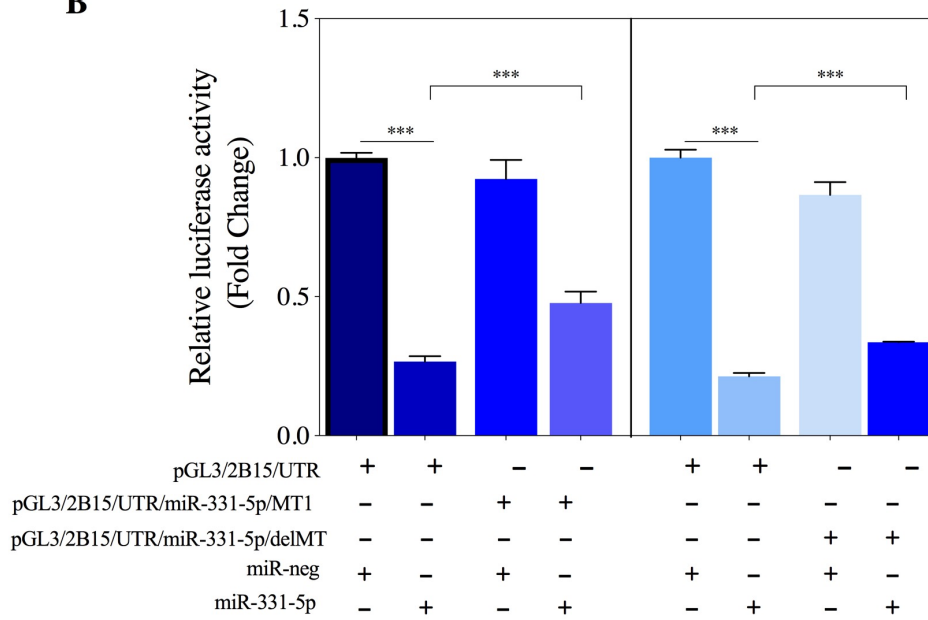
Luciferase reporter assays. LNCaP cells were co-transfected with either UGT2B15 3'UTR reporter construct (A) or UGT2B17 3'UTR reporter construct (B), along with miR331-5p mimics or miR-neg. The activity of the reporter constructs was first normalized to the activity of the pRL-null vector and then presented relative to that of pGL3-promoter vector activity (set at a value of 1). Data shown are from two or three independent experiment performed in quadruplicate, the error bar representing \pm S.E.M, *** $p < 0.0001$. ns, not statistically significant. Luciferase reporter assays in Du145, HEK293T and HepG2 cells where the cells were co-transfected with either the pGL3/2B15/UTR construct (C), or the pGL3/2B17/UTR construct (D), along with miR331-5p mimics or miR-neg. The activity of the reporter constructs was first normalized to the activity of the pRL-null vector and then presented relative to that of pGL3-promoter vector activity (set at a value of 100). Data shown are from a representative experiment of three or more independent experiments performed in quadruplicate, the error bar representing \pm S.D.

To examine whether miR-331-5p regulates UGT2B15 expression via the 3'UTR, the pGL3/2B15/UTR vector which contained the UGT2B15 3'-UTR, was used (Chapter 3). The pGL3/2B17/UTR vector containing the UGT2B17 3'UTR was used as a negative control. The two reporter constructs were cotransfected with miR-331-5p mimics or miR-neg into LNCaP cells. As expected, miR-331-5p significantly reduced UGT2B15 3'-UTR-containing reporter activity in LNCaP cells by ~70% (Figure 4.4 A) and did not affect UGT2B17 3'UTR-containing reporter activity (Figure 4.4 B). A similar reduction of the UGT2B15 3'-UTR-containing reporter activity was seen when the experiment was repeated in Du145 cells (75%), HEK293T cells (65%) and HepG2 cells by (80%) (Figure 4.4 C). These cells were chosen for this repeat experiment as they showed lower expression of UGT2B15 basal levels than LNCaP but similar miR-331-5p levels (Figure 4.2 A, B). The UGT2B17 3'UTR-containing reporter activity was not altered by miR-331-5p in these cell lines (Figure 4.4 D).

A



B



C

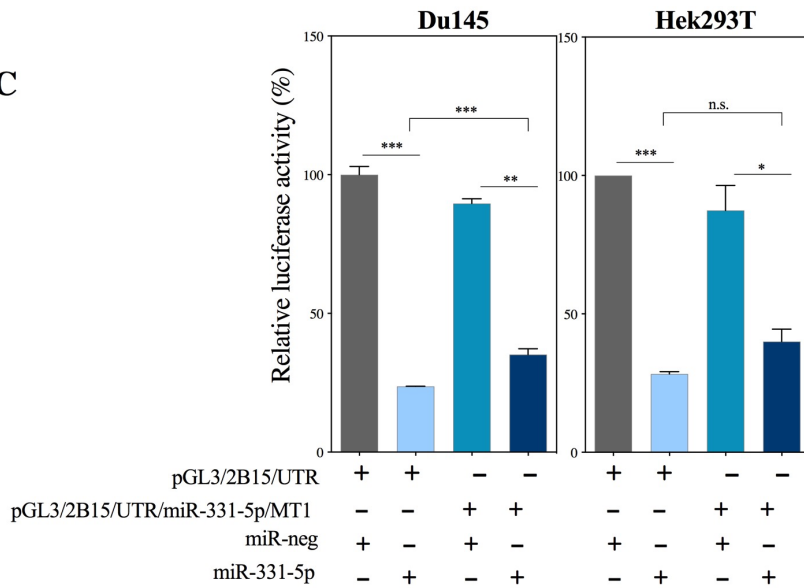


Figure 4.5: miR-331-5p reduces the activity of a luciferase reporter construct containing the UGT2B15 3'-UTR via a canonical target site (site 1) in LNCaP cells

(A) Shown is the predicted pairing between miR-331-5p and its target site in the UGT2B15 3'-UTR by RNAhybrid. The seed binding site is boxed. Schematic representation of firefly luciferase reporter constructs containing either the wild-type 2B15 (pGL3/2B15/UTR), mutated 2B15 (pGL3/2B15/UTR/miR331-5p/MT1) or deleted 2B15 (pGL3/2B15/UTR/miR331-5p/delMT) predicted miR-331-5p seed site sequence. Mutated or deleted seed sequences are boxed and highlighted (B) Luciferase reporter assays in LNCaP cells. Cells were co-transfected with either wild-type UGT2B15 3'UTR reporter construct, or the mutated or deleted miR331-5p binding site containing UGT2B15 3'UTR reporter constructs, along with miR331-5p mimics or miR-neg. The activity of the reporter constructs was first normalized to the activity of the pRL-null vector and then presented relative to that of pGL3-promoter vector activity (set at a value of 1). Data shown are from two or three independent experiment performed in quadruplicate, the error bar representing \pm S.E.M, *** $p < 0.0001$. ns, not statistically significant. (C) Luciferase reporter assays in Du145 and HEK293T cells. Cells were co-transfected with either wild-type UGT2B15 3'UTR reporter construct or mutated construct (pGL3/2B15/UTR/miR331-5p/MT1), along with miR331-5p mimics or miR-neg. The activity of the reporter constructs was first normalized to the activity of the pRL-null vector and then presented relative to that of pGL3-promoter vector activity (set at a value of 100). Data shown are from a representative experiment of two or three independent experiments performed in quadruplicate, the error bar representing \pm S.D. *** $p < 0.0001$. ** $p < 0.005$. * $p < 0.05$. ns, not statistically significant

The predicted canonical miR-331-5p binding site in the UGT2B15 3'UTR-containing reporter construct was mutated to define the role of this site in regulation (Figure 4.5 A). Wild-type (pGL3/2B15/UTR) or mutated (pGL3/2B15/UTR/miR-331-5p/MT1) reporter constructs were transfected into LNCaP cells together with miR-331-5p mimics or miR-neg control. Surprisingly, mutation of the miR-331-5p binding site, did not completely abrogate repression of miR-331-5p as reported by Margailan *et al* (Margailan et al., 2016) and Papageorgiou and Court (Papageorgiou and Court, 2017b). As shown in Figure 4.5 B, the mutation led to only a slight, albeit significant ($p < 0.005$), reduction in miR-331-5p-mediated repression of the UGT2B15 3'UTR-containing reporter (Figure 4.5 B). Similar results were also seen in Du145 and HEK293T cells (Figure 4.5 C). Because it was possible that the

mutations did not fully disrupt the miRNA-3'UTR association, an additional construct was generated in which the seed sequence binding site in the UGT2B15 3'UTR (pGL3/2B15/UTR/miR-331-5p/delMT) was completely deleted. However, this deletion also had only a very modest effect on the ability of miR-331-5p to repress 3'UTR activity (Figure 4.5 B). These data suggested the possibility of a second miR-331-5p target site in the 3'UTR of UGT2B15.

4.3.4 A non-canonical miR-331-5p target site is present in the UGT2B15 3'UTR

Attempts to predict a second binding site for miR-331-5p using bioinformatics programs yielded no candidate sites. Because these programs usually rely on seed sequence matching between the miRNA and the target, it was considered possible that any second binding site may involve non-seed based interactions. To find such a site empirically, different segments of UGT2B15 3'UTR were cloned into the pGL3-promoter luciferase reporter vector, and the resultant constructs transfected along with miR-331-5p mimics or miR-neg control into LNCaP cells. As expected, the luciferase activities of the two constructs carrying the canonical miR-331-5p target site [nucleotides (nt) 1-314 and nt 1-384] were significantly reduced by miR-331-5p mimics as compared to miR-neg (Figure 4.6 A). Three constructs that lacked the canonical miR-331-5p binding site (nt 244-318, nt 244-384, nt 244-454), showed no reduction in luciferase activity by miR-331-5p mimics. However, two other constructs that lacked the canonical miR-331-5p binding site (nt 1-150 and nt 1-225) were significantly repressed by the mimics. A construct containing the region from nt 1-75 was not affected by miR-331-5p mimics (Figure 4.6 A). Together these data suggested that there was a second miR-331-5p target site between nucleotides 75-150 of the UGT2B15 3'UTR.

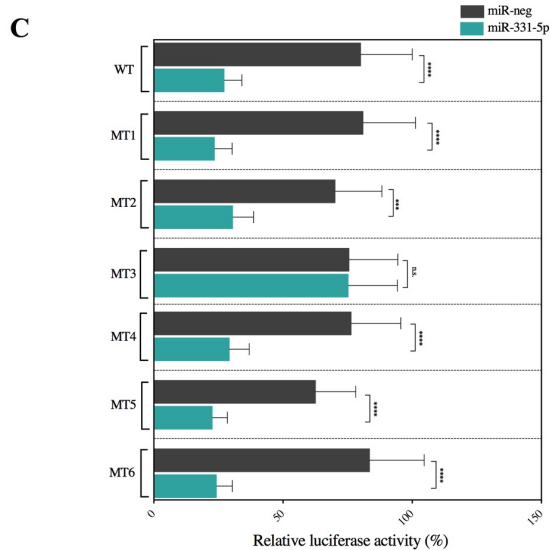
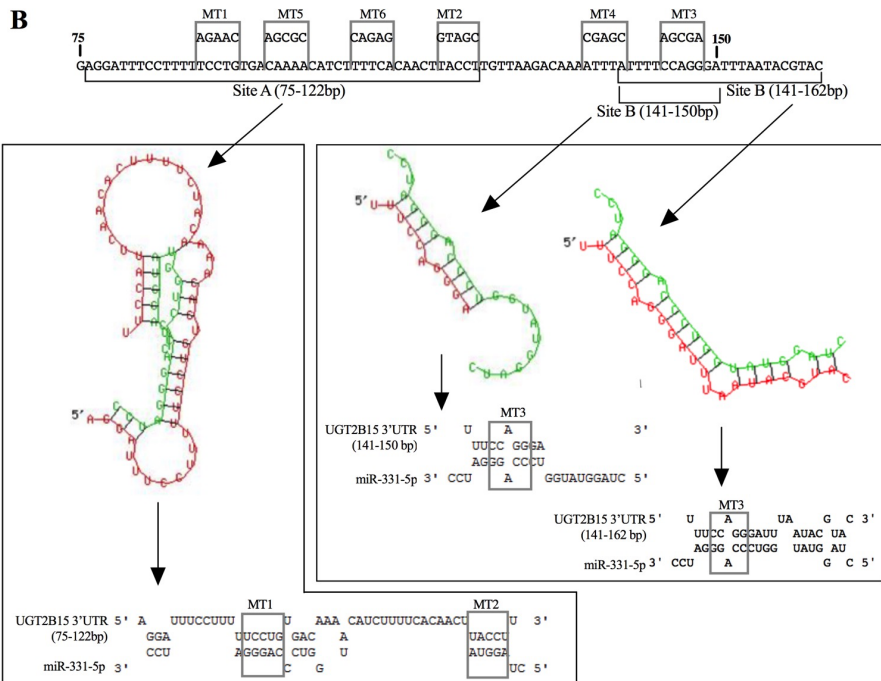
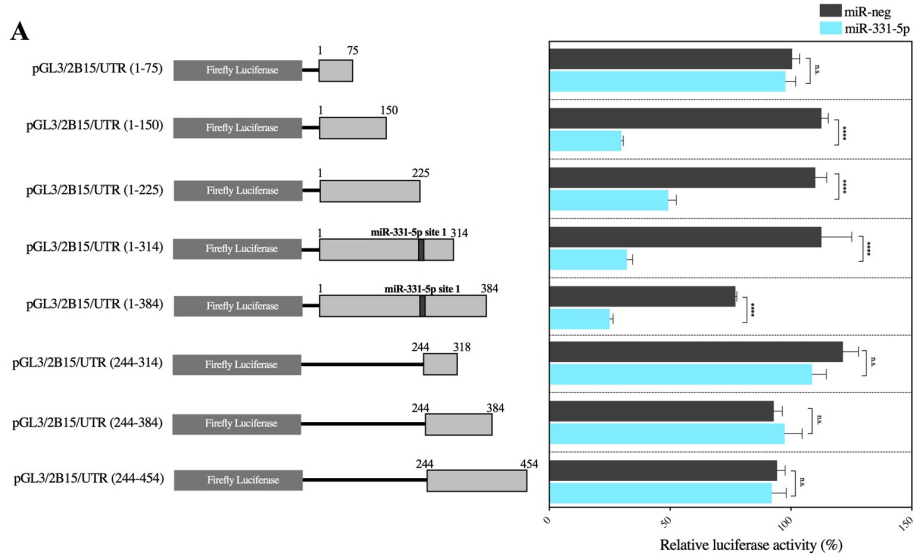


Figure 4.6: Discovery of a noncanonical miR-331-5p target site (site 2) in the UGT2B15 3'UTR

(A) Schematic representation of firefly luciferase reporter constructs containing either the wild-type UGT2B15 3'UTR (pGL3/2B15/UTR) or different segments of 2B15 3'UTR (nt 1-75, nt 1-150, nt 1-225, nt 1-314, nt 1-384, nt 224-318, nt 224-384, nt 224-454) as described under Materials and Methods (left diagram, the nucleotides are numbered relative to the stop codon; TAG with G positioned as -1 of UGT2B15 mRNA). Luciferase reporter assays were performed using LNCaP cells cotransfected with miR-neg or miR-331-5p and the 8 reporter constructs containing the UGT2B15 3'-UTR (right diagram). (B) Shown are the six mutations of the 2B15 3'UTR between nucleotides 75 and 150 that were based on the prediction of a second miR-331-5p binding site by RNAhybrid (MT 1, MT 2 are from the duplex formation site A and MT 3 is from duplex formation site B), an RNA-binding protein site (MT 4), or random sequences (MT 5 and MT 6). Mutated sequences are boxed with the mutations shown above the wild type sequences. (C) Luciferase reporter assays using LNCaP cells cotransfected with miR-neg or miR-331-5p and the wild-type or mutant reporter constructs containing the UGT2B15 3'-UTRs. The activity of the reporter constructs (A and C) was first normalized to the activity of the pRL-null vector and then presented relative to those of the empty pGL3-promoter vector (set at a value of 100%). All data shown are from two independent experiments performed in quadruplicate; the error bar represents \pm S.E.M. *** $p < 0.0001$. n.s., not statistically significant.

To further narrow the miRNA binding site, the 150 bp 3'UTR containing reporter vector was mutated at 6 sites between nucleotides 75-150 (Figure 4.6 B). As miRNA binding may not always follow the seed pairing rule, RNAhybrid was used to predict the energetically most favourable miRNA:mRNA duplex formation sites in the 75-150 nucleotide portion of the UGT2B15 3'UTR. RNAhybrid predicted two energetically favorable duplex formation sites between miR-331-5p and UGT2B15 mRNA at nucleotides 76–122 [termed site A: minimum folding energy (mfe): -18.8 kcal/mol) and at nucleotides 141–150 (termed site B: mfe: -15.7 kcal/mol) (Figure 4.6 B). Mutations MT1 and MT2 were located within site A and MT3 was located within site B (Figure 4.6 B). The mutation MT4 was located within a putative RNA protein binding site 'AUUUA'. Mutations MT5 and MT6 were located away from any of these predicted binding sites in the UGT2B15 3'UTR. Analysis of these constructs indicated that the stretch of nucleotides 144-148 in the UGT2B15 3'UTR

(complementary to nucleotides 11-19 of the miR-331-5p 3' end) are part of a second binding site for miR331-5p (Figure 4.6 C). As shown in Figure 4.6 B (site B; 141-162bp and in Figure 4.11), RNAhybrid predicted Watson-Crick pairing at 16 nt between this site and miR-331-5p, including pairing in the seed site but with a 1-bp mismatch in the full length 3'UTR of UGT2B15; hence, this was defined as a non-canonical miR-331-5p target site. For simplicity, this non-canonical miR-331 site was named miR-331-5p site 2 and the canonical seed-matched miR-331-5p site was named miR-331-5p site 1.

4.3.5 MiR-331-5p cooperatively regulates UGT2B15 via two target sites

Mutations in the miR-331-5p sites 1 and 2 were generated separately or in combination in the full-length pGL3/2B15/UTR reporter to see whether the two sites may act synergistically. (Figure 4.7 A). The MT A construct contains a mutation in the seed region of the miR-331-5p site 1 (also known as pGL3/2B15/UTR/MT1). MT B and MT D constructs contain mutations in the miR-331-5p site 2. In MT B, a mutation that disrupts the 3' pairing is present and in MT D, a mutation in the seed site is present. MT C contains a mutation in the seed site of miR-331-5p site 1 and a mutation in the 3' pairing site of the miR-331-5p site 2. MT E contains mutations in the seed sites of both miR-331-5p site 1 and 2. When the two miR-331-5p sites are mutated separately (MT A, B and D), miR-331-5p mimics were still able to partially but significantly reduce the reporter activity, but when the two sites were mutated simultaneously as in MT C, the mimics had no effect on reporter activity (Figure 4.7 B). This demonstrates a synergistic regulation of UGT2B15 by the two miR-331-5p sites. In addition, it appears that this synergy depends on the 3' sequence of miR-331-5p site 2, rather than its seed sequence.

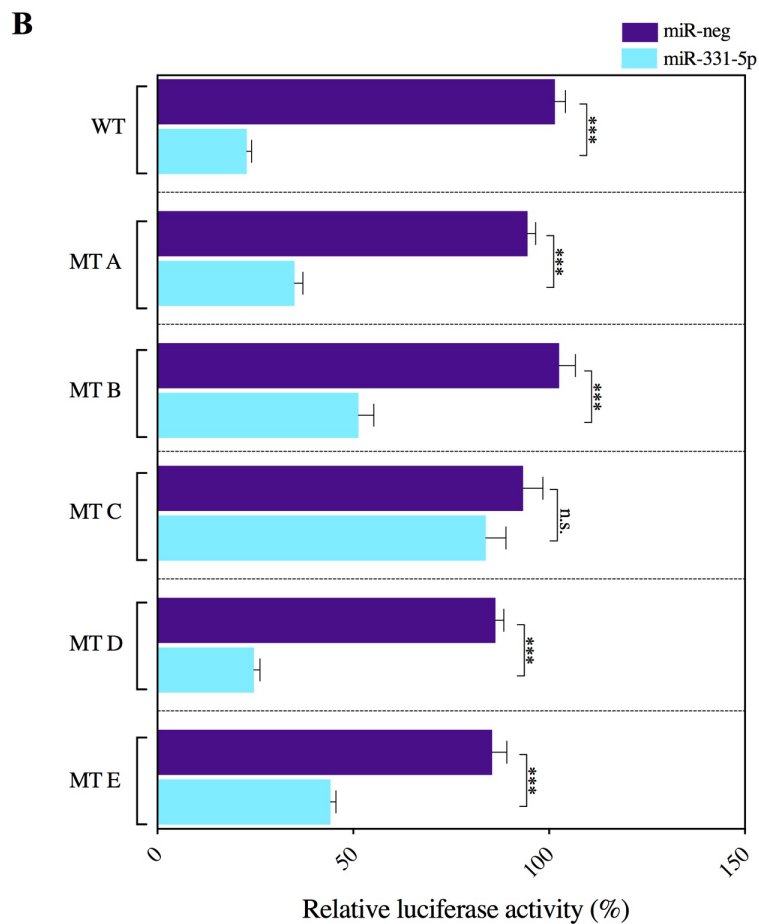
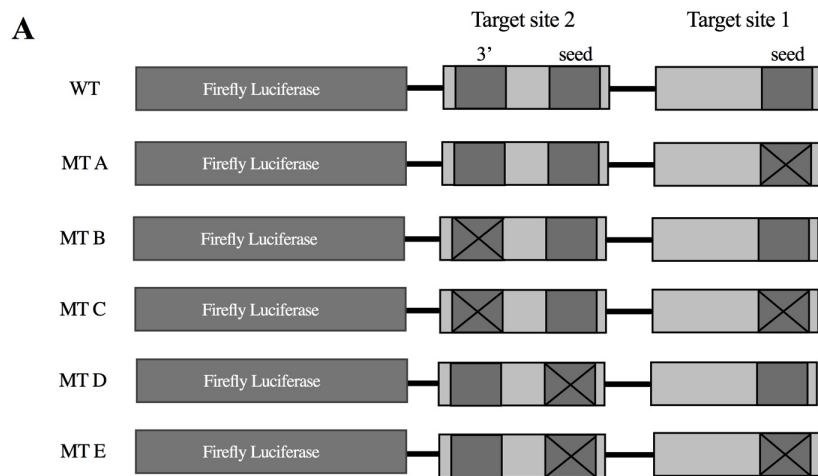


Figure 4.7: Cooperative regulation of UGT2B15 3'UTR by miR-331-5p via two target sites

(A) Schematic representation of firefly luciferase reporter constructs containing either wild-type 2B15 (pGL3/2B15/UTR) or two miR-331-5p sites mutated

[mutation at the seed site of site 1 (MT A) or mutation at either the 3'pairing site (MT B) or seed site (MT D) of site 2) separately or in different combinations (MT C and MT D). (B) Luciferase reporter assays were performed in LNCaP cells transfected with miR-neg or miR-331-5p and the wild-type (WT) or mutant reporter constructs (as described in Materials and Methods). The activity of the reporter constructs was first normalized to the activity of the pRL-null vector and then presented relative to those of the empty pGL3-promoter vector (set at a value of 1). Data shown are from two independent experiments performed in quadruplicate; the error bar represents \pm S.E.M, *** $p < 0.001$. n.s., not statistically significant.

4.3.6 MiR-331-5p and miR-376c function additively in UGT2B15 regulation

The miR-376c target site (reported in Chapter 3) is located between the two miR-331-5p sites (Figure 4.8 A). As a single mRNA can be regulated by more than one miRNA in a combinatorial way (Doench and Sharp, 2004), whether miR-376c and miR-331-5p cooperatively regulate the UGT2B15 3'UTR was investigated. The UGT2B15 3'UTR reporter construct (pGL3/2B15/UTR) was co-transfected with miR-331-5p, miR-376c or a combination of miR-331-5p and miR376c mimics in LNCaP cells. When both miRNAs were present, there was an additive inhibitory effect on UGT2B15 reporter activity (55%-65% reduction in reporter activity when present alone and 80% reduction in activity when transfected together; Figure 4.8 B). This suggests that both microRNAs can directly bind to the UGT2B15 3'UTR simultaneously and regulate UGT2B15 mRNA.

Figure 4.8: Additive regulation of UGT2B15 3'UTR by miR-331-5p and miR-376c

(A) Shown are the miR-376c and miR-331-5p target sites (all miRNA target sites are boxed and the seed sites of miR-376c and miR-331-5p site 1 are in bold) in the 3'UTRs of UGT2B15 (NM_001076.3) and/ or UGT2B17 (NM_001077.3). The 3'UTRs of the two UGTs are aligned and nucleotide sequences are numbered relative to the stop codon (TAG with G positioned as 0). (B) Luciferase assays in cells transfected with UGT2B15 3'UTR reporter construct along with either miR-neg, miR-331-5p, miR-376c or combination of miR331-5p and miR376c mimics. The activity of the reporter constructs was first normalized to the activity of the pRL-null vector and then presented relative to those of the empty pGL3-promoter vector (set at a value of 1). Data shown are from two independent experiments performed in triplicate; error bar represents \pm S.E.M. ***P < 0.0001. ns, not statistically significant.

4.3.7 The expression of miR-331-5p inversely correlates with UGT2B15 mRNA expression in human tissues and hepatocellular carcinoma

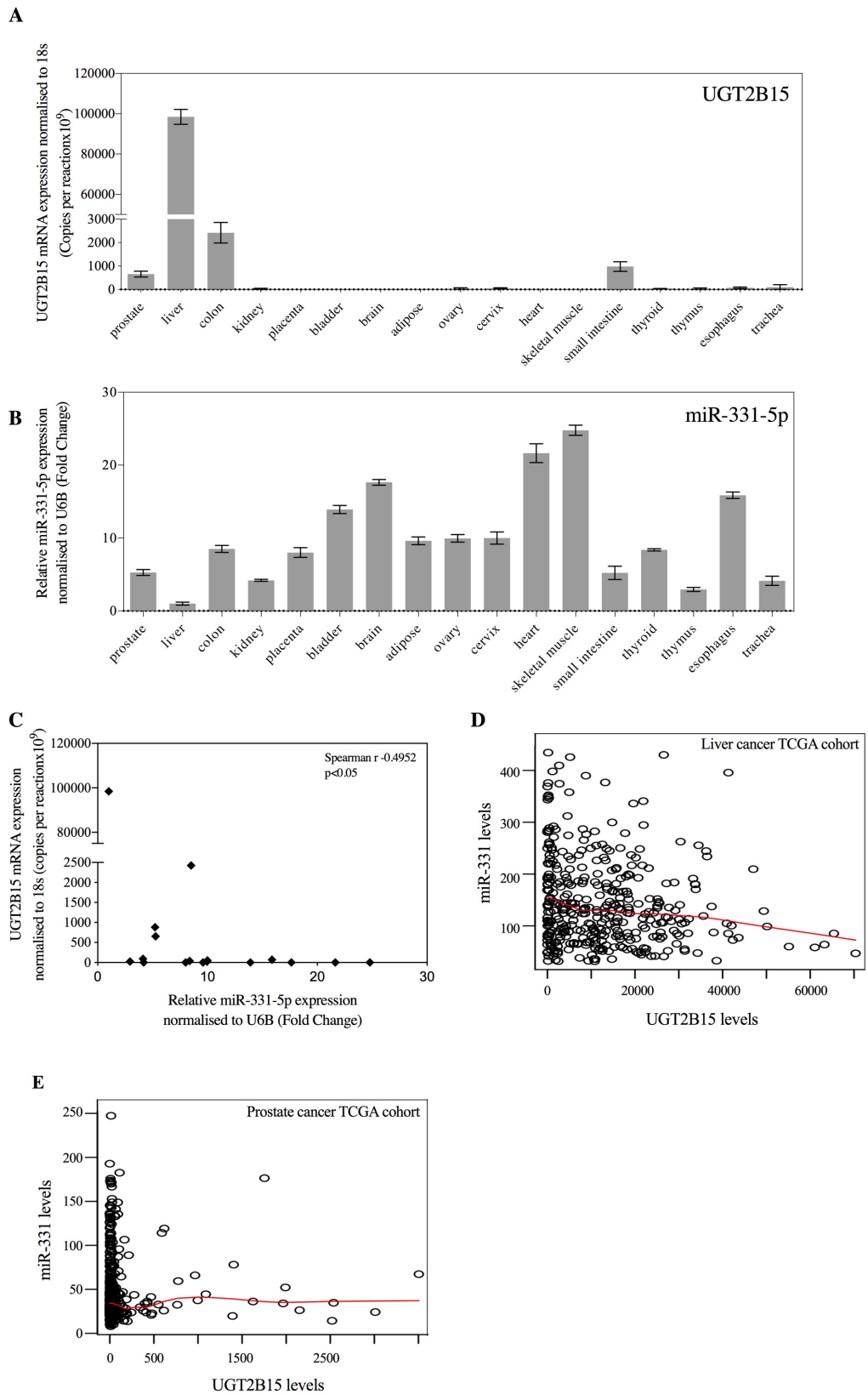


Figure 4.9: The miR-331-5p and UGT2B15 levels are significantly inversely correlated in a human tissue panel and the TCGA hepatocellular carcinoma cohort

Expression of (A) UGT2B15 mRNA (Data taken from fig 3.16 A) and (B) miR-331-5p in human tissues. MiR-331-5p expression is normalized to RNU6-2 presented relative to that of liver (set at a value of 1). Data shown are from a representative experiment performed in triplicate, the error bar representing \pm SD. (C) Expression of UGT2B15 mRNA versus miR-331-5p expression in human tissues. Data were examined using the Spearman Method. Each dot (\blacklozenge) represents the value of an independent replicate. $p < 0.05$. (D) Transcriptome profiling data (RNA sequencing and miRNA sequencing) from the TCGA hepatocellular carcinoma cohort (371 samples) were downloaded from the TCGA data portal. Data were normalized and correlation analysis between miR-331 and UGT2B15 mRNA levels was conducted using the Spearman rank method; the graph was drawn using the R statistical package as described in Materials and Methods. (E) The miR-331 and UGT2B15 levels are not significantly correlated in the TCGA prostate adenocarcinoma (TCGA-PRAD) cohort ($\rho = -0.043$, $p = 0.335$). Transcriptome profiling data (RNAseq and miRNAseq) from the TCGA-PRAD cohort (498 samples) were downloaded from the TCGA data portal. Data were normalized and correlation analysis between miR-331 and UGT2B15 mRNA levels was conducted using the Spearman rank method; the graph was drawn using the R statistical package as described in the Materials and Methods section.

The expression levels of UGT2B15 in human tissue samples were discussed previously in Chapter 3 (Figure 3.16 A). Briefly, liver shows the highest level of UGT2B15 expression followed by colon, small intestine and prostate (Figure 4.9 A). Low expression of UGT2B15 was also seen in trachea, esophagus, cervix, thyroid, ovary and thymus. Quantitative real time PCR revealed the highest miR-331-5p expression in the skeletal muscle and heart (Figure 4.9 B). Interestingly, miR-331-5p had the lowest expression levels in the liver where UGT2B15 is expressed at high levels. Spearman's correlation analysis showed a significant negative correlation between miR331-5p expression and UGT2B15 mRNA expression ($\rho = -0.4952$; $p < 0.05$; Figure 4.9 C), suggesting that miR-331-5p may regulate UGT2B15 in these tissues. As expected, there was no significant correlation between miR-331-5p and UGT2B17 expression in these tissues ($p > 0.05$; data not shown). Moreover, analysis

of the TCGA hepatocellular carcinoma RNA- and miRNA-seq data sets (TCGA-LIHC, 371 specimens) showed a significant inverse correlation between miR-331 and UGT2B15 levels ($\rho = -0.171$, $P = 0.0009$) (Figure 4.9 D). Similar analysis of the TCGA-PRAD cohort (498 specimens) also suggested an inverse correlation between levels of miR-331 and UGT2B15, but this correlation was not statistically significant ($\rho = -0.043$, $P = 0.335$) (Figure 4.9 E).

4.4 Discussion

Preliminary bioinformatic analyses revealed that the 3'-UTRs of human UGTs have many target sequences for microRNAs. Direct impact of microRNA on UGT2B15 and/or UGT2B17 expression has only been investigated by a handful of research groups including our laboratory, Margaillan *et al*, and Papageorgiou and Court (Margaillan *et al.*, 2016, Papageorgiou and Court, 2017b). In this chapter, miR-331-5p was shown to regulate UGT2B15 3'-UTR via two sites; a previously identified canonical target site (site 1) (Margaillan *et al.*, 2016) and a second non-canonical site (site 2). Moreover, the present study provides a clear example of combinatorial regulation by two miRNA target sites.

In animals, miRNAs interact with target mRNAs in an imperfect base pairing manner leading to translational repression. Nucleotides 2-7 of the 5' end of the miRNA is known as the seed sequence and early studies have considered seed pairing to be a primary determinant of miRNA target recognition (Grimson *et al.*, 2007, Bartel, 2009, Friedman *et al.*, 2009). In addition to seed pairing, supplementary Watson-crick pairing at the 3' region of miRNA (position 13-16) to the mRNA has been known to enhance the efficacy of miRNA targeting as well (Grimson *et al.*, 2007).

However, experimental data from recent studies show the existence of non-canonical miRNA binding sites (Cloonan, 2015) including compensatory pairing of miRNA 3' bases 12-17 in addition to seed pairing with a single nucleotide mismatch (Bartel, 2009, Brennecke et al., 2005, Grimson et al., 2007), seed pairing with a single G-bulge mismatch (Chi et al., 2012, Loeb et al., 2012), seedless pairing (Ghosal et al., 2016, Lal et al., 2009) such as interaction in the mid region of the miRNA (11-12 nucleotides of the mRNA bind in perfect complementarity to the 5' bases 4-15 of miRNA) known as centered sites (Shin et al., 2010) and imperfect centered sites with a GU wobble or one mismatch (Martin et al., 2014) (Figure 4.10). However, non-canonical target site predictions are omitted by most current miRNA target prediction tools to reduce false-positive predictions (Martin et al., 2014). Therefore, in this study RNAhybrid was utilized to predict the most energetically favourable miRNA:mRNA hybridization in order to predict the noncanonical miR-331-5p target site in the UGT2B15 3' UTR. (Kruger and Rehmsmeier, 2006, Rehmsmeier et al., 2004).

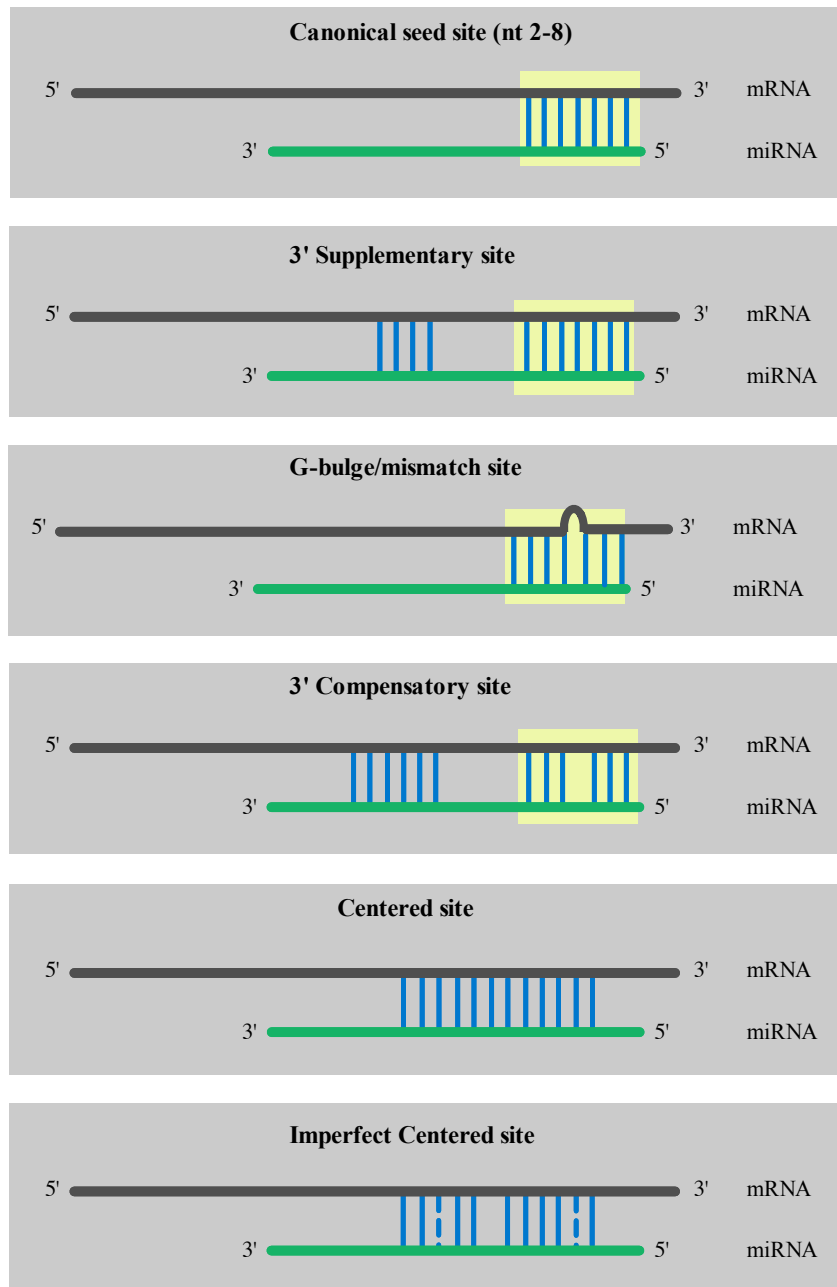


Figure 4.10: Types of canonical and non-canonical miRNA:mRNA interactions
Seed sites are highlighted in yellow.

As demonstrated in the current study, miR-331-5p downregulates basal UGT2B15 mRNA levels and 4-MU glucuronidation activity. However, it is yet to be investigated if miR-331-5p has any translational inhibitory effect on UGT2B15. Moreover, miR-331 and UGT2B15 levels were inversely correlated in a

hepatocellular carcinoma cohort (371 specimens), suggesting that miR-331-5p plays an important role in defining the basal level of UGT2B15 expression in liver cancer. However, there was no significant correlation between miR-331 and UGT2B15 expression levels in a large prostate cancer cohort. Further work is required to understand the relative importance of miR-331-5p in control of UGT2B15 levels in various tissues, either as a central determinant of expression or a more subtle fine-tuning regulator.

Luciferase reporter assays indicated that miR-331-5p reduces UGT2B15 levels by direct binding to the 3'UTR. However in contrast to the study conducted by Margailan *et al* (Margailan et al., 2016) and Papageorgiou and Court (Papageorgiou and Court, 2017b), mutating the canonical miR-331-5p site (site 1) in the UGT2B15 3'UTR reporter only partially abrogated the miRNA-mediated repression. As a single miRNA may have multiple binding sites in a target mRNA (Doench and Sharp, 2004) and having multiple binding sites for the same miRNA in the 3'UTR causes a higher degree of repression (Doench et al., 2003), this result implied that miR-331-5p may have an alternative binding site(s) in the UGT2B15 3'UTR. The second non-canonical binding site of miR-331-5p (site 2) was identified by deletion and mutation analysis and shown to involve a 3' compensatory pairing site rather than a seed match. Overall, this data confirm that perfect miRNA:mRNA seed pairing may not be sufficient and not always necessary for miRNA targeting (Betel et al., 2010). We also demonstrated that these two sites regulate UGT2B15 in a cooperative way.

The miR-331 gene located on chromosome 12q22 generates two mature miRNAs, miR-331-3p and miR-331-5p [National Center for Biotechnology Information

(NCBI): <https://www.ncbi.nlm.nih.gov/gene/442903>, miRBase: http://www.mirbase.org/cgi-bin/mirna_entry.pl?acc=MI0000812]. miR-331-5p is implicated in a number of cancers including leukemia (Feng et al., 2011), colorectal adenomas (Verma et al., 2015), and lung cancer (Zhan et al., 2017); it is also considered to be a biomarker for Parkinson's disease (Cardo et al., 2013) and facioscapulohumeral muscular dystrophy (Portilho et al., 2015). However the current study is the first to suggest a role for this miRNA in regulating genes in prostate or liver contexts.

This study also examined whether the miR-331-5p sites and the miR-376c site may function cooperatively. Several studies have investigated the cooperative regulation of single-target mRNAs by multiple miRNAs and revealed that the efficacy and cooperativity between miRNA target sites is predominantly determined by the interval spacing between seed sites (Doench and Sharp, 2004, Grimson et al., 2007, Pasquinelli, 2012, Saetrom et al., 2007). Specifically, the most effective cooperative downregulation is seen when the distance between two seed sites is between 13 and 35 nucleotides; however, this cooperativity becomes less likely when the internal spacing between miRNA seed sites is over 70 nucleotides (Saetrom et al., 2007). The miR-376c site is located between the two miR-331-5p sites: 62 bp upstream of miR-331-5p site 2 and 15 bp downstream from miR-331-5p site 1 (Figure 4.8 A). Therefore, the distance between the seed sites of miR-331-5p site 2 and miR-376c falls within the proposed optimal spacing range and thus cooperative regulation is highly possible. The distance between miR-331-5p site 1 and the miR-376c seed site falls outside the optimal spacing range but still below the 70-nucleotide space limit for cooperative regulation. In addition, cooperative regulation seems to be more effective with 3 individual sites compared to 2 individual sites (Saetrom et al., 2007).

According to a study conducted by Saetrom *et al*, when 2 seed sites are optimally spaced (17 nucleotides between them) and the third site is 50 nucleotides away, higher cooperative regulation was detected when compared to having all 3 seed sites optimally spaced (17 nucleotides). Interactions between the miRNA complexes may play a role in this type of dependence upon distance between the seed sites (Saetrom *et al.*, 2007). The spacing between the 2 miR-331-5p and miR-376c seed sites is somewhat consistent with the arrangement described above. Consistent with this, the current study showed miR-331-5p and miR-376c can simultaneously repress the UGT2B15 3'UTR through these closely located target sites, although the effect appeared to be additive.

The sequences of the UGT2B15 and UGT2B17 3'UTRs are highly conserved at their 5'-ends (approximately 210 nt after the TAG codon) but diverge at their 3'-ends (Figure 4.8 A). The canonical miR-331-5p target site (site 1) lies in the divergent region; hence, the UGT2B17 3'UTR does not contain a site that is equivalent to UGT2B15 miR-331-5p site 1 (Figure 4.8 A). The noncanonical miR-331-5p site (site 2) resides in the region that is conserved between the UGT2B15 and UGT2B17 3'UTRs (Figure 4.8 A) and a sequence similar to miR-331-5p site 2 can be identified in the UGT2B17 3'UTR. As shown in Figure 4.11, there is only two nucleotide differences between UGT2B15 and UGT2B17 3'UTR in the miR-331-5p site 2 (a G/A mismatch in the 3' pairing sequence of the miR-331-5p target site and a C/T mismatch in the seed site) and yet UGT2B17 is not a miR-331-5p target. In support of this observation, RNAhybrid predicted the formation of a miR-331-5p/mRNA duplex (mfe: -14.9 kcal/mol) at this putative site that was less energetically favorable compared with that (mfe: -22.1 kcal/mol) formed at the UGT2B15 miR-331-5p site 2 (Figure 4.11). The 2nt- difference in UGT2B17 possibly interferes with the

secondary structure of the miRNA/target mRNA duplexes or the accessibility of the miRNA to the target site. Thus, the UGT2B17 3'UTR lacks a functional miR-331-5p target site and is not regulated by miR-331-5p. This provides the first evidence for a posttranscriptional mechanism that can differentially regulate these two major androgen-metabolizing UGTs. This is an important finding because currently there is no identified mechanism allowing differential regulation of these two UGTs at the transcriptional level. In Chapter 3, two other potential specific regulators of UGT2B15 were also identified: miR-376b and miR-222. The differential regulation of UGT2B15 and UGT2B17 may allow specific tuning of testosterone and DHT levels and well as other divergent substrates of these enzymes. The biological significance of this requires further study.

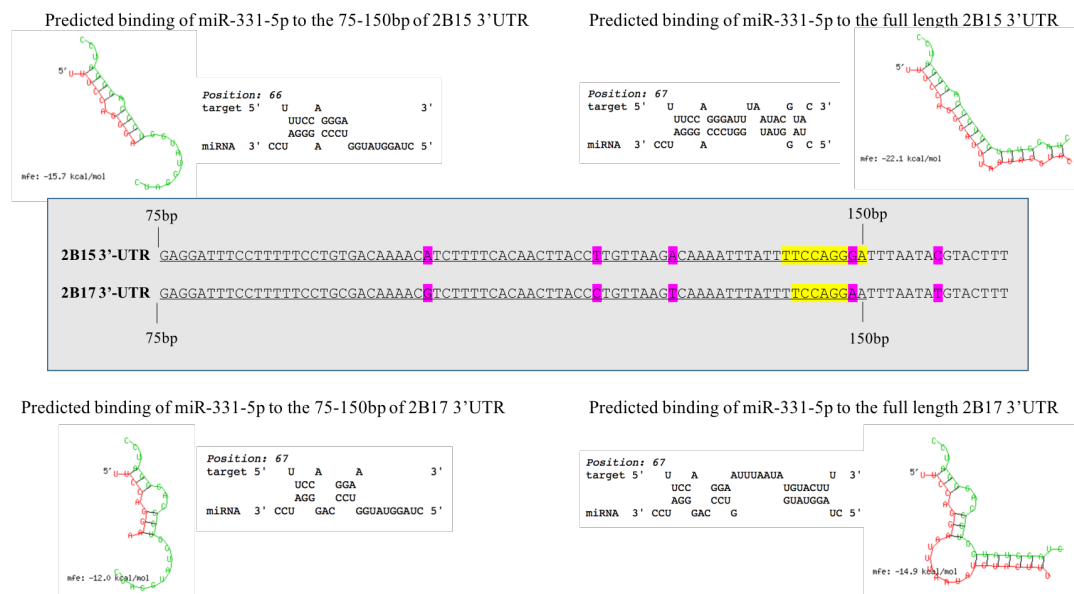


Figure 4.11: Interaction of 75-150 bp or full-length 3'UTRs of UGT2B15 and UGT2B17, with miR-331-5p predicted by RNAhybrid

The miRNA 3' pairing site is highlighted in the 3'UTRs of UGT2B15 and UGT2B17 in yellow. The nucleotide differences between the two 3'UTRs are highlighted in pink.

CHAPTER 5

REGULATION OF *UGT2B7* AND *UGT2B4* BY MICRORNAS

Published in part as: Wijayakumara DD, Mackenzie PI, McKinnon RA, Hu DG, Meech R (2017), 'Regulation of UDP-Glucuronosyltransferases UGT2B4 and UGT2B7 by MicroRNAs in Liver Cancer Cells'. *Journal of Pharmacology and Experimental Therapeutics*, 361(3):386-397.

Reproduced with permission of the American Society for Pharmacology and Experimental Therapeutics. All rights reserved.

5.1 Introduction

UGTs mediate 35% of the phase II metabolism of therapeutic drugs (Guillemette, 2003). UGTs also protect the body for exogenous carcinogens, and other toxins, and are involved in the homeostasis of various endogenous signalling molecules (Guillemette, 2003, Mackenzie et al., 1997). The primary glucuronidation site is the liver and thus the hepatic expression and activity of UGTs is vital for systemic metabolism and clearance of UGT substrates (Hu et al., 2015). Human liver expresses UGT2B7 and UGT2B4 predominantly among all UGT2B subfamily isoforms (Congiu et al., 2002). UGT2B7 has high affinity towards various endogenous compounds including bile acids, retinoic acids, steroids, mineralocorticoid and glucocorticoid hormones and fatty acids (Hu et al., 2014b) as

well as exogenous compounds including carcinogens, and a wide range of therapeutic drugs such as morphine (Coffman et al., 1997), codeine (Raungrut et al., 2010), epirubicin (Innocenti et al., 2001), valproic acid (Argikar and Remmel, 2009) and nonsteroidal anti-inflammatories (Jin et al., 1993). Williams et al. estimated that 20 out of the top 200 drugs prescribed in 2002 in the United States are glucuronidated by UGTs and 35% of these glucuronidated drugs, are, in fact, UGT2B7 substrates (Williams et al., 2004). UGT2B4 is involved in the glucuronidation of bile acids (Fournel-Gigleux et al., 1989), catechol-estrogens (Ritter et al., 1992) and various phenols and is thus important for their detoxification (Guillemette, 2003). In addition to the liver, UGT2B7 is expressed in the small intestine, colon (Ohno and Nakajin, 2009), kidney, and breast (Hu et al., 2014b) whereas UGT2B4 is also expressed in kidney and esophagus (Ohno and Nakajin, 2009).

The regulation of UGT2B7 and UGT2B4 expression and activity has been investigated in several studies. As reviewed in Hu *et al* 2015, multiple transcription factors including HNF1 α (Ishii et al., 2000), HNF4 α , Cdx2 (Gregory et al., 2006), Nuclear factor erythroid 2-related factor 2 (Nrf2) (Nakamura et al., 2008), FXR (Lu et al., 2005), p53 (Hu et al., 2014c)(Hu et al. 2014b) and AP-1 proteins (Hu et al., 2014a) have been identified as regulators of UGT2B7 expression at the transcriptional level. Transcription factors FXR, retinoid X receptor (RXR) (Barbier et al., 2003b) and PPAR α (Barbier et al., 2003a) are known to regulate UGT2B4 expression at the transcriptional level. However, the mechanisms controlling UGT mRNA stability at the post-transcriptional level remain poorly characterized, but could include miRNA mediated effects. A recent study (Dluzen et al., 2016) reported regulation of UGT2B4, UGT2B7 and UGT2B10 by miR-216b-5p in HuH7 and

Hep3B cells. In order to further investigate post-transcriptional regulation of UGT2B7 and UGT2B4, a series of experiments were performed in the hepatic cell line HepG2, revealing that UGT2B7 is a direct target of miR-3664-3p and that UGT2B4 is a direct target of miR-135a-5p and miR-410-3p. These data contribute substantially to our understanding of the regulation of UGT2B7 and UGT2B4 expression.

5.2 Methods

5.2.1 Luciferase Plasmid Construction

The 3'UTR of UGT2B7 mRNA (NM_001074.2) is 264-base pair (bp) in length whereas the 3'UTR of UGT2B4 mRNA (NM_021139.2) is 486-bp in length. In order to generate a reporter construct containing the 3'UTR of UGT2B7 (pGL3/2B7/UTR), the 251 bp region between the stop codon (TAG) and the poly(A) tail of the UGT2B7 3'UTR was initially amplified from human genomic DNA (Roche Diagnostic, Indianapolis, IN) by Phusion hot-start high-fidelity DNA polymerase (Thermo Fisher Scientific, Pittsburgh, PA). The amplified region was then cloned into the pGL3- promoter vector at the XbaI restriction site which is located downstream of the luciferase coding sequence. Similarly, to generate a construct containing the UGT2B4 3'UTR (pGL3/2B4/UTR), the 469 bp region between the stop codon and the poly(A) tail was amplified and cloned into the pGL3- promoter vector at the XbaI restriction site. The primers used for cloning are listed in Table 5.1.

Using the pGL3/2B7/UTR construct as a template and the QuikChange site-directed mutagenesis kit (Stratagene, La Jolla, CA), the miR-3664 seed sequence (3'-

GGACUC-5'), which is complementary to the miR-3664 seed site in UGT2B7 3'UTR (5'-CCUGAG-3'), was changed to 5'-AGCTAG-3' producing the mutated construct pGL3/2B7/UTR/miR-3664/MT. Similarly, the miR-135a-5p seed sequence in the predicted target site was mutated from 5'-AGCCAU-3' to 5'-AUGACU-3' in the wild type construct to generate the mutated construct pGL3/2B4/UTR/miR-135a/MT. The miR-410-3p seed sequence in the predicted target site was mutated from 5'-UUAUAU-3' to 5'-UCCGCU-3' in the wild type construct to generate the mutated construct pGL3/2B4/UTR/miR-410/MT. The identities of all constructs were confirmed by DNA sequencing. The sequences of the primers used for mutagenesis are given in Table 5.1.

5.2.2 Western Blotting

HepG2 cells were transfected with miRNA mimics (miR-3664-3p or miR-neg) at 30 nM and 72 hours post-transfection, whole cell lysates were prepared with RIPA buffer (50mM Tris-HCl, pH 7.4, 150 mM NaCl, 1% NP-40, 2mM EDTA, 0.5% sodium deoxycholate, 0.1% SDS). The cell lysate concentrations were measured using the Bradford Protein Assay according to the manufacturer's protocol (Bio-Rad, Hercules, CA). Fifty micro-grams of each cell lysate or 5 µg of recombinant human UGT2B7 proteins expressed in baculovirus-infected insect cells (Supersomes from In vitro Technologies, VIC, Australia) were subjected to SDS-polyacrylamide gel electrophoresis on 12% acrylamide gels and transferred onto nitrocellulose membranes. The anti-UGT2B7 antibody used in Western blotting was developed in our laboratory as previously reported (Kerdpin et al. 2009, Hu et al. 2014) and the anti-calnexin antibody was obtained from Sigma-Aldrich. After the membranes were probed with primary antibodies (anti-UGT2B7 1:2000 or anti-Calnexin antibody

1:2000), the membranes were probed with a horseradish peroxidase-conjugated donkey anti-rabbit secondary antibody (1:2000) (NeoMarkers). SuperSignal®West Pico Chemiluminescent kit (Thermo Fisher Scientific) was used for visualizing the Immunosignals in the ImageQuant LAS4000 luminescent image analyzer (GE Healthcare Life Sciences, Piscataway, NJ). Multi Gauge Version 3.0 image software (FUJIFILM, Tokyo, Japan) was utilized for the quantification of band intensity.

5.2.3 Morphine Glucuronidation Assay

HepG2 cells were plated in 6-well plates and cultured overnight before transfection with miR-neg or miR-3664-3p at 30nM. Whole cell lysates were prepared after 24 hours post-transfection with 80 µl of TE buffer (10 mM Tris-HCl, 1 mM EDTA, pH 7.6) and the protein concentrations of the lysates were determined as described above. Two-hundred µl reactions of each sample containing 100 mM potassium phosphate pH 7.4, 4 mM MgCl₂, 5 mM morphine, 125 µg lysate protein and 5 mM UDPGA, were incubated for 2 hours at 37°C in a shaking water bath. The glucuronidation reaction was terminated by the addition of 2 µl of 70% (v/v) perchloric acid and samples were kept on ice for 30 minutes before centrifugation at 5000g for 10 minutes at 4°C. The supernatant fraction (40-µl) was analysed by HPLC using an Agilent 1100 series instrument (Agilent Technologies, Sydney, Australia) as previously described (Uchaipichat et al., 2004). Quantification of morphine-3-glucuronide concentrations in the samples was performed by comparing peak areas of the samples to those of standard curves prepared over the concentration range of 0.5 to 40 µM. Morphine-6-glucuronide was not detected in the samples.

5.2.4 Data Analyses of Liver Hepatocellular Carcinoma.

Liver hepatocellular carcinoma (LIHC) RNA-seq and miRNA-Seq datasets were downloaded from The Cancer Genome Atlas (TCGA) data portal (<https://portal.gdc.cancer.gov/>). The LIHC RNAseq data (371 HCC samples) were represented in the form of high-throughput sequencing counts. Genes (protein coding and noncoding) with a mean of less than 10 counts were discarded; the counts of the remaining genes were normalized using the upper quantile normalization method. Correlation analyses between the expression levels of UGT and miRNA gene sets were conducted using the Spearman rank method and plots were drawn using the R statistical package (<https://cran.r-project.org/>; R Foundation for Statistical Computing, Vienna, Austria).

5.2.5 Statistical Analysis.

Statistical analyses of all data were performed using GraphPad Prism 6 software (GraphPad Inc., La Jolla, CA), as mentioned in Materials and Methods (Chapter 2). Correlation analyses between expression levels of a UGT gene and a miRNA were conducted by Spearman correlation. A P value of 0.05 was considered statistically significant.

Table 5.1: Primers used in this study for mutagenesis, cloning and qPCR (5'–3')

Primer	Sequence (5' - 3')
<i>Cloning</i>	
UGT2B7_3UTR_F	CCGCTCTAGATTATATCTGAGATTTGAAGC
UGT2B7_3UTR_R	CCGGTCTAGACCGTAGTGTTTTCTTCATTG
UGT2B4_3UTR_F	CCGGTCTAGATTACGTCTGAGGCTGGAAGC
UGT2B4_3UTR_R	CCGATCTAGAGCTTCCTCAACAACAGTTAA

<p><u>Site-directed mutagenesis</u></p> <p>2B7_miR3664_MT_F 2B7_miR3664_MT_R</p> <p>2B4_miR135a_MT_F 2B4_miR135a_MT_R</p> <p>2B4_miR410_MT_F 2B4_miR410_MT_R</p>	<p>AGATTTCTTTCTTAGCTAGACAAAAAAAAAAAAAAG TTTTTTTTTTTTGTCTAGCTAAGAAAGAAATCTTG</p> <p>CAAAAATGATATAAATGACTATGAGGTTATATTG CAATATAACCTCATAGTCATTTATATCATTTTTG</p> <p>AAAGCCATATGAGGTCCGCTTGAAATGTATTGAG CTCAATACATTTCAAGCGGACCTCATATGGCTTT</p>
<p><u>RT-qPCR</u></p> <p>miR3664-3p_qPCR_F miR3664-3p_qPCR_R</p> <p>miR-1266-5p_qPCR_F miR-1266-5p_qPCR_R</p> <p>miR-4483_qPCR_F miR-4483_qPCR_R</p> <p>miR-4317_qPCR_F miR-4317_qPCR_R</p> <p>miR-216b-5p_qPCR_F miR-216b-5p_qPCR_R</p> <p>miR-135a_qPCR_F miR-135a_qPCR_R</p> <p>miR-410_qPCR_F miR-410_qPCR_R</p> <p>miR-489_qPCR_F miR-489_qPCR_R</p> <p>miR-4691-5p_qPCR_F miR-4691-5p_qPCR_R</p> <p>miR-101_qPCR_F miR-101_qPCR_R</p>	<p>GCAGTCTCAGGAGTAAAGACA AGGTCCAGTTTTTTTTTTTTTTTAACTC</p> <p>GCC TCA GGG CTG TAG AAC A GTC CAG TTT TTT TTT TTT TTT AGC CC</p> <p>GCA GGG GGT GGT CTG T GGT CCA GTT TTT TTT TTT TTT TCA ACA</p> <p>GCA GAC ATT GCC AGG GA CAG GTC CAG TTT TTT TTT TTT TTT AAA C</p> <p>GCA GAA ATC TCT GCA GGC A GGT CCA GTT TTT TTT TTT TTT TTC ACA TT</p> <p>CGC AGT ATG GCT TTT TAT TCC T GGT CCA GTT TTT TTT TTT TTT TTC ACA T</p> <p>CGC AGA ATA TAA CAC AGA TGG C AGG TCC AGT TTT TTT TTT TTT TTA CAG</p> <p>CGC AGG TGA CAT CAC ATA TAC CCA GTT TTT TTT TTT TTT TGC TGC C</p> <p>GGT CCT CCA GGC CAT GA AGT TTT TTT TTT TTT TTC CGC AGC</p> <p>CGC AGT ACA GTA CTG TGA TA GGT CCA GTT TTT TTT TTT TTT TTT CAG T</p>

5.3 Results

5.3.1 The UGT2B7 and UGT2B4 3'UTRs contain putative target sites for miRNAs

TargetScan (version 6.2) predicted 10 microRNA binding sites in the 3'UTRs of UGT2B7 and/or UGT2B4. MiR-3664-3p, miR-1266-5p, miR-4483, and miR-4317 were predicted to target the UGT2B7 3'UTR (Figure 5.1 A) whereas miR-135a-5p, miR-410-3p, miR-489-3p, miR-4691-5p and miR-101-3p were predicted to target the UGT2B4 3'UTR (Figure 5.1 B). Both UGT2B7 and UGT2B4 3'UTRs contained putative binding sites for miR-216b-5p (Figure 5.1).

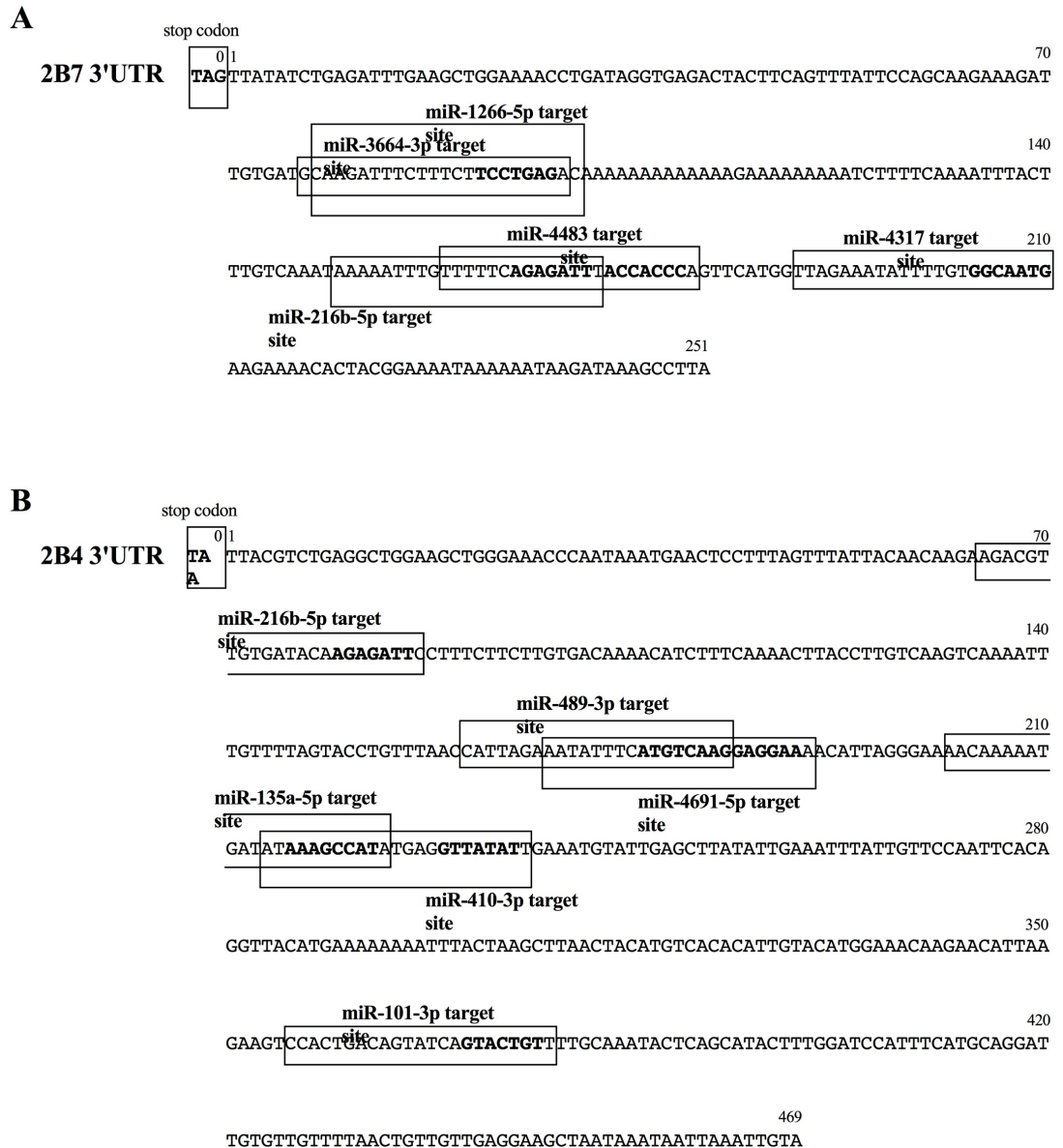


Figure 5.1: The 3'UTRs of UGT2B7 and UGT2B4 mRNAs contain putative miRNA binding sites

Schematic diagram of the UGT2B7 (A) and UGT2B4 (B) 3'-UTR regions with predicted miRNA binding sites indicated by boxes.

UGT2B4 has three transcript variants. Isoform 1 is the longest UGT2B4 transcript. Compared to isoform 1, isoform 2 has a frame-shift due to a lack of an exon in the 3' coding region. It also has a shorter C-terminus. Isoform 3 has differences in the 5' coding region and the 5'UTR compared to isoform 1, and it also has a shorter N-

terminus (NCBI database, <http://www.ncbi.nlm.nih.gov/gene/7363>). In addition, isoform 1 and 3, contain the same 3'UTR of 469 nucleotides whereas the 3'UTR of isoform 2 contains 726 nucleotides. Despite the differences in the transcript variants, the five predicted miRNA target sites are present in all three variants.

According to the TargetScan classification (explained in detail in Chapter 1) (Grimson et al., 2007, Nielsen et al., 2007), three UGT2B7 targeting miRNAs (miR-3664-3p, miR-4317 and miR-4483) are 8mer target sites with context score percentiles of 99% each. In addition, the predicted miR-4483 target site is also conserved in human and chimp. The predicted miR-216b-5p and miR-1266-5p target sites are 7mer-m8 and 7mer-A1 sites respectively, both with 97% context score percentiles. The miR-216b-5p target site is conserved in human, chimp and rhesus whereas miR-1266-5p is conserved in human and chimp. The UGT2B4 3'UTR targeting microRNAs miR-410-3p, miR-101-3p and miR-216b-5p are all 7mer-m8 target sites with context score percentiles of 97%, 96% and 97% respectively and they are all conserved in human and chimp. The miR-135a-5p target site is an 8mer site with a context score percentile of 99% which is conserved in human, chimp and rhesus. Both miR-489-3p and miR-4691-5p target sites are 7mer-A1 sites with 81% and 97% respective context score percentiles; miR-489-3p is conserved in human and chimp.

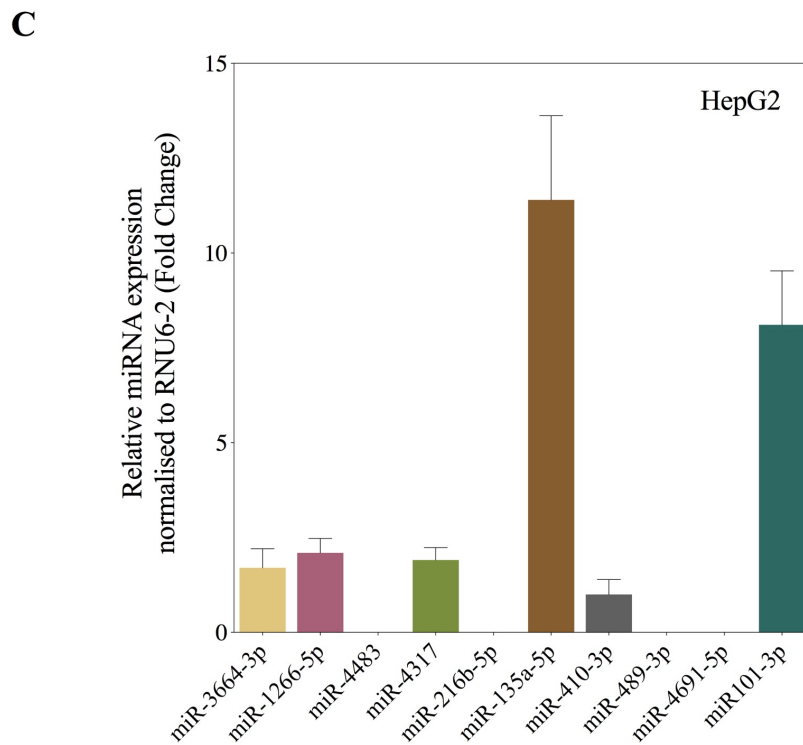
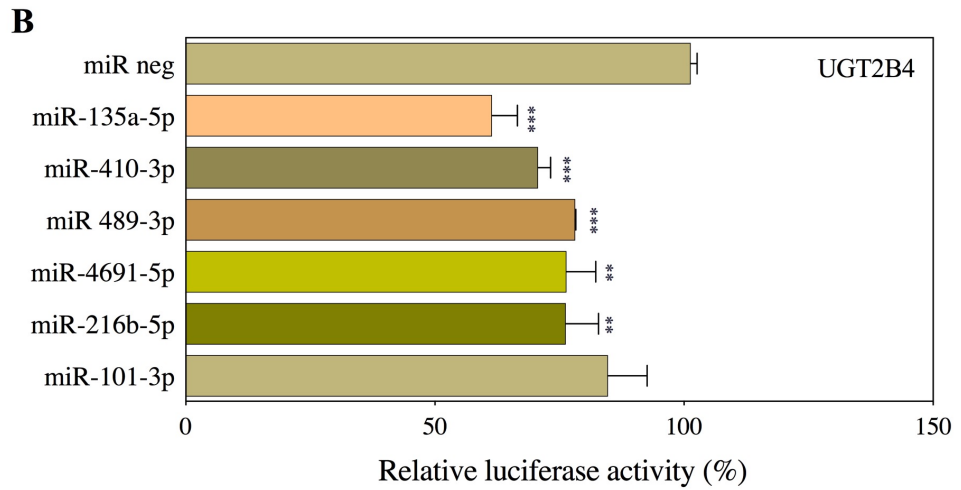
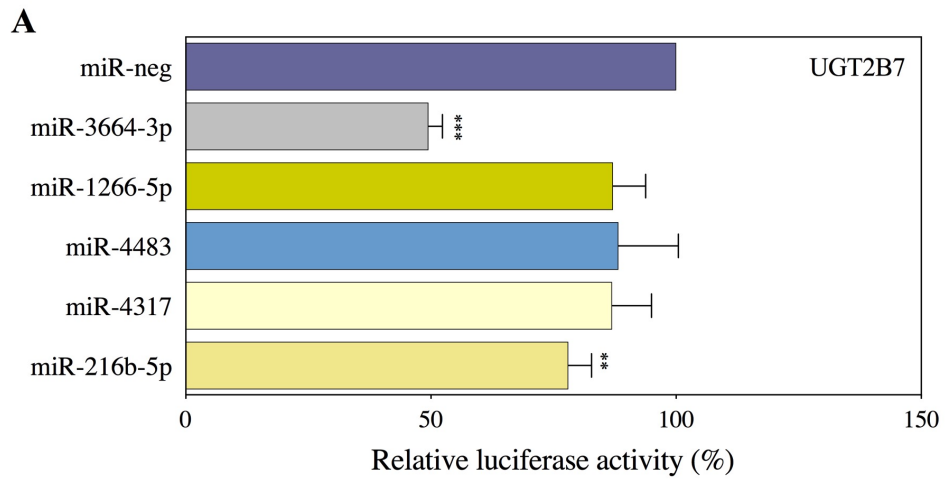


Figure 5.2: Effects of miRNA mimics on a luciferase reporter containing the UGT2B7 3'-UTR or UGT2B4 3'-UTR and expression of miRNAs in HepG2 cells

HepG2 cells were cotransfected with miR-neg or miRNA mimics and the reporter construct containing (A) UGT2B7 3'UTR and (B) UGT2B4 3'UTR. Firefly luciferase signal was normalized to renilla luciferase signal and presented relative to that of pGL3-promoter vector activity (set at a value of 100%). pRL-null vector was used as an internal control. Data shown are means from two independent experiments performed in quadruplicate, the error bar representing \pm S.E.M., *** $p < 0.0005$, ** $p < 0.005$. (C) The relative miRNA expression in HepG2 cells. The data was normalised to RNU6-2 and presented relative to the miR-410-3p expression (set at a value of 1).

To investigate the potential downregulation of UGT mRNAs by miRNAs in vitro, the 3'UTRs of UGT2B7 and UGT2B4 (isoform1) were cloned into the pGL3 promoter luciferase vector, downstream of the luciferase gene as described in Materials and Methods. Transfection of miRNA mimics along with the reporter constructs showed that miR-3664-3p and miR-216b-5p significantly reduced the UGT2B7 3'UTR reporter activity by 51% and 22% respectively, whereas miR-1266-5p, miR-4483, and miR-4317 did not significantly reduce reporter activity (Figure 5.2 A). Similarly, a significant reduction of 39%, 30%, 22%, 24% and 24% was seen in the UGT2B4 3'UTR containing reporter by miR-135a-5p, miR-410-3p, miR-489-3p, miR-4691-5p and miR-216b-5p respectively. No reduction in reporter activity was seen with miR-101-3p (Figure 5.2 B).

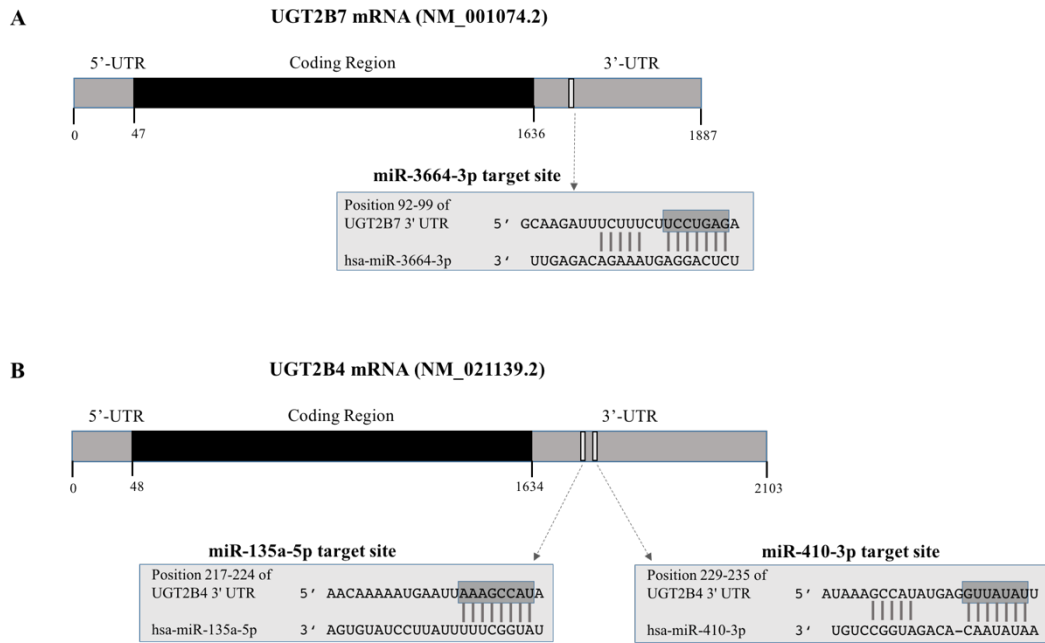


Figure 5.3: The putative interaction of the microRNAs with the 3'UTRs of UGT2B7 and UGT2B4 mRNAs

Shown are the seed pairings (highlighted in grey) and 3'-pairing between miR-3664-3p and its predicted binding site in the UGT2B7 3'UTR (A), miR-135a-5p and miR-410-3p and their predicted binding sites in the UGT2B4 3'UTR (B). The nucleotides of the miR-binding sites are numbered relative to the stop codon (TAG with G positioned as -1) of UGT2B7 (NM_001074.2) and UGT2B4 (NM_021139.2) mRNAs.

The subsequent studies focused on regulation of UGT2B7 and UGT2B4 by the miRNAs that showed the most efficient 3'UTR targeting: miR-3664-3p with the target site at nucleotides 92-99 in the 3'UTR of UGT2B7, and miRs-135a-5p and 410-3p with target sites at nucleotides 217-224 and 229-235 respectively in the 3'UTR of UGT2B4 (Figure 5.3). All three UGT2B4 transcript variants contain the miRs-135a-5p and 410-3p binding sites. Additional 3' compensation pairing of nucleotides 12-17 of the miRNA, has been known to augment specific miRNA targeting (Bartel, 2009, Grimson et al., 2007, Brennecke et al., 2005). Such 3' end-

pairing is seen at nucleotides 11-15 of the miR3664-3p target site in UGT2B7 and nucleotides 13-17 of the miR410-3p target site in UGT2B4.

5.3.2 The 3'UTR of UGT2B7 is a direct target of miR-3664-3p and the 3'UTR of UGT2B4 is a direct target of miR-135a-5p and miR-410-3p in HepG2 cells

To assess the direct interaction of miR-3664-3p with the UGT2B7 3'UTR, four contiguous bases within the predicted miRNA seed site sequence were mutated in the pGL3/2B7/UTR construct as described in Materials and Methods (Figure 5.4Ai). The wild-type and mutated constructs (pGL3/2B7/miR3664/MT) were cotransfected into HepG2 cells with miRNA mimics, and the luciferase activity of each reporter construct was measured. Consistent with data in Figure 5.2 A, miR-3664-3p significantly reduced the luciferase activity of the wild-type pGL3/2B7/UTR and this reduction was significantly abrogated in the pGL3/2B7/miR3664/MT construct (Figure 5.4 Aii). Similar results were seen in HuH7 cells; however, the inhibitory effect of miR-3664-3p was only partially abrogated in the mutant construct (Figure 5.5 A).

The role of miR-3664-3p in regulation of the UGT2B7 3'UTR was also assessed using a specific miRNA inhibitor. Cotransfection of the wild-type pGL3/2B7/UTR with a miR-3664-inhibitor did not significantly affect reporter luciferase activity in HepG2 cells. This was expected as the basal miR-3664-3p expression in HepG2 cells is very low (Figure 5.2 C). When the reporter was cotransfected with both miR-3664 mimics and inhibitors, there was no reduction in reporter activity showing that the miR-3664 inhibitor could abrogate repression of the pGL3/2B7/UTR reporter by

miR-3664 mimic. Collectively, these data show that the predicted miR-3664-3p target site in UGT2B7 is functional.

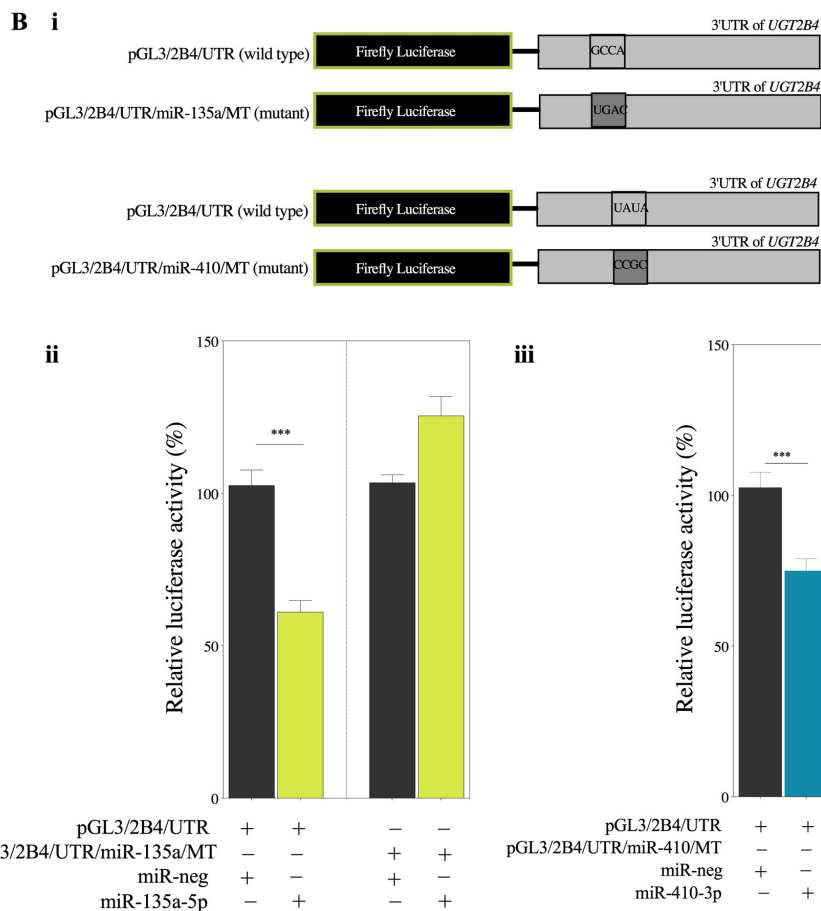
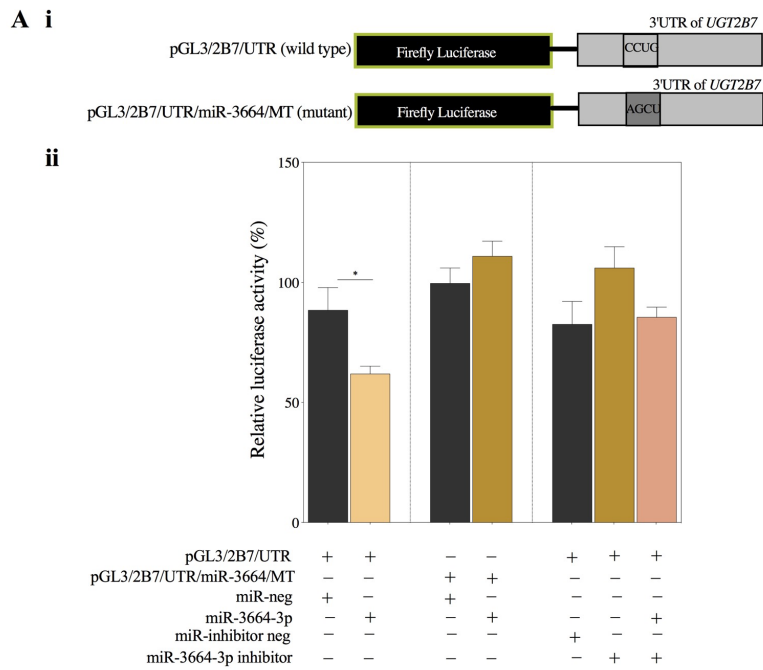


Figure 5.4: The UGT2B7 3'UTR contains a functional miR-3664-3p target site and the UGT2B4 3'UTR contains a functional miR-135a-5p site and a functional miR-410-3p site

(A i) Schematic representation of firefly luciferase reporter constructs containing either the wild type UGT2B7 3'UTR (pGL3/2B7/UTR) or mutated UGT2B7 3'UTR (pGL3/2B7/miR3664/MT) at the seed site for miR3664-3p. The seed site sequence is boxed and mutated seed site sequence is highlighted. (ii) Luciferase reporter assays in HepG2 cells cotransfected with miR-neg, miR-3664-3p mimics or miR-3664-3p inhibitors along with either the wild type or mutated UGT2B7 3'UTR reporter constructs. (B i) Schematic representation of firefly luciferase reporter constructs containing either the wild type UGT2B4 3'UTR (pGL3/2B4/UTR) or mutated UGT2B4 3'UTR at the seed site for miR-135a-5p (pGL3/2B4/miR135a/MT) or at the seed site for miR-410-3p (pGL3/2B4/miR410/MT). The seed site sequences are boxed and mutated seed site sequences are highlighted. (B ii, iii) Luciferase reporter assays in HepG2 cells cotransfected with either miR-neg, miR-135a-5p mimics or miR-410-3p mimics along with either the wild type or specific mutated UGT2B4 reporter constructs. Firefly luciferase signal was normalized to renilla luciferase signal and presented relative to that of pGL3-promoter vector activity (set at a value of 100%). pRL-null vector was used as an internal control. Data shown are the mean from two independent experiments performed in quadruplicate, the error bar representing \pm S.E.M., *** $p < 0.0005$, * $p < 0.05$.

Similar mutational analysis of the UGT2B4 3'UTR luciferase reporter construct was used to assess direct interaction of miR-135a-5p and miR-410-3p with the UGT2B4 3'UTR. Four contiguous bases within the predicted miRNA seed site sequences were mutated in the pGL3/2B4/3UTR reporter to generate constructs pGL3/2B4/miR135a/MT and pGL3/2B4/miR410/MT (Figure 5.4 Bi). These constructs were cotransfected with miR-135a-5p and miR-410-3p mimics in HepG2 cells. Both mimics reduced the activity of the wild type pGL3/2B4/UTR but did not affect the activity of their respective mutant constructs. This suggests that UGT2B4 is a direct target of miR-135a-5p and miR-410-3p in HepG2 cells (Figure 5.4 B ii, iii).

To assess whether the regulation of the UGT2B7 and UGT2B4 3'UTRs by these miRNAs is a consistent feature of liver cancer cells, an attempt was made to replicate the results from HepG2 cells in the Huh7 cell line. As in HepG2 cells, miR-3664-3p

mimics significantly reduced the luciferase activity of the wild-type pGL3/2B7/UTR in Huh7 cells, although this reduction was only partly abrogated in the pGL3/2B7/miR3664/MT construct (Figure 5.5 A). Similarly, miR-135a-5p mimics repressed wild type pGL3/2B4/UTR activity in Huh7 cells and this was abrogated by the seed site mutation (Figure 5.5 B). Interestingly however, miR-410-3p mimics did not alter either wild type or mutant pGL3/2B4/UTR activity in Huh7 cells (not shown).

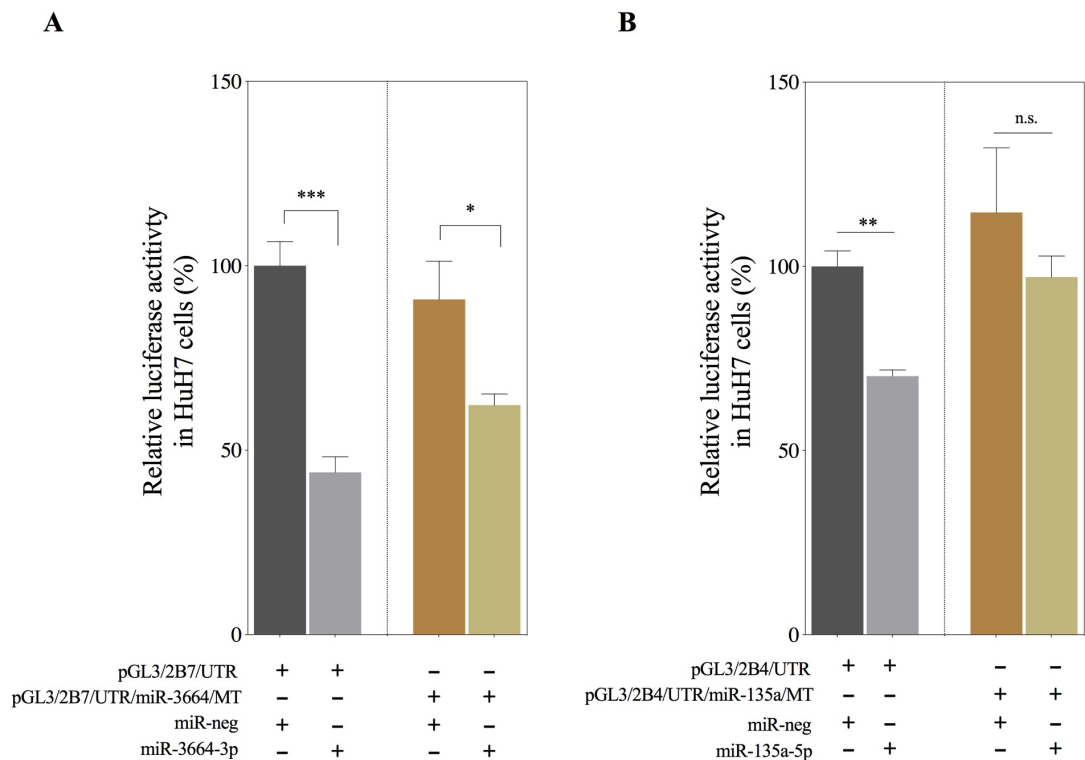


Figure 5.5: MiR-3664-3p and miR-135a-5p mimics reduce the activity of the pGL3-promoter construct carrying the UGT2B7 and UGT2B4 3'UTR respectively, via their binding to the predicted target site in Huh7 cells

(A) Luciferase reporter assays in Huh7 cells cotransfected with miR-neg, miR-3664 mimics along with either the wild type or mutated UGT2B7 3'UTR reporter constructs. (B) Luciferase reporter assays in Huh7 cells cotransfected with either miR-neg or miR-135a-5p mimics along with either the wild type or mutated UGT2B4 reporter constructs. Firefly luciferase signal was normalized to renilla

luciferase signal and presented relative to that of pGL3-promoter vector activity (set at a value of 1). pRL-null vector was used as an internal control. Data shown are representative of two independent experiments performed in triplicates, the error bar representing \pm S.D. *** $p < 0.0005$, ** $p < 0.005$, * $p < 0.05$.

5.3.3 MiR-3664-3p reduces UGT2B7 mRNA, protein, and glucuronidation activity in human liver HepG2 cells

To investigate the negative regulation of endogenous UGT2B7 mRNA by miR-3664-3p, miRNA mimics or inhibitors (miR-neg, miR-3664-3p mimic or miR-3664-3p inhibitor) were transfected into HepG2 cells and UGT2B7 mRNA levels were quantified using RT-qPCR. Figure 5.6 A and B confirm the effective over-expression and knockdown of miR-3664-3p after transient transfection of miR-3664-3p mimics and inhibitors respectively. The expression of miR-3664-3p was measured at 2 time points after miR-inhibitor transfection revealing that expression was reduced by 90% and 37% at 24h and 48h post-transfection respectively (data not shown). As shown in Figure 5.6 C, UGT2B7 mRNA levels were \sim 25% lower in miR-3664-3p mimic-transfected cells as compared with those in miR-neg-transfected cells. In addition, UGT2B7 mRNA levels were \sim 17% higher in miR-3664-3p inhibitor-transfected cells as compared with those in miR-neg-transfected cells. GAPDH mRNA levels were not significantly altered either by miR-3664-3p mimic or inhibitor as compared to miR-neg (Figure 5.6 D).

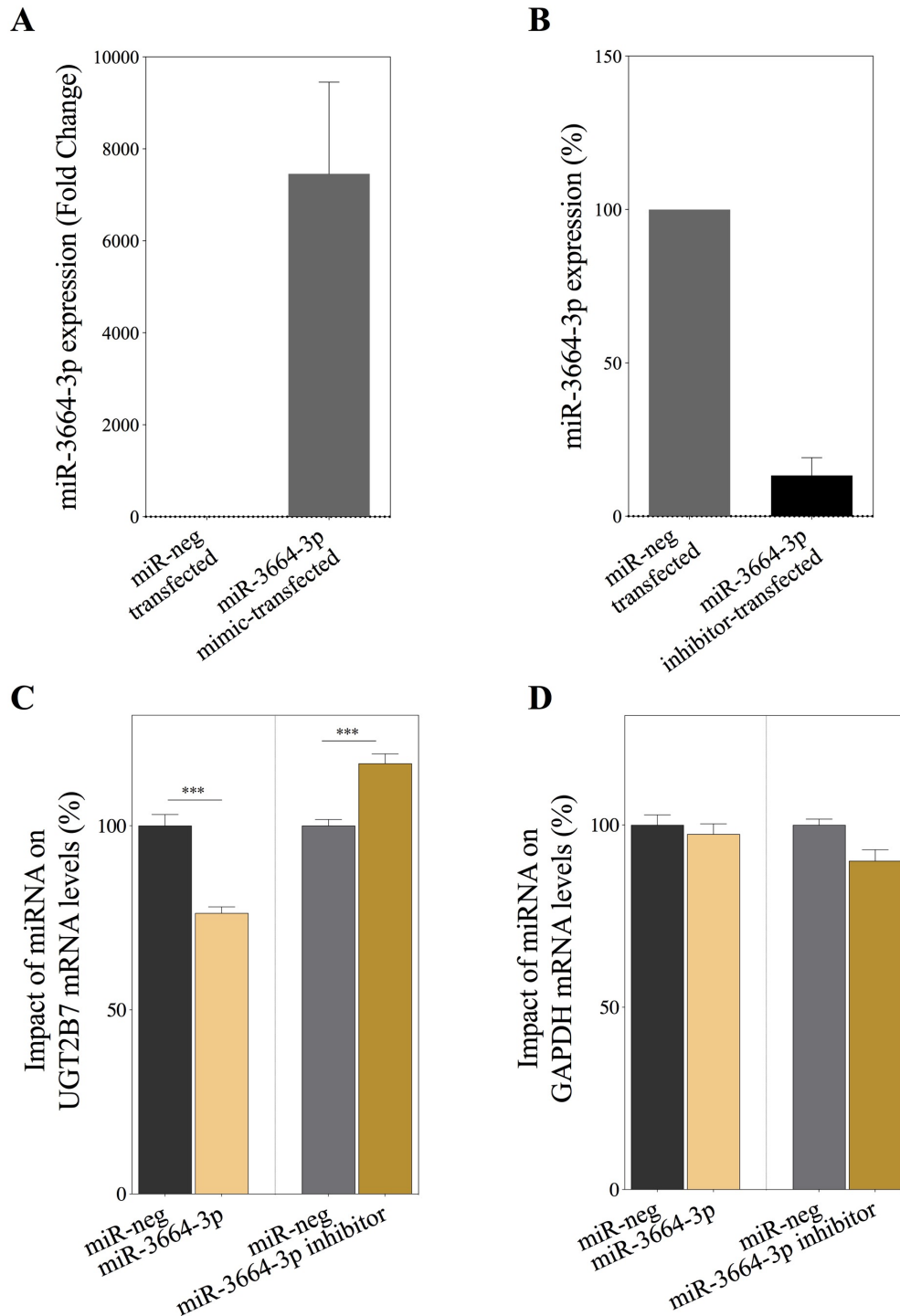


Figure 5.6: MiR-3664-3p mimics reduce the expression of endogenous UGT2B7 mRNA

(A) Overexpression of miR-3664-3p with miR-mimics in HepG2 cells 24h post transfection. MiR-3664-3p levels are normalised to RNU6-2 and fold change is presented relative to that of miR-neg-transfected cells (set at a value of 1). (B) Knockdown of miR-3664-3p expression with miR-inhibitors in HepG2 cells 24h post transfection. After normalization with RNU6-2, the miR-3664-3p levels were

presented relative to that of their respective vehicle-treated cells (miR-neg, set at a value of 100%). (C) Expression of UGT2B7 mRNA and (D) GAPDH mRNA, in HepG2 cells transfected with either miR-neg, miR-3664-3p mimics or miR-3664-3p inhibitors. Total RNA was extracted from the cells 24h post-transfection and then subjected to quantitative real-time RT-qPCR for measuring target gene mRNA levels. After normalization with 18S rRNA, the mRNA levels of target genes were presented relative to that of their respective vehicle-treated cells (miR-neg, set at a value of 100%). Data shown are means from three independent experiments performed in triplicate, the error bar representing \pm S.E.M., *** $p < 0.0005$.

To assess the effect of miR-3364 on UGT2B7 protein levels, Western blotting was performed with a UGT2B7 specific antibody after mimic transfection of HepG2 cells. The UGT2B7 protein levels were significantly reduced by 28% in miR-3664 mimic-transfected cells as compared to miR-neg transfected cells (Figure 5.7 A). Finally, UGT2B7 activity was assessed in miR-3664 mimic-transfected HepG2 whole cell lysates. Morphine was used as a specific substrate for this assay as UGT2B7 is the primary UGT that catalyses morphine glucuronidation (Coffman et al., 1997). Morphine can be metabolized into its major inactive metabolite, morphine-3-glucuronide (M3G) or a potent analgesic compound, morphine-6-glucuronide (M6G). The production of both metabolites was examined using HPLC-based assays. The results indicated a significant 41% reduction in the rate of M3G formation, with ectopic expression of miR-3664-3p (Figure 5.7 B). However, M6G formation was not detected in HepG2 cells.

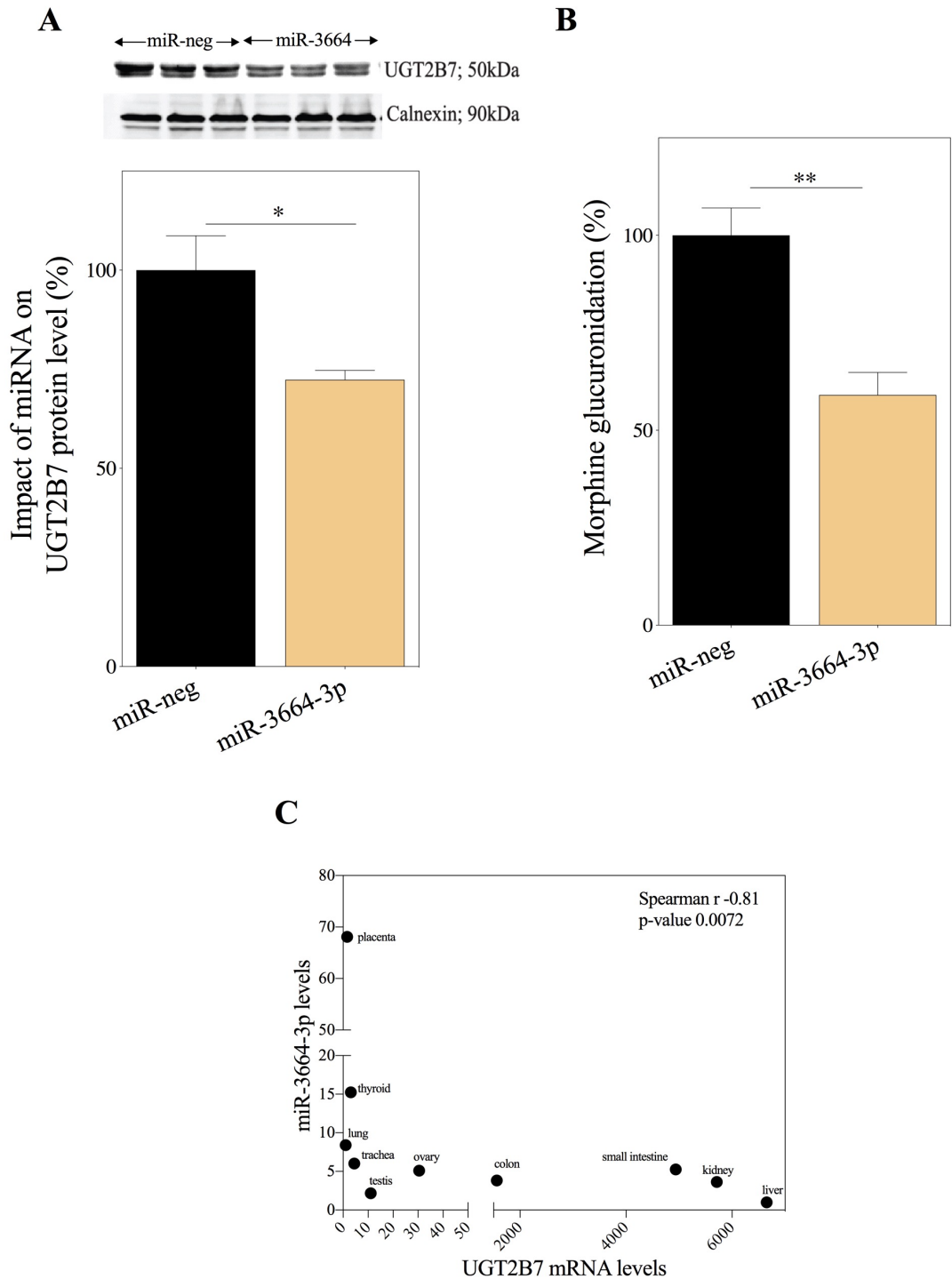


Figure 5.7: miR-3664-3p mimics reduce the protein expression of endogenous UGT2B7, and miR-3664 levels are negatively correlated to UGT2B7 mRNA in a tissue RNA panel

(A) MiR-3664 mimics reduce the protein levels of UGT2B7 in HepG2 cells transfected with either miR-neg or miR-3664 mimics. Cells were harvested 72 hours post-transfection, and the lysates were used to perform Western Blotting with anti-UGT2B7 and anti-Calnexin antibodies. Quantification of reduction in UGT2B7 protein levels relative to Calnexin levels in cells transfected with miR-3664 mimics

are presented relative to those with miR-neg-transfected cells (set at a value of 100%). Data shown are the immune signals of a representative experiment performed in triplicate (top) and the means \pm S.E.M. from two independent experiments performed in triplicate (bottom). *P < 0.05. (B) Quantification of reduction in morphine-3-glucuronide formation in HepG2 cells transfected with miR-3664 mimics as compared to miR-neg-transfected cells (set at a value of 100%). Cells were harvested 24h post-transfection and glucuronidation assays were performed using HPLC. (C) Negative correlation between the expression of miR-3664-3p and UGT2B7 in a panel of human tissues. MiR-3664-3p expression in tissues were quantified using RT-qPCR, normalized to RNU6-2 and presented as fold change relative to that of the liver tissue (set at a value of 1). Expression of UGT2B7 mRNA was normalized to 18S and presented as fold change relative to that of lung tissue (set at a value of 1) and data were examined using the Spearman correlation method as described in Materials and Methods. Each dot (●) represents the value of an independent tissue sample. p<0.05.

The expression miR-3664-3p was measured by RT-qPCR in a panel of 10 human tissues that express significant levels of UGT2B7 (liver, kidney, colon, small intestine, ovary, testis, trachea, lung, thyroid, and placenta). As shown in Figure 5.7 C, there was a significant negative correlation between UGT2B7 mRNA and miR-3664-3p in these tissues (Spearman's $r=0.8061$, $p<0.0072$). An analysis of RNAseq data from a TCGA cohort of 371 LIHCs also revealed high levels of UGT2B7 mRNA and extremely low levels of miR-3664 (data not shown). These observations suggest a negative correlation between miR-3664 and UGT2B7 mRNA levels in both normal and cancerous liver tissues. However, an overall correlation analysis between miR-3664-3p and UGT2B7 mRNA levels in liver cancer/liver tissue was not possible due to the lack of miR-3664-3p expression in most samples.

The negative regulation of endogenous UGT2B4 mRNA by miR-135a-5p and miR-410-3p was examined in HuH7 cells as these cells express higher levels of UGT2B4 relative to HepG2 cells (Figure 5.9 B). MiRNA mimics were transfected into Huh7 cells and UGT2B4 mRNA levels were quantified using RT-qPCR. Both miR-135a-

5p and miR-410-3p mimics decreased UGT2B4 mRNA expression to control miR-neg transfected cells (Figure 5.8 A). No reduction in GAPDH mRNA levels was observed as expected (Figure 5.8 B). As there are no commercially available UGT2B4-specific antibodies or identified UGT2B4-specific substrate, the effect of these miRNAs on UGT2B4 protein levels or enzymatic activity could not be assessed.

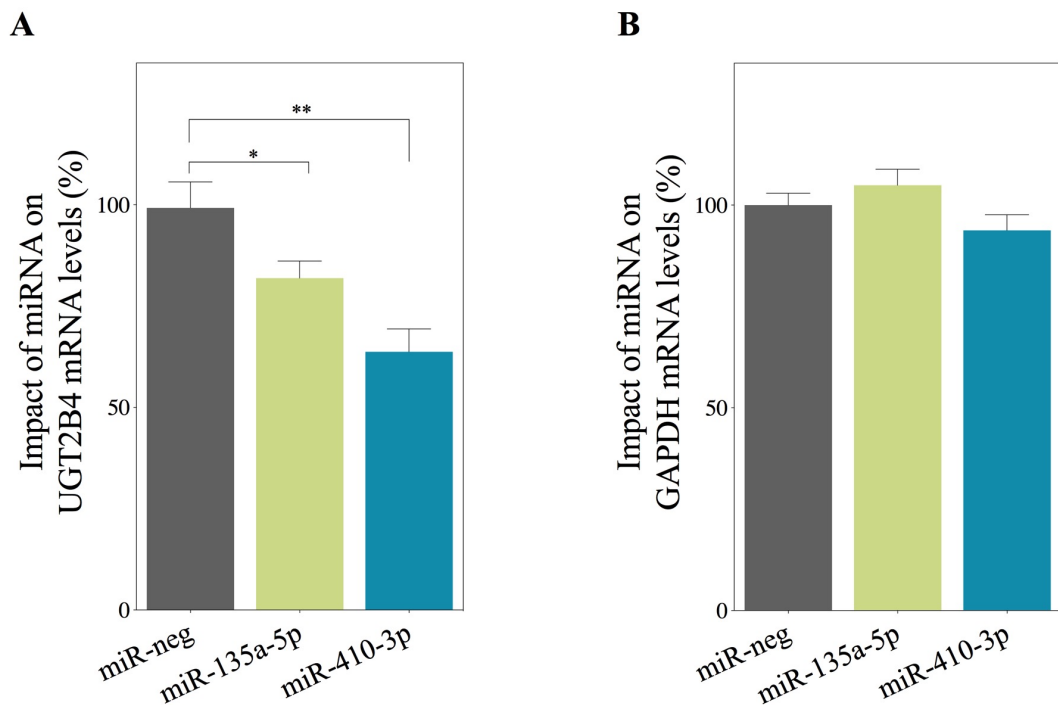


Figure 5.8: miR-135a-5p and miR-410-3p mimics reduce UGT2B4 mRNA levels in HuH7 cells

(A) Expression of UGT2B4 mRNA and (B) GAPDH mRNA, in HuH7 cells transfected with either miR-neg, miR-135a-5p or miR-410-3p mimics. Total RNA was extracted from the cells 24h post-transfection and then subjected to quantitative real-time RT-qPCR for measuring target gene mRNA levels. After normalising to 18S, the mRNA levels of target genes were presented relative to that of their respective vehicle-treated cells (miR-neg, set at a value of 100%). Data shown are means \pm S.E.M. from two independent experiments performed in triplicate. *P<0.05; **P<0.005

Next, the expression patterns of UGT2B4 and its target miRNAs were investigated in 18 human liver tissue samples. All the liver tissues expressed high levels of UGT2B4 but miR-410-3p expression was not detectable at significant levels. Interestingly, a significant negative correlation between UGT2B4 expression and miR-135a-5p expression was seen in these liver tissues (Spearman $r = -0.473$, $P < 0.0474$) (Figure 5.9 A). Levels of miR-135a-5p and UGT2B4 were also measured in HepG2 and Huh7 cells, revealing that miR-135a-5p levels are significantly lower in Huh7 cells than in HepG2 cells; conversely, UGT2B4 levels are significantly higher in Huh7 cells than in HepG2 cells (Figure 5.9 B). Thus the negative correlation between miR-135a-5p and UGT2B4 levels in liver tissues may also be observed in liver cancer cell lines. However, such no correlation between miR-135a-1 or miR-135a-2 primary transcripts and UGT2B4 mRNA was observed in the TCGA-LIHC RNAseq dataset containing 371 hepatocellular carcinoma specimens (UGT2B4/miR-135a-1 Spearman's $r = 0.040$, $p = 0.43959$; UGT2B4/miR-135a-2 Spearman's $r = 0.0055$, $p = 0.9152$) (Figure 5.9 C and D) or in a panel of 10 normal human tissues that express UGT2B4 (liver, kidney, testis, lung, thyroid, placenta, prostate, heart, and cervix) (Spearman's $r = -0.1667$, $p = 0.3389$).

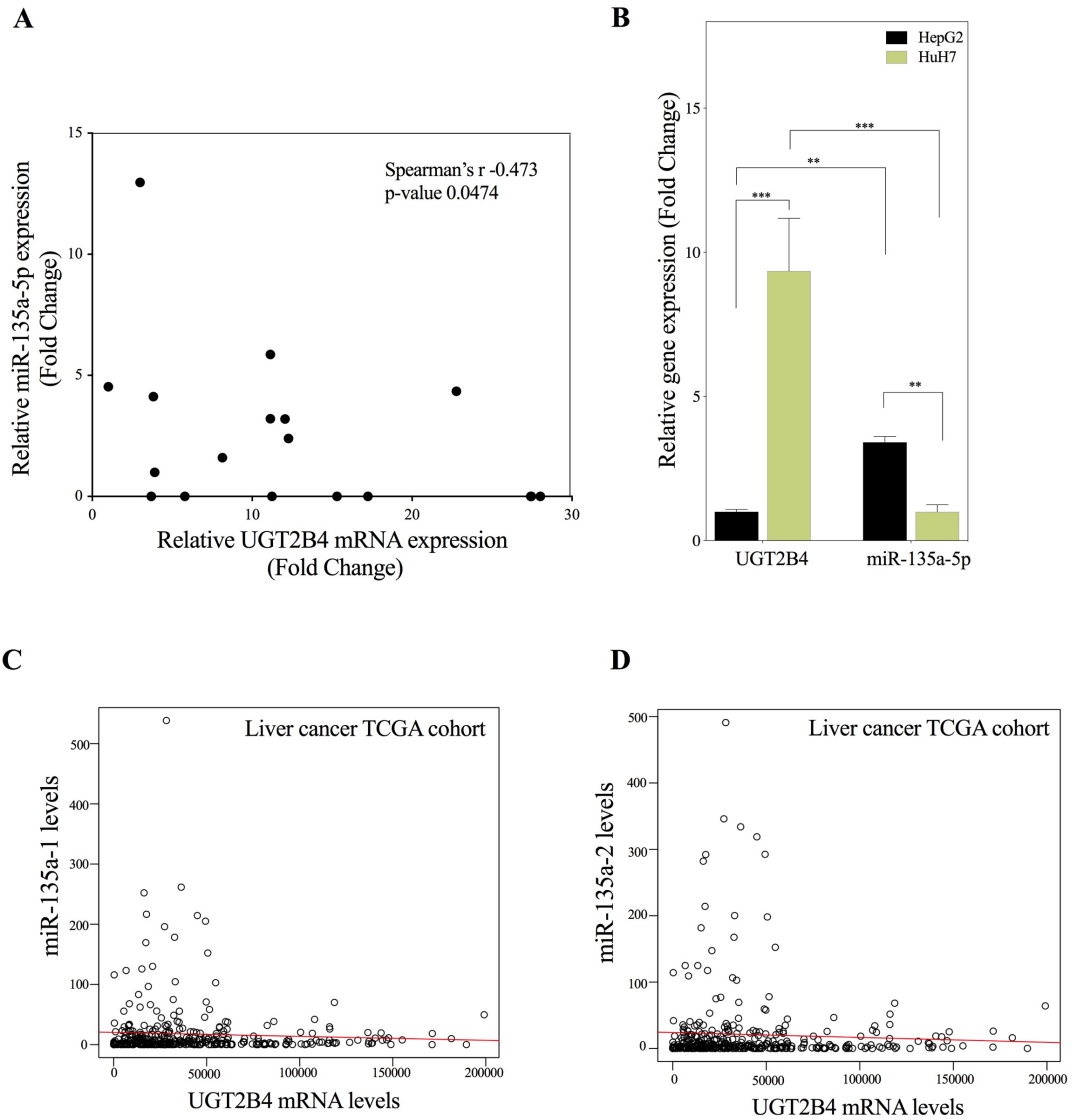


Figure 5.9: Correlation analyses between UGT2B4 and miR-135a-5p (or pri-miR-135a-1/2) levels in normal human liver tissues and liver cancer specimens

(A) Negative correlation between UGT2B4 and miR-135a-5p in a panel of normal human liver tissues. Data were quantified using RT-qPCR (expression of miR-135a-5p in liver tissues were normalized to RNU6-2 and expression of UGT2B4 mRNA was normalized to 18S), followed by correlation analyses between miR-135a-5p and UGT2B4 mRNA levels using GraphPad Prism 6 software as described in the Materials and Methods. (B) UGT2B4 and miR-135a-5p levels were measured in HepG2 and HuH7 cells. The expression of UGT2B4 in HepG2 cells is set as 1 (after normalising to 18S rRNA) showing that UGT2B4 has higher expression in HuH7 than HepG2 cells. The expression of miR-135a-5p in HuH7 cells is set as 1 (after normalising to RNU6-2) showing that miR-135a-5p has higher expression in HepG2 than in HuH7 cells. Data are means from an experiment performed in quadruplicate, the error bar represents \pm S.D., ** $p < 0.005$, *** $p < 0.0005$. (C and D) The correlation analysis of UGT2B4 and miR-135a primary transcript levels in the TCGA liver cancer cohort (371 specimens). Both the pri-miR-135a-1 (C) and pri-miR135a-2 (D) transcripts were examined because they both give rise to mature miR-135a-5p. Data

were normalized and correlation analysis between pri-miR-135a-1/miR-135a-2 and UGT2B4 mRNA levels were conducted using the Spearman rank method; the graphs were drawn using the R statistical package as described in the Materials and Methods.

As mentioned previously, the expression of miR-410-3p was not detectable at a significant level in the 10 human liver tissues and no correlation was observed between miR-410-3p and UGT2B4 expression levels. Despite this, we observed a significant negative correlation between miR-410-3p and UGT2B4 expression levels in the panel of 10 normal human tissues that express UGT2B4 (liver, kidney, testis, lung, thyroid, placenta, prostate, heart, and cervix) (Pearson $r = -0.77$, $P = 0.010$) (Figure 5.10 A). In addition, a significant negative correlation between the miR-410 primary transcript and UGT2B4 was also observed in TCGA-LIHC RNAseq dataset containing 371 hepatocellular carcinoma specimens (Spearman $r = -0.15$, $P = 0.002$) (Figure 5.10 B).

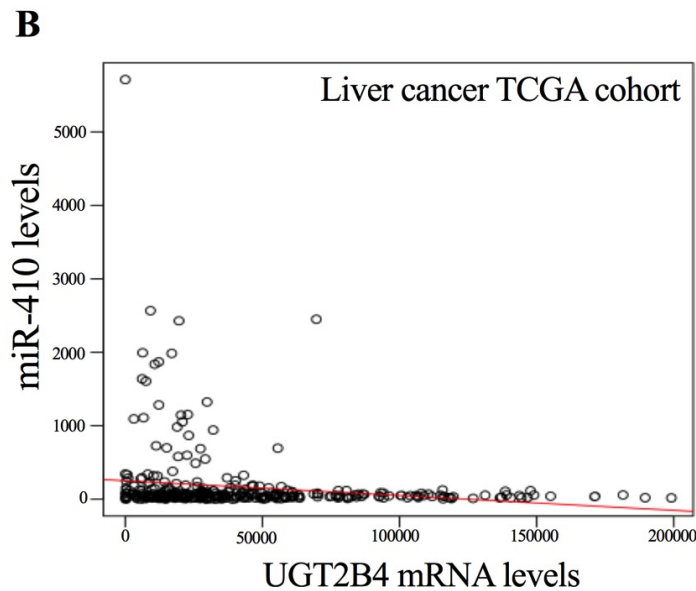
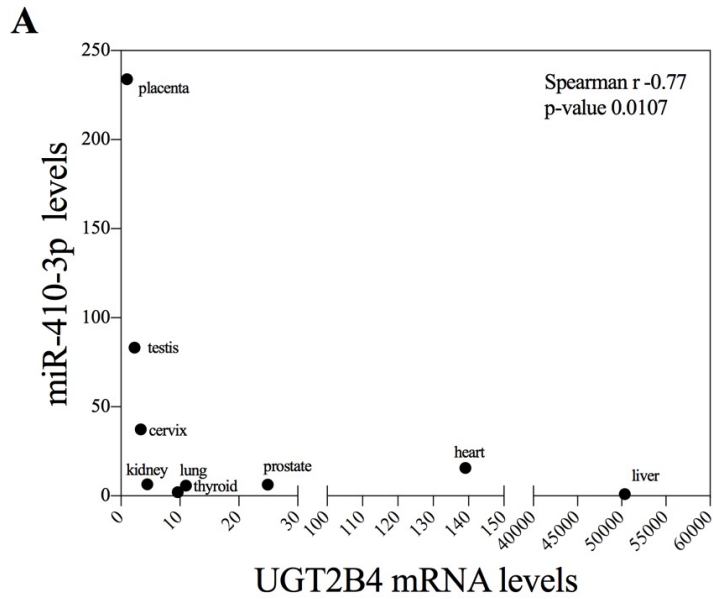


Figure 5.10: Negative correlation between UGT2B4 and miR-410-3p in a human tissue panel and a liver cancer cohort

(A) MiR-410-3p expression in tissues were quantified using RT-qPCR and normalized to RNU6-2 and presented as fold change relative to that of the liver tissue (set at a value of 1). Expression of UGT2B4 mRNA was normalized to 18S and presented as fold change relative to that of the placental tissue which showed the lowest UGT2B4 expression among tissue samples in the tissue panel (set at a value of 1). (B) Negative correlation between UGT2B4 and pri-miR-410 in the TCGA liver cancer cohort (371 specimens). Data were normalized and a correlation analysis between pri-miR-410 and UGT2B4 mRNA levels was conducted using the Spearman rank method; the graph was drawn using the R statistical package as described in the Materials and Methods.

5.4 Discussion

Given the importance of UGT2B7 and UGT2B4 in detoxification and systemic clearance of various endogenous and exogenous compounds especially via the liver, understanding control of their expression and activity is crucial. As UGT2B7 is a major drug metabolizing enzyme, changes in its expression may alter target drug pharmacokinetic properties leading to variability in drug levels that may impact on drug efficacy and/or toxicity. Moreover, inter-individual variation in drug metabolizing enzymes can alter risk of disease. Transcriptional regulation, mRNA processing (splicing and stability), epigenetic effects of small regulatory RNAs such as miRNAs and post-translational modifications are some factors that account for inter-individual variation in drug-metabolizing enzymes (Sadee et al 2005). Even though several transcriptional regulators have been identified for UGT2B7 and UGT2B4, little is known about post-transcriptional mechanisms that impact on UGT2B7/UGT2B4 gene regulation and to date there has been only one report of their post-transcriptional regulation by miR-216b-5p in liver cancer cell lines (Dluzen et al., 2016). Therefore, the present investigation on the post-transcriptional regulation of UGT2B7 by microRNAs is extremely timely.

In this chapter, potential binding sites for 5 different miRNAs were identified in the 3'-untranslated regions (3'-UTR) of UGT2B7 and/or UGT2B4 by bioinformatic analysis. Experiments in HepG2 cells with miR-mimics demonstrated that miR-3664-3p significantly reduced mRNA, protein and activity levels of UGT2B7. Furthermore, the direct binding of miR-3664-3p to the 3'UTR of UGT2B7 was demonstrated using luciferase reporter assays. Human chromosome 11 encodes pri-miR-3664 (11q13.4), which is processed into 2 mature miRNAs, miR-3664-3p and

miR-3664-5p (NCBI: <https://www.ncbi.nlm.nih.gov/gene/100500844> and miRBase: http://www.mirbase.org/cgi-bin/mirna_entry.pl?acc=MI0016065). Not much is known about miR-3664-3p but microarray data suggests it is upregulated in the peripheral blood of glioblastoma patients compared to control cases (Dong et al 2014) and in individuals with gastric cancer (Liu et al., 2014). Thus, its biological role in liver cancer remains to be investigated. So far only one study has evaluated correlation between UGT2B7 activities and miR-3664-5p concentrations in 27 liver specimens but unfortunately found no association (Papageorgiou and Court, 2017b). In the future it might also be possible to examine relationships between levels of this miRNA and UGT2B7-related drug metabolic capacity and drug responses in larger liver cohorts.

Two miRNAs, miR-135a-5p and miR-410-3p, were found to negatively regulate UGT2B4 expression by binding directly to its 3'UTR. Even though UGT2B7 and UGT2B4 share high sequence similarity (~85%), miR-3664-3p did not target the 3'UTR of UGT2B4 and neither miR-135a-5p nor miR-410-3p targeted the 3'UTR of UGT2B7, indicating specificity of miRNA targeting. Human chromosome 3 encodes miR-135a-1 (3p21.2) and human chromosome 12 encodes miR-135a-2 (12q23.1) primary transcripts that both give rise to miR-13a-5p mature miRNA (NCBI: <https://www.ncbi.nlm.nih.gov/gene/406925> and <https://www.ncbi.nlm.nih.gov/gene/406926>, miRBase: http://www.mirbase.org/cgi-bin/mirna_entry.pl?acc=MI0000452 and http://www.mirbase.org/cgi-bin/mirna_entry.pl?acc=MI0000453). In liver cancer, both miR-135a (Liu et al., 2012, Zeng et al., 2016) and miR-410 (Wang et al., 2014, Marrone et al., 2016) are reported to be upregulated and are considered as liver onco-miRs. However, downregulation of these two miRNAs have been reported in certain cancers such as

prostate, neuroblastoma and epithelial ovarian cancer (Theodore et al., 2014, Gattolliat et al., 2011, Tang et al., 2014).

In accordance with the possibility that miR-3664-3p negatively regulates UGT2B7 expression in vivo, there was an inverse correlation in the levels of miR-3664-3p and UGT2B7 mRNAs in a panel of 10 human tissues (including 9 extra hepatic tissues). However, some tissues such as testis, ovary and trachea had low/ absent levels of UGT2B7 as well as low/absent miR-3664-3p levels. One possible explanation for this would be the effects of transcriptional regulation of UGT2B7 expression in these tissues. The key transcriptional regulators such as HNFs that activate the UGT2B7 promoter, have low expression in these tissues which may result in low levels of UGT2B7 transcription. In cell types where UGT transcription is low or absent, post-transcriptional regulation likely has little relevance. Furthermore, correlation analysis of TCGA-LIHC database (371 specimens) found that miR-3664 and UGT2B7 levels were in fact negatively correlated in both normal and cancerous liver tissues. The data showed high expression of UGT2B7 and low/absent expression of miR-3664 in these tissue specimens, suggesting that low/absent miR-3664 may permit high UGT2B7 levels to be maintained.

A negative correlation between miR-410 and UGT2B4 mRNA levels in the liver cancer TCGA cohort was also observed. In addition, miR-410-3p showed a negative correlation with UGT2B4 levels in a panel of 10 normal human tissues. However, there was no correlation in panel of 18 normal liver tissues. This may relate to the low sample numbers and further studies involving examining larger cohort of liver tissues should be performed for clarification. In terms of the relationship between UGT2B4 and miR-135a-5p, there was a negative correlation in the panel of 18

normal liver tissues as well as the 2 liver cancer cell lines, but unexpectedly, no correlation in the cohort of TCGA-LIHC specimens. Many factors including both transcriptional and post-transcriptional regulators, are involved in the regulation of a given gene. Deregulation of transcription factors and other miRNAs that are involved in UGT2B4 expression in liver cancer has been previously reported (Callegari et al., 2015, Negrini et al., 2011); these other regulatory factors may have greater impact on UGT2B4 levels than miR-135a-5p.

As mentioned previously in Chapter 4, the spacing between the seed sites of miRNAs determine the efficacy and the cooperativity of these target sites on the 3' UTR (optimal spacing range is 13-35 nucleotides between the seed pairs) (Saetrom et al., 2007). Our study combined with a study conducted by Dluzen et al indicate that miR-135a-5p, miR-410-3p and miR-216b-5p all directly target UGT2B4 and that miR-3664-3p and miR-216b-5p directly target UGT2B7. As mentioned earlier, the 5' 11 nucleotides of the miR-135a-5p site overlap with the 3' 11 nucleotides of the miR-410-3p site in the UGT2B4 3'-UTR (Figure 5.1 B) and the distance between the 2 seed sites of 12 nucleotides falls just outside the optimal spacing range. Even though the probability of cooperative regulation by these 2 miRNAs on UGT2B4 is low, it could be investigated in future studies. The distance between the miR-216b-5p and miR-135a-5p seed sites is 137 nucleotides and the distance between the miR-216b-5p and miR-410-3p seed sites is 149 nucleotides in the UGT2B4 3'UTR (Figure 5.1 B). The distance between miR-216b-5p and miR-3664-3p seed sites is 73 nucleotides in the UGT2B7 3'UTR (Figure 5.1 A). Therefore, cooperativity between these miRNA target sites is also predicted to be unlikely; however, this also remains to be tested empirically.

In summary, the present study demonstrates that the UGT2B7 mRNA is a direct target of miR-3664-3p and that UGT2B4 mRNA is a direct target of miR-135a-5p and miR-410-3p and that many of the relationships defined in vitro using cell lines are supported by correlation analyses in human tissues. This provides novel evidence for post-transcriptional regulation of UGT2B7 and UGT2B4 by miRNAs in hepatic cells. Altered expression of miRNAs, such as miR-3664-3p and possibly miR-135a-5p and miR-410-3p in the liver, may have a role in endobiotic homeostasis and/or detoxification and clearance of xenobiotics including therapeutic drugs.

CHAPTER 6

**INVESTIGATION OF UGT2B15 AND UGT2B17
POST-TRANSCRIPTIONAL REGULATION BY
ANDROGENS**

**6.1 PART 1: INVESTIGATION OF THE INVOLVEMENT OF
RNA-BINDING PROTEINS IN UGT2B15 AND UGT2B17
REGULATION**

6.1.1 Introduction

The expression and activity of UGT2B15 and UGT2B17 in the prostate cancer line LNCaP has been shown to be repressed by both natural DHT and the synthetic androgen R1881 (Chouinard et al., 2006). Studies presented in this chapter using LNCaP cells are consistent with this finding (Figure 6.2.1 A, B). The mechanisms behind these effects both at the transcriptional level and post-transcriptional level have yet to be identified. CHIP assays have shown androgen induced binding of AR to the UGT2B15 proximal promoter in LNCaP cells (Bao et al., 2008) suggesting a possible transcriptional repression mechanism; although the regulatory elements that mediate this repression have not been defined. Importantly, the contribution of post-transcriptional regulation towards this regulation remains unexplored.

Apart from miRNAs, RNA-binding proteins (RBPs) are another major class of molecules involved in post-transcriptional gene regulation (Ciafrè and Galardi, 2013, Lukong et al., 2008). They are key players that govern RNA metabolism via regulating processes such as RNA splicing, export, localization, stability and

translation [(Keene, 2007) and Figure 6.1.1]. RBPs function in ribonucleoprotein complexes (RNPs) that associate with untranslated (pre-mRNAs), protein-coding (mRNAs) or non-protein-coding RNAs and can act as either activators or repressors depending on the mRNA, protein and the biological context (Lukong et al., 2008, Ciafrè and Galardi, 2013). They are classified into different categories based on their expression patterns and target RNAs (Anji and Kumari, 2016, Sanchez-Diaz and Penalva, 2006).

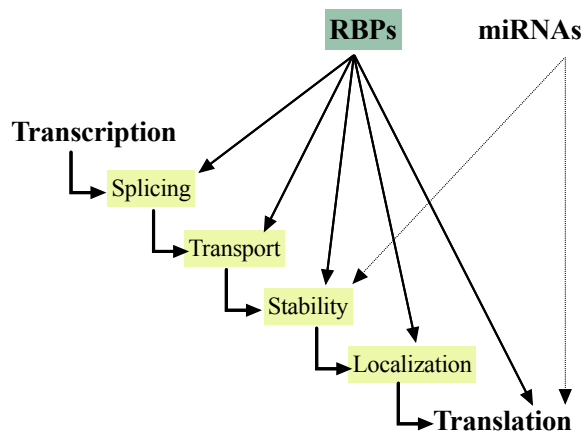


Figure 6.1.1: Post-transcriptional regulation of gene expression by RBPs and miRNAs at different levels

The levels at which RBPs and miRNAs regulate target mRNAs are shown by arrows [modified from (Keene, 2007)]. RBPs target RNA splicing, export, localization, stability and translation whereas miRNAs target RNA stability and translation.

RBPs contain single or multiple RNA-binding domains that can recognize specific sequences in either single stranded or double stranded RNA. It is believed that a single RBP may have a vast number of targets and multiple RBPs could bind to a single RNA and regulate its expression in a combinatorial way (Anji and Kumari, 2016, Kishore et al., 2010, Keene and Tenenbaum, 2002, Smith and Valcarcel, 2000). In addition, it is speculated that stability, localization and translation of many RNAs are regulated coordinately by RBPs (Keene and Tenenbaum, 2002, Selbach et

al., 2008, Baek et al., 2008). To date, several hundred RBPs have been identified and 3-11% of the genes in bacteria, archaea and eukaryotes are estimated to encode RBPs (Baltz et al., Anantharaman et al., 2002). Most RBPs show evolutionary conservation among various species but some are restricted to single species (Anji and Kumari, 2016).

Many RBPs bind to uridine (U)- or adenosine-uridine (AU)-rich sequences known as AU-rich elements (AREs) on target mRNAs to modulate their expression post-transcriptionally. A typical ARE consists of two to five copies of the sequence AUUUA (Lal et al., 2004, Chen and Shyu, 1995, Wilson and Brewer, 1999). These AREs are predicted to be present in 5-8% of all mRNA transcripts in humans (Shen and Malter, 2015). ARE-binding proteins include AU-binding factor 1 (AUF1) also known as heterogeneous nuclear ribonucleoprotein D (hnRNP D) (Zhang et al., 1993), tristetraprolin (TTP) (Lai et al., 2003), T-cell internal antigen-1 (TIA-1), TIA-1-related protein (TIAR) (Piecyk et al., 2000, Gueydan et al., 1999), KH-type splicing regulatory protein (KSRP) (Gherzi et al., 2004), butyrate response factor 1 (BRF1) (Stoecklin et al., 2002), and the Hu proteins HuB, HuC, HuD, and HuR (Brennan and Steitz, 2001).

Of specific relevance to this project, ARE binding proteins such as AUF1 have been shown to be regulated by androgens in a tissue-specific pattern (Sheflin and Spaulding, 2000, Sheflin et al., 2001, Sheflin et al., 2004). Hence we hypothesized that AUF and other RNA binding proteins (RBPs) may be involved in the downregulation of UGT2B15 and UGT2B17 by androgens in prostate cells. In support of this hypothesis, bioinformatic analysis showed that the 3'UTRs of UGT2B15 and UGT2B17 mRNAs each contain three AU-rich (AUUUA) regions. In

the current study, the possible role of ARE-binding RBPs in regulation of UGT2B15 and UGT2B17 was examined, particularly TTP, TIAR, KSRP, HuR and AUF1.

The TTP protein is a predominant cytoplasmic RBP that is known to destabilize many target RNAs including several inflammatory mediators (Barreau et al., 2005). TIAR is a nuclear protein that could shuttle to the cytoplasm under stimuli (Taupin et al., 1995). This protein has been reported to post-transcriptionally regulate target genes by repressing translation (Anderson and Kedersha, 2002b, Anderson and Kedersha, 2002a). KSRP is a multifunctional protein that is involved in mRNA stability, splicing and localization. It's key targets include several genes involved in inflammation, lipid metabolism, tissue regeneration and cell fate (Winzen et al., 2007, Gherzi et al., 2014). HuR is a predominant nuclear RBP, which shuttles from the nucleus into the cytoplasm under various stimulations (Barreau et al., 2005, Wang et al., 2013). It is ubiquitously expressed in many tissues including intestine, spleen, adipose and testis (Wang et al., 2013) and has been reported to regulate expression of various genes involved in cell division, stress response, immune response mainly via mRNA stabilization and targeting protein translation (Wang et al., 2013, Lal et al., 2004).

The AUF1 protein is also ubiquitously expressed and regulates gene expression through multiple post-transcriptional mechanisms including RNA stability. It can act to either stabilize or destabilize target mRNAs depending on the cell type and the type of ARE (Xu et al., 2001). AUF1 has four isoforms; p37, p40, p42 and p45 due to alternative splicing of its pre-mRNA transcript encoded by the chromosome 4 locus 4q21. p37 AUF1 is a 37kDa core protein, p40 AUF1 is a 40kDa protein containing an N-terminal 19 amino acid exon 2 insertion, p42 AUF1 is a 42kDa

protein containing a C-terminal 49 amino acid exon 7 insertion, and p45 AUF1 is a 45kDa protein containing both exon 2 and exon 7 insertions (Wagner et al., 1998). These isoforms possess different binding affinity towards target mRNAs (p37 > p42 > p45 > p40) and show a differential cell specific expression pattern (Wagner et al., 1998, Shen and Malter, 2015). Similar to HuR, this nuclear RBP is shown to shuttle from nucleus to cytoplasm (Barreau et al., 2005). AUF1 key targets include mRNAs involved in processes such as cell-cycle progression, immune response, apoptosis, stress response and telomere maintenance (Lal et al., 2004, Kiledjian et al., 1997, Gratacos and Brewer, 2010, Zucconi and Wilson, 2011, Eversole and Maizels, 2000).

Emerging evidence shows that dysfunction of RBPs is associated with various human diseases including neurological diseases, muscular atrophies and cancer (Lukong et al., 2008, Castello et al., 2013, Musunuru, 2003, Cooper et al., Darnell, 2010, Neelamraju et al., 2015, Kechavarzi and Janga, 2014). Especially in cancer, aberrant expression of several RBPs has been reported (Tessier et al., 2004, Sanchez-Diaz and Penalva, 2006) and dysfunction of RBPs has been shown to affect alternative splicing or alternative cleavage mechanisms of target RNAs leading to tumorigenesis (Kechavarzi and Janga, 2014). Of note, KSRP has been reported to be involved in leukemias and lymphomas via post-transcriptionally regulating specific genes or miRNAs (Baou et al., 2011). Additionally, HuR is involved in tumourigenesis and cancer progression by acting either as a tumour suppressor or an oncogene via regulating many target genes. Its involvement in various human cancers including breast, lung, ovarian and colon cancers has been reported (Wang et al., 2013). Furthermore, high levels of AUF1 have been reported in several cancers including breast, skin, thyroid and liver cancers, and involvement of AUF1 in sarcoma development has been reported (Abdelmohsen et al., 2012).

In studies described in this Chapter, the potential role of the above-mentioned ARE-binding RBPs in post-transcriptional regulation of UGT2B15 and UGT2B17 was explored in prostate cancer cell lines.

6.1.2 Materials and Methods

6.1.2.1 PCR amplification of the RBPs from cell lines

The expression levels of RBPs were detected by PCR amplification of target RBP transcripts from cDNA of VCaP, LNCaP, ZR75, T47D and MDA-MB-453 cells. PCR reactions consisted of 3 μ l of cDNA from cell lines (prepared as described in Materials and Methods in Chapter 2) as the template, 1 unit of Taq polymerase, 0.4 mM dNTPs, and 0.5 μ M of each primer (Table 6.1) in a 25 μ l reaction of 1 x ThermoPol® buffer. The reactions were run for 1 cycle at 95°C for 5 minutes, 30 cycles of 94°C for 45 seconds, 58°C for 1 minute and 72°C for 1 minute, followed by a final extension cycle of 72°C for 10 minutes. PCR products (10 μ l) were run on an ethidium bromide-stained 1.5 % agarose gel for 25 minutes at 80V for detection.

6.1.2.2 Extraction of pCMV-AUF1 vectors

The AUF1 expression vectors; pCMV-AUF1(p37), pCMV-AUF1(p40), pCMV-AUF1(p42) and pCMV-AUF1(p45) used in this study were generated in Dr. Gary Brewer's laboratory (UMDNJ). All the vectors including the control empty pCMV were kindly provided to us by Dr. Myriam Gorospe (Laboratory of Cellular and Molecular Biology, National Institute on Aging, 251 Bayview Blvd, suite 100, Baltimore, Maryland, USA) with the consent of Dr. Gary Brewer.

Each vector was provided on Whatman paper that was immersed in 100 μ l of filtered EB buffer in 1.5 ml sterile eppendorf tubes for 3 hours at room temperature. The tubes were vortexed to completely resuspend the vectors in EB buffer. A 3 μ l aliquot of the resultant samples was used for transformation into DH5 α cells as described in Materials and Methods in Chapter 2.

6.1.2.3 Verification of the identity of AUF1 expression vectors

After transformation, 200 μ l of bacterial culture was spread on LB agar plates and incubated at 37°C overnight. Colonies were analysed for appropriate inserts by PCR of miniprep DNA. PCR reactions consisted of 50 ng of AUF1 isoform expression vector, 2 units of Taq polymerase, 0.4 mM dNTPs, and 0.5 μ M of each primer (Table 6.1) in a 50 μ l reaction of 1 x ThermoPol® buffer. The same PCR conditions were used as above, and the PCR products (10 μ l) were run on an ethidium bromide-stained 1.5 % agarose gel for 25 minutes at 80V for detection (Figure 6.1.2).

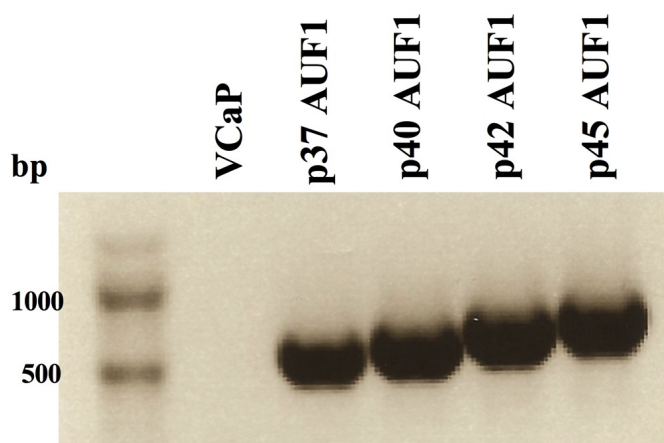


Figure 6.1.2: AUF1 isoform detection in AUF1 expression vectors

Shown is the PCR amplification of AUF1 isoforms using specific primers. The amplified PCR products of target transcripts were run on an ethidium bromide-stained 1% agarose gel.

6.1.2.4 Transient Transfection of AUF1 expression vectors into cell lines

All transfections were performed using Lipofectamine 2000 according to the manufacturer's protocol. For VCaP transfections, cells were first plated in DMEM medium supplemented with 10% FBS and 0.1 nM DHT in 6-well plates at approximately 1×10^5 cells per well and grown overnight (16 hours) at 37°C in 5% CO₂ before the transient transfection with pCMV-AUF1 vectors at 2.5 µg per well. Transfections were performed when cells reached 60 to 70% confluence. Cells were harvested 24 hours after transfection for RNA analysis. For LNCaP transfections, cells were plated in RPMI 1640 medium supplemented with 5% FBS in 6-well plates at approximately 1×10^6 cells per well and transfected under the same conditions as above.

6.1.2.5 DHT Treatment of LNCaP and VCaP cells

VCaP cells were firstly plated in phenol red-free DMEM medium supplemented with 5% dextran-coated charcoal-stripped FBS for 48 hours in 6-well plates. LNCaP cells were plated in phenol red-free RPMI 1640 medium supplemented with 5% dextran-coated charcoal-stripped FBS for 48 hours in 6-well plates. All cells were treated either with DHT at 10 nM final concentration or 0.1% ethanol (EtOH) as a control. Cells were harvested 24 hours after treatment for RNA analysis.

6.1.2.6 Primers

Table 6.1: Primers used in this study for PCR and qPCR (5'–3')

Primer	Sequence (5' - 3')
<i>PCR and qPCR</i>	
TIAR_F	AAACCCACAACAGTATGGAC
TIAR_R	AAATCCACCCATCCAAGCAG
TTP_F	GTTACACCATGGATCCTGAC
TTP_R	TGACCCCAGACGGGCTGGAGT
KSRP_F	AATACCTACCCCCAGTGGCA
KSRP_R	CTTAGTGTAGTCCGACTGGC
HuR_F	CCAGAACAAAAACGTGGCAC
HuR_R	GGAGGCGTTTCCTGGCACGT
AUF1_F	TAAGAACGAGGAGGATGAAGG
AUF1_R	TTCCATAACCACTCTGCTGG
ADCY9_F	ACAGCGTCATCAGGGAATGT
ADCY9_R	TGTTTTTATGCTCGTCTTGG
PSMB2_F	TGGCCGCCAGCAATATTGTC
PSMB2_R	GCATCTTATAAAGTTGCACG
UBE2W_F	TGGCTTTGCAAAATGACCC
UBE2W_R	AGAGTCAAAAGGATATCGAC

6.1.3 Results

6.1.3.1 Investigation of RBP expression in human cell lines

Initially, the expression levels of TIAR, TTP, KSRP and HuR were investigated by performing PCR in the prostate cancer cell lines VCaP and LNCaP. TIAR and KSRP were expressed in these two cell lines as shown in Figure 6.1.3A. TTP and

HuR were expressed in the breast cancer cell lines ZR75, T47D and MDA-MB-453 but not in the prostate VCaP or LNCaP cell lines (Figure 6.1.3B). The highest expression of these two proteins were seen in MDA-MB-453 cells and lowest in ZR75 cells.

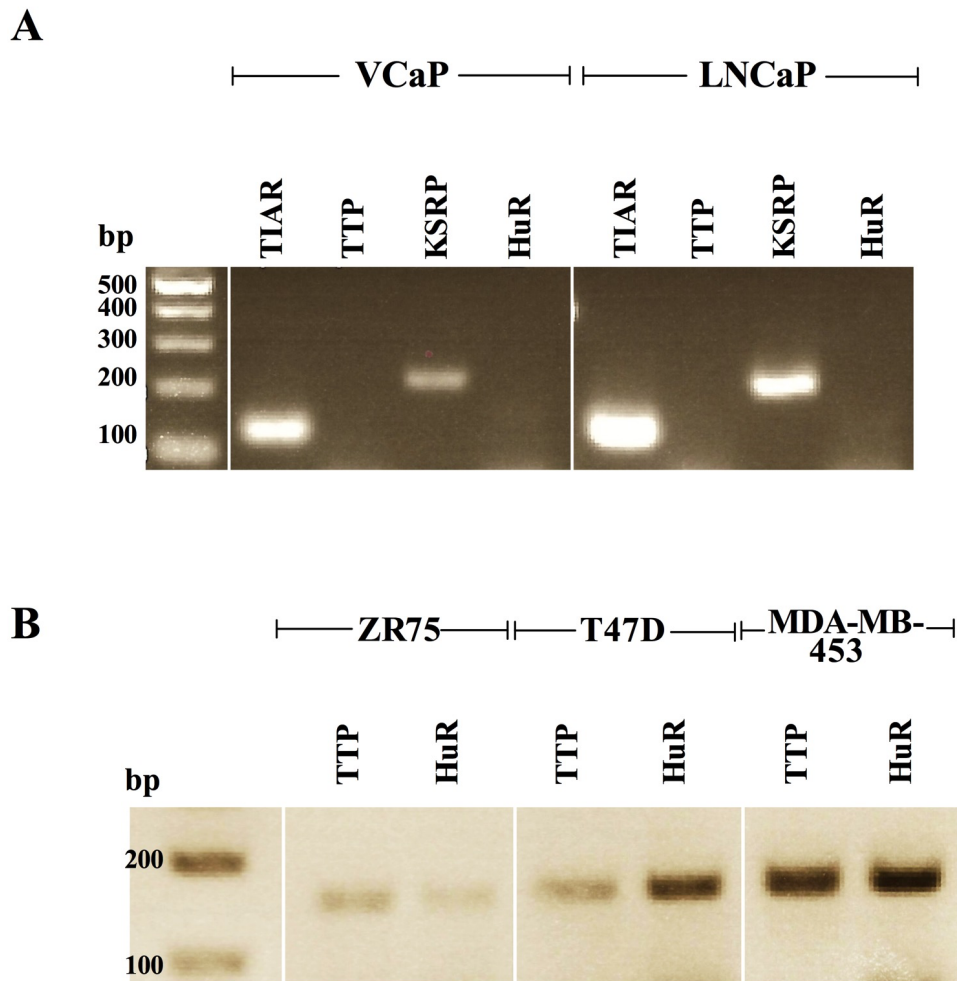


Figure 6.1.3: Expression of RNA-binding proteins in human prostate and breast cancer cell lines

(A) TIAR, TTP, KSRP and HuR expression in prostate cancer VCaP and LNCaP cells. (B) TTP and HuR expression in breast cancer ZR75, T47D and MDA-MB-453 cells. Total RNA from all five cell lines was extracted and reverse transcribed to generate cDNA, followed by PCR amplification using specific RBP primers. Shown are the PCR products of target transcripts on ethidium bromide-stained 1% agarose gels.

The expression of all four isoforms of AUF1: p37, p40, p42 and p45, were also examined in the prostate and breast cancer cell lines. All the cell lines expressed all four isoforms of AUF1 with MDA-MB-453 cells showing the highest expression (Figure 6.1.4). It was also noted that p40 AUF1 was expressed at high levels compared to the other 3 isoforms in all cell lines except for LNCaP cells.

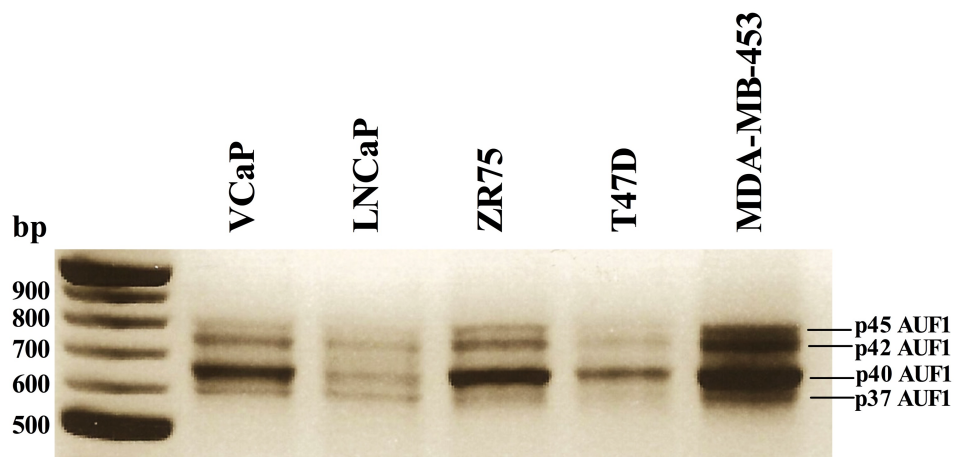


Figure 6.1.4: Expression of AUF1 isoforms in human prostate and breast cancer cell lines

Total RNA from all five cell lines was extracted and reverse transcribed to generate cDNA, followed by PCR amplification using a specific AUF1 primer set that amplifies all isoforms. Shown are the PCR products of target transcripts on ethidium bromide-stained 1% agarose gels.

6.1.3.2 Changes in RBP mRNA expression in VCaP and LNCaP cells with DHT treatment

A downregulation of UGT2B15 and UGT2B17 is seen with androgen treatment in the prostate cancer cell line LNCaP; however, the mechanism behind this is unknown (Guillemette et al., 1996). As RBPs (especially AUF1) have been reported to be upregulated by DHT in mice (Sheflin and Spaulding, 2000), it was hypothesized that DHT may upregulate RBPs that can in turn downregulate UGT2B15 and UGT2B17

at the post-transcriptional level. Hence, the effects of DHT on RBP mRNA expression levels was examined in VCaP and LNCaP cells. Cells were harvested 24 hours post-DHT treatment and qRT-PCR was used to measure levels of AUF1 (using a primer set that amplifies all isoforms) and TIAR. As shown in Figure 6.1.5, none of the RBP mRNA levels were significantly affected by DHT. This suggested that downregulation of UGT2B15 and UGT2B17 by DHT is unlikely to be caused by regulation of RBP proteins AUF1 or TIAR.

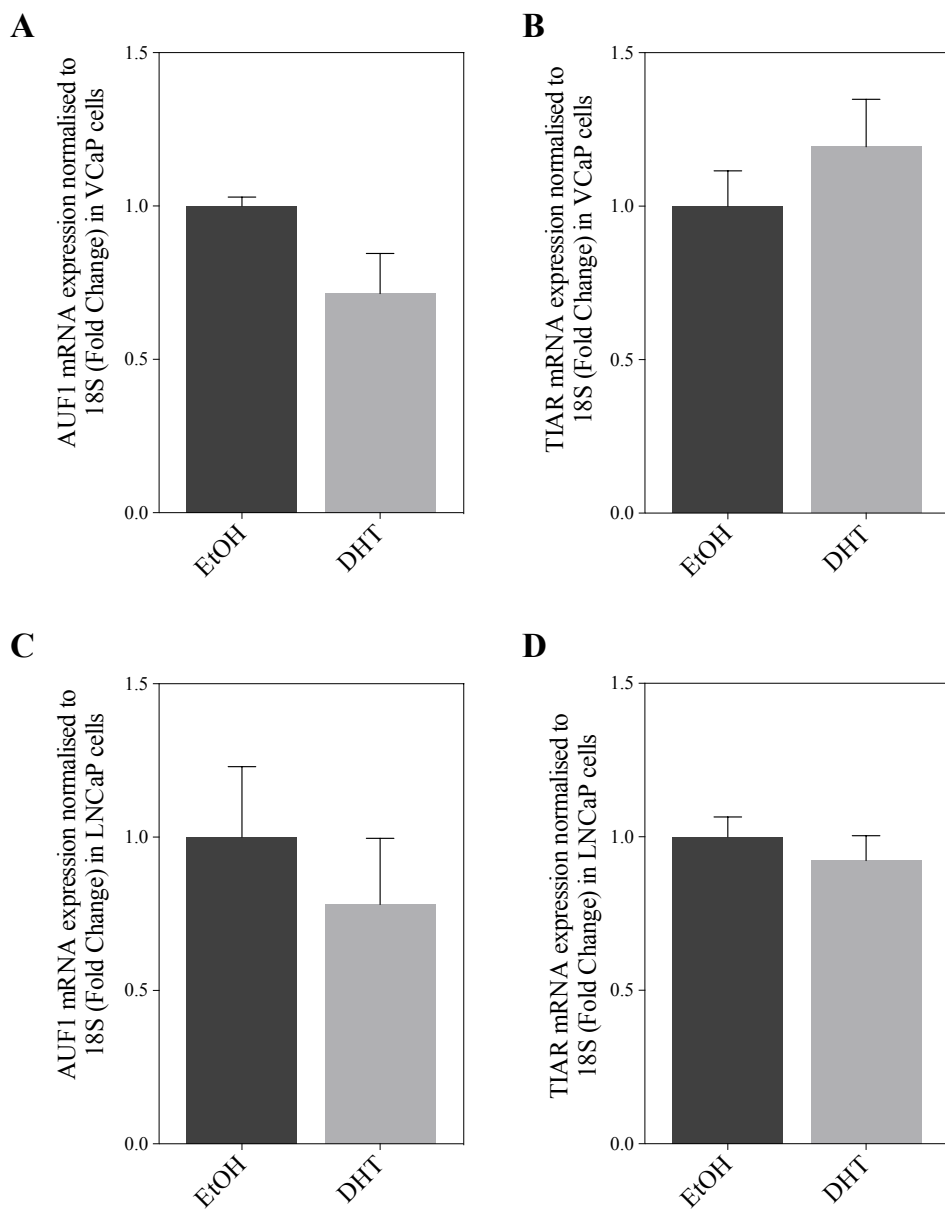


Figure 6.1.5: Expression of AUF1 and TIAR in VCaP and LNCaP cells treated with DHT

Changes in AUF1 mRNA (A, C) and TIAR mRNA (B, D) in VCaP and LNCaP cells. Cells were treated with 10nM DHT and the total RNA from cells were extracted 24 hours after and subjected to RT-qPCR for measuring target gene mRNA levels. Target gene mRNA levels were normalized to 18S rRNA levels presented relative to that of the control sample (EtOH, set at a value of 1). Data shown are from a representative experiment performed in triplicate, the error bar representing \pm S.D.

6.1.3.3 Regulation of UGT2B15 and UGT2B17 mRNA expression by AUF1 isoforms in VCaP and LNCaP cells.

Although total AUF1 levels were not altered by DHT in prostate cancer cells, the possibility that one or more of the AUF1 isoforms regulate UGT2B15 and/or UGT2B17 was still possible and this was examined using overexpression of AUF1 proteins in cells. Four vectors expressing the AUF1 isoforms: pCMV-AUF1(p37), pCMV-AUF1(p40), pCMV-AUF1(p42) and pCMV-AUF1(p45) were transfected into cells and pCMV empty vector was used as a control.

After transfection of LNCaP cells with the AUF1 expression vectors pCMV-AUF1(p37), pCMV-AUF1(p40), pCMV-AUF1(p42) and pCMV-AUF1(p45), the expression of AUF1 isoforms was confirmed by qRT-PCR. As shown in Figure 6.1.6 Ei, total AUF1 mRNA levels were increased in cells transfected with each of the AUF1 expression vectors. The expression of each AUF1 isoform was also confirmed by non-quantitative PCR and analyzing the products by agarose gel electrophoresis (Figure 6.1.6 Eii).

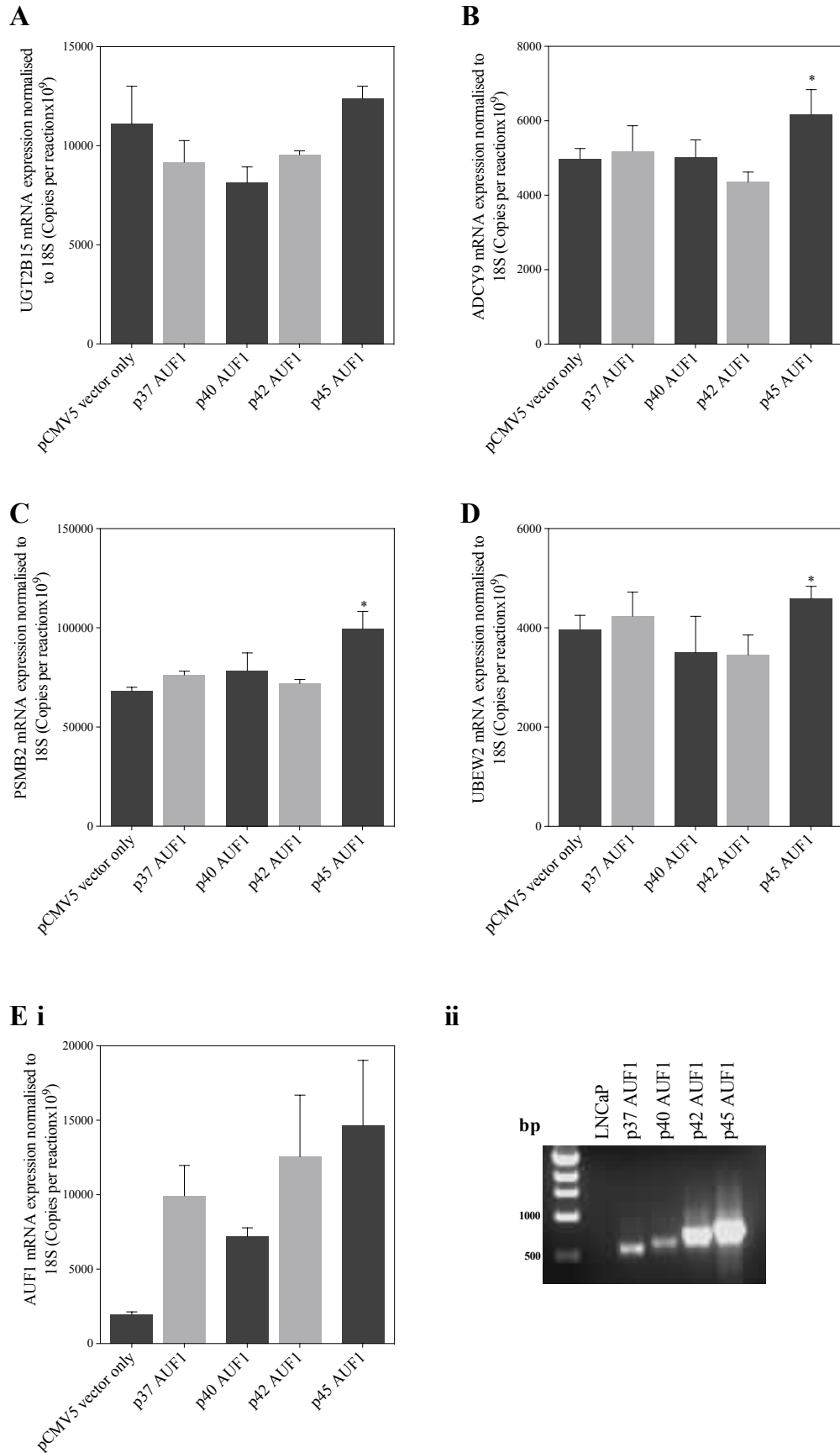


Figure 6.1.6: Target gene expression in AUF1 overexpressed VCaP cells

The expression of UGT2B15 mRNA (A), ADCY9 mRNA (B), PSMB2 mRNA (C) and UBE2W mRNA (D) and AUF1 mRNA (Ei) in LNCaP cells transfected with AUF1 expression vectors. Total RNA from cells were extracted 36 hours after transfection and subjected to quantitative real-time RT-qPCR for measuring target gene mRNA levels. Target gene mRNA levels were normalized to 18S RNA levels and presented as copy number per reaction. Data shown are from an experiment performed in triplicate, the error bar representing \pm S.D. * $p < 0.05$. (E) Expression of specific AUF1 isoforms in LNCaP cells transfected with AUF1 expression vectors. Total RNA from all five cell lines was extracted and reverse transcribed to generate cDNA, followed by PCR amplification using a set of AUF1 specific primers. (ii) Shown are the PCR products of AUF1 transcripts on ethidium bromide-stained 1% agarose gels.

The expression of UGT2B15 was measured in AUF1 transfected LNCaP cells. The expression of three other genes that contain ARE-binding sites: adenylate cyclase 9 (ADCY9), proteasome subunit beta 2 (PSMB2) and ubiquitin conjugating enzyme E2 W (UBE2W), were measured as positive controls. There was no significant change in expression of UGT2B15 after transfection of any of the AUF1 isoforms. The three positive control genes were modestly but significantly upregulated by the over-expression of p45 AUF1 isoform only (Figure 6.1.6 B and C).

VCaP cells were also transfected with the AUF1 expression vectors and the expression of UGT2B15 and UGT2B17 mRNA was measured using qRT-PCR. Similar to the results in LNCaP cells, there was no significant change in either UGT2B15 or UGT2B17 mRNA levels with the overexpression of AUF1. GAPDH was used as a control (Figure 6.1.7 C).

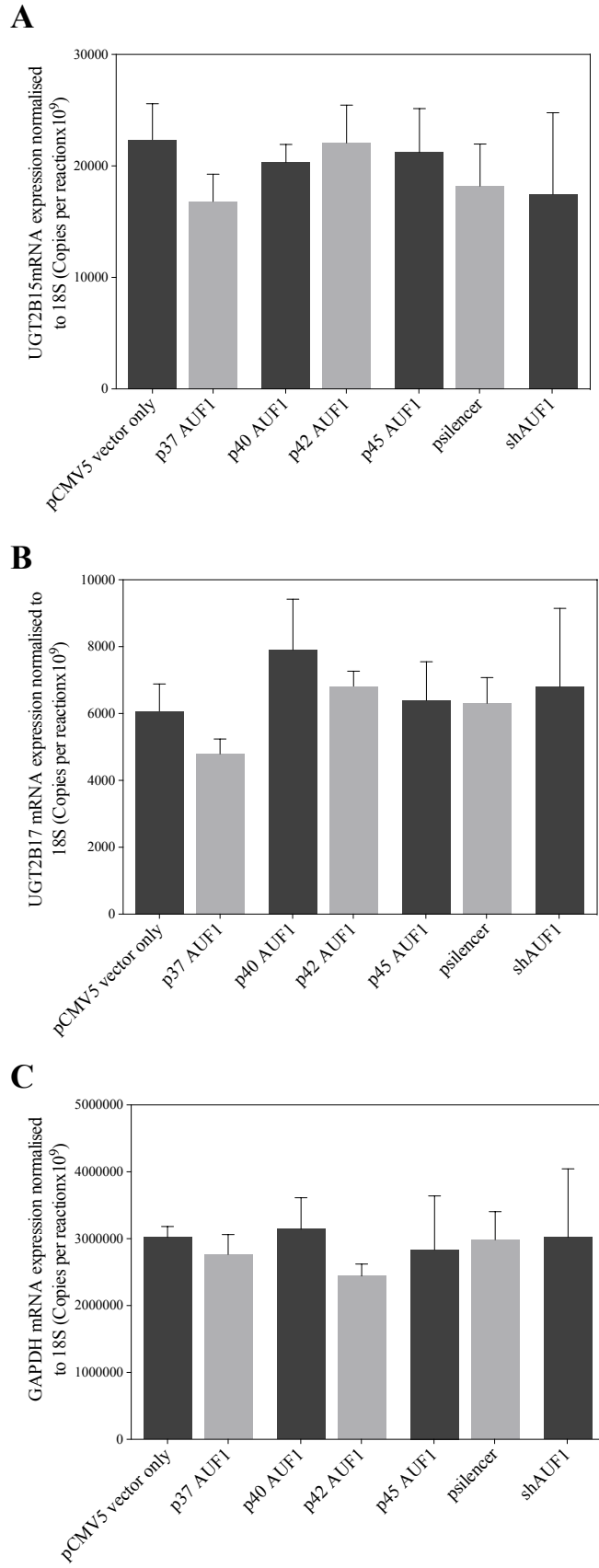


Figure 6.1.7: Changes in UGT2B15 and UGT2B17 mRNA expression in AUF1 overexpressed VCaP cells

The expression of UGT2B15 mRNA (A), UGT2B17 mRNA (B) and GAPDH mRNA (C) in VCaP cells transfected with AUF1 expression vectors. Total RNA from cells were extracted 36 hours after and subjected to quantitative real-time RT-qPCR for measuring target gene mRNA levels. Target gene mRNA levels were normalized to 18S rRNA levels and presented as copy number per reaction. Data shown are from an experiment performed in triplicate, the error bar representing \pm S.D.

6.2 PART 2: INVESTIGATION OF THE ROLE OF miRNAs IN ANDROGEN-INDUCED UGT2B15 AND UGT2B17 REGULATION

6.2.1 Results

To further investigate androgen regulation of UGT2B15 and UGT2B17 at the post-transcriptional level, possible miRNA mediated involvement was examined. As miR-376c and miR-331-5p directly target UGT2B15 and/or UGT2B17 and regulate their expression, it was of interest to determine whether these two miRNA are regulated by DHT in prostate cancer cells. As shown in Figure 6.2.1 D, no significant change in miRNA expression was seen in DHT-treated compared to control LNCaP cells. The expression of miR-3664-3p, miR-410-3p and miR-135a-5p (which target UGT2B7 or UGT2B4) was also examined in these cells. Interestingly, miR-135a-5p showed a significant 5-fold increase in expression in DHT-treated LNCaP cells compared to non-treated control cells (Figure 6.2.1 D). Consistent with data from previously reported studies (Bao et al., 2008, Chouinard et al., 2006, Guillemette et al., 1996, Guillemette et al., 1997, Sheflin et al., 2004), our experiment showed that UGT2B15 and UGT2B17 mRNA levels were reduced by 77-80% by DHT in the same cell samples (Figure 6.2.1 A, B). GAPDH was not affected by DHT as seen in Figure 6.2.1 C.

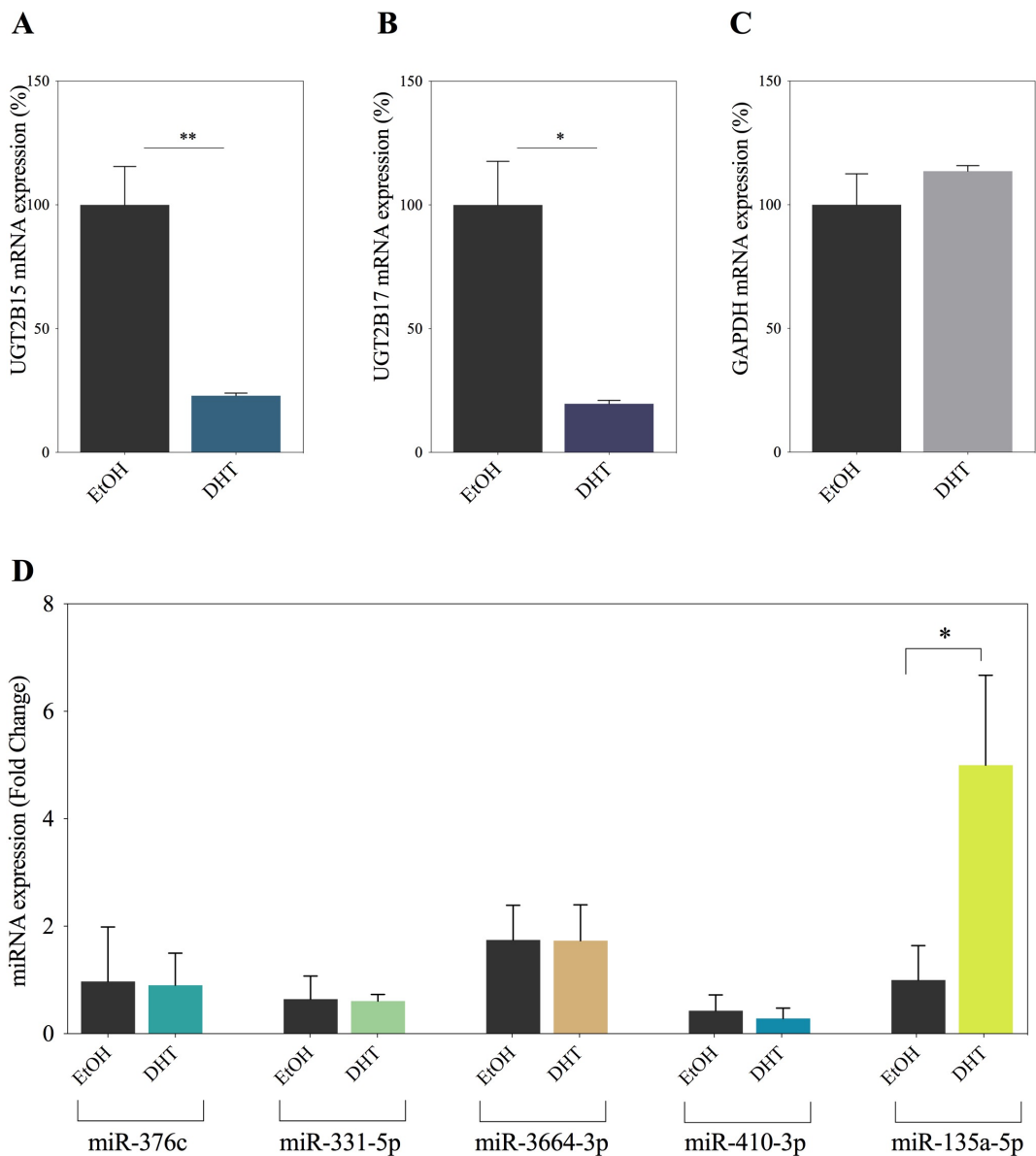


Figure 6.2.1: Expression of UGT2B15, UGT2B17 and miRNAs in LNCaP cells treated with DHT

Changes in UGT2B15 mRNA (A), UGT2B17 mRNA (B), GAPDH mRNA (C) in LNCaP cells treated with 10nM DHT for 24 hours. Target gene mRNA levels were measured by qRT-PCR, normalized to 18S RNA levels and presented relative to that of the control sample (EtOH, set at a value of 1). (D) Changes in miR-376c, miR-331-5p, miR-3664-3p, miR-410-3p and miR-135a-5p in DHT-treated LNCaP cells. All miRNA levels were normalized to RNU6-2 and presented relative to miR-135a-5p levels in the EtOH treated LNCaP cells (set at a value of 1). All data shown are from a representative experiment performed in triplicate, the error bar representing 1 S.D.

To determine whether there was any correlation between miR-135a-5p and UGT2B15/UGT2B17 levels and prostate cancer, expression data from normal and prostate cancer specimens was obtained from MSKCC database using cbiportal (Taylor et al., 2010). Levels of miR-135a-5p were highest in normal prostate followed by primary tumour and lowest in metastatic tumour; conversely UGT2B15/UGT2B17 levels were higher in metastatic prostate tumours than in normal prostate and primary prostate tumours (Figure 6.2.2). This suggests a negative correlation between UGT2B15/UGT2B17 and miR-135a-5p in prostate cancer progression. This data was consistent with the findings of Kroiss et al (Kroiss et al., 2015).

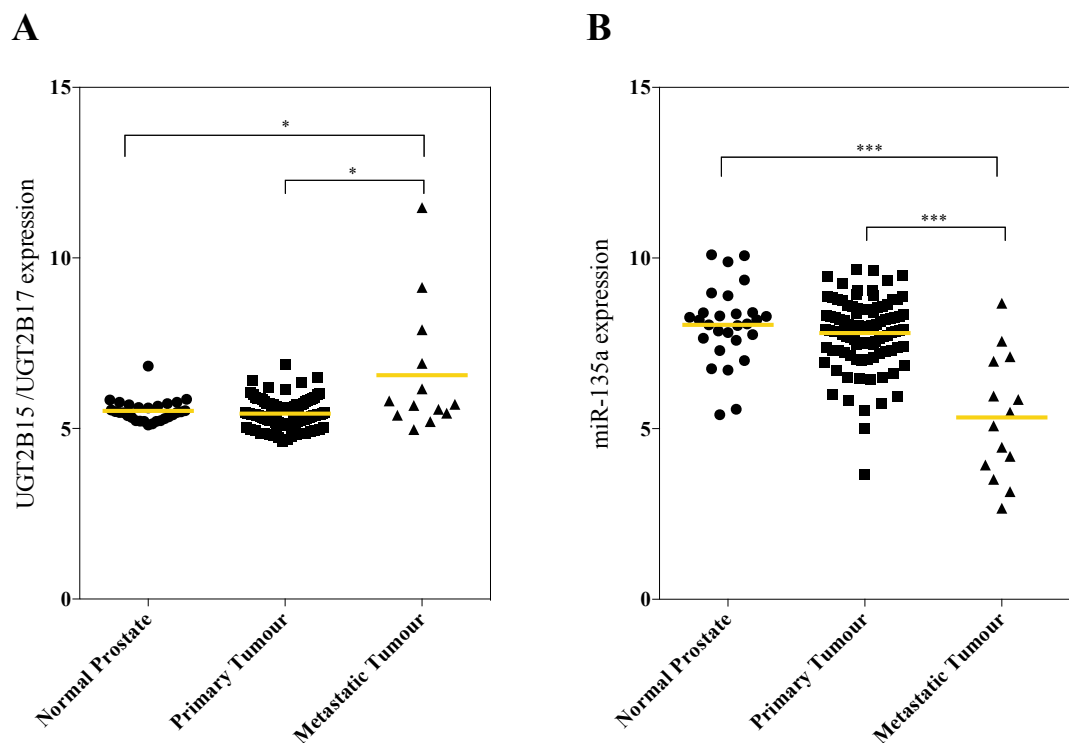


Figure 6.2.2: Relationship between miR-135a-5p versus UGT2B15 and UGT2B17 in normal prostate tissues, primary prostate tumours and metastatic prostate tumours

Analysis of UGT2B15 and UGT2B17 mRNA (A) and miR-135a-5p expression (B) in normal, primary tumour and metastatic prostate tumour tissues. Data was obtained

from MSKCC database using cbiportal (www.cbiportal.org), from a study performed by Taylor et al (Taylor et al., 2010). Mean expression levels of either UGT2B15/ UGT2B17 or miR-135a-5p in prostatic tissues (yellow lines) were compared to each prostatic classification group using a 2-tailed Student's t-test. ***P<0.0005, *p<0.05.

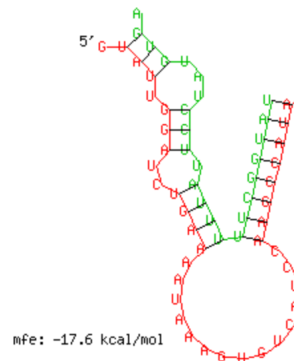
No miR-135a-5p target sites were predicted in the UGT2B17/UGT2B17 3'UTRs by TargetScan (version 6.2) (see section 3.3.1). Therefore, RNAhybrid was used to identify potential miR-135a-5p binding sites in both UGT2B15 and UGT2B17 3'UTRs (Figure 6.2.3). As shown in Figure 6.2.3, two miR-135a-5p target sites with seed pairing (mfe: -17.6 kcal/mol and mfe: -15.3 kcal/mol) were predicted. However, further studies are needed to confirm if these miR-135a-5p target sites are functional and if their effects on UGT2B15 and UGT2B17 expression are androgen-mediated.

A

Target: *gi/353411935/ref/NM_001076.3/*
length: 513
MiRNA: *hsa-miR-135a-5p*
length: 23

mfe: -17.6 kcal/mol
p-value: 1.000000e+00

Position: 430
target 5' G U UC AAUAAAGUGUCAUCC A 3'
UUAU GGA UGAA AAGCCAU
GUG CCU AUUU UUCGGUAU
miRNA 3' A UAU U 5'



B

Target: *gi/294345383/ref/NM_001077.3/*
length: 463
MiRNA: *hsa-miR-135a-5p*
length: 23

mfe: -15.3 kcal/mol
p-value: 1.000000e+00

Position: 177
target 5' U UC UUUUU A 3'
UC UAUG AAUGA AAGCUAUG
AG GUAU UUAUU UUCGGUAU
miRNA 3' U CC U 5'

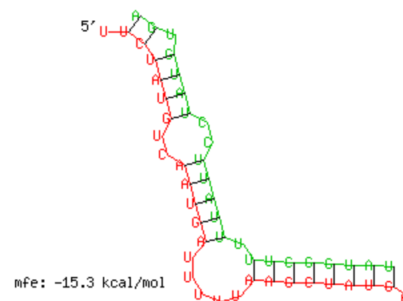


Figure 6.2.3: 3'UTRs of UGT2B15 and UGT2B17 contain predicted miR-135a-5p binding sites

Shown are the predicted pairing between miR-135a-5p and its target site in the UGT2B15 3'UTR (A) and UGT2B17 3'UTR (B), by RNAhybrid (<http://bibiserv.techfak.uni-bielefeld.de/rnahybrid>). The mRNA sequences are in red and miR-135a-5p sequence is in green.

6.3 Discussion

The downregulation of UGT2B15 and UGT2B17 by androgens is not understood mechanistically. The inability of our group and others to define DNA regulatory elements directly involved in transcriptional downregulation by AR led to a hypothesis that post-transcriptional mechanisms may be involved. Consistent with this idea, ARE-binding RBPs have been shown to be androgen regulated and the UGT2B15 and UGT2B17 3'UTR contain several AREs. However, neither AUF1 or TIAR expression was induced by DHT in androgen-dependent prostate cancer cells. Moreover, over-expression of AUF1 isoforms in VCaP or LNCaP cells did not alter the expression of UGT2B15 or UGT2B17 mRNA levels. Together these data suggest that these RBPs are not involved in the post-transcriptional regulation of UGT2B15 and UGT2B17. HuR is also known to be regulated by androgens (Sheflin et al., 2001, Sheflin et al., 2004). However, HuR was not expressed in LNCaP or VCaP cells and there was insufficient time to study post-transcriptional regulation of UGT2B15 and UGT2B17 by HuR.

As aforementioned, both UGT2B15 and UGT2B17 contain three ARE binding sequences in their 3'UTRs. In order to determine whether these elements are involved in regulation of 3'UTR activity, they were mutated in a 2B15/3UTR luciferase reporter vector; however, there was insufficient time to analyse these constructs within this project and this may be a useful future direction.

The induction of miR-135a-5p by DHT in LNCaP cells and the negative correlation between UGT2B15/UGT2B17 and miR-135a-5p in normal and cancerous prostate tissues, suggested that miR-135a-5p could be involved in androgen-mediated regulation of these UGTs. However, further studies are required to test this hypothesis.

CHAPTER 7

GENERAL DISCUSSION AND CONCLUSIONS

Note: This chapter contains written work directly taken from three published peer-reviewed journal articles generated from this PhD project;

1. Wijayakumara DD, Hu DG, Meech R, McKinnon RA, Mackenzie PI. (2015) Regulation of Human UGT2B15 and UGT2B17 by miR-376c in Prostate Cancer Cell Lines. *J Pharmacol Exp Ther* 354(3): 417-25. (**Appendix 2**)
2. Wijayakumara DD, Mackenzie PI, McKinnon RA, Hu DG, Meech R (2017) Regulation of UDP-Glucuronosyltransferases UGT2B4 and UGT2B7 by MicroRNAs in Liver Cancer Cells. *J Pharmacol Exp Ther* 361(3):386-397. (**Appendix 3**)
3. Wijayakumara DD, Mackenzie PI, McKinnon RA, Hu DG, Meech R (2018) Regulation of UDP-Glucuronosyltransferase 2B15 by miR-331-5p in prostate cancer cells involves canonical and non-canonical target sites. *J Pharmacol Exp Ther* 365(1):48-59. (**Appendix 4**)

Reproduced with permission of the American Society for Pharmacology and Experimental Therapeutics. All rights reserved.

Glucuronidation is a robust metabolic pathway in humans, however, it is susceptible to changes in either UGT enzyme expression or activity, which may be due to diverse exogenous and endogenous factors. UGT substrates include endogenous molecules such as steroid hormones and xenobiotics including numerous pharmaceutical drugs. Deviations from normal rates of glucuronidation can alter substrate concentrations and/or activities, which may lead to clinically relevant outcomes such as altered drug efficacy and increased risk of diseases such as cancer. The expression of UGTs is tightly controlled at the transcriptional level and this has been studied extensively for the past few decades. However, UGT regulation by post-transcriptional mechanisms remains poorly understood, and hence the studies presented in this thesis investigated the regulation of UGTs specifically by miRNAs, which are an emerging class of major post-transcriptional gene regulators. The

studies focussed on UGT2B family members that are involved in critical endogenous signalling processes and/or drug metabolism. In particular, UGT2B15 and UGT2B17 are involved in the control of androgen signaling in the prostate by inactivating testosterone and DHT (Turgeon et al., 2001; Chouinard et al., 2007, 2008); UGT2B7 is metabolizes various important compounds and is known as a major drug metabolizing enzyme; UGT2B4 is an important player in hepatic glucuronidation of various compounds including potentially toxic bile acids.

Common and Differential Regulation of UGT2B15 and UGT2B17 by miRNAs.

The proximal UGT2B15 and UGT2B17 promoters have similar sequences and contain highly conserved response elements for the AR and estrogen receptor. They are both downregulated by androgens in prostate cancer cells (Chouinard et al., 2007; Bao et al., 2008) and upregulated by estrogens in breast cancer cells (Hu and Mackenzie, 2009; Hu et al., 2016). The proximal 3'UTRs of UGT2B15 and UGT2B17 also exhibit high homology regions and are similar in length. Specifically, a 210-bp sequence at the 5'-terminus of each 3'UTR exhibits high homology with the remaining sequence being highly divergent. This sequence similarity and divergence may allow regulation of both UGTs by common miRNAs with target sites in their conserved 3'-UTR sequences but could also permit their differential regulation by miRNAs with target sites in the divergent 3'-UTR sequences. Indeed, multiple examples of this joint- and differential-regulation were identified in this project. In particular, miR-376c was identified as a regulator of both UGT2B15 and UGT2B17 via a target site within their conserved 3'-UTR sequences. In contrast, miR-222 was identified as a specific regulator of UGT2B15 and not UGT2B17 via a target site present only in the divergent UGT2B15 3'-UTR region. Interestingly,

miR-376b was also identified as a negative regulator of UGT2B15 and not UGT2B17, even though the miR-376b target site is highly conserved in the UGT2B15 and UGT2B17 3'-UTR sequences. This may be an example of context-dependent miRNA function; however, the differences in sequence/structure context that render the site non-functional in UGT2B17 remain to be defined. Moreover, UGT2B15 was found to be regulated via 2 miR-331-5p target sites; with one site present in the highly homologous proximal region, and the other site in the distal part of the UGT2B15 3'UTR which is divergent from the UGT2B17 3'UTR.

UGT2B15 and UGT2B17 may be regulated by miRNA-mediated mRNA degradation.

miRNAs can repress gene expression through mRNA degradation and/or translational repression depending on the degree and nature of sequence complementarity between the miRNA guide and mRNA target (Macfarlane and Murphy, 2010). Extensive base-pairing between the miRNA guide and mRNA target permits mRNA cleavage by Argonaute (Ago2) (Macfarlane and Murphy, 2010); expression levels of such miRNAs and their target mRNAs may thus be negatively correlated due to miRNA-mediated mRNA degradation. The miR-376c target site in the UGT2B15/UGT2B17 3'UTR, is classified as a 7mer-8m site (which is one of the four canonical site types as mentioned in Chapter 1), with only a C/U mismatch at position 19 between the two sites and a G-deletion at position 17 in the UGT2B15 site. The ability of miR-376c to promote UGT2B15 and UGT2B17 mRNA degradation was confirmed by reduced UGT2B15/17 mRNA levels, and reduced UGT2B15/UGT2B17 protein and activity levels may be a secondary result of mRNA degradation. As miR-376c shows extensive seed pairing and additional 3'-sequence pairing to both UGT2B15 and UGT2B17 mRNAs, it would suggest that the mRNA

degradation pathway is favoured in this instance. However, its involvement in translational inhibition is yet to be elucidated. It is also possible that other screened miRNAs that did not alter UGT mRNA levels may specifically alter translation and this warrants further study.

Identification of a critical non-canonical miRNA target site in UGT2B15.

A miRNA target site can either be canonical or non-canonical (details of types of miRNA target sites are presented in Chapter 1, figure 1.11 and Chapter 4, figure 4.10). Even though initial miRNA-related studies mainly explored canonical miRNA binding sites, experimental data from recent studies show the existence of other non-canonical miRNA binding sites (Cloonan, 2015). Even though 40-60% of miRNA binding sites are now thought to be non-canonical and include centered sites and 3' compensatory sites (Shin et al., 2010; Loeb et al., 2012; Helwak et al., 2013; Martin et al., 2014), most current microRNA target prediction tools avoid non-canonical target site predictions to reduce the generation of false-positive results. An intriguing aspect of the current studies was the identification of two miR-331-5p sites that mediate the repression of UGT2B15. Site 1 is a canonical 8-mer site with perfect seed pairing with additional supplementary pairing to miR-331-5p at nucleotides 13-15, which is believed to enhance miRNA targeting. Site 2 is a 'non-canonical' target site which contains a 1-bp mismatch in its seed site and extensive 3' pairing to miR-331-5p. This site is defined as a typical 3' compensatory site. Site 2 was found by analyzing regions of UGT2B15 3'UTR with the RNAhybrid tool for an energetically favourable miRNA:mRNA hybridization, in combination with empirical deletion/mutation studies. This emphasizes that classical prediction programs may be insufficient to identify critical miRNA:mRNA interactions.

Another interesting aspect of miR-331-5p mediated regulation of UGT2B15, is that site 1 is located in the distal part of the UGT2B15 3' UTR which diverges from the UGT2B17 3'UTR, while site 2 is located in the proximal region of the UGT2B15 3'UTR which is highly conserved with the UGT2B17 3'UTR. However, the region of the UGT2B17 3'UTR that is putatively analogous to UGT2B15 miR-331-5p site 2 shows 2 nucleotide mismatches; a G/A mismatch in the 3' pairing sequence of the miR-331-5p target site and a C/T mismatch in the seed site. The two mismatches in this site seem to be sufficient to prohibit the interaction between UGT2B17 3'UTR and miR-331-5p and thus the site is non-functional. This work provided the first evidence for a posttranscriptional mechanism that can differentially regulate these two important androgen-metabolizing UGTs. The work also showed that 3' seed pairing, rather than the seed site, plays a pivotal role in miR-331-5p targeting in this instance (in site 2) as complete abolishment of the regulation of the UGT2B15 3'UTR by miR-331-5p was achieved by disrupting the 3' pairing and not seed pairing.

Cooperative regulation of UGT2B15 by two different miRNAs.

Several studies have investigated the cooperative regulation of single-target mRNAs by multiple miRNAs and revealed that the efficacy and cooperativity between miRNA target sites is predominantly determined by the interval spacing between seed sites (Doench and Sharp, 2004; Grimson et al., 2007; Saetrom et al., 2007; Pasquinelli, 2012). The miR-376c site is located upstream of miR-331-5p site 2 and downstream from miR-331-5p site 1 and the spacing between the sites falls just within the proposed constraints for effective cooperativity. Consistent with this, miR-376c and miR-331-5p could function together additively to repress UGT2B15

3'UTR reporter activity. Similar cooperative regulation of UGT2B4 3'UTR by miRNAs in liver cancer cell lines via adjacent target sites was also suggested by the studies discussed below. It remains to be determined whether other UGT gene transcripts are also cooperatively regulated by multiple miRNAs.

Negative correlations between UGT and miRNA levels in tissues suggest that miRNA-mediated regulation occurs in vivo

The expression of several of the miRNAs studied here was negatively correlated with target mRNAs in various tissues. For example, the expression of miR-376c and expression of UGT2B15 and UGT2B17 exhibit an inverse correlation in normal prostate tissues. Several recent studies show that UGT2B15 and/or UGT2B17 expression is upregulated in metastatic androgen independent prostate cancer as compared with primary prostate cancer. Elevated UGT2B17 protein levels have been reported in metastatic prostate tumors compared to benign tumors (Paquet et al., 2012) and in castrate-resistant metastasis compared to primary prostate tumours (Montgomery et al., 2008). In fact, higher UGT2B17 protein levels in prostate tumours were associated with higher Gleason score as well as higher metastasis, and CRPC progression (Li et al., 2016). Elevated UGT2B15 levels have also been reported in androgen-independent prostate cancer (Stanbrough et al., 2006). Our findings raise the possibility that higher expression of UGT2B15 and UGT2B17 might be a result of reduced miR-376c levels in prostate cancer. Consistent with this possibility, Ozen and colleagues reported widespread deregulation of miRNA expression in prostate cancer (Ozen et al., 2008). In particular, miR-376c has been shown to be downregulated in prostate cancer tissues (especially in advanced metastatic and invasive tumors) as compared with normal prostate tissues. Srivastava

et al report that miR-376 is reduced by 10.1 fold in prostate cancer (Srivastava et al., 2013). Formosa et al report that miR-376c is significantly reduced in metastatic prostate tumours compared to normal prostate tissue and non-metastatic prostate tumours (Formosa et al., 2014). These findings were similar to those derived from analysis of prostate cancer cohorts from the MSKCC database in Chapter 3. This work is an important step towards understanding the regulation of UGT2B15 and UGT2B17 at different stages of prostate cancer progression, which may also help understanding modulation of steroid activity with different cancer staging.

Similar to miR-376c, miR-222 also showed reduced levels in primary prostate tumours and metastatic prostate tumours as compared to normal prostate tissues. Consistent with these findings, a recent study shows that miR-222 is downregulated in prostate cancer tissues and CRPC tissues and is involved in prostate cancer progression (Goto et al., 2015). Therefore, reduced levels of both miR-222 and miR-376c could both contribute to elevated UGT2B15/UGT2B17 expression in prostate cancer, especially at the metastatic/castrate resistant stage.

Some other miRNAs that were found to regulate UGT2B15 such as miR-331-5p and miR-376b did not show a negative expression correlation with UGT2B15/UGT2B17 in tissues including prostate and prostate tumours. When interpreting this data, it is important to consider that correlation alone does not imply causation, and many regulatory factors, both transcriptional and posttranscriptional, are involved in the regulation of a given gene. Therefore, one reasonable explanation for the lack of correlation between specific miRNAs and UGT2B15/UGT2B17 in prostate cancer, could be the extent of contribution by other factors such as transcription factors in determining overall UGT levels. In prostate cancer, androgens and AR signaling

tightly control UGT2B15 (and UGT2B17) transcription and strongly repress its expression. Therefore, in this context, the contribution of miR-331-5p (in particular) to post-transcriptional regulation of UGT2B15 may have little impact on overall expression levels. Adding further complexity to the regulatory model, the miR-331 gene generates both miR-331-5p and miR-331-3p; miR-331-3p was reported to repress the AR-signaling pathway through targeting the human epidermal growth factor receptor 2 and PI3k/AKT signaling in prostate cancer cells (Epis et al., 2009). This ability of miR-331-3p to repress AR signaling suggests that it might also indirectly modulate UGT2B15 expression at the transcriptional level; moreover, repression of AR activity could potentially increase UGT2B15 transcription. It is tempting to suggest that the lack of a significant correlation between UGT2B15 and miR-331 levels in prostate cancer tissues might partly reflect the opposing effects of miR-331-5p and miR-331-3p. However, understanding the complex network of direct and indirect effects of miR-331-derived miRNAs on androgen signaling and UGT2B15 expression will require further study. Furthermore, the data on expression levels of UGT2B15 and UGT2B17 cannot be distinguished from one another in the MSKCC database. Therefore, the results do not essentially reflect the precise correlation of miR-331-5p and UGT2B15 expression levels. However, an inverse correlation between miR-331 and UGT2B15 levels was observed in a cohort of hepatocellular carcinoma (TCGA database) and a human tissue panel, and this may justify future studies on the possible role of miR-331-5p in liver cancer.

Another research group recently reported that miR-376c regulates UGT2B15 expression and activity and that miR-409, miR-494 and miR-331-5p can repress a UGT2B17 3'UTR containing luciferase reporter in HEK293 cells (Margaillan et al., 2016). In addition, miR-770-5p, miR-103b, miR-3924, miR-376b-3p, miR-455-5p,

miR-605, miR-624-3p, miR-47125p, miR-3675-3p, miR-6500-5p, miR-548as-3p, and miR-4292 were reported to reduce the activity of UGT2B15 3'UTR-containing luciferase reporters in HEK293 cells. Furthermore, miR-455-5p levels showed a significant negative correlation with the S-oxazepam glucuronidation activity of UGT2B15 (Papageorgiou and Court, 2017b). These different studies emphasize the broad interest in the research community in understanding the posttranscriptional control of these important steroid conjugating UGTs.

The mechanism underlying the profound down regulation of UGT2B15 and UGT2B17 by androgens in prostate cells is still not fully elucidated. The possibility that post-transcriptional events mediated by RNA binding proteins and miRNAs are involved was investigated in Chapter 6, but concrete evidence for their involvement was not found. However, these were preliminary studies and further work is required to determine if post transcriptional regulation by miRNAs and RNA binding proteins is involved in androgen modulation of UGT2B15 and UGT2B17 expression.

Novel miRNA mediated regulation of UGT2B7 and UGT2B4 in liver cancer cells

Transcriptional regulation of UGT2B4 and UGT2B7 is well studied (summarised in Hu et al 2014) but to date only a handful of studies have investigated their post-transcriptional regulation by miRNA. The first identification of a miRNA involved in UGT2B4 and UGT2B7 regulation was recently reported (Dluzen et al., 2016). According to their study, miR-216-5p regulates both UGT2B4 and UGT2B7 in liver cancer cell lines. In addition to this, Papageorgiou and Court reported that miR-1293, miR-3664-3p, miR-4317, miR-513c-3p, miR-4483, and miR-142-3p can reduce the activity of a luciferase reporter carrying the UGT2B7 3'UTR in HEK293 cells

(Papageorgiou and Court, 2017b). MiR-485-5p has also been shown to reduce the expression and activity of UGT2B7 (and UGT2B10) (Sutliff et al., 2019).

This project provided an in-depth characterization of the roles of three additional miRNAs (miR-135a-5p, miR-410-3p and miR-3664-3p) in regulation of UGT2B4 and UGT2B7 in liver cancer cell lines. MiR-3664-3p regulates UGT2B7 via a target site in its 3'UTR and reduces UGT2B7 mRNA and protein levels. Consistent with this finding, another study recently confirmed that miR-3664-3p targets UGT2B7 cells utilizing luciferase reporter assays in HEK293 cells (Papageorgiou and Court, 2017b). Two other miRNAs, miR135a-5p and miR-410-3p, regulate UGT2B4 via target sites within its 3'UTR. The miR-3664-3p and miR-135a-5p target sites in UGT2B7 and UGT2B4 (respectively), are classified as 8mer target sites while the miR-410-3p target site is a 7mer-m8 site. Therefore, these miRNAs show extensive seed pairing (and additional 3'-sequence pairings) with their targets as seen for the other miRNAs discussed above, and this would suggest favouring regulation by a mRNA degradation pathway.

The 5' 11 nucleotides of the miR-135a-5p site overlap with the 3' 11 nucleotides of the miR-410-3p site in the UGT2B4 3'-UTR and their seed sites are separated by 12 nucleotides. This falls just outside of the proposed optimal spacing range for cooperativity between miRNA target sites. Whether these sites can function together remains to be tested. In contrast, cooperative regulation between miR-135a-3p and the 2 other miRNAs which repressed UGT2B4 3'UTR reporter activity; miR-4691-5p or miR-489-3p, might be possible as the spacing between their seed sites is within the optimal range for cooperativity. However, future studies are required to test these possibilities.

High UGT2B7 expression levels and low miR-3664 levels were seen in both normal and cancerous liver tissues. An overall negative correlation was observed in a human tissue panel as well. Therefore, miR-3664-3p might be an important endogenous regulator of basal UGT2B7 levels. However, to come to such a conclusion, further studies are needed. The negative correlation between miR-410 and UGT2B4 mRNA levels in the liver cancer TCGA cohort but not in the panel of 18 normal livers is a discrepancy that remains to be resolved; possibly by examining a larger set of normal livers. Conversely, miR-135a and UGT2B4 mRNA levels were negatively correlated in the normal liver panel but not in the liver cancer TCGA cohort. This could be related to deregulation of other miRNAs and transcription factors that are involved in controlling UGT2B4 expression in liver cancer (Negrini et al., 2011; Callegari et al., 2015).

Overall Summary and Future Directions

In summary, this project identified several new miRNA regulators of key UGT2B enzymes in relevant cellular contexts such as prostate and liver cancer cells. Post-transcriptional regulation of UGTs by miRNAs may have an important role in fine-tuning glucuronidation activity in the liver as well as in extrahepatic tissues. Although none of the miRNAs characterized in this study are predicted to have a role in cancer-specific UGT regulation, further analysis of the functional significance of the miRNA-regulatory network is ongoing. In particular, it is interesting to consider whether deregulation of miRNA expression due to cellular stress or inflammation could alter UGT levels and hence the capacity for detoxification, which in turn may affect cancer risk and progression. As UGT2B15 and UGT2B17 are major determinants of the androgen response, miRNAs that regulate their expression might

be valuable as biomarkers of androgen-dependent (or indeed independent) cancer progression, or even as targets for novel approaches to prostate cancer therapy. As UGT2B7 is a major enzyme involved in drug metabolism, miRNAs that significantly regulate its expression and activity could conceivably act as biomarkers of drug metabolic capacity and thus potentially drug efficacy and toxicity. Future studies could investigate such potential translational applications of these important basic research findings.

APPENDIX 1:
INVESTIGATION OF SNPS IN UGT2B15 AND
UGT2B17 REGULATION

A1. Introduction

As miRNAs play important roles in a vast number of biological processes by binding to target mRNA transcripts, mutations that could affect miRNA binding and their function could possibly play pathogenic roles in human diseases. Among germline variations, single nucleotide polymorphisms (SNPs) are the most common sequence variations that influence cancer susceptibility (Pharoah et al., 2004). A SNP within a miRNA binding site could cause alteration in binding affinity or capacity, create an erroneous binding site or alter RNA secondary structure (Chen et al., 2008, Haas et al., 2012, Saunders et al., 2007). Thus, it could result in adverse changes in gene expression (Yu et al., 2007, Pelletier and Weidhaas, 2010). Studies have shown that SNPs located within miRNA binding sites of protein-coding genes correlate to alterations in gene expression and protein function, and lead to various cancer susceptibilities (Pelletier and Weidhaas, 2010). According to Sun et al (Sun et al., 2011), a SNP (rs3100 c.1761 C/T) within the UGT2B15 3'UTR causes an alteration in UGT2B15 enzymatic activity. Luciferase reporter gene assays using plasmid constructs containing different rs3100 alleles (either C or T) in LNCaP, MCF7, HepG2 and Caco2 cells showed that the T allele containing reporter showed higher activity than the C allele containing reporter by 61.5%, 21.5%, 14.3% and 31.5% respectively (Sun et al., 2011). These data suggested that the T allele correlates with higher UGT2B15 expression compared to the C allele. Therefore, it was speculated

that the SNP could be within a miRNA target site; however, no miRNA that could bind to the SNP site was identified in the study (Sun et al., 2011). Moreover, although SNP rs3100 resides within the miR-376c target site in the UGT2B15 3'UTR; Papageorgiou and Court showed that it does not alter miR-376c mediated regulation of the UGT2B15 3'UTR (Papageorgiou and Court, 2017b). The present study attempted to determine whether this SNP has any influence on miRNA-mediated regulation of UGT2B15.

A2. Results

A2.1 Putative miRNA binding to the SNP (rs3100) located in the 3'UTR of UGT2B15

A bioinformatic approach was taken to identify possible miRNA binding sites that overlap the SNP rs3100 c.1761 C/T. As Sun et al used TargetScan and MicroInspector as miRNA target prediction programs, we utilized a different program FINDTAR3 (<http://bio.sz.tsinghua.edu.cn>). This programs predicts miRNA targets based on criteria including seed pairing, free energy and partial complementarity of the miRNA:mRNA duplex (Ye et al., 2008). As shown in Figure A1, FINDTAR3 predicted that miR-3160 and miR-3679-5p could target the UGT2B15 3'UTR site where the SNP (rs3100) is located.

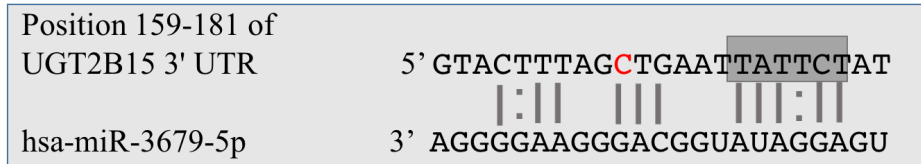
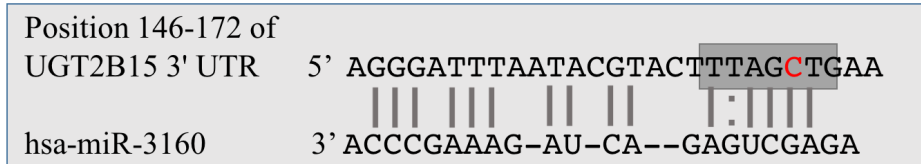


Figure A1: Predicted binding of miRNAs to the the UGT2B15 3'UTR target site where the SNP (rs3100) is located

Shown are the watson-crick pairing between miR-3160 and miR-3679-5p seeds and their respective predicted binding sites in the UGT2B15 3'UTR. The SNP is shown in red and the seed binding sites of the mRNAs are boxed and highlighted in grey.

To investigate the direct binding of these miRNAs to the SNP site in the UGT2B15 3'UTR, miRNA mimics (miR-3160, miR-3679-5p or miR-neg) were cotransfected with the UGT2B15 3'UTR reporter vector (pGL3/2B15/UTR) in LNCaP cells. The vector contained the C allele. The alignment of UGT2B15 and UGT2B17 3'UTRs show that the T is found in this position in the 3'UTR of UGT2B17 (Figure A2) (confirmed by sequencing). Therefore, the mimics were also cotransfected with the pGL3/2B17/UTR vector as a possible negative control.

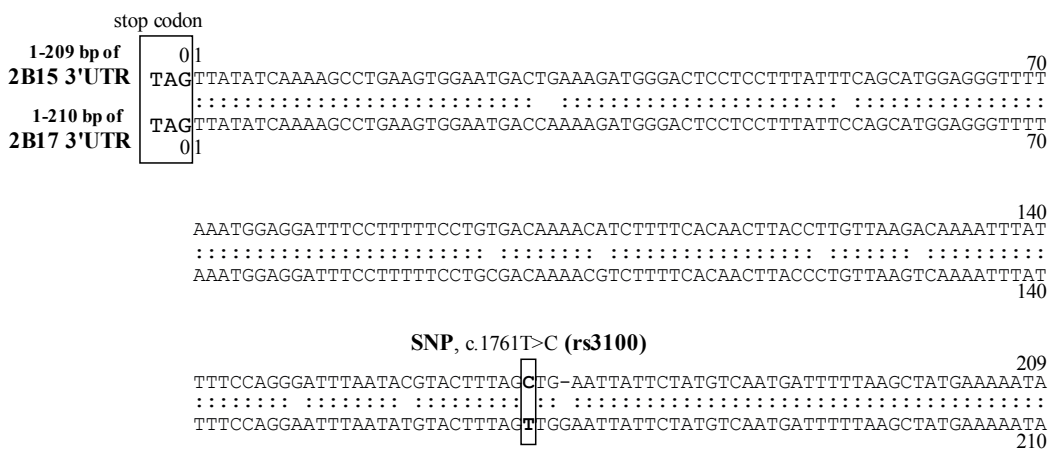


Figure A2: The position of the SNP, c.1761T>C (rs3100) site in the 3'UTR of UGT2B15

The 3'UTRs of UGT2B15 and UGT2B17 (up to 210 bp) are aligned and the nucleotide sequences are numbered relative to the stop codon (TAG with G positioned as 0). The SNP site is in bold and boxed. The C allele is seen in the UGT2B15 3'UTR (NM_001076.3) whereas the T allele of the SNP is found in the UGT2B17 3'UTR (NM_001077.3).

The luciferase assay results showed that miR-3679-5p decreased the pGL3/2B15/UTR reporter activity by 21.5% in LNCaP cells (Figure A3 A). The activity of the pGL3/2B17/UTR reporter was not significantly affected by this miRNA (Figure A3 B). However, miR-3160 did not affect the activity of either reporter (Figure A3).

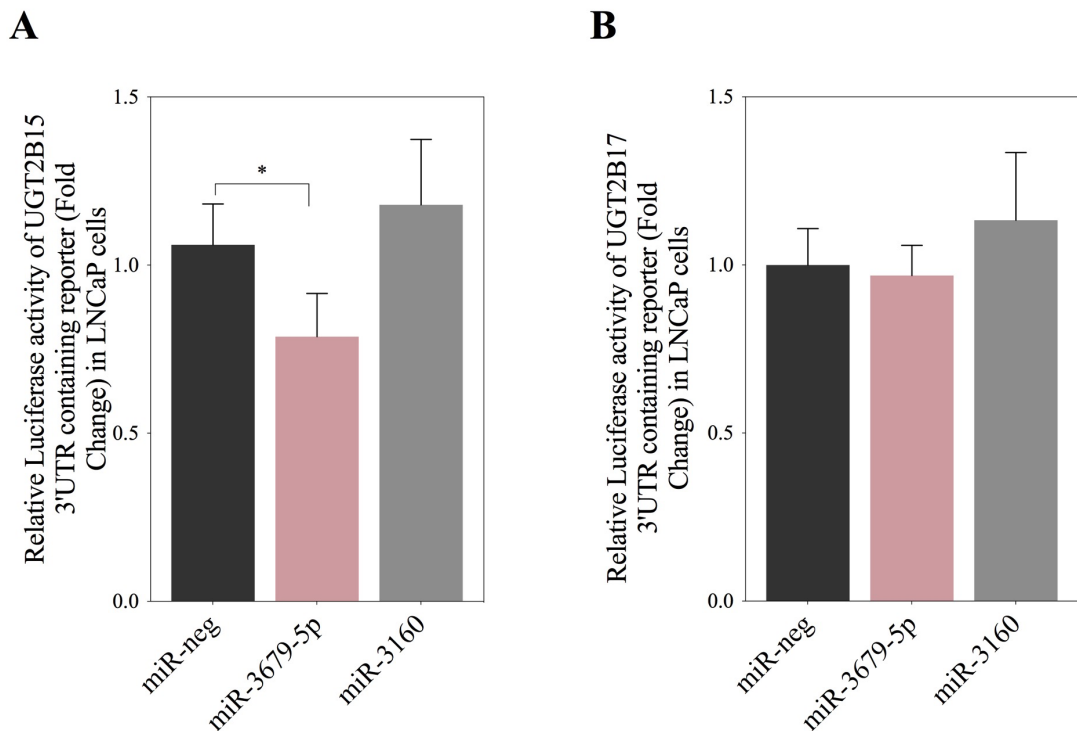


Figure A3: MiR-3679-5p mimics reduce the activity of the pGL3-reporter construct carrying the UGT2B15 3'UTR containing the C allele of the SNP, rs3100 in LNCaP cells

Luciferase reporter activity in LNCaP cells co-transfected either with UGT2B15 3'UTR containing reporter (A) or UGT2B17 3'UTR containing reporter (B), along with miR-neg, miR-3679-5p or miR-3160 mimics. The activities of the reporter constructs were first normalized to the empty pGL3-promoter vector and then presented relative to that of miR-neg transfected cells (set at a value of 1). pRL-null

was used as an internal control. Data shown are mean \pm S.D. from a single experiment performed in quadruplicate. *p, 0.05.

The experiment was repeated in the kidney HEK293T cell line as this cell line has a high transfection efficiency. However, the miR-3679-5p mimics had no effect on the pGL3/2B15/UTR reporter in this line (Figure A4 A). Consistent with LNCaP cell data, miR-3160 mimics had no effect on either of the reporters as expected (Figure A4 B).

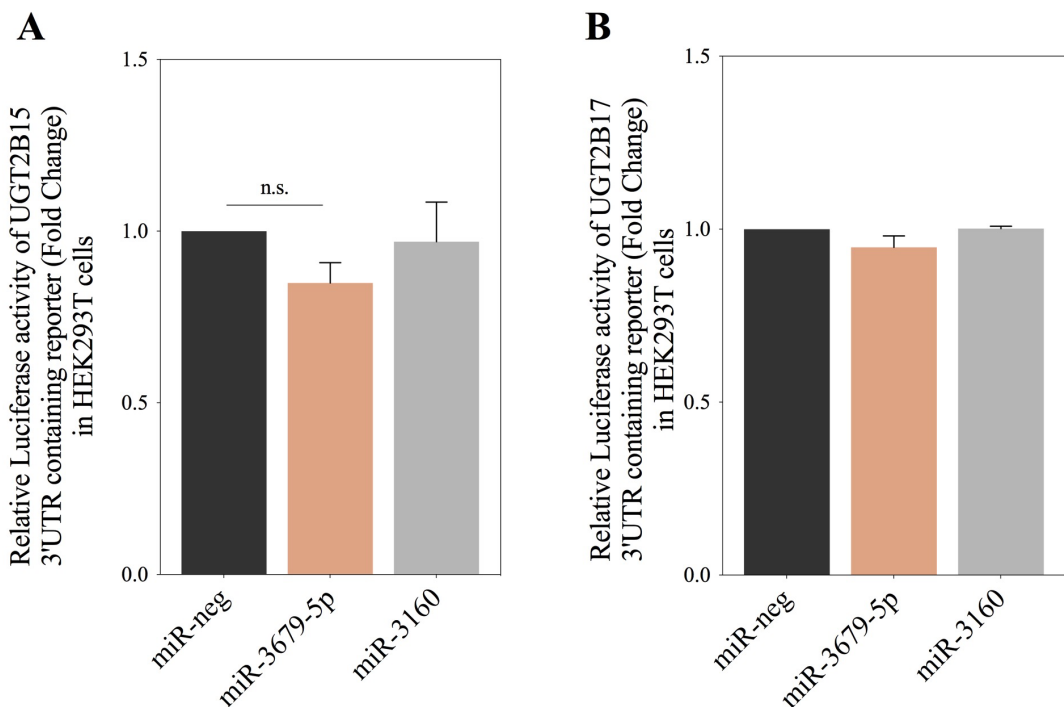


Figure A4: Luciferase assays in HEK293T cells transfected with miRNA mimics and the reporter construct carrying the UGT2B15 3'UTR with the C allele at the SNP site, or the UGT2B17 3'UTR containing reporter

The activities of the reporter constructs were first normalized to the empty pGL3-promoter vector and then presented relative to that of miR-neg transfected cells (set at a value of 1). pRL-null was used as an internal control. Data shown are mean \pm S.E.M. from two experiments performed in quadruplicate.

The ability of miR-3679-5p to alter UGT2B15 mRNA levels was investigated in LNCaP and Huh7 cells by qRT-PCR analysis performed 24 h post-transfection of

miRNA mimics. The miR-3679-5p mimics did not significantly affect UGT2B15 mRNA levels in LNCaP (Figure A5 A) or HuH7 cells (Figure A5 B). Thus, we were unable to identify a miRNA that could affect UGT2B15 expression by targeting the 3'UTR in region that overlaps SNP rs3100.

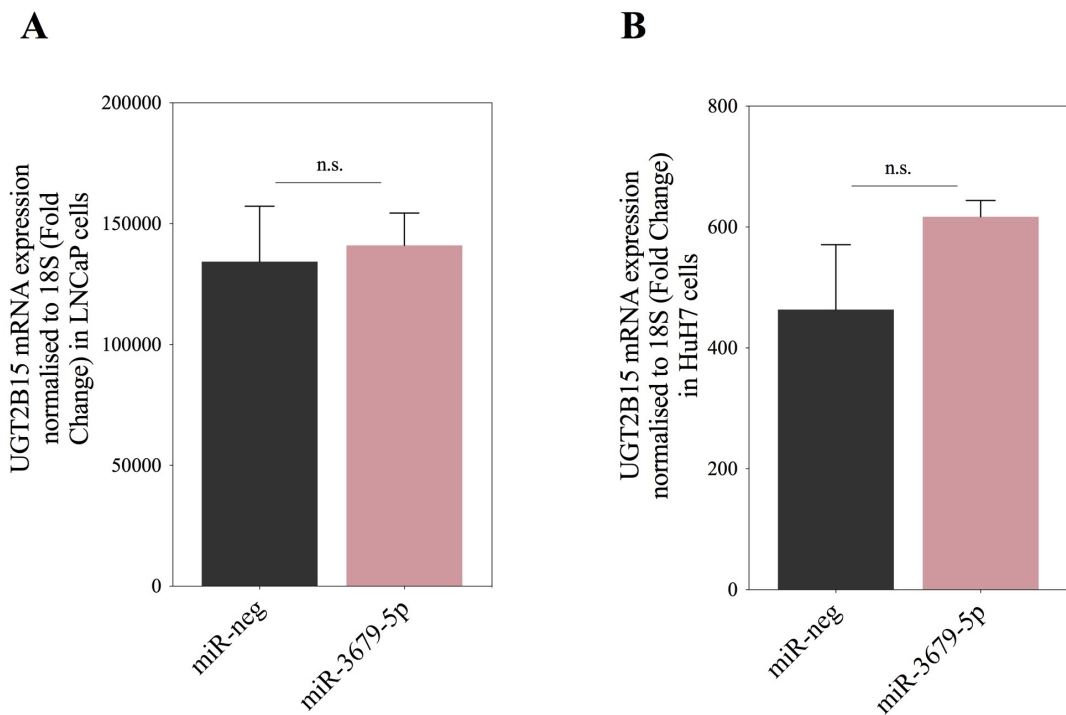


Figure A5: UGT2B15 mRNA expression in miR-3679-5p mimic-transfected cells

The expression of UGT2B15 mRNA in LNCaP cells (A) and HuH7 cells (B), transfected with miR-3679-5p mimics. Total RNA from cells were extracted 24 hours post-transfection and subjected to quantitative real-time RT-qPCR for measuring UGT2B15 mRNA levels. UGT2B15 mRNA levels were normalized to 18S RNA levels and presented as copy number per reaction. Data shown are from an experiment performed in triplicate, the error bar representing \pm S.D.

A3 Discussion

The ability of miRNAs to bind to target mRNA transcripts is critical for fine-tuning various cellular functions. SNPs that reside within miRNA target sites may affect this binding (Chen et al., 2008), disturb cellular functions or play a role in various

diseases. Hence, SNPs in miRNA target genes may function as regulatory SNPs. Currently, research is being focussed on defining the role of SNPs residing within miRNA target sites in diseases including cancer (Haas et al., 2012, Pelletier and Weidhaas, 2010, Bhaumik et al., 2014, Dzikiewicz-Krawczyk, 2014, Landi et al., 2012, Manikandan and Munirajan, 2014). Some SNPs lead to alterations in gene expression and protein function that influence cancer susceptibility. Therefore, SNPs present within miRNA binding sites may be useful as novel biomarkers of cancer risk, diagnosis and outcome (Pelletier and Weidhaas, 2010). Several databases and bioinformatics web tools are available to predict effects of SNPs on putative miRNA targets or RNA secondary structure. These include miRNASNP, MirSNP, mrSNP, miRdSNP, miRNA SNIper, MicroSNIper, RNAsnp and PolymiRTS (Gong et al., 2015). It has been reported that many xenobiotic metabolizing enzymes and transporters (including cytochrome P450 family and UGTs) are regulated by miRNAs, and that SNPs in the 3'UTR of these genes show differences in enzymatic activity (Saunders et al., 2007, Wei et al., 2012). Unfortunately, although miR-3679-5p and miR-3160 were novel candidates for binding to the region of the UGT2B15 3'UTR that overlaps the SNP rs3100, these studies did not provide definitive evidence that either of these miRNAs control expression of UGT2B15. Since the completion of this study, more advanced bioinformatic prediction tools have become available. The recent updated version of TargetScan (version 7.2) has predicted that this SNP resides within the seed binding site for miR-5690 (Figure A6). Future studies are required to elucidate if this SNP affects the binding of this or any other miRNA to the UGT2B15 3'UTR and possibly alter the post-transcriptional regulation of UGT2B15.

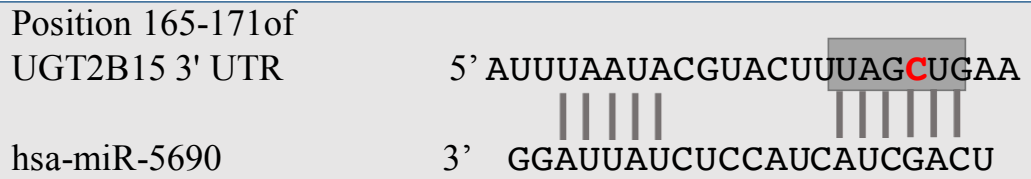


Figure A6: SNP (rs3100) is located within the predicted miR-5690 target site in the UGT2B15 3'UTR

Shown is the Watson-Crick pairing between miR-5690 and its respective predicted binding site in the UGT2B15 3'UTR according to TargetScan (release 7.2). The SNP is shown in red and the seed binding site of the mRNA is boxed and highlighted in grey.

Bibliography

- ABDELMOHSEN, K., TOMINAGA-YAMANAKA, K., SRIKANTAN, S., YOON, J. H., KANG, M. J. & GOROSPE, M. 2012. RNA-binding protein AUF1 represses Dicer expression. *Nucleic Acids Res*, 40, 11531-44.
- AGARWAL, V., BELL, G. W., NAM, J. W. & BARTEL, D. P. 2015. Predicting effective microRNA target sites in mammalian mRNAs. *Elife*, 4.
- ALMEIDA, M. I., NICOLOSO, M. S., ZENG, L., IVAN, C., SPIZZO, R., GAFA, R., XIAO, L., ZHANG, X., VANNINI, I., FANINI, F., FABBRI, M., LANZA, G., REIS, R. M., ZWEIDLER-MCKAY, P. A. & CALIN, G. A. 2012. Strand-specific miR-28-5p and miR-28-3p have distinct effects in colorectal cancer cells. *Gastroenterology*, 142, 886-896.e9.
- AMBROS, V. 2004. The functions of animal microRNAs. *Nature*, 431, 350-5.
- AMBS, S., PRUEITT, R. L., YI, M., HUDSON, R. S., HOWE, T. M., PETROCCA, F., WALLACE, T. A., LIU, C. G., VOLINIA, S., CALIN, G. A., YFANTIS, H. G., STEPHENS, R. M. & CROCE, C. M. 2008. Genomic profiling of microRNA and messenger RNA reveals deregulated microRNA expression in prostate cancer. *Cancer Res*, 68, 6162-70.
- ANANTHARAMAN, V., KOONIN, E. V. & ARAVIND, L. 2002. Comparative genomics and evolution of proteins involved in RNA metabolism. *Nucleic Acids Research*, 30, 1427-1464.
- ANDERSON, P. & KEDERSHA, N. 2002a. Stressful initiations. *J Cell Sci*, 115, 3227-34.
- ANDERSON, P. & KEDERSHA, N. 2002b. Visibly stressed: the role of eIF2, TIA-1, and stress granules in protein translation. *Cell Stress Chaperones*, 7, 213-21.
- ANJI, A. & KUMARI, M. 2016. Guardian of Genetic Messenger-RNA-Binding Proteins. *Biomolecules*, 6, 4.
- ARCAROLI, J. J., QUACKENBUSH, K. S., POWELL, R. W., PITTS, T. M., SPREAFICO, A., VARELLA-GARCIA, M., BEMIS, L., TAN, A. C., REINEMANN, J. M., TOUBAN, B. M., DASARI, A., ECKHARDT, S. G. & MESSERSMITH, W. A. 2012. Common PIK3CA mutants and a novel 3' UTR mutation are associated with increased sensitivity to saracatinib. *Clin Cancer Res*, 18, 2704-14.
- ARGIKAR, U. A. & REMMEL, R. P. 2009. Effect of aging on glucuronidation of valproic acid in human liver microsomes and the role of UDP-glucuronosyltransferase UGT1A4, UGT1A8, and UGT1A10. *Drug Metab Dispos*, 37, 229-36.
- ARMSTRONG, R. N. 1987. Enzyme-catalyzed detoxication reactions: mechanisms and stereochemistry. *CRC Crit Rev Biochem*, 22, 39-88.
- BACHMANN, K. 2009. Chapter 8 - Drug Metabolism. In: HACKER, M., MESSER, W. & BACHMANN, K. (eds.) *Pharmacology*. San Diego: Academic Press.
- BAEK, D., VILLEN, J., SHIN, C., CAMARGO, F. D., GYGI, S. P. & BARTEL, D. P. 2008. The impact of microRNAs on protein output. *Nature*, 455, 64-71.
- BAKER, A. H. & DELLES, C. 2013. Is MicroRNA-376c a biomarker or mediator of preeclampsia? *Hypertension*, 61, 767-769.

-
- BALCELLS, I., CIRERA, S. & BUSK, P. K. 2011. Specific and sensitive quantitative RT-PCR of miRNAs with DNA primers. *BMC Biotechnol*, 11, 70.
- BALTZ, ALEXANDER G., MUNSCHAUER, M., SCHWANHÄUSSER, B., VASILE, A., MURAKAWA, Y., SCHUELER, M., YOUNGS, N., PENFOLD-BROWN, D., DREW, K., MILEK, M., WYLER, E., BONNEAU, R., SELBACH, M., DIETERICH, C. & LANDTHALER, M. 2012. The mRNA-Bound Proteome and Its Global Occupancy Profile on Protein-Coding Transcripts. *Molecular Cell*, 46, 674-690.
- BANDYOPADHYAY, S. & MITRA, R. 2009. TargetMiner: microRNA target prediction with systematic identification of tissue-specific negative examples. *Bioinformatics*, 25, 2625-31.
- BAO, B.-Y., CHUANG, B.-F., WANG, Q., SARTOR, O., BALK, S. P., BROWN, M., KANTOFF, P. W. & LEE, G.-S. M. 2008. Androgen receptor mediates the expression of UDP-glucuronosyltransferase 2 B15 and B17 genes. *The Prostate*, 68, 839-848.
- BAOU, M., NORTON, J. D. & MURPHY, J. J. 2011. AU-rich RNA binding proteins in hematopoiesis and leukemogenesis. *Blood*, 118, 5732-40.
- BARBIER, O. & BELANGER, A. 2008. Inactivation of androgens by UDP-glucuronosyltransferases in the human prostate. *Best Pract Res Clin Endocrinol Metab*, 22, 259-70.
- BARBIER, O., DURAN-SANDOVAL, D., PINEDA-TORRA, I., KOSYKH, V., FRUCHART, J. C. & STAELS, B. 2003a. Peroxisome proliferator-activated receptor alpha induces hepatic expression of the human bile acid glucuronidating UDP-glucuronosyltransferase 2B4 enzyme. *J Biol Chem*, 278, 32852-60.
- BARBIER, O., LAPOINTE, H., EL ALFY, M., HUM, D. W. & BELANGER, A. 2000. Cellular localization of uridine diphosphoglucuronosyltransferase 2B enzymes in the human prostate by in situ hybridization and immunohistochemistry. *J Clin Endocrinol Metab*, 85, 4819-26.
- BARBIER, O., TORRA, I. P., SIRVENT, A., CLAUDEL, T., BLANQUART, C., DURAN-SANDOVAL, D., KUIPERS, F., KOSYKH, V., FRUCHART, J. C. & STAELS, B. 2003b. FXR induces the UGT2B4 enzyme in hepatocytes: a potential mechanism of negative feedback control of FXR activity. *Gastroenterology*, 124, 1926-40.
- BARREAU, C., PAILLARD, L. & OSBORNE, H. B. 2005. AU-rich elements and associated factors: are there unifying principles? *Nucleic Acids Research*, 33, 7138-7150.
- BARRETT, K. G., FANG, H., CUKOVIC, D., DOMBKOWSKI, A. A., KOCAREK, T. A. & RUNGE-MORRIS, M. 2015. Upregulation of UGT2B4 Expression by 3'-Phosphoadenosine-5'-Phosphosulfate Synthase Knockdown: Implications for Coordinated Control of Bile Acid Conjugation. *Drug Metab Dispos*, 43, 1061-70.
- BARTEL, D. P. 2009. MicroRNAs: target recognition and regulatory functions. *Cell*, 136, 215-33.
- BASU, N. K., KOLE, L., BASU, M., CHAKRABORTY, K., MITRA, P. S. & OWENS, I. S. 2008. The major chemical-detoxifying system of UDP-glucuronosyltransferases requires regulated phosphorylation supported by protein kinase C. *J Biol Chem*, 283, 23048-61.

-
- BASU, N. K., KOLE, L. & OWENS, I. S. 2003. Evidence for phosphorylation requirement for human bilirubin UDP-glucuronosyltransferase (UGT1A1) activity. *Biochem Biophys Res Commun*, 303, 98-104.
- BASU, N. K., KOVAROVA, M., GARZA, A., KUBOTA, S., SAHA, T., MITRA, P. S., BANERJEE, R., RIVERA, J. & OWENS, I. S. 2005. Phosphorylation of a UDP-glucuronosyltransferase regulates substrate specificity. *Proc Natl Acad Sci U S A*, 102, 6285-90.
- BEAULIEU, M., LEVESQUE, E., HUM, D. W. & BELANGER, A. 1996. Isolation and characterization of a novel cDNA encoding a human UDP-glucuronosyltransferase active on C19 steroids. *J Biol Chem*, 271, 22855-62.
- BEHM-ANSMANT, I., REHWINKEL, J., DOERKS, T., STARK, A., BORK, P. & IZAURRALDE, E. 2006. mRNA degradation by miRNAs and GW182 requires both CCR4:NOT deadenylase and DCP1:DCP2 decapping complexes. *Genes & development*, 20, 1885-1898.
- BELANGER, A., HUM, D. W., BEAULIEU, M., LEVESQUE, E., GUILLEMETTE, C., TCHERNOF, A., BELANGER, G., TURGEON, D. & DUBOIS, S. 1998. Characterization and regulation of UDP-glucuronosyltransferases in steroid target tissues. *J Steroid Biochem Mol Biol*, 65, 301-10.
- BELANGER, A., PELLETIER, G., LABRIE, F., BARBIER, O. & CHOUINARD, S. 2003. Inactivation of androgens by UDP-glucuronosyltransferase enzymes in humans. *Trends Endocrinol Metab*, 14, 473-9.
- BELANGER, A. S., TOJCIC, J., HARVEY, M. & GUILLEMETTE, C. 2010. Regulation of UGT1A1 and HNF1 transcription factor gene expression by DNA methylation in colon cancer cells. *BMC Mol Biol*, 11, 9.
- BETEL, D., KOPPAL, A., AGIUS, P., SANDER, C. & LESLIE, C. 2010. Comprehensive modeling of microRNA targets predicts functional non-conserved and non-canonical sites. *Genome Biology*, 11, R90.
- BHASKER, C. R., MCKINNON, W., STONE, A., LO, A. C., KUBOTA, T., ISHIZAKI, T. & MINERS, J. O. 2000. Genetic polymorphism of UDP-glucuronosyltransferase 2B7 (UGT2B7) at amino acid 268: ethnic diversity of alleles and potential clinical significance. *Pharmacogenetics*, 10, 679-685.
- BHAUMIK, P., GOPALAKRISHNAN, C., KAMARAJ, B. & PUROHIT, R. 2014. Single nucleotide polymorphisms in microRNA binding sites: implications in colorectal cancer. *ScientificWorldJournal*, 2014, 547154.
- BIZUAYEHU, T. T. & BABIAK, I. 2014. MicroRNA in Teleost Fish. *Genome Biology and Evolution*, 6, 1911-1937.
- BOCK, K. W., LILIENBLUM, W., FISCHER, G., SCHIRMER, G. & BOCK-HENNIG, B. S. 1987. The role of conjugation reactions in detoxication. *Archives of Toxicology*, 60, 22-29.
- BOSSUYT, X. & BLANCKAERT, N. 1997. Carrier-mediated transport of uridine diphosphoglucuronic acid across the endoplasmic reticulum membrane is a prerequisite for UDP-glucuronosyltransferase activity in rat liver. *The Biochemical journal*, 323 (Pt 3), 645-648.
- BRAUN, J. E., TRUFFAULT, V., BOLAND, A., HUNTZINGER, E., CHANG, C. T., HAAS, G., WEICHENRIEDER, O., COLES, M. & IZAURRALDE, E. 2012. A direct interaction between DCP1 and XRN1 couples mRNA decapping to 5' exonucleolytic degradation. *Nat Struct Mol Biol*, 19, 1324-31.
- BRENNAN, C. M. & STEITZ, J. A. 2001. HuR and mRNA stability. *Cell Mol Life Sci*, 58, 266-77.
-

-
- BRENNECKE, J., STARK, A., RUSSELL, R. B. & COHEN, S. M. 2005. Principles of microRNA-target recognition. *PLoS Biol*, 3, e85.
- BRODERSEN, P. & VOINNET, O. 2009. Revisiting the principles of microRNA target recognition and mode of action. *Nat Rev Mol Cell Biol*, 10, 141-8.
- BRUMMER, A. & HAUSSER, J. 2014. MicroRNA binding sites in the coding region of mRNAs: extending the repertoire of post-transcriptional gene regulation. *Bioessays*, 36, 617-26.
- BURCHELL, B., BRIERLEY, C. H. & RANCE, D. 1995. Specificity of human UDP-glucuronosyltransferases and xenobiotic glucuronidation. *Life Sci*, 57, 1819-31.
- BURCHELL, B., COUGHTRIE, M., JACKSON, M., HARDING, D., FOURNEL-GIGLEUX, S., LEAKEY, J. & HUME, R. 1989. Development of Human Liver UDP-Glucuronosyltransferases. *Developmental Pharmacology and Therapeutics*, 13, 70-77.
- CAI, L., HUANG, W. & CHOU, K. C. 2012. Prostate cancer with variants in CYP17 and UGT2B17 genes: a meta-analysis. *Protein Pept Lett*, 19, 62-9.
- CAI, X., HAGEDORN, C. H. & CULLEN, B. R. 2004. Human microRNAs are processed from capped, polyadenylated transcripts that can also function as mRNAs. *Rna*, 10, 1957-66.
- CALLEGARI, E., GRAMANTIERI, L., DOMENICALI, M., D'ABUNDO, L., SABBIONI, S. & NEGRINI, M. 2015. MicroRNAs in liver cancer: a model for investigating pathogenesis and novel therapeutic approaches. *Cell Death Differ*, 22, 46-57.
- CARDO, L. F., COTO, E., DE MENA, L., RIBACOBIA, R., MORIS, G., MENÉNDEZ, M. & ALVAREZ, V. 2013. Profile of microRNAs in the plasma of Parkinson's disease patients and healthy controls. *Journal of neurology*, 260, 1420-1422.
- CARSON, C., 3RD & RITTMASER, R. 2003. The role of dihydrotestosterone in benign prostatic hyperplasia. *Urology*, 61, 2-7.
- CARTHEW, R. W. & SONTHEIMER, E. J. 2009. Origins and Mechanisms of miRNAs and siRNAs. *Cell*, 136, 642-55.
- CASTELLO, A., FISCHER, B., HENTZE, M. W. & PREISS, T. 2013. RNA-binding proteins in Mendelian disease. *Trends Genet*, 29, 318-27.
- CHANAWONG, A., HU, D. G., MEECH, R., MACKENZIE, P. I. & MCKINNON, R. A. 2015. Induction of UDP-glucuronosyltransferase 2B15 gene expression by the major active metabolites of tamoxifen, 4-hydroxytamoxifen and endoxifen, in breast cancer cells. *Drug Metab Dispos*, 43, 889-97.
- CHANAWONG, A., MACKENZIE, P. I., MCKINNON, R. A., HU, D. G. & MEECH, R. 2017. Exemestane and Its Active Metabolite 17-Hydroxyexemestane Induce UDP-Glucuronosyltransferase (UGT) 2B17 Expression in Breast Cancer Cells. *J Pharmacol Exp Ther*, 361, 482-491.
- CHANG, I., MITSUI, Y., FUKUHARA, S., GILL, A., WONG, D. K., YAMAMURA, S., SHAHRYARI, V., TABATABAI, Z. L., DAHIYA, R., SHIN, D. M. & TANAKA, Y. 2015. Loss of miR-200c up-regulates CYP1B1 and confers docetaxel resistance in renal cell carcinoma. *Oncotarget*, 6, 7774-87.
- CHELOUFI, S., DOS SANTOS, C. O., CHONG, M. M. & HANNON, G. J. 2010. A dicer-independent miRNA biogenesis pathway that requires Ago catalysis. *Nature*, 465, 584-9.
-

-
- CHEN, C. Y. & SHYU, A. B. 1995. AU-rich elements: characterization and importance in mRNA degradation. *Trends Biochem Sci*, 20, 465-70.
- CHEN, F., CHEN, C., YANG, S., GONG, W., WANG, Y., CIANFLONE, K., TANG, J. & WANG, D. W. 2012. Let-7b inhibits human cancer phenotype by targeting cytochrome P450 epoxygenase 2J2. *PLoS One*, 7, e39197.
- CHEN, K., SONG, F., CALIN, G. A., WEI, Q., HAO, X. & ZHANG, W. 2008. Polymorphisms in microRNA targets: a gold mine for molecular epidemiology. *Carcinogenesis*, 29, 1306-11.
- CHEN, Y., ZENG, L., WANG, Y., TOLLESON, W. H., KNOX, B., CHEN, S., REN, Z., GUO, L., MEI, N., QIAN, F., HUANG, K., LIU, D., TONG, W., YU, D. & NING, B. 2017. The expression, induction and pharmacological activity of CYP1A2 are post-transcriptionally regulated by microRNA hsa-miR-132-5p. *Biochemical pharmacology*, 145, 178-191.
- CHENDRIMADA, T. P., FINN, K. J., JI, X., BAILLAT, D., GREGORY, R. I., LIEBHABER, S. A., PASQUINELLI, A. E. & SHIEKHATTAR, R. 2007. MicroRNA silencing through RISC recruitment of eIF6. *Nature*, 447, 823-8.
- CHI, S. W., HANNON, G. J. & DARNELL, R. B. 2012. An alternative mode of microRNA target recognition. *Nat Struct Mol Biol*, 19, 321-7.
- CHIANG, H. R., SCHOENFELD, L. W., RUBY, J. G., AUYEUNG, V. C., SPIES, N., BAEK, D., JOHNSTON, W. K., RUSS, C., LUO, S., BABIARZ, J. E., BLELLOCH, R., SCHROTH, G. P., NUSBAUM, C. & BARTEL, D. P. 2010. Mammalian microRNAs: experimental evaluation of novel and previously annotated genes. *Genes Dev*, 24, 992-1009.
- CHOI, Y. M., AN, S., LEE, E. M., KIM, K., CHOI, S. J., KIM, J. S., JANG, H. H., AN, I. S. & BAE, S. 2012. CYP1A1 is a target of miR-892a-mediated post-transcriptional repression. *Int J Oncol*, 41, 331-6.
- CHOUDHURY, Y., TAY, F. C., LAM, D. H., SANDANARAJ, E., TANG, C., ANG, B. T. & WANG, S. 2012. Attenuated adenosine-to-inosine editing of microRNA-376a* promotes invasiveness of glioblastoma cells. *J Clin Invest*, 122, 4059-76.
- CHOUINARD, S., BARBIER, O. & BELANGER, A. 2007. UDP-glucuronosyltransferase 2B15 (UGT2B15) and UGT2B17 enzymes are major determinants of the androgen response in prostate cancer LNCaP cells. *J Biol Chem*, 282, 33466-74.
- CHOUINARD, S., PELLETIER, G., BELANGER, A. & BARBIER, O. 2006. Isoform-specific regulation of uridine diphosphate-glucuronosyltransferase 2B enzymes in the human prostate: differential consequences for androgen and bioactive lipid inactivation. *Endocrinology*, 147, 5431-42.
- CHOUINARD, S., YUEH, M. F., TUKEY, R. H., GITON, F., FIET, J., PELLETIER, G., BARBIER, O. & BELANGER, A. 2008. Inactivation by UDP-glucuronosyltransferase enzymes: the end of androgen signaling. *J Steroid Biochem Mol Biol*, 109, 247-53.
- CHRISTODOULOU, F., RAIBLE, F., TOMER, R., SIMAKOV, O., TRACHANA, K., KLAUS, S., SNYMAN, H., HANNON, G. J., BORK, P. & ARENDT, D. 2010. Ancient animal microRNAs and the evolution of tissue identity. *Nature*, 463, 1084-1088.
- CHU, C.-Y. & RANA, T. M. 2006. Translation Repression in Human Cells by MicroRNA-Induced Gene Silencing Requires RCK/p54. *PLOS Biology*, 4, e210.
-

-
- CHU, C. Y. & RANA, T. M. 2007. Small RNAs: regulators and guardians of the genome. *J Cell Physiol*, 213, 412-9.
- CIAFRE, S. A. & GALARDI, S. 2013. microRNAs and RNA-binding proteins: A complex network of interactions and reciprocal regulations in cancer. *RNA Biology*, 10, 934-942.
- CIAFRE, S. A., GALARDI, S., MANGIOLA, A., FERRACIN, M., LIU, C. G., SABATINO, G., NEGRINI, M., MAIRA, G., CROCE, C. M. & FARACE, M. G. 2005. Extensive modulation of a set of microRNAs in primary glioblastoma. *Biochem Biophys Res Commun*, 334, 1351-8.
- CIFUENTES, D., XUE, H., TAYLOR, D. W., PATNODE, H., MISHIMA, Y., CHELOUFI, S., MA, E., MANE, S., HANNON, G. J., LAWSON, N. D., WOLFE, S. A. & GIRALDEZ, A. J. 2010. A novel miRNA processing pathway independent of Dicer requires Argonaute2 catalytic activity. *Science*, 328, 1694-8.
- CLOONAN, N. 2015. Re-thinking miRNA-mRNA interactions: Intertwining issues confound target discovery. *BioEssays*, 37, 379-388.
- COCCO, E., PALADINI, F., MACINO, G., FULCI, V., FIORILLO, M. T. & SORRENTINO, R. 2010. The expression of vasoactive intestinal peptide receptor 1 is negatively modulated by microRNA 525-5p. *PLoS One*, 5, e12067.
- COFFMAN, B. L., RIOS, G. R., KING, C. D. & TEPHLY, T. R. 1997. Human UGT2B7 catalyzes morphine glucuronidation. *Drug Metab Dispos*, 25, 1-4.
- CONGIU, M., MASHFORD, M. L., SLAVIN, J. L. & DESMOND, P. V. 2002. UDP glucuronosyltransferase mRNA levels in human liver disease. *Drug Metab Dispos*, 30, 129-34.
- COOPER, T. A., WAN, L. & DREYFUSS, G. 2009. RNA and Disease. *Cell*, 136, 777-793.
- COURT, M. H. 2005. Isoform-selective probe substrates for in vitro studies of human UDP-glucuronosyltransferases. *Methods Enzymol*, 400, 104-16.
- COURT, M. H. 2010. Interindividual variability in hepatic drug glucuronidation: studies into the role of age, sex, enzyme inducers, and genetic polymorphism using the human liver bank as a model system. *Drug Metab Rev*, 42, 209-24.
- COURT, M. H., ZHANG, X., DING, X., YEE, K. K., HESSE, L. M. & FINEL, M. 2012. Quantitative distribution of mRNAs encoding the 19 human UDP-glucuronosyltransferase enzymes in 26 adult and 3 fetal tissues. *Xenobiotica*, 42, 266-77.
- CUI, Y., KONIG, J., LEIER, I., BUCHHOLZ, U. & KEPPLER, D. 2001. Hepatic uptake of bilirubin and its conjugates by the human organic anion transporter SLC21A6. *J Biol Chem*, 276, 9626-30.
- CUK, K., ZUCKNICK, M., HEIL, J., MADHAVAN, D., SCHOTT, S., TURCHINOVICH, A., ARLT, D., RATH, M., SOHN, C., BENNER, A., JUNKERMANN, H., SCHNEEWEISS, A. & BURWINKEL, B. 2013a. Circulating microRNAs in plasma as early detection markers for breast cancer. *International Journal of Cancer*, 132, 1602-1612.
- CUK, K., ZUCKNICK, M., MADHAVAN, D., SCHOTT, S., GOLATTA, M., HEIL, J., MARMÉ, F., TURCHINOVICH, A., SINN, P., SOHN, C., JUNKERMANN, H., SCHNEEWEISS, A. & BURWINKEL, B. 2013b. Plasma MicroRNA Panel for Minimally Invasive Detection of Breast Cancer. *PLoS ONE*, 8.
-

-
- CURTIS, H. J., SIBLEY, C. R. & WOOD, M. J. 2012. Mirtrons, an emerging class of atypical miRNA. *Wiley Interdiscip Rev RNA*, 3, 617-32.
- DAHIYA, N., SHERMAN-BAUST, C. A., WANG, T. L., DAVIDSON, B., SHIH IE, M., ZHANG, Y., WOOD, W., 3RD, BECKER, K. G. & MORIN, P. J. 2008. MicroRNA expression and identification of putative miRNA targets in ovarian cancer. *PLoS One*, 3, e2436.
- DARNELL, R. B. 2010. RNA Regulation in Neurologic Disease and Cancer. *Cancer Research and Treatment : Official Journal of Korean Cancer Association*, 42, 125-129.
- DELLINGER, R. W., MATUNDAN, H. H., AHMED, A. S., DUONG, P. H. & MEYSKENS, F. L., JR. 2012. Anti-Cancer Drugs Elicit Re-Expression of UDP-Glucuronosyltransferases in Melanoma Cells. *PLOS ONE*, 7, e47696.
- DHARAP, A., POKRZYWA, C., MURALI, S., PANDI, G. & VEMUGANTI, R. 2013. MicroRNA miR-324-3p Induces Promoter-Mediated Expression of RelA Gene. *PLOS ONE*, 8, e79467.
- DIXON-MCIVER, A., EAST, P., MEIN, C. A., CAZIER, J.-B., MOLLOY, G., CHAPLIN, T., ANDREW LISTER, T., YOUNG, B. D. & DEBERNARDI, S. 2008. Distinctive Patterns of MicroRNA Expression Associated with Karyotype in Acute Myeloid Leukaemia. *PLoS ONE*, 3, e2141.
- DLUZEN, D. F. & LAZARUS, P. 2015. MicroRNA regulation of the major drug-metabolizing enzymes and related transcription factors. *Drug Metab Rev*, 47, 320-34.
- DLUZEN, D. F., SUN, D., SALZBERG, A. C., JONES, N., BUSHEY, R. T., ROBERTSON, G. P. & LAZARUS, P. 2014. Regulation of UDP-glucuronosyltransferase 1A1 expression and activity by microRNA 491-3p. *J Pharmacol Exp Ther*, 348, 465-77.
- DLUZEN, D. F., SUTLIFF, A., CHEN, G., WATSON, C., ISHMAEL, F. T. & LAZARUS, P. 2016. Regulation of UGT2B expression and activity by miR-216b in liver cancer cell lines. *J Pharmacol Exp Ther*.
- DOENCH, J. G., PETERSEN, C. P. & SHARP, P. A. 2003. siRNAs can function as miRNAs. *Genes Dev*, 17, 438-42.
- DOENCH, J. G. & SHARP, P. A. 2004. Specificity of microRNA target selection in translational repression. *Genes & Development*, 18, 504-511.
- DUSKOVA, K., NAGILLA, P., LE, H.-S., IYER, P., THALAMUTHU, A., MARTINSON, J., BAR-JOSEPH, Z., BUCHANAN, W., RINALDO, C. & AYYAVOO, V. 2013. MicroRNA regulation and its effects on cellular transcriptome in Human Immunodeficiency Virus-1 (HIV-1) infected individuals with distinct viral load and CD4 cell counts. *BMC Infectious Diseases*, 13, 250.
- DUTTON, G. J. 1980. *Glucuronidation of drugs and other compounds*, Boca Raton (Florida), CRC Press.
- DUTTON, G. J. & STOREY, I. D. 1953. The isolation of a compound of uridine diphosphate and glucuronic acid from liver. *Biochem J*, 53, xxxvii-xxxviii.
- DUURSMA, A. M., KEDDE, M., SCHRIER, M., LE SAGE, C. & AGAMI, R. 2008. miR-148 targets human DNMT3b protein coding region. *RNA*, 14, 872-877.
- DZIKIEWICZ-KRAWCZYK, A. 2014. MicroRNA-binding site polymorphisms in hematological malignancies. *Journal of Hematology & Oncology*, 7, 83.
- EKIMLER, S. & SAHIN, K. 2014. Computational Methods for MicroRNA Target Prediction. *Genes (Basel)*, 5, 671-83.
-

-
- ESQUELA-KERSCHER, A. & SLACK, F. J. 2006. Oncomirs - microRNAs with a role in cancer. *Nat Rev Cancer*, 6, 259-69.
- EVANS, W. E. & RELLING, M. V. 1999. Pharmacogenomics: translating functional genomics into rational therapeutics. *Science*, 286, 487-91.
- EVERSOLE, A. & MAIZELS, N. 2000. In vitro properties of the conserved mammalian protein hnRNP D suggest a role in telomere maintenance. *Mol Cell Biol*, 20, 5425-32.
- FABIAN, M. R., SONENBERG, N. & FILIPOWICZ, W. 2010. Regulation of mRNA translation and stability by microRNAs. *Annu Rev Biochem*, 79, 351-79.
- FELICETTI, F., ERRICO, M. C., BOTTERO, L., SEGNALE, P., STOPPACCIARO, A., BIFFONI, M., FELLI, N., MATTIA, G., PETRINI, M., COLOMBO, M. P., PESCHLE, C. & CARE, A. 2008. The promyelocytic leukemia zinc finger-microRNA-221/-222 pathway controls melanoma progression through multiple oncogenic mechanisms. *Cancer Res*, 68, 2745-54.
- FENG, D.-D., ZHANG, H., ZHANG, P., ZHENG, Y.-S., ZHANG, X.-J., HAN, B.-W., LUO, X.-Q., XU, L., ZHOU, H., QU, L.-H. & CHEN, Y.-Q. 2011. Down-regulated miR-331-5p and miR-27a are associated with chemotherapy resistance and relapse in leukaemia. *Journal of cellular and molecular medicine*, 15, 2164-2175.
- FERLAY, J., SOERJOMATARAM, I., DIKSHIT, R., ESER, S., MATHERS, C., REBELO, M., PARKIN, D. M., FORMAN, D. & BRAY, F. 2015. Cancer incidence and mortality worldwide: Sources, methods and major patterns in GLOBOCAN 2012. *International Journal of Cancer*, 136, E359-E386.
- FILIPOWICZ, W., BHATTACHARYYA, S. N. & SONENBERG, N. 2008. Mechanisms of post-transcriptional regulation by microRNAs: are the answers in sight? *Nat Rev Genet*, 9, 102-14.
- FISHER, M. B., PAINE, M. F., STRELEVITZ, T. J. & WRIGHTON, S. A. 2001. The role of hepatic and extrahepatic UDP-glucuronosyltransferases in human drug metabolism. *Drug Metab Rev*, 33, 273-97.
- FORMAN, J. J., LEGESSE-MILLER, A. & COLLIER, H. A. 2008. A search for conserved sequences in coding regions reveals that the let-7 microRNA targets Dicer within its coding sequence. *Proc Natl Acad Sci U S A*, 105, 14879-84.
- FORMOSA, A., MARKERT, E. K., LENA, A. M., ITALIANO, D., FINAZZI-AGRO, E., LEVINE, A. J., BERNARDINI, S., GARABADGIU, A. V., MELINO, G. & CANDI, E. 2014. MicroRNAs, miR-154, miR-299-5p, miR-376a, miR-376c, miR-377, miR-381, miR-487b, miR-485-3p, miR-495 and miR-654-3p, mapped to the 14q32.31 locus, regulate proliferation, apoptosis, migration and invasion in metastatic prostate cancer cells. *Oncogene*, 33, 5173-82.
- FOURNEL-GIGLEUX, S., JACKSON, M. R., WOOSTER, R. & BURCHELL, B. 1989. Expression of a human liver cDNA encoding a UDP-glucuronosyltransferase catalysing the glucuronidation of hyodeoxycholic acid in cell culture. *FEBS Lett*, 243, 119-22.
- FREMONT, J. J., WANG, R. W. & KING, C. D. 2005. Coimmunoprecipitation of UDP-glucuronosyltransferase isoforms and cytochrome P450 3A4. *Mol Pharmacol*, 67, 260-2.
-

-
- FRIEDMAN, R. C., FARH, K. K., BURGE, C. B. & BARTEL, D. P. 2009. Most mammalian mRNAs are conserved targets of microRNAs. *Genome Res*, 19, 92-105.
- FUJIWARA, R. & ITOH, T. 2014. Extensive protein-protein interactions involving UDP-glucuronosyltransferase (UGT) 2B7 in human liver microsomes. *Drug Metab Pharmacokinet*, 29, 259-65.
- FUJIWARA, R., NAKAJIMA, M., YAMANAKA, H., KATOH, M. & YOKOI, T. 2007. Interactions between human UGT1A1, UGT1A4, and UGT1A6 affect their enzymatic activities. *Drug Metab Dispos*, 35, 1781-7.
- GAGNON, J. F., BERNARD, O., VILLENEUVE, L., TETU, B. & GUILLEMETTE, C. 2006. Irinotecan inactivation is modulated by epigenetic silencing of UGT1A1 in colon cancer. *Clin Cancer Res*, 12, 1850-8.
- GALARDI, S., MERCATELLI, N., GIORDA, E., MASSALINI, S., FRAJESE, G. V., CIAFRE, S. A. & FARACE, M. G. 2007. miR-221 and miR-222 expression affects the proliferation potential of human prostate carcinoma cell lines by targeting p27Kip1. *J Biol Chem*, 282, 23716-24.
- GALL, W. E., ZAWADA, G., MOJARRABI, B., TEPHLY, T. R., GREEN, M. D., COFFMAN, B. L., MACKENZIE, P. I. & RADOMINSKA-PANDYA, A. 1999. Differential glucuronidation of bile acids, androgens and estrogens by human UGT1A3 and 2B7. *J Steroid Biochem Mol Biol*, 70, 101-8.
- GALLAGHER, C. J., KADLUBAR, F. F., MUSCAT, J. E., AMBROSONE, C. B., LANG, N. P. & LAZARUS, P. 2007. The UGT2B17 gene deletion polymorphism and risk of prostate cancer. A case-control study in Caucasians. *Cancer Detect Prev*, 31, 310-5.
- GARDNER-STEPHEN, D. A. 2008. *Transcriptional Regulation of Human UDP glucuronosyltransferases*. Doctor of Philosophy PhD, Flinders University.
- GARDNER-STEPHEN, D. A. & MACKENZIE, P. I. 2008. Liver-enriched transcription factors and their role in regulating UDP glucuronosyltransferase gene expression. *Curr Drug Metab*, 9, 439-52.
- GATTOLLIAT, C. H., THOMAS, L., CIAFRÈ, S. A., MEURICE, G., LE TEUFF, G., JOB, B., RICHON, C., COMBARET, V., DESSEN, P., VALTEAU-COUANET, D., MAY, E., BUSSON, P., DOUC-RASY, S. & BÉNARD, J. 2011. Expression of miR-487b and miR-410 encoded by 14q32.31 locus is a prognostic marker in neuroblastoma. *British Journal of Cancer*, 105, 1352-1361.
- GAUTHIER-LANDRY, L., BELANGER, A. & BARBIER, O. 2015. Multiple roles for UDP-glucuronosyltransferase (UGT)2B15 and UGT2B17 enzymes in androgen metabolism and prostate cancer evolution. *J Steroid Biochem Mol Biol*, 145, 187-92.
- GEBERT, L. F. R. & MACRAE, I. J. 2019. Regulation of microRNA function in animals. *Nat Rev Mol Cell Biol*, 20, 21-37.
- GHERZI, R., CHEN, C. Y., RAMOS, A. & BRIATA, P. 2014. KSRP controls pleiotropic cellular functions. *Semin Cell Dev Biol*, 34, 2-8.
- GHERZI, R., LEE, K. Y., BRIATA, P., WEGMULLER, D., MORONI, C., KARIN, M. & CHEN, C. Y. 2004. A KH domain RNA binding protein, KSRP, promotes ARE-directed mRNA turnover by recruiting the degradation machinery. *Mol Cell*, 14, 571-83.
- GHOSAL, S., SAHA, S., DAS, S., SEN, R., GOSWAMI, S., JANA, S. S. & CHAKRABARTI, J. 2016. miRepress: modelling gene expression regulation by microRNA with non-conventional binding sites. *Sci Rep*, 6, 22334.
-

-
- GHOSH, S. S., SAPPAL, B. S., KALPANA, G. V., LEE, S. W., CHOWDHURY, J. R. & CHOWDHURY, N. R. 2001. Homodimerization of human bilirubin-uridine-diphosphoglucuronate glucuronosyltransferase-1 (UGT1A1) and its functional implications. *J Biol Chem*, 276, 42108-15.
- GOMES, C. P., CHO, J. H., HOOD, L., FRANCO, O. L., PEREIRA, R. W. & WANG, K. 2013. A Review of Computational Tools in microRNA Discovery. *Front Genet*, 4, 81.
- GONG, J., LIU, C., LIU, W., WU, Y., MA, Z., CHEN, H. & GUO, A.-Y. 2015. An update of miRNASNP database for better SNP selection by GWAS data, miRNA expression and online tools. *Database: The Journal of Biological Databases and Curation*, 2015, bav029.
- GONG, Q. H., CHO, J. W., HUANG, T., POTTER, C., GHOLAMI, N., BASU, N. K., KUBOTA, S., CARVALHO, S., PENNINGTON, M. W., OWENS, I. S. & POPESCU, N. C. 2001. Thirteen UDPglucuronosyltransferase genes are encoded at the human UGT1 gene complex locus. *Pharmacogenetics*, 11, 357-68.
- GOTO, Y., KOJIMA, S., NISHIKAWA, R., KUROZUMI, A., KATO, M., ENOKIDA, H., MATSUSHITA, R., YAMAZAKI, K., ISHIDA, Y., NAKAGAWA, M., NAYA, Y., ICHIKAWA, T. & SEKI, N. 2015. MicroRNA expression signature of castration-resistant prostate cancer: the microRNA-221/222 cluster functions as a tumour suppressor and disease progression marker. *Br J Cancer*, 113, 1055-65.
- GOTTARDO, F., LIU, C. G., FERRACIN, M., CALIN, G. A., FASSAN, M., BASSI, P., SEVIGNANI, C., BYRNE, D., NEGRINI, M., PAGANO, F., GOMELLA, L. G., CROCE, C. M. & BAFFA, R. 2007. Micro-RNA profiling in kidney and bladder cancers. *Urol Oncol*, 25, 387-92.
- GRAMANTIERI, L., FORNARI, F., CALLEGARI, E., SABBIONI, S., LANZA, G., CROCE, C. M., BOLONDI, L. & NEGRINI, M. 2008. MicroRNA involvement in hepatocellular carcinoma. *J Cell Mol Med*, 12, 2189-204.
- GRANT, D. J., CHEN, Z., HOWARD, L. E., WIGGINS, E., DE HOEDT, A., VIDAL, A. C., CARNEY, S. T., SQUIRES, J., MAGYAR, C. E., HUANG, J. & FREEDLAND, S. J. 2017. UDP-glucuronosyltransferases and biochemical recurrence in prostate cancer progression. *BMC cancer*, 17, 463-463.
- GRATACOS, F. M. & BREWER, G. 2010. The role of AUF1 in regulated mRNA decay. *Wiley Interdiscip Rev RNA*, 1, 457-73.
- GREEN, M. D., OTURU, E. M. & TEPHLY, T. R. 1994. Stable expression of a human liver UDP-glucuronosyltransferase (UGT2B15) with activity toward steroid and xenobiotic substrates. *Drug Metab Dispos*, 22, 799-805.
- GREGORY, P. A. 2004. *Transcriptional regulation of UDPglucuronosyltransferases in extrahepatic tissues*. Doctor of Philosophy PhD, Flinders University.
- GREGORY, P. A., GARDNER-STEPHEN, D. A., ROGERS, A., MICHAEL, M. Z. & MACKENZIE, P. I. 2006. The caudal-related homeodomain protein Cdx2 and hepatocyte nuclear factor 1alpha cooperatively regulate the UDP-glucuronosyltransferase 2B7 gene promoter. *Pharmacogenet Genomics*, 16, 527-36.
- GREGORY, P. A., LEWINSKY, R. H., GARDNER-STEPHEN, D. A. & MACKENZIE, P. I. 2004. Coordinate regulation of the human UDP-glucuronosyltransferase 1A8, 1A9, and 1A10 genes by hepatocyte nuclear
-

-
- factor 1alpha and the caudal-related homeodomain protein 2. *Mol Pharmacol*, 65, 953-63.
- GRIMSON, A., FARH, K. K., JOHNSTON, W. K., GARRETT-ENGELE, P., LIM, L. P. & BARTEL, D. P. 2007. MicroRNA targeting specificity in mammals: determinants beyond seed pairing. *Mol Cell*, 27, 91-105.
- GRIMSON, A., SRIVASTAVA, M., FAHEY, B., WOODCROFT, B. J., CHIANG, H. R., KING, N., DEGNAN, B. M., ROKHSAR, D. S. & BARTEL, D. P. 2008. Early origins and evolution of microRNAs and Piwi-interacting RNAs in animals. *Nature*, 455, 1193-1197.
- GRISHOK, A., PASQUINELLI, A. E., CONTE, D., LI, N., PARRISH, S., HA, I., BAILLIE, D. L., FIRE, A., RUVKUN, G. & MELLO, C. C. 2001. Genes and mechanisms related to RNA interference regulate expression of the small temporal RNAs that control *C. elegans* developmental timing. *Cell*, 106, 23-34.
- GROSSE, L., PAQUET, S., CARON, P., FAZLI, L., RENNIE, P. S., BELANGER, A. & BARBIER, O. 2013. Androgen glucuronidation: an unexpected target for androgen deprivation therapy, with prognosis and diagnostic implications. *Cancer Res*, 73, 6963-71.
- GSUR, A., PREYER, M., HAIDINGER, G., SCHATZL, G., MADERSBACHER, S., MARBERGER, M., VUTUC, C. & MICKSCHE, M. 2002. A Polymorphism in the *UDP-Glucuronosyltransferase 2B15* Gene (D⁸⁵Y) Is Not Associated with Prostate Cancer Risk. *Cancer Epidemiology Biomarkers & Prevention*, 11, 497-498.
- GUEYDAN, C., DROOGMANS, L., CHALON, P., HUEZ, G., CAPUT, D. & KRUYSS, V. 1999. Identification of TIAR as a protein binding to the translational regulatory AU-rich element of tumor necrosis factor alpha mRNA. *J Biol Chem*, 274, 2322-6.
- GUILLEMETTE, C. 2003. Pharmacogenomics of human UDP-glucuronosyltransferase enzymes. *Pharmacogenomics J*, 3, 136-58.
- GUILLEMETTE, C., HUM, D. W. & BELANGER, A. 1996. Regulation of steroid glucuronosyltransferase activities and transcripts by androgen in the human prostatic cancer LNCaP cell line. *Endocrinology*, 137, 2872-9.
- GUILLEMETTE, C., LEVESQUE, E., BEAULIEU, M., TURGEON, D., HUM, D. W. & BELANGER, A. 1997. Differential regulation of two uridine diphospho-glucuronosyltransferases, UGT2B15 and UGT2B17, in human prostate LNCaP cells. *Endocrinology*, 138, 2998-3005.
- GUILLEMETTE, C., LEVESQUE, E., HARVEY, M., BELLEMARE, J. & MENARD, V. 2010. UGT genomic diversity: beyond gene duplication. *Drug Metab Rev*, 42, 24-44.
- GUILLEMETTE, C., LEVESQUE, E. & ROULEAU, M. 2014. Pharmacogenomics of human uridine diphospho-glucuronosyltransferases and clinical implications. *Clin Pharmacol Ther*, 96, 324-39.
- GUO, Z., DAI, B., JIANG, T., XU, K., XIE, Y., KIM, O., NESHEIWAT, I., KONG, X., MELAMED, J., HANDRATTA, V. D., NJAR, V. C. O., BRODIE, A. M. H., YU, L.-R., VEENSTRA, T. D., CHEN, H. & QIU, Y. 2006. Regulation of androgen receptor activity by tyrosine phosphorylation. *Cancer Cell*, 10, 309-319.
- HA, M. & KIM, V. N. 2014. Regulation of microRNA biogenesis. *Nat Rev Mol Cell Biol*, 15, 509-24.
-

-
- HAAS, U., SCZAKIEL, G. & LAUFER, S. D. 2012. MicroRNA-mediated regulation of gene expression is affected by disease-associated SNPs within the 3'-UTR via altered RNA structure. *RNA Biol*, 9, 924-37.
- HABIBI, M., MIRFAKHRAIE, R., KHANI, M., RAKHSHAN, A., AZARGASHB, E. & POURSMAEILI, F. 2017. Genetic variations in UGT2B28, UGT2B17, UGT2B15 genes and the risk of prostate cancer: A case-control study. *Gene*, 634, 47-52.
- HAMMOND, S. M. 2015. An overview of microRNAs. *Adv Drug Deliv Rev*, 87, 3-14.
- HAN, J., LEE, Y., YEOM, K. H., NAM, J. W., HEO, I., RHEE, J. K., SOHN, S. Y., CHO, Y., ZHANG, B. T. & KIM, V. N. 2006. Molecular basis for the recognition of primary microRNAs by the Drosha-DGCR8 complex. *Cell*, 125, 887-901.
- HAUSER, S. C., ZIURYS, J. C. & GOLLAN, J. L. 1988. A membrane transporter mediates access of uridine 5'-diphosphoglucuronic acid from the cytosol into the endoplasmic reticulum of rat hepatocytes: implications for glucuronidation reactions. *Biochim Biophys Acta*, 967, 149-57.
- HE, L. & HANNON, G. J. 2004. MicroRNAs: small RNAs with a big role in gene regulation. *Nat Rev Genet*, 5, 522-31.
- HEINLEIN, C. A. & CHANG, C. 2004. Androgen receptor in prostate cancer. *Endocr Rev*, 25, 276-308.
- HIROHASHI, T., SUZUKI, H. & SUGIYAMA, Y. 1999. Characterization of the transport properties of cloned rat multidrug resistance-associated protein 3 (MRP3). *J Biol Chem*, 274, 15181-5.
- HOFACKER, I. L. 2007. How microRNAs choose their targets. *Nat Genet*, 39, 1191-1192.
- HOMBACH, S. & KRETZ, M. 2016. Non-coding RNAs: Classification, Biology and Functioning. *Adv Exp Med Biol*, 937, 3-17.
- HORNBERG, E., YLITALO, E. B., CRNALIC, S., ANTTI, H., STATTIN, P., WIDMARK, A., BERGH, A. & WIKSTROM, P. 2011. Expression of androgen receptor splice variants in prostate cancer bone metastases is associated with castration-resistance and short survival. *PLoS One*, 6, e19059.
- HSU, J. B.-K., CHIU, C.-M., HSU, S.-D., HUANG, W.-Y., CHIEN, C.-H., LEE, T.-Y. & HUANG, H.-D. 2011. miRTar: an integrated system for identifying miRNA-target interactions in human. *BMC Bioinformatics*, 12, 300.
- HU, D. G., GARDNER-STEPHEN, D., SEVERI, G., GREGORY, P. A., TRELOAR, J., GILES, G. G., ENGLISH, D. R., HOPPER, J. L., TILLEY, W. D. & MACKENZIE, P. I. 2010. A Novel Polymorphism in a Forkhead Box A1 (FOXA1) Binding Site of the Human UDP Glucuronosyltransferase 2B17 Gene Modulates Promoter Activity and Is Associated with Altered Levels of Circulating Androstane-3 α ,17 β -diol Glucuronide. *Molecular Pharmacology*, 78, 714-722.
- HU, D. G. & MACKENZIE, P. I. 2009. Estrogen receptor alpha, fos-related antigen-2, and c-Jun coordinately regulate human UDP glucuronosyltransferase 2B15 and 2B17 expression in response to 17beta-estradiol in MCF-7 cells. *Mol Pharmacol*, 76, 425-39.
- HU, D. G. & MACKENZIE, P. I. 2010. Forkhead Box Protein A1 Regulates UDP-Glucuronosyltransferase 2B15 Gene Transcription in LNCaP Prostate Cancer Cells. *Drug Metabolism and Disposition*, 38, 2105-2109.
-

-
- HU, D. G., MACKENZIE, P. I., LU, L., MEECH, R. & MCKINNON, R. A. 2015. Induction of human UDP-Glucuronosyltransferase 2B7 gene expression by cytotoxic anticancer drugs in liver cancer HepG2 cells. *Drug Metab Dispos*, 43, 660-8.
- HU, D. G., MACKENZIE, P. I., MCKINNON, R. A. & MEECH, R. 2016a. Genetic polymorphisms of human UDP-glucuronosyltransferase (UGT) genes and cancer risk. *Drug Metab Rev*, 48, 47-69.
- HU, D. G., MEECH, R., LU, L., MCKINNON, R. A. & MACKENZIE, P. I. 2014a. Polymorphisms and haplotypes of the UDP-glucuronosyltransferase 2B7 gene promoter. *Drug Metab Dispos*, 42, 854-62.
- HU, D. G., MEECH, R., MCKINNON, R. A. & MACKENZIE, P. I. 2014b. Transcriptional regulation of human UDP-glucuronosyltransferase genes. *Drug Metab Rev*, 46, 421-58.
- HU, D. G., ROGERS, A. & MACKENZIE, P. I. 2014c. Epirubicin upregulates UDP glucuronosyltransferase 2B7 expression in liver cancer cells via the p53 pathway. *Mol Pharmacol*, 85, 887-97.
- HU, D. G., SELTH, L. A., TARULLI, G. A., MEECH, R., WIJAYAKUMARA, D., CHANAWONG, A., RUSSELL, R., CALDAS, C., ROBINSON, J. L., CARROLL, J. S., TILLEY, W. D., MACKENZIE, P. I. & HICKEY, T. E. 2016b. Androgen and Estrogen Receptors in Breast Cancer Coregulate Human UDP-Glucuronosyltransferases 2B15 and 2B17. *Cancer Res*, 76, 5881-5893.
- HU, W. & COLLER, J. 2012. What comes first: translational repression or mRNA degradation? The deepening mystery of microRNA function. *Cell Res*, 22, 1322-4.
- HUTVAGNER, G., MCLACHLAN, J., PASQUINELLI, A. E., BALINT, E., TUSCHL, T. & ZAMORE, P. D. 2001. A cellular function for the RNA-interference enzyme Dicer in the maturation of the let-7 small temporal RNA. *Science*, 293, 834-8.
- IKUSHIRO, S., EMI, Y. & IYANAGI, T. 1997. Protein-protein interactions between UDP-glucuronosyltransferase isozymes in rat hepatic microsomes. *Biochemistry*, 36, 7154-61.
- INGELMAN-SUNDBERG, M., SIM, S. C., GOMEZ, A. & RODRIGUEZ-ANTONA, C. 2007. Influence of cytochrome P450 polymorphisms on drug therapies: pharmacogenetic, pharmacoeconomic and clinical aspects. *Pharmacol Ther*, 116, 496-526.
- INNOCENTI, F., IYER, L., RAMIREZ, J., GREEN, M. D. & RATAIN, M. J. 2001. Epirubicin glucuronidation is catalyzed by human UDP-glucuronosyltransferase 2B7. *Drug Metab Dispos*, 29, 686-92.
- ISHII, Y., HANSEN, A. J. & MACKENZIE, P. I. 2000. Octamer transcription factor-1 enhances hepatic nuclear factor-1alpha-mediated activation of the human UDP glucuronosyltransferase 2B7 promoter. *Mol Pharmacol*, 57, 940-7.
- ITAAHO, K., MACKENZIE, P. I., IKUSHIRO, S., MINERS, J. O. & FINEL, M. 2008. The configuration of the 17-hydroxy group variably influences the glucuronidation of beta-estradiol and epiestradiol by human UDP-glucuronosyltransferases. *Drug Metab Dispos*, 36, 2307-15.
- IWAKI, J., KIKUCHI, K., MIZUGUCHI, Y., KAWAHIGASHI, Y., YOSHIDA, H., UCHIDA, E. & TAKIZAWA, T. 2013. MiR-376c down-regulation

-
- accelerates EGF-dependent migration by targeting GRB2 in the HuCCT1 human intrahepatic cholangiocarcinoma cell line. *PLoS One*, 8, e69496.
- IZUKAWA, T., NAKAJIMA, M., FUJIWARA, R., YAMANAKA, H., FUKAMI, T., TAKAMIYA, M., AOKI, Y., IKUSHIRO, S., SAKAKI, T. & YOKOI, T. 2009. Quantitative analysis of UDP-glucuronosyltransferase (UGT) 1A and UGT2B expression levels in human livers. *Drug Metab Dispos*, 37, 1759-68.
- JACOBSEN, A., KROGH, A., KAUPPINEN, S. & LINDOW, M. 2010. miRMaid: a unified programming interface for microRNA data resources. *BMC Bioinformatics*, 11, 29.
- JANCOVA, P., ANZENBACHER, P. & ANZENBACHEROVA, E. 2010. Phase II drug metabolizing enzymes. *Biomed Pap Med Fac Univ Palacky Olomouc Czech Repub*, 154, 103-16.
- JEDLITSCHKY, G., LEIER, I., BUCHHOLZ, U., HUMMEL-EISENBEISS, J., BURCHELL, B. & KEPPLER, D. 1997. ATP-dependent transport of bilirubin glucuronides by the multidrug resistance protein MRP1 and its hepatocyte canalicular isoform MRP2. *The Biochemical journal*, 327 (Pt 1), 305-310.
- JIN, C., MINERS, J. O., LILLYWHITE, K. J. & MACKENZIE, P. I. 1993. Complementary deoxyribonucleic acid cloning and expression of a human liver uridine diphosphate-glucuronosyltransferase glucuronidating carboxylic acid-containing drugs. *J Pharmacol Exp Ther*, 264, 475-9.
- JIN, Y., PENG, D., SHEN, Y., XU, M., LIANG, Y., XIAO, B. & LU, J. 2013. MicroRNA-376c inhibits cell proliferation and invasion in osteosarcoma by targeting to transforming growth factor- α . *DNA Cell Biol*, 32, 302-9.
- JONAS, S. & IZAURRALDE, E. 2015. Towards a molecular understanding of microRNA-mediated gene silencing. *Nat Rev Genet*, 16, 421-33.
- KAARBO, M., KLOKK, T. I. & SAATCIOGLU, F. 2007. Androgen signaling and its interactions with other signaling pathways in prostate cancer. *Bioessays*, 29, 1227-38.
- KAEDING, J., BELANGER, J., CARON, P., VERREAULT, M., BELANGER, A. & BARBIER, O. 2008a. Calcitrol (1 α ,25-dihydroxyvitamin D3) inhibits androgen glucuronidation in prostate cancer cells. *Mol Cancer Ther*, 7, 380-90.
- KAEDING, J., BOUCHAERT, E., BELANGER, J., CARON, P., CHOUINARD, S., VERREAULT, M., LAROUCHE, O., PELLETIER, G., STAELS, B., BELANGER, A. & BARBIER, O. 2008b. Activators of the farnesoid X receptor negatively regulate androgen glucuronidation in human prostate cancer LNCAP cells. *Biochem J*, 410, 245-53.
- KANG, M. J., SONG, W. H., SHIM, B. H., OH, S. Y., LEE, H. Y., CHUNG, E. Y., SOHN, Y. & LEE, J. 2010. Pharmacologically Active Metabolites of Currently Marketed Drugs: Potential Resources for New Drug Discovery and Development. *YAKUGAKU ZASSHI*, 130, 1325-1337.
- KARYPIDIS, A. H., OLSSON, M., ANDERSSON, S. O., RANE, A. & EKSTROM, L. 2008. Deletion polymorphism of the UGT2B17 gene is associated with increased risk for prostate cancer and correlated to gene expression in the prostate. *Pharmacogenomics J*, 8, 147-51.
- KAWAHARA, Y., ZINSHTEYN, B., SETHUPATHY, P., IIZASA, H., HATZIGEORGIOU, A. G. & NISHIKURA, K. 2007. Redirection of silencing targets by adenosine-to-inosine editing of miRNAs. *Science*, 315, 1137-40.
-

-
- KEBAMO, S., TESEMA, S. & GELETA, B. 2015. The Role of Biotransformation in Drug Discovery and Development. *Journal of Drug Metabolism and Toxicology*, 6, 196.
- KECHAVARZI, B. & JANGA, S. C. 2014. Dissecting the expression landscape of RNA-binding proteins in human cancers. *Genome Biol*, 15, R14.
- KEENE, J. D. 2007. RNA regulons: coordination of post-transcriptional events. *Nat Rev Genet*, 8, 533-43.
- KEENE, J. D. & TENENBAUM, S. A. 2002. Eukaryotic mRNPs may represent posttranscriptional operons. *Mol Cell*, 9, 1161-7.
- KEPPLER, D., LEIER, I. & JEDLITSCHKY, G. 1997. Transport of glutathione conjugates and glucuronides by the multidrug resistance proteins MRP1 and MRP2. *Biol Chem*, 378, 787-91.
- KERTESZ, M., IOVINO, N., UNNERSTALL, U., GAUL, U. & SEGAL, E. 2007. The role of site accessibility in microRNA target recognition. *Nature Genetics*, 39, 1278.
- KETTING, R. F., FISCHER, S. E., BERNSTEIN, E., SIJEN, T., HANNON, G. J. & PLASTERK, R. H. 2001. Dicer functions in RNA interference and in synthesis of small RNA involved in developmental timing in *C. elegans*. *Genes Dev*, 15, 2654-9.
- KHVOROVA, A., REYNOLDS, A. & JAYASENA, S. D. 2003. Functional siRNAs and miRNAs exhibit strand bias. *Cell*, 115, 209-16.
- KIANG, T. K., ENSOM, M. H. & CHANG, T. K. 2005. UDP-glucuronosyltransferases and clinical drug-drug interactions. *Pharmacol Ther*, 106, 97-132.
- KILEDJIAN, M., DEMARIA, C. T., BREWER, G. & NOVICK, K. 1997. Identification of AUF1 (heterogeneous nuclear ribonucleoprotein D) as a component of the alpha-globin mRNA stability complex. *Mol Cell Biol*, 17, 4870-6.
- KIM, V. N. 2005. MicroRNA biogenesis: coordinated cropping and dicing. *Nat Rev Mol Cell Biol*, 6, 376-85.
- KIM, Y. K., YU, J., HAN, T. S., PARK, S. Y., NAMKOONG, B., KIM, D. H., HUR, K., YOO, M. W., LEE, H. J., YANG, H. K. & KIM, V. N. 2009. Functional links between clustered microRNAs: suppression of cell-cycle inhibitors by microRNA clusters in gastric cancer. *Nucleic Acids Res*, 37, 1672-81.
- KIRIAKIDOU, M., TAN, G. S., LAMPRIKAKI, S., DE PLANELL-SAGUER, M., NELSON, P. T. & MOURELATOS, Z. 2007. An mRNA m7G cap binding-like motif within human Ago2 represses translation. *Cell*, 129, 1141-51.
- KISHORE, S., LUBER, S. & ZAVOLAN, M. 2010. Deciphering the role of RNA-binding proteins in the post-transcriptional control of gene expression. *Brief Funct Genomics*, 9, 391-404.
- KOMAGATA, S., NAKAJIMA, M., TAKAGI, S., MOHRI, T., TANIYA, T. & YOKOI, T. 2009. Human CYP24 catalyzing the inactivation of calcitriol is post-transcriptionally regulated by miR-125b. *Mol Pharmacol*, 76, 702-9.
- KONIG, J., ROST, D., CUI, Y. & KEPPLER, D. 1999. Characterization of the human multidrug resistance protein isoform MRP3 localized to the basolateral hepatocyte membrane. *Hepatology*, 29, 1156-63.
- KORKMAZ, G., LE SAGE, C., TEKIRDAG, K. A., AGAMI, R. & GOZUACIK, D. 2012. miR-376b controls starvation and mTOR inhibition-related autophagy by targeting ATG4C and BECN1. *Autophagy*, 8, 165-76.
-

-
- KOSIK, K. S. 2010. MicroRNAs and cellular phenotypy. *Cell*, 143, 21-6.
- KOTURBASH, I., TOLLESON, W. H., GUO, L., YU, D., CHEN, S., HONG, H., MATTES, W. & NING, B. 2015. microRNAs as pharmacogenomic biomarkers for drug efficacy and drug safety assessment. *Biomarkers in medicine*, 9, 1153-1176.
- KOZOMARA, A. & GRIFFITHS-JONES, S. 2011. miRBase: integrating microRNA annotation and deep-sequencing data. *Nucleic acids research*, 39, D152-D157.
- KPOGHOMOU, M.-A., SOATIANA, J. E., KALEMBO, F. W., BISHWAJIT, G. & SHENG, W. 2013. UGT2B17 Polymorphism and Risk of Prostate Cancer: A Meta-Analysis. *ISRN oncology*, 2013, 465916-465916.
- KREK, A., GRÜN, D., POY, M. N., WOLF, R., ROSENBERG, L., EPSTEIN, E. J., MACMENAMIN, P., DA PIEDADE, I., GUNSALUS, K. C., STOFFEL, M. & RAJEWSKY, N. 2005. Combinatorial microRNA target predictions. *Nature Genetics*, 37, 495.
- KROISS, A., VINCENT, S., DECAUSSIN-PETRUCCI, M., MEUGNIER, E., VIALLET, J., RUFFION, A., CHALMEL, F., SAMARUT, J. & ALLIOLI, N. 2015. Androgen-regulated microRNA-135a decreases prostate cancer cell migration and invasion through downregulating ROCK1 and ROCK2. *Oncogene*, 34, 2846-55.
- KRUGER, J. & REHMSMEIER, M. 2006. RNAhybrid: microRNA target prediction easy, fast and flexible. *Nucleic Acids Res*, 34, W451-4.
- LAGOS-QUINTANA, M., RAUHUT, R., LENDECKEL, W. & TUSCHL, T. 2001. Identification of novel genes coding for small expressed RNAs. *Science*, 294, 853-8.
- LAGOS-QUINTANA, M., RAUHUT, R., MEYER, J., BORKHARDT, A. & TUSCHL, T. 2003. New microRNAs from mouse and human. *Rna*, 9, 175-9.
- LAI, W. S., KENNINGTON, E. A. & BLACKSHEAR, P. J. 2003. Tristetraprolin and its family members can promote the cell-free deadenylation of AU-rich element-containing mRNAs by poly(A) ribonuclease. *Mol Cell Biol*, 23, 3798-812.
- LAL, A., MAZAN-MAMCZARZ, K., KAWAI, T., YANG, X., MARTINDALE, J. L. & GOROSPE, M. 2004. Concurrent versus individual binding of HuR and AUF1 to common labile target mRNAs. *Embo j*, 23, 3092-102.
- LAL, A., NAVARRO, F., MAHER, C. A., MALISZEWSKI, L. E., YAN, N., O'DAY, E., CHOWDHURY, D., DYKXHOORN, D. M., TSAI, P., HOFMANN, O., BECKER, K. G., GOROSPE, M., HIDE, W. & LIEBERMAN, J. 2009. miR-24 Inhibits cell proliferation by targeting E2F2, MYC, and other cell-cycle genes via binding to "seedless" 3'UTR microRNA recognition elements. *Mol Cell*, 35, 610-25.
- LAMBA, V., GHODKE, Y., GUAN, W. & TRACY, T. S. 2014. microRNA-34a is associated with expression of key hepatic transcription factors and cytochromes P450. *Biochem Biophys Res Commun*, 445, 404-11.
- LANDI, D., GEMIGNANI, F. & LANDI, S. 2012. Role of variations within microRNA-binding sites in cancer. *Mutagenesis*, 27, 205-10.
- LAU, N. C., LIM, L. P., WEINSTEIN, E. G. & BARTEL, D. P. 2001. An abundant class of tiny RNAs with probable regulatory roles in *Caenorhabditis elegans*. *Science*, 294, 858-62.
- LAZARUS, P., ZHENG, Y., RUNKLE, E. A., MUSCAT, J. E. & WIENER, D. 2005. Genotype-phenotype correlation between the polymorphic UGT2B17
-

-
- gene deletion and NNAL glucuronidation activities in human liver microsomes. *Pharmacogenet Genomics*, 15, 769-78.
- LEE, E. J., GUSEV, Y., JIANG, J., NUOVO, G. J., LERNER, M. R., FRANKEL, W. L., MORGAN, D. L., POSTIER, R. G., BRACKETT, D. J. & SCHMITTGEN, T. D. 2007. Expression profiling identifies microRNA signature in pancreatic cancer. *Int J Cancer*, 120, 1046-54.
- LEE, R. C. & AMBROS, V. 2001. An extensive class of small RNAs in *Caenorhabditis elegans*. *Science*, 294, 862-4.
- LEE, R. C., FEINBAUM, R. L. & AMBROS, V. 1993. The *C. elegans* heterochronic gene *lin-4* encodes small RNAs with antisense complementarity to *lin-14*. *Cell*, 75, 843-54.
- LEE, Y., AHN, C., HAN, J., CHOI, H., KIM, J., YIM, J., LEE, J., PROVOST, P., RADMARK, O., KIM, S. & KIM, V. N. 2003. The nuclear RNase III Droscha initiates microRNA processing. *Nature*, 425, 415-9.
- LEE, Y., JEON, K., LEE, J. T., KIM, S. & KIM, V. N. 2002. MicroRNA maturation: stepwise processing and subcellular localization. *Embo j*, 21, 4663-70.
- LEE, Y., KIM, M., HAN, J., YEOM, K. H., LEE, S., BAEK, S. H. & KIM, V. N. 2004. MicroRNA genes are transcribed by RNA polymerase II. *Embo j*, 23, 4051-60.
- LEIVONEN, S. K., ROKKA, A., OSTLING, P., KOHONEN, P., CORTHALS, G. L., KALLIONIEMI, O. & PERALA, M. 2011. Identification of miR-193b targets in breast cancer cells and systems biological analysis of their functional impact. *Mol Cell Proteomics*, 10, M110.005322.
- LÉPINE, J., BERNARD, O., PLANTE, M., TÊTU, B., PELLETIER, G., LABRIE, F., BÉLANGER, A. & GUILLEMETTE, C. 2004. Specificity and Regioselectivity of the Conjugation of Estradiol, Estrone, and Their Catecholestrogen and Methoxyestrogen Metabolites by Human Uridine Diphospho-glucuronosyltransferases Expressed in Endometrium. *The Journal of Clinical Endocrinology & Metabolism*, 89, 5222-5232.
- LEVESQUE, E., BEAULIEU, M., GREEN, M. D., TEPHLY, T. R., BELANGER, A. & HUM, D. W. 1997. Isolation and characterization of UGT2B15(Y85): a UDP-glucuronosyltransferase encoded by a polymorphic gene. *Pharmacogenetics*, 7, 317-25.
- LEVESQUE, E., BEAULIEU, M., GUILLEMETTE, C., HUM, D. W. & BELANGER, A. 1998. Effect of interleukins on UGT2B15 and UGT2B17 steroid uridine diphosphate-glucuronosyltransferase expression and activity in the LNCaP cell line. *Endocrinology*, 139, 2375-81.
- LÉVESQUE, E., GIRARD, H., JOURNAULT, K., LÉPINE, J. & GUILLEMETTE, C. 2007. Regulation of the UGT1A1 bilirubin-conjugating pathway: Role of a new splicing event at the UGT1A locus. *Hepatology*, 45, 128-138.
- LEVESQUE, E., TURGEON, D., CARRIER, J. S., MONTMINY, V., BEAULIEU, M. & BELANGER, A. 2001. Isolation and characterization of the UGT2B28 cDNA encoding a novel human steroid conjugating UDP-glucuronosyltransferase. *Biochemistry*, 40, 3869-81.
- LEWIS, B. P., BURGE, C. B. & BARTEL, D. P. 2005. Conserved seed pairing, often flanked by adenosines, indicates that thousands of human genes are microRNA targets. *Cell*, 120, 15-20.
- LEWIS, B. P., SHIH, I. H., JONES-RHOADES, M. W., BARTEL, D. P. & BURGE, C. B. 2003. Prediction of mammalian microRNA targets. *Cell*, 115, 787-98.
-

-
- LI, C. H., TO, K. F., TONG, J. H., XIAO, Z., XIA, T., LAI, P. B., CHOW, S. C., ZHU, Y. X., CHAN, S. L., MARQUEZ, V. E. & CHEN, Y. 2013. Enhancer of zeste homolog 2 silences microRNA-218 in human pancreatic ductal adenocarcinoma cells by inducing formation of heterochromatin. *Gastroenterology*, 144, 1086-1097.e9.
- LI, H., XIE, N., CHEN, R., VERREAULT, M., FAZLI, L., GLEAVE, M. E., BARBIER, O. & DONG, X. 2016. UGT2B17 Expedites Progression of Castration-Resistant Prostate Cancers by Promoting Ligand-Independent AR Signaling. *Cancer Res*, 76, 6701-6711.
- LI, L. J., HUANG, Q., ZHANG, N., WANG, G. B. & LIU, Y. H. 2014. miR-376b-5p regulates angiogenesis in cerebral ischemia. *Mol Med Rep*, 10, 527-35.
- LI, S. C., CHAN, W. C., HU, L. Y., LAI, C. H., HSU, C. N. & LIN, W. C. 2010. Identification of homologous microRNAs in 56 animal genomes. *Genomics*, 96, 1-9.
- LIU, D., HU, X., ZHOU, H., SHI, G. & WU, J. 2014. Identification of Aberrantly Expressed miRNAs in Gastric Cancer. *Gastroenterol Res Pract*, 2014, 473817.
- LIU, H., YUE, D., CHEN, Y., GAO, S. J. & HUANG, Y. 2010. Improving performance of mammalian microRNA target prediction. *BMC Bioinformatics*, 11, 476.
- LIU, J., CARMELL, M. A., RIVAS, F. V., MARSDEN, C. G., THOMSON, J. M., SONG, J. J., HAMMOND, S. M., JOSHUA-TOR, L. & HANNON, G. J. 2004. Argonaute2 is the catalytic engine of mammalian RNAi. *Science*, 305, 1437-41.
- LIU, J.-E., REN, B., TANG, L., TANG, Q.-J., LIU, X.-Y., LI, X., BAI, X., ZHONG, W.-P., MENG, J.-X., LIN, H.-M., WU, H., CHEN, J.-Y. & ZHONG, S.-L. 2016. The independent contribution of miRNAs to the missing heritability in CYP3A4/5 functionality and the metabolism of atorvastatin. *Scientific Reports*, 6, 26544.
- LIU, S., GUO, W., SHI, J., LI, N., YU, X., XUE, J., FU, X., CHU, K., LU, C., ZHAO, J., XIE, D., WU, M., CHENG, S. & LIU, S. 2012. MicroRNA-135a contributes to the development of portal vein tumor thrombus by promoting metastasis in hepatocellular carcinoma. *J Hepatol*, 56, 389-96.
- LIU, W. & WANG, X. 2019. Prediction of functional microRNA targets by integrative modeling of microRNA binding and target expression data. *Genome Biology*, 20, 18.
- LIU, Y., YE, X., JIANG, F., LIANG, C., CHEN, D., PENG, J., KINCH, L. N., GRISHIN, N. V. & LIU, Q. 2009. C3PO, an endoribonuclease that promotes RNAi by facilitating RISC activation. *Science*, 325, 750-3.
- LIVAK, K. J. & SCHMITTGEN, T. D. 2001. Analysis of relative gene expression data using real-time quantitative PCR and the 2(-Delta Delta C(T)) Method. *Methods*, 25, 402-8.
- LOEB, G. B., KHAN, A. A., CANNER, D., HIATT, J. B., SHENDURE, J., DARNELL, R. B., LESLIE, C. S. & RUDENSKY, A. Y. 2012. Transcriptome-wide miR-155 binding map reveals widespread noncanonical microRNA targeting. *Mol Cell*, 48, 760-70.
- LOOKINGBILL, D. P., DEMERS, L. M., WANG, C., LEUNG, A., RITTMASER, R. S. & SANTEN, R. J. 1991. Clinical and biochemical parameters of androgen action in normal healthy Caucasian versus Chinese subjects. *J Clin Endocrinol Metab*, 72, 1242-8.
-

-
- LU, Y., HEYDEL, J. M., LI, X., BRATTON, S., LINDBLOM, T. & RADOMINSKA-PANDYA, A. 2005. Lithocholic acid decreases expression of UGT2B7 in Caco-2 cells: a potential role for a negative farnesoid X receptor response element. *Drug Metab Dispos*, 33, 937-46.
- LUKONG, K. E., CHANG, K. W., KHANDJIAN, E. W. & RICHARD, S. 2008. RNA-binding proteins in human genetic disease. *Trends Genet*, 24, 416-25.
- MACFARLANE, L. A. & MURPHY, P. R. 2010. MicroRNA: Biogenesis, Function and Role in Cancer. *Curr Genomics*, 11, 537-61.
- MACKENZIE, P. I., BOCK, K. W., BURCHELL, B., GUILLEMETTE, C., IKUSHIRO, S., IYANAGI, T., MINERS, J. O., OWENS, I. S. & NEBERT, D. W. 2005. Nomenclature update for the mammalian UDP glycosyltransferase (UGT) gene superfamily. *Pharmacogenet Genomics*, 15, 677-85.
- MACKENZIE, P. I., GREGORY, P. A., GARDNER-STEPHEN, D. A., LEWINSKY, R. H., JORGENSEN, B. R., NISHIYAMA, T., XIE, W. & RADOMINSKA-PANDYA, A. 2003. Regulation of UDP glucuronosyltransferase genes. *Curr Drug Metab*, 4, 249-57.
- MACKENZIE, P. I., HU, D. G. & GARDNER-STEPHEN, D. A. 2010. The regulation of UDP-glucuronosyltransferase genes by tissue-specific and ligand-activated transcription factors. *Drug Metab Rev*, 42, 99-109.
- MACKENZIE, P. I., MINERS, J. O. & MCKINNON, R. A. 2000. Polymorphisms in UDP glucuronosyltransferase genes: functional consequences and clinical relevance. *Clin Chem Lab Med*, 38, 889-92.
- MACKENZIE, P. I., OWENS, I. S., BURCHELL, B., BOCK, K. W., BAIROCH, A., BELANGER, A., FOURNEL-GIGLEUX, S., GREEN, M., HUM, D. W., IYANAGI, T., LANCET, D., LOUISOT, P., MAGDALOU, J., CHOWDHURY, J. R., RITTER, J. K., SCHACHTER, H., TEPHLY, T. R., TIPTON, K. F. & NEBERT, D. W. 1997. The UDP glycosyltransferase gene superfamily: recommended nomenclature update based on evolutionary divergence. *Pharmacogenetics*, 7, 255-69.
- MACKENZIE, P. I., ROGERS, A., ELLIOT, D. J., CHAU, N., HULIN, J. A., MINERS, J. O. & MEECH, R. 2011. The novel UDP glycosyltransferase 3A2: cloning, catalytic properties, and tissue distribution. *Mol Pharmacol*, 79, 472-8.
- MACKENZIE, P. I., ROGERS, A., TRELOAR, J., JORGENSEN, B. R., MINERS, J. O. & MEECH, R. 2008. Identification of UDP glycosyltransferase 3A1 as a UDP N-acetylglucosaminyltransferase. *J Biol Chem*, 283, 36205-10.
- MACLEOD, S. L., NOWELL, S., PLAXCO, J. & LANG, N. P. 2000. An allele-specific polymerase chain reaction method for the determination of the D85Y polymorphism in the human UDP-glucuronosyltransferase 2B15 gene in a case-control study of prostate cancer. *Ann Surg Oncol*, 7, 777-82.
- MANIKANDAN, M. & MUNIRAJAN, A. K. 2014. Single Nucleotide Polymorphisms in MicroRNA Binding Sites of Oncogenes: Implications in Cancer and Pharmacogenomics. *OMICS : a Journal of Integrative Biology*, 18, 142-154.
- MAO, M., WU, Z. & CHEN, J. 2016. MicroRNA-187-5p suppresses cancer cell progression in non-small cell lung cancer (NSCLC) through down-regulation of CYP1B1. *Biochem Biophys Res Commun*, 478, 649-55.

-
- MARGAILLAN, G., LEVESQUE, E. & GUILLEMETTE, C. 2016. Epigenetic regulation of steroid inactivating UDP-glucuronosyltransferases by microRNAs in prostate cancer. *J Steroid Biochem Mol Biol*, 155, 85-93.
- MARRONE, A. K., SHPYLEVA, S., CHAPPELL, G., TRYNDYAK, V., UEHARA, T., TSUCHIYA, M., BELAND, F. A., RUSYN, I. & POGRIBNY, I. P. 2016. Differentially expressed MicroRNAs provide mechanistic insight into fibrosis-associated liver carcinogenesis in mice. *Mol Carcinog*, 55, 808-17.
- MARTIN, H. C., WANI, S., STEPTOE, A. L., KRISHNAN, K., NONES, K., NOURBAKHS, E., VLASSOV, A., GRIMMOND, S. M. & CLOONAN, N. 2014. Imperfect centered miRNA binding sites are common and can mediate repression of target mRNAs. *Genome Biol*, 15, R51.
- MATHONNET, G., FABIAN, M. R., SVITKIN, Y. V., PARSYAN, A., HUCK, L., MURATA, T., BIFFO, S., MERRICK, W. C., DARZYNKIEWICZ, E., PILLAI, R. S., FILIPOWICZ, W., DUCHAINE, T. F. & SONENBERG, N. 2007. MicroRNA inhibition of translation initiation in vitro by targeting the cap-binding complex eIF4F. *Science*, 317, 1764-7.
- MATHYS, H., BASQUIN, J., OZGUR, S., CZARNOCKI-CIECIURA, M., BONNEAU, F., AARTSE, A., DZIEMBOWSKI, A., NOWOTNY, M., CONTI, E. & FILIPOWICZ, W. 2014. Structural and biochemical insights to the role of the CCR4-NOT complex and DDX6 ATPase in microRNA repression. *Mol Cell*, 54, 751-65.
- MATRANGA, C., TOMARI, Y., SHIN, C., BARTEL, D. P. & ZAMORE, P. D. 2005. Passenger-strand cleavage facilitates assembly of siRNA into Ago2-containing RNAi enzyme complexes. *Cell*, 123, 607-20.
- MAZARIS, E. & TSIOTRAS, A. 2013. Molecular pathways in prostate cancer. *Nephro-urology monthly*, 5, 792-800.
- MEECH, R., HU, D. G., MCKINNON, R. A., MUBAROKAH, S. N., HAINES, A. Z., NAIR, P. C., ROWLAND, A. & MACKENZIE, P. I. 2019. The UDP-Glycosyltransferase (UGT) Superfamily: New Members, New Functions, and Novel Paradigms. *Physiol Rev*, 99, 1153-1222.
- MEECH, R. & MACKENZIE, P. I. 1997a. Structure and function of uridine diphosphate glucuronosyltransferases. *Clin Exp Pharmacol Physiol*, 24, 907-15.
- MEECH, R. & MACKENZIE, P. I. 1997b. UDP-Glucuronosyltransferase, the Role of the Amino Terminus in Dimerization. *Journal of Biological Chemistry*, 272, 26913-26917.
- MEECH, R. & MACKENZIE, P. I. 2010. UGT3A: novel UDP-glycosyltransferases of the UGT superfamily. *Drug Metab Rev*, 42, 45-54.
- MEECH, R., MINERS, J. O., LEWIS, B. C. & MACKENZIE, P. I. 2012. The glycosidation of xenobiotics and endogenous compounds: versatility and redundancy in the UDP glycosyltransferase superfamily. *Pharmacol Ther*, 134, 200-18.
- MEECH, R., MUBAROKAH, N., SHIVASAMI, A., ROGERS, A., NAIR, P. C., HU, D. G., MCKINNON, R. A. & MACKENZIE, P. I. 2015. A novel function for UDP glycosyltransferase 8: galactosidation of bile acids. *Mol Pharmacol*, 87, 442-50.
- MEISTER, G., LANDTHALER, M., PETERS, L., CHEN, P. Y., URLAUB, H., LUHRMANN, R. & TUSCHL, T. 2005. Identification of novel argonaute-associated proteins. *Curr Biol*, 15, 2149-55.
-

-
- MEISTER, G. & TUSCHL, T. 2004. Mechanisms of gene silencing by double-stranded RNA. *Nature*, 431, 343-9.
- MIAO, L., YAO, H., LI, C., PU, M., YAO, X., YANG, H., QI, X., REN, J. & WANG, Y. 2016. A dual inhibition: microRNA-552 suppresses both transcription and translation of cytochrome P450 2E1. *Biochim Biophys Acta*, 1859, 650-62.
- MILLER, E. C. & MILLER, J. A. 1981. Searches for ultimate chemical carcinogens and their reactions with cellular macromolecules. *Cancer*, 47, 2327-45.
- MINERS, J. O., KNIGHTS, K. M., HOUSTON, J. B. & MACKENZIE, P. I. 2006. In vitro-in vivo correlation for drugs and other compounds eliminated by glucuronidation in humans: pitfalls and promises. *Biochem Pharmacol*, 71, 1531-9.
- MINERS, J. O. & MACKENZIE, P. I. 1991. Drug glucuronidation in humans. *Pharmacol Ther*, 51, 347-69.
- MINERS, J. O., MACKENZIE, P. I. & KNIGHTS, K. M. 2010. The prediction of drug-glucuronidation parameters in humans: UDP-glucuronosyltransferase enzyme-selective substrate and inhibitor probes for reaction phenotyping and in vitro-in vivo extrapolation of drug clearance and drug-drug interaction potential. *Drug Metab Rev*, 42, 196-208.
- MINERS, J. O., SMITH, P. A., MICHAEL J. SORICH, MCKINNON, R. A. & MACKENZIE, P. I. 2004. Predicting Human Drug Glucuronidation Parameters: Application of In Vitro and In Silico Modeling Approaches. *Annual Review of Pharmacology and Toxicology*, 44, 1-25.
- MIRANDA, K. C., HUYNH, T., TAY, Y., ANG, Y. S., TAM, W. L., THOMSON, A. M., LIM, B. & RIGOUTSOS, I. 2006. A pattern-based method for the identification of MicroRNA binding sites and their corresponding heteroduplexes. *Cell*, 126, 1203-17.
- MITRA, P. S., BASU, N. K., BASU, M., CHAKRABORTY, S., SAHA, T. & OWENS, I. S. 2011. Regulated Phosphorylation of a Major UDP-glucuronosyltransferase Isozyme by Tyrosine Kinases Dictates Endogenous Substrate Selection for Detoxification. *Journal of Biological Chemistry*, 286, 1639-1648.
- MITSIADES, N., SUNG, C. C., SCHULTZ, N., DANILA, D. C., HE, B., EEDUNURI, V. K., FLEISHER, M., SANDER, C., SAWYERS, C. L. & SCHER, H. I. 2012. Distinct patterns of dysregulated expression of enzymes involved in androgen synthesis and metabolism in metastatic prostate cancer tumors. *Cancer Res*, 72, 6142-52.
- MIURA, K., HIGASHIJIMA, A., MURAKAMI, Y., TSUKAMOTO, O., HASEGAWA, Y., ABE, S., FUCHI, N., MIURA, S., KANEUCHI, M. & MASUZAKI, H. 2015. Circulating chromosome 19 miRNA cluster microRNAs in pregnant women with severe pre-eclampsia. *J Obstet Gynaecol Res*, 41, 1526-32.
- MOHRI, T., NAKAJIMA, M., FUKAMI, T., TAKAMIYA, M., AOKI, Y. & YOKOI, T. 2010. Human CYP2E1 is regulated by miR-378. *Biochem Pharmacol*, 79, 1045-52.
- MONTGOMERY, R. B., MOSTAGHEL, E. A., VESSELLA, R., HESS, D. L., KALHORN, T. F., HIGANO, C. S., TRUE, L. D. & NELSON, P. S. 2008. Maintenance of intratumoral androgens in metastatic prostate cancer: a mechanism for castration-resistant tumor growth. *Cancer Res*, 68, 4447-54.

-
- MORIYA, Y., NOHATA, N., KINOSHITA, T., MUTALLIP, M., OKAMOTO, T., YOSHIDA, S., SUZUKI, M., YOSHINO, I. & SEKI, N. 2012. Tumor suppressive microRNA-133a regulates novel molecular networks in lung squamous cell carcinoma. *J Hum Genet*, 57, 38-45.
- MOROZOVA, N., ZINOVYEV, A., NONNE, N., PRITCHARD, L. L., GORBAN, A. N. & HAREL-BELLAN, A. 2012. Kinetic signatures of microRNA modes of action. *Rna*, 18, 1635-55.
- MOSTAGHEL, E. A. 2013. Steroid hormone synthetic pathways in prostate cancer. *Translational andrology and urology*, 2, 212-227.
- MUBAROKAH, S. N. 2018. *Regulation of UDP-glucuronosyltransferase 1A genes in the intestine*. Doctor of Philosophy PhD, Flinders University.
- MUKHERJI, S., EBERT, M. S., ZHENG, G. X. Y., TSANG, J. S., SHARP, P. A. & VAN OUDENAARDEN, A. 2011. MicroRNAs can generate thresholds in target gene expression. *Nature Genetics*, 43, 854.
- MULLANY, L. E., WOLFF, R. K., HERRICK, J. S., BUAS, M. F. & SLATTERY, M. L. 2015. SNP Regulation of microRNA Expression and Subsequent Colon Cancer Risk. *PLoS One*, 10, e0143894.
- MURAOKA, M., MIKI, T., ISHIDA, N., HARA, T. & KAWAKITA, M. 2007. Variety of Nucleotide Sugar Transporters with Respect to the Interaction with Nucleoside Mono- and Diphosphates. *Journal of Biological Chemistry*, 282, 24615-24622.
- MUSUNURU, K. 2003. Cell-Specific RNA-Binding Proteins in Human Disease. *Trends in Cardiovascular Medicine*, 13, 188-195.
- NADEAU, G., BELLEMARE, J., AUDET-WALSH, E., FLAGEOLE, C., HUANG, S. P., BAO, B. Y., DOUVILLE, P., CARON, P., FRADET, Y., LACOMBE, L., GUILLEMETTE, C. & LEVESQUE, E. 2011. Deletions of the androgen-metabolizing UGT2B genes have an effect on circulating steroid levels and biochemical recurrence after radical prostatectomy in localized prostate cancer. *J Clin Endocrinol Metab*, 96, E1550-7.
- NAGAR, S. & REMMEL, R. P. 2006. Uridine diphosphoglucuronosyltransferase pharmacogenetics and cancer. *Oncogene*, 25, 1659-72.
- NAKAMURA, A., NAKAJIMA, M., HIGASHI, E., YAMANAKA, H. & YOKOI, T. 2008. Genetic polymorphisms in the 5'-flanking region of human UDP-glucuronosyltransferase 2B7 affect the Nrf2-dependent transcriptional regulation. *Pharmacogenet Genomics*, 18, 709-20.
- NAKANO, M., MOHRI, T., FUKAMI, T., TAKAMIYA, M., AOKI, Y., MCLEOD, H. L. & NAKAJIMA, M. 2015. Single-Nucleotide Polymorphisms in Cytochrome P450 2E1 (CYP2E1) 3'-Untranslated Region Affect the Regulation of CYP2E1 by miR-570. *Drug Metab Dispos*, 43, 1450-7.
- NEBERT, D. W. 1994. Drug-metabolizing enzymes in ligand-modulated transcription. *Biochem Pharmacol*, 47, 25-37.
- NEELAMRAJU, Y., HASHEMIKHABIR, S. & JANGA, S. C. 2015. The human RBPome: from genes and proteins to human disease. *J Proteomics*, 127, 61-70.
- NEGRINI, M., GRAMANTIERI, L., SABBIONI, S. & CROCE, C. M. 2011. microRNA involvement in hepatocellular carcinoma. *Anticancer Agents Med Chem*, 11, 500-21.
- NIELSEN, C. B., SHOMRON, N., SANDBERG, R., HORNSTEIN, E., KITZMAN, J. & BURGE, C. B. 2007. Determinants of targeting by endogenous and exogenous microRNAs and siRNAs. *Rna*, 13, 1894-910.

-
- NISHIMURA, M. & NAITO, S. 2006. Tissue-specific mRNA expression profiles of human phase I metabolizing enzymes except for cytochrome P450 and phase II metabolizing enzymes. *Drug Metab Pharmacokinet*, 21, 357-74.
- NOTTROT, S., SIMARD, M. J. & RICHTER, J. D. 2006. Human let-7a miRNA blocks protein production on actively translating polyribosomes. *Nat Struct Mol Biol*, 13, 1108-14.
- O'BRIEN, J., HAYDER, H., ZAYED, Y. & PENG, C. 2018. Overview of MicroRNA Biogenesis, Mechanisms of Actions, and Circulation. *Frontiers in endocrinology*, 9, 402-402.
- ODA, S., FUKAMI, T., YOKOI, T. & NAKAJIMA, M. 2013. Epigenetic regulation is a crucial factor in the repression of UGT1A1 expression in the human kidney. *Drug Metab Dispos*, 41, 1738-43.
- ODA, S., FUKAMI, T., YOKOI, T. & NAKAJIMA, M. 2014. Epigenetic regulation of the tissue-specific expression of human UDP-glucuronosyltransferase (UGT) 1A10. *Biochem Pharmacol*, 87, 660-7.
- OHANIAN, M., HUMPHREYS, D. T., ANDERSON, E., PREISS, T. & FATKIN, D. 2013. A heterozygous variant in the human cardiac miR-133 gene, MIR133A2, alters miRNA duplex processing and strand abundance. *BMC Genet*, 14, 18.
- OHNO, S., KAWANA, K. & NAKAJIN, S. 2008. Contribution of UDP-glucuronosyltransferase 1A1 and 1A8 to morphine-6-glucuronidation and its kinetic properties. *Drug Metab Dispos*, 36, 688-94.
- OHNO, S. & NAKAJIN, S. 2009. Determination of mRNA expression of human UDP-glucuronosyltransferases and application for localization in various human tissues by real-time reverse transcriptase-polymerase chain reaction. *Drug Metab Dispos*, 37, 32-40.
- OKAMURA, K., HAGEN, J. W., DUAN, H., TYLER, D. M. & LAI, E. C. 2007. The mirtron pathway generates microRNA-class regulatory RNAs in *Drosophila*. *Cell*, 130, 89-100.
- OLSSON, M., LINDSTROM, S., HAGGKVIST, B., ADAMI, H. O., BALTER, K., STATTIN, P., ASK, B., RANE, A., EKSTROM, L. & GRONBERG, H. 2008. The UGT2B17 gene deletion is not associated with prostate cancer risk. *Prostate*, 68, 571-5.
- OPERANA, T. N. & TUKEY, R. H. 2007. Oligomerization of the UDP-glucuronosyltransferase 1A proteins: homo- and heterodimerization analysis by fluorescence resonance energy transfer and co-immunoprecipitation. *J Biol Chem*, 282, 4821-9.
- OSBORNE, R., JOEL, S., TREW, D. & SLEVIN, M. 1988. ANALGESIC ACTIVITY OF MORPHINE-6-GLUCURONIDE. *The Lancet*, 331, 828.
- OSBORNE, R., THOMPSON, P., JOEL, S., TREW, D., PATEL, N. & SLEVIN, M. 1992. The analgesic activity of morphine-6-glucuronide. *British journal of clinical pharmacology*, 34, 130-138.
- OZEN, M., CREIGHTON, C. J., OZDEMIR, M. & ITTMANN, M. 2008. Widespread deregulation of microRNA expression in human prostate cancer. *Oncogene*, 27, 1788-93.
- PAN, Y. Z., GAO, W. & YU, A. M. 2009. MicroRNAs regulate CYP3A4 expression via direct and indirect targeting. *Drug Metab Dispos*, 37, 2112-7.
- PANDA, H., CHUANG, T. D., LUO, X. & CHEGINI, N. 2012. Endometrial miR-181a and miR-98 expression is altered during transition from normal into

-
- cancerous state and target PGR, PGRMC1, CYP19A1, DDX3X, and TIMP3. *J Clin Endocrinol Metab*, 97, E1316-26.
- PAPAGEORGIOU, I. & COURT, M. H. 2017a. Identification and validation of microRNAs directly regulating the UDP-glucuronosyltransferase 1A subfamily enzymes by a functional genomics approach. *Biochemical Pharmacology*, 137, 93-106.
- PAPAGEORGIOU, I. & COURT, M. H. 2017b. Identification and validation of the microRNA response elements in the 3'-untranslated region of the UDP glucuronosyltransferase (UGT) 2B7 and 2B15 genes by a functional genomics approach. *Biochem Pharmacol*, 146, 199-213.
- PAQUET, S., FAZLI, L., GROSSE, L., VERREAULT, M., TETU, B., RENNIE, P. S., BELANGER, A. & BARBIER, O. 2012. Differential expression of the androgen-conjugating UGT2B15 and UGT2B17 enzymes in prostate tumor cells during cancer progression. *J Clin Endocrinol Metab*, 97, E428-32.
- PARASKEVOPOULOU, M. D., GEORGAKILAS, G., KOSTOULAS, N., VLACHOS, I. S., VERGOULIS, T., RECZKO, M., FILIPPIDIS, C., DALAMAGAS, T. & HATZIGEORGIOU, A. G. 2013. DIANA-microT web server v5.0: service integration into miRNA functional analysis workflows. *Nucleic Acids Res*, 41, W169-73.
- PARK, J., CHEN, L., SHADE, K., LAZARUS, P., SEIGNE, J., PATTERSON, S., HELAL, M. & POW-SANG, J. 2004. Asp85tyr polymorphism in the udp-glucuronosyltransferase (UGT) 2B15 gene and the risk of prostate cancer. *J Urol*, 171, 2484-8.
- PARK, J. Y., TANNER, J. P., SELLERS, T. A., HUANG, Y., STEVENS, C. K., DOSSETT, N., SHANKAR, R. A., ZACHARIAH, B., HEYSEK, R. & POW-SANG, J. 2007. Association between polymorphisms in HSD3B1 and UGT2B17 and prostate cancer risk. *Urology*, 70, 374-9.
- PASQUINELLI, A. E. 2012. MicroRNAs and their targets: recognition, regulation and an emerging reciprocal relationship. *Nat Rev Genet*, 13, 271-82.
- PATRON, J. P., FENDLER, A., BILD, M., JUNG, U., MULLER, H., ARNTZEN, M. O., PISO, C., STEPHAN, C., THIEDE, B., MOLLENKOPF, H. J., JUNG, K., KAUFMANN, S. H. & SCHREIBER, J. 2012. MiR-133b targets antiapoptotic genes and enhances death receptor-induced apoptosis. *PLoS One*, 7, e35345.
- PELLETIER, C. & WEIDHAAS, J. B. 2010. MicroRNA binding site polymorphisms as biomarkers of cancer risk. *Expert Rev Mol Diagn*, 10, 817-29.
- PETERSEN, C. P., BORDELEAU, M. E., PELLETIER, J. & SHARP, P. A. 2006. Short RNAs repress translation after initiation in mammalian cells. *Mol Cell*, 21, 533-42.
- PETERSON, S. M., THOMPSON, J. A., UFKIN, M. L., SATHYANARAYANA, P., LIAW, L. & CONGDON, C. B. 2014. Common features of microRNA target prediction tools. *Front Genet*, 5, 23.
- PHAROAH, P. D. P., DUNNING, A. M., PONDER, B. A. J. & EASTON, D. F. 2004. Association studies for finding cancer-susceptibility genetic variants. *Nat Rev Cancer*, 4, 850-860.
- PIECYK, M., WAX, S., BECK, A. R., KEDERSHA, N., GUPTA, M., MARITIM, B., CHEN, S., GUEYDAN, C., KRUYSS, V., STREULI, M. & ANDERSON, P. 2000. TIA-1 is a translational silencer that selectively regulates the expression of TNF-alpha. *Embo j*, 19, 4154-63.
-

-
- PORKKA, K. P., PFEIFFER, M. J., WALTERING, K. K., VESSELLA, R. L., TAMMELA, T. L. J. & VISAKORPI, T. 2007. MicroRNA Expression Profiling in Prostate Cancer. *Cancer Research*, 67, 6130-6135.
- PORTILHO, D. M., ALVES, M. R., KRATASSIOUK, G., ROCHE, S., MAGDINIER, F., DE SANTANA, E. C., POLESSKAYA, A., HARELBELLAN, A., MOULY, V., SAVINO, W., BUTLER-BROWNE, G. & DUMONCEAUX, J. 2015. miRNA Expression in Control and FSHD Fetal Human Muscle Biopsies. *PLOS ONE*, 10, e0116853.
- RADOMINSKA-PANDYA, A., CZERNIK, P. J., LITTLE, J. M., BATTAGLIA, E. & MACKENZIE, P. I. 1999. Structural and functional studies of UDP-glucuronosyltransferases. *Drug Metab Rev*, 31, 817-99.
- RAMIREZ, J., MIRKOV, S., ZHANG, W., CHEN, P., DAS, S., LIU, W., RATAIN, M. J. & INNOCENTI, F. 2008. Hepatocyte nuclear factor-1 alpha is associated with UGT1A1, UGT1A9 and UGT2B7 mRNA expression in human liver. *Pharmacogenomics J*, 8, 152-61.
- RAUNGRUT, P., UCHAIPICHAT, V., ELLIOT, D. J., JANCHAWEE, B., SOMOGYI, A. A. & MINERS, J. O. 2010. In vitro-in vivo extrapolation predicts drug-drug interactions arising from inhibition of codeine glucuronidation by dextropropoxyphene, fluconazole, ketoconazole, and methadone in humans. *J Pharmacol Exp Ther*, 334, 609-18.
- REHMSMEIER, M., STEFFEN, P., HOCHSMANN, M. & GIEGERICH, R. 2004. Fast and effective prediction of microRNA/target duplexes. *Rna*, 10, 1507-17.
- RIEGER, J. K., REUTTER, S., HOFMANN, U., SCHWAB, M. & ZANGER, U. M. 2015. Inflammation-associated microRNA-130b down-regulates cytochrome P450 activities and directly targets CYP2C9. *Drug Metab Dispos*, 43, 884-8.
- RITTER, J. K., CHEN, F., SHEEN, Y. Y., LUBET, R. A. & OWENS, I. S. 1992. Two human liver cDNAs encode UDP-glucuronosyltransferases with 2 log differences in activity toward parallel substrates including hyodeoxycholic acid and certain estrogen derivatives. *Biochemistry*, 31, 3409-14.
- RITTER, J. K., SHEEN, Y. Y. & OWENS, I. S. 1990. Cloning and expression of human liver UDP-glucuronosyltransferase in COS-1 cells. 3,4-catechol estrogens and estriol as primary substrates. *Journal of Biological Chemistry*, 265, 7900-6.
- RITTMASER, R. S., THOMPSON, D. L., LISTWAK, S. & LORIAUX, D. L. 1988. Androstanediol glucuronide isomers in normal men and women and in men infused with labeled dihydrotestosterone. *J Clin Endocrinol Metab*, 66, 212-6.
- RITTMASER, R. S., ZWICKER, H., THOMPSON, D. L., KONOK, G. & NORMAN, R. W. 1993. Androstanediol glucuronide production in human liver, prostate, and skin. Evidence for the importance of the liver in 5 alpha-reduced androgen metabolism. *J Clin Endocrinol Metab*, 76, 977-82.
- ROBB, G. B. & RANA, T. M. 2007. RNA helicase A interacts with RISC in human cells and functions in RISC loading. *Mol Cell*, 26, 523-37.
- RODRIGUEZ, A., GRIFFITHS-JONES, S., ASHURST, J. L. & BRADLEY, A. 2004. Identification of mammalian microRNA host genes and transcription units. *Genome Res*, 14, 1902-10.
- ROSS, R. K., BERNSTEIN, L., LOBO, R. A., SHIMIZU, H., STANCZYK, F. Z., PIKE, M. C. & HENDERSON, B. E. 1992. 5-alpha-reductase activity and risk of prostate cancer among Japanese and US white and black males. *Lancet*, 339, 887-9.
-

-
- ROTH, C., RACK, B., MULLER, V., JANNI, W., PANTEL, K. & SCHWARZENBACH, H. 2010. Circulating microRNAs as blood-based markers for patients with primary and metastatic breast cancer. *Breast Cancer Research*, 12, R90.
- ROWLAND, A., MINERS, J. O. & MACKENZIE, P. I. 2013. The UDP-glucuronosyltransferases: their role in drug metabolism and detoxification. *Int J Biochem Cell Biol*, 45, 1121-32.
- RUBY, J. G., JAN, C. H. & BARTEL, D. P. 2007. Intronic microRNA precursors that bypass Drosha processing. *Nature*, 448, 83-6.
- SAETROM, P., HEALE, B. S., SNOVE, O., JR., AAGAARD, L., ALLUIN, J. & ROSSI, J. J. 2007. Distance constraints between microRNA target sites dictate efficacy and cooperativity. *Nucleic Acids Res*, 35, 2333-42.
- SAITO, T. & SAETROM, P. 2010. A two-step site and mRNA-level model for predicting microRNA targets. *BMC Bioinformatics*, 11, 612.
- SALZMAN, D. W., SHUBERT-COLEMAN, J. & FURNEAUX, H. 2007. P68 RNA helicase unwinds the human let-7 microRNA precursor duplex and is required for let-7-directed silencing of gene expression. *J Biol Chem*, 282, 32773-9.
- SANCHEZ-DIAZ, P. & PENALVA, L. O. 2006. Post-transcription meets post-genomic: the saga of RNA binding proteins in a new era. *RNA Biol*, 3, 101-9.
- SATOH, J.-I. & TABUNOKI, H. 2011. Comprehensive analysis of human microRNA target networks. *BioData Mining*, 4, 17.
- SAUNDERS, M. A., LIANG, H. & LI, W. H. 2007. Human polymorphism at microRNAs and microRNA target sites. *Proc Natl Acad Sci U S A*, 104, 3300-5.
- SCHAEFER, O., OHTSUKI, S., KAWAKAMI, H., INOUE, T., LIEHNER, S., SAITO, A., SAKAMOTO, A., ISHIGURO, N., MATSUMARU, T., TERASAKI, T. & EBNER, T. 2012. Absolute quantification and differential expression of drug transporters, cytochrome P450 enzymes, and UDP-glucuronosyltransferases in cultured primary human hepatocytes. *Drug Metab Dispos*, 40, 93-103.
- SCHWARZ, D. S., HUTVAGNER, G., DU, T., XU, Z., ARONIN, N. & ZAMORE, P. D. 2003. Asymmetry in the assembly of the RNAi enzyme complex. *Cell*, 115, 199-208.
- SELBACH, M., SCHWANHAUSSER, B., THIERFELDER, N., FANG, Z., KHANIN, R. & RAJEWSKY, N. 2008. Widespread changes in protein synthesis induced by microRNAs. *Nature*, 455, 58-63.
- SHEFLIN, L. G. & SPAULDING, S. W. 2000. Testosterone and dihydrotestosterone regulate AUF1 isoforms in a tissue-specific fashion in the mouse. *American Journal of Physiology-Endocrinology and Metabolism*, 278, E50-E57.
- SHEFLIN, L. G., ZHANG, W. & SPAULDING, S. W. 2001. Androgen regulates the level and subcellular distribution of the AU-rich ribonucleic acid-binding protein HuR both in vitro and in vivo. *Endocrinology*, 142, 2361-8.
- SHEFLIN, L. G., ZOU, A. P. & SPAULDING, S. W. 2004. Androgens regulate the binding of endogenous HuR to the AU-rich 3'UTRs of HIF-1alpha and EGF mRNA. *Biochem Biophys Res Commun*, 322, 644-51.
- SHEN, Z. J. & MALTER, J. S. 2015. Regulation of AU-Rich Element RNA Binding Proteins by Phosphorylation and the Prolyl Isomerase Pin1. *Biomolecules*, 5, 412-34.
-

-
- SHI, X. B., XUE, L., YANG, J., MA, A. H., ZHAO, J., XU, M., TEPPER, C. G., EVANS, C. P., KUNG, H. J. & DEVERE WHITE, R. W. 2007. An androgen-regulated miRNA suppresses Bak1 expression and induces androgen-independent growth of prostate cancer cells. *Proc Natl Acad Sci U S A*, 104, 19983-8.
- SHIN, C. 2008. Cleavage of the star strand facilitates assembly of some microRNAs into Ago2-containing silencing complexes in mammals. *Mol Cells*, 26, 308-13.
- SHIN, C., NAM, J. W., FARH, K. K., CHIANG, H. R., SHKUMATAVA, A. & BARTEL, D. P. 2010. Expanding the microRNA targeting code: functional sites with centered pairing. *Mol Cell*, 38, 789-802.
- SHUKLA, G. C., SINGH, J. & BARIK, S. 2011. MicroRNAs: Processing, Maturation, Target Recognition and Regulatory Functions. *Mol Cell Pharmacol*, 3, 83-92.
- SHUKLA, U., TUMMA, N., GRATSCHEV, T., DOMBKOWSKI, A. & NOVAK, R. F. 2013. Insights into insulin-mediated regulation of CYP2E1: miR-132/-212 targeting of CYP2E1 and role of phosphatidylinositol 3-kinase, Akt (protein kinase B), mammalian target of rapamycin signaling in regulating miR-132/-212 and miR-122/-181a expression in primary cultured rat hepatocytes. *Drug Metab Dispos*, 41, 1769-77.
- SMALE, S. T. 2001. Core promoters: active contributors to combinatorial gene regulation. *Genes Dev*, 15, 2503-8.
- SMALE, S. T. & KADONAGA, J. T. 2003. The RNA polymerase II core promoter. *Annu Rev Biochem*, 72, 449-79.
- SMITH, C. W. & VALCARCEL, J. 2000. Alternative pre-mRNA splicing: the logic of combinatorial control. *Trends Biochem Sci*, 25, 381-8.
- SNEITZ, N., COURT, M. H., ZHANG, X., LAAJANEN, K., YEE, K. K., DALTON, P., DING, X. & FINEL, M. 2009. Human UDP-glucuronosyltransferase UGT2A2: cDNA construction, expression, and functional characterization in comparison with UGT2A1 and UGT2A3. *Pharmacogenet Genomics*, 19, 923-34.
- SONG, G. & WANG, L. 2008. MiR-433 and miR-127 Arise from Independent Overlapping Primary Transcripts Encoded by the miR-433-127 Locus. *PLOS ONE*, 3, e3574.
- SONG, K.-H., LI, T., OWSLEY, E. & CHIANG, J. Y. L. 2010. A putative role of micro RNA in regulation of cholesterol 7 α -hydroxylase expression in human hepatocytes. *Journal of Lipid Research*, 51, 2223-2233.
- SONG, M.-Y., PAN, K.-F., SU, H.-J., ZHANG, L., MA, J.-L., LI, J.-Y., YUASA, Y., KANG, D., KIM, Y. S. & YOU, W.-C. 2012. Identification of Serum MicroRNAs as Novel Non-Invasive Biomarkers for Early Detection of Gastric Cancer. *PLoS ONE*, 7, e33608.
- SPAHN, M., KNEITZ, S., SCHOLZ, C. J., STENGER, N., RUDIGER, T., STROBEL, P., RIEDMILLER, H. & KNEITZ, B. 2010. Expression of microRNA-221 is progressively reduced in aggressive prostate cancer and metastasis and predicts clinical recurrence. *Int J Cancer*, 127, 394-403.
- SRIVASTAVA, A., GOLDBERGER, H., DIMTCHEV, A., RAMALINGA, M., CHIJOKE, J., MARIAN, C., OERMANN, E. K., UHM, S., KIM, J. S., CHEN, L. N., LI, X., BERRY, D. L., KALLAKURY, B. V., CHAUHAN, S. C., COLLINS, S. P., SUY, S. & KUMAR, D. 2013. MicroRNA profiling in

-
- prostate cancer--the diagnostic potential of urinary miR-205 and miR-214. *PLoS One*, 8, e76994.
- STANBROUGH, M., BUBLEY, G. J., ROSS, K., GOLUB, T. R., RUBIN, M. A., PENNING, T. M., FEBBO, P. G. & BALK, S. P. 2006. Increased expression of genes converting adrenal androgens to testosterone in androgen-independent prostate cancer. *Cancer Res*, 66, 2815-25.
- STOECKLIN, G., COLOMBI, M., RAINERI, I., LEUENBERGER, S., MALLAUN, M., SCHMIDLIN, M., GROSS, B., LU, M., KITAMURA, T. & MORONI, C. 2002. Functional cloning of BRF1, a regulator of ARE-dependent mRNA turnover. *Embo j*, 21, 4709-18.
- STRASSBURG, C. P., MANNS, M. P. & TUKEY, R. H. 1998. Expression of the UDP-glucuronosyltransferase 1A locus in human colon identification and characterization of the novel extrahepatic UGT1A8. *Journal of Biological Chemistry*, 273, 8719-8726.
- STRASSBURG, C. P., OLDHAFFER, K., MANNS, M. P. & TUKEY, R. H. 1997. Differential Expression of the UGT1A Locus in Human Liver, Biliary, and Gastric Tissue: Identification of UGT1A7 and UGT1A10 Transcripts in Extrahepatic Tissue. *Molecular Pharmacology*, 52, 212-220.
- SUN, C., SOUTHARD, C., OLOPADE, O. I. & DI RIENZO, A. 2011. Differential allelic expression of c.1568C > A at UGT2B15 is due to variation in a novel cis-regulatory element in the 3'UTR. *Gene*, 481, 24-8.
- SUTLIFF, A. K., SHI, J., WATSON, C. J. W., HUNT, M., CHEN, G., ZHU, H.-J. & LAZARUS, P. 2019. Potential Regulation of UGT2B10 and UGT2B7 by miR-485-5p in human liver. *Molecular Pharmacology*, mol.119.115881.
- SZCZESNIAK, M. W. & MAKALOWSKA, I. 2014. miRNEST 2.0: a database of plant and animal microRNAs. *Nucleic Acids Res*, 42, D74-7.
- TAITT, H. E. 2018. Global Trends and Prostate Cancer: A Review of Incidence, Detection, and Mortality as Influenced by Race, Ethnicity, and Geographic Location. *Am J Mens Health*, 12, 1807-1823.
- TANG, W., JIANG, Y., MU, X., XU, L., CHENG, W. & WANG, X. 2014. MiR-135a functions as a tumor suppressor in epithelial ovarian cancer and regulates HOXA10 expression. *Cell Signal*, 26, 1420-6.
- TATAROV, O., MITCHELL, T. J., SEYWRIGHT, M., LEUNG, H. Y., BRUNTON, V. G. & EDWARDS, J. 2009. SRC family kinase activity is up-regulated in hormone-refractory prostate cancer. *Clin Cancer Res*, 15, 3540-9.
- TATSUMI, N., TOKUMITSU, S., NAKANO, M., FUKAMI, T. & NAKAJIMA, M. 2018. miR-141-3p commonly regulates human UGT1A isoforms via different mechanisms. *Drug Metab Pharmacokinet*, 33, 203-210.
- TAUPIN, J. L., TIAN, Q., KEDERSHA, N., ROBERTSON, M. & ANDERSON, P. 1995. The RNA-binding protein TIAR is translocated from the nucleus to the cytoplasm during Fas-mediated apoptotic cell death. *Proc Natl Acad Sci U S A*, 92, 1629-33.
- TAURA, K., NAITO, E., ISHII, Y., MORI, M. A., OGURI, K. & YAMADA, H. 2004. Cytochrome P450 1A1 (CYP1A1) inhibitor alpha-naphthoflavone interferes with UDP-glucuronosyltransferase (UGT) activity in intact but not in permeabilized hepatic microsomes from 3-methylcholanthrene-treated rats: possible involvement of UGT-P450 interactions. *Biol Pharm Bull*, 27, 56-60.
- TAURA, K. I., YAMADA, H., HAGINO, Y., ISHII, Y., MORI, M. A. & OGURI, K. 2000. Interaction between cytochrome P450 and other drug-metabolizing enzymes: evidence for an association of CYP1A1 with microsomal epoxide
-

-
- hydrolase and UDP-glucuronosyltransferase. *Biochem Biophys Res Commun*, 273, 1048-52.
- TAYLOR, B. S., SCHULTZ, N., HIERONYMUS, H., GOPALAN, A., XIAO, Y., CARVER, B. S., ARORA, V. K., KAUSHIK, P., CERAMI, E., REVA, B., ANTIPIN, Y., MITSIADES, N., LANDERS, T., DOLGALEV, I., MAJOR, J. E., WILSON, M., SOCCI, N. D., LASH, A. E., HEGUY, A., EASTHAM, J. A., SCHER, H. I., REUTER, V. E., SCARDINO, P. T., SANDER, C., SAWYERS, C. L. & GERALD, W. L. 2010. Integrative genomic profiling of human prostate cancer. *Cancer Cell*, 18, 11-22.
- TEPHLY, T. R. & BURCHELL, B. 1990. UDP-glucuronosyltransferases: a family of detoxifying enzymes. *Trends Pharmacol Sci*, 11, 276-9.
- TESSIER, C. R., DOYLE, G. A., CLARK, B. A., PITOT, H. C. & ROSS, J. 2004. Mammary tumor induction in transgenic mice expressing an RNA-binding protein. *Cancer Res*, 64, 209-14.
- THADANI, R. & TAMMI, M. T. 2006. MicroTar: predicting microRNA targets from RNA duplexes. *BMC Bioinformatics*, 7, S20.
- THEODORE, S. C., DAVIS, M., ZHAO, F., WANG, H., CHEN, D., RHIM, J., DEAN-COLOMB, W., TURNER, T., JI, W., ZENG, G., GRIZZLE, W. & YATES, C. 2014. MicroRNA profiling of novel African American and Caucasian Prostate Cancer cell lines reveals a reciprocal regulatory relationship of miR-152 and DNA methyltransferase 1. *Oncotarget*, 5, 3512-25.
- TOIDE, K., TAKAHASHI, Y., YAMAZAKI, H., TERAUCHI, Y., FUJII, T., PARKINSON, A. & KAMATAKI, T. 2002. Hepatocyte nuclear factor-1alpha is a causal factor responsible for interindividual differences in the expression of UDP-glucuronosyltransferase 2B7 mRNA in human livers. *Drug Metab Dispos*, 30, 613-5.
- TONG, A. W., FULGHAM, P., JAY, C., CHEN, P., KHALIL, I., LIU, S., SENZER, N., EKLUND, A. C., HAN, J. & NEMUNAITIS, J. 2009. MicroRNA profile analysis of human prostate cancers. *Cancer Gene Ther*, 16, 206-16.
- TSAI, N. P., LIN, Y. L. & WEI, L. N. 2009. MicroRNA mir-346 targets the 5'-untranslated region of receptor-interacting protein 140 (RIP140) mRNA and up-regulates its protein expression. *Biochem J*, 424, 411-8.
- TSUCHIYA, Y., NAKAJIMA, M., TAKAGI, S., TANIYA, T. & YOKOI, T. 2006. MicroRNA regulates the expression of human cytochrome P450 1B1. *Cancer Res*, 66, 9090-8.
- TUKEY, R. H. & STRASSBURG, C. P. 2000. Human UDP-glucuronosyltransferases: metabolism, expression, and disease. *Annu Rev Pharmacol Toxicol*, 40, 581-616.
- TUKEY, R. H. & STRASSBURG, C. P. 2001. Genetic multiplicity of the human UDP-glucuronosyltransferases and regulation in the gastrointestinal tract. *Mol Pharmacol*, 59, 405-14.
- TURGEON, D., CARRIER, J. S., LEVESQUE, E., BEATTY, B. G., BELANGER, A. & HUM, D. W. 2000. Isolation and characterization of the human UGT2B15 gene, localized within a cluster of UGT2B genes and pseudogenes on chromosome 4. *J Mol Biol*, 295, 489-504.
- TURGEON, D., CARRIER, J. S., LEVESQUE, E., HUM, D. W. & BELANGER, A. 2001. Relative enzymatic activity, protein stability, and tissue distribution of human steroid-metabolizing UGT2B subfamily members. *Endocrinology*, 142, 778-87.
-

-
- UCHAIPICHAT, V., MACKENZIE, P. I., GUO, X. H., GARDNER-STEPHEN, D., GALETIN, A., HOUSTON, J. B. & MINERS, J. O. 2004. Human udp-glucuronosyltransferases: isoform selectivity and kinetics of 4-methylumbelliferone and 1-naphthol glucuronidation, effects of organic solvents, and inhibition by diclofenac and probenecid. *Drug Metab Dispos*, 32, 413-23.
- UCHIDA, Y., CHIYOMARU, T., ENOKIDA, H., KAWAKAMI, K., TATARANO, S., KAWAHARA, K., NISHIYAMA, K., SEKI, N. & NAKAGAWA, M. 2013. MiR-133a induces apoptosis through direct regulation of GSTP1 in bladder cancer cell lines. *Urol Oncol*, 31, 115-23.
- VALINEZHAD ORANG, A., SAFARALIZADEH, R. & KAZEMZADEH-BAVILI, M. 2014. Mechanisms of miRNA-Mediated Gene Regulation from Common Downregulation to mRNA-Specific Upregulation. *Int J Genomics*, 2014, 970607.
- VAN SCHOONEVELD, E., WOUTERS, M. C., VAN DER AUWERA, I., PEETERS, D. J., WILDIERS, H., VAN DAM, P. A., VERGOTE, I., VERMEULEN, P. B., DIRIX, L. Y. & VAN LAERE, S. J. 2012. Expression profiling of cancerous and normal breast tissues identifies microRNAs that are differentially expressed in serum from patients with (metastatic) breast cancer and healthy volunteers. *Breast Cancer Res*, 14, R34.
- VERGARA, A. G., WATSON, C. J. & LAZARUS, P. 2017. Characterization of UDP-glycosyltransferase 3A (UGT3A) Variants in Tobacco Carcinogen Metabolism. *The FASEB Journal*, 31, 821.2-821.2.
- VERMA, A. M., PATEL, M., ASLAM, M. I., JAMESON, J., PRINGLE, J. H., WURM, P. & SINGH, B. 2015. Circulating plasma microRNAs as a screening method for detection of colorectal adenomas. *Lancet (London, England)*, 385 Suppl 1, S100-S100.
- VIDAL, A. C., TUCKER, C., SCHILDKRAUT, J. M., RICHARDSON, R. M., MCPHAIL, M., FREEDLAND, S. J., HOYO, C. & GRANT, D. J. 2013. Novel associations of UDP-glucuronosyltransferase 2B gene variants with prostate cancer risk in a multiethnic study. *BMC Cancer*, 13, 556.
- VISONE, R., RUSSO, L., PALLANTE, P., DE MARTINO, I., FERRARO, A., LEONE, V., BORBONE, E., PETROCCA, F., ALDER, H., CROCE, C. M. & FUSCO, A. 2007. MicroRNAs (miR)-221 and miR-222, both overexpressed in human thyroid papillary carcinomas, regulate p27Kip1 protein levels and cell cycle. *Endocr Relat Cancer*, 14, 791-8.
- WAGNER, B. J., DEMARIA, C. T., SUN, Y., WILSON, G. M. & BREWER, G. 1998. Structure and genomic organization of the human AUF1 gene: alternative pre-mRNA splicing generates four protein isoforms. *Genomics*, 48, 195-202.
- WANG, B., YANEZ, A. & NOVINA, C. D. 2008. MicroRNA-repressed mRNAs contain 40S but not 60S components. *Proceedings of the National Academy of Sciences*, 105, 5343.
- WANG, J., GUO, Y., CHU, H., GUAN, Y., BI, J. & WANG, B. 2013. Multiple functions of the RNA-binding protein HuR in cancer progression, treatment responses and prognosis. *Int J Mol Sci*, 14, 10015-41.
- WANG, P., NIE, Y.-L., WANG, S.-J., YANG, L.-L., YANG, W.-H., LI, J.-F., LI, X.-T. & ZHANG, L.-R. 2018. Regulation of UGT1A expression by miR-298 in human livers from the Han Chinese population and in human cell lines. *Epigenomics*, 10, 43-57.
-

-
- WANG, Y., FU, J., JIANG, M., ZHANG, X., CHENG, L., XU, X., FAN, Z., ZHANG, J., YE, Q. & SONG, H. 2014. MiR-410 is overexpressed in liver and colorectal tumors and enhances tumor cell growth by silencing FHL1 via a direct/indirect mechanism. *PLoS One*, 9, e108708.
- WEI, R., YANG, F., URBAN, T. J., LI, L., CHALASANI, N., FLOCKHART, D. A. & LIU, W. 2012. Impact of the Interaction between 3'-UTR SNPs and microRNA on the Expression of Human Xenobiotic Metabolism Enzyme and Transporter Genes. *Frontiers in Genetics*, 3, 248.
- WEI, Z., JIANG, S., ZHANG, Y., WANG, X., PENG, X., MENG, C., LIU, Y., WANG, H., GUO, L., QIN, S., HE, L., SHAO, F., ZHANG, L. & XING, Q. 2014. The effect of microRNAs in the regulation of human CYP3A4: a systematic study using a mathematical model. *Sci Rep*, 4, 4283.
- WELLS, P. G., MACKENZIE, P. I., CHOWDHURY, J. R., GUILLEMETTE, C., GREGORY, P. A., ISHII, Y., HANSEN, A. J., KESSLER, F. K., KIM, P. M., CHOWDHURY, N. R. & RITTER, J. K. 2004. Glucuronidation and the UDP-glucuronosyltransferases in health and disease. *Drug Metab Dispos*, 32, 281-90.
- WHITTEMORE, A. S., KOLONEL, L. N., WU, A. H., JOHN, E. M., GALLAGHER, R. P., HOWE, G. R., BURCH, J. D., HANKIN, J., DREON, D. M., WEST, D. W. & ET AL. 1995. Prostate cancer in relation to diet, physical activity, and body size in blacks, whites, and Asians in the United States and Canada. *J Natl Cancer Inst*, 87, 652-61.
- WIGHTMAN, B., HA, I. & RUVKUN, G. 1993. Posttranscriptional regulation of the heterochronic gene *lin-14* by *lin-4* mediates temporal pattern formation in *C. elegans*. *Cell*, 75, 855-62.
- WILLIAMS, J. A., HYLAND, R., JONES, B. C., SMITH, D. A., HURST, S., GOOSEN, T. C., PETERKIN, V., KOUP, J. R. & BALL, S. E. 2004. Drug-Drug Interactions For Udp-Glucuronosyltransferase Substrates: A Pharmacokinetic Explanation For Typically Observed Low Exposure (Auc_i/Auc) Ratios. *Drug Metabolism and Disposition*, 32, 1201-1208.
- WILLIAMS, J. A., RING, B. J., CANTRELL, V. E., CAMPANALE, K., JONES, D. R., HALL, S. D. & WRIGHTON, S. A. 2002. Differential modulation of UDP-glucuronosyltransferase 1A1 (UGT1A1)-catalyzed estradiol-3-glucuronidation by the addition of UGT1A1 substrates and other compounds to human liver microsomes. *Drug Metab Dispos*, 30, 1266-73.
- WILSON, G. M. & BREWER, G. 1999. The search for trans-acting factors controlling messenger RNA decay. *Prog Nucleic Acid Res Mol Biol*, 62, 257-91.
- WINTER, J., JUNG, S., KELLER, S., GREGORY, R. I. & DIEDERICHS, S. 2009. Many roads to maturity: microRNA biogenesis pathways and their regulation. *Nat Cell Biol*, 11, 228-34.
- WINZEN, R., THAKUR, B. K., DITTRICH-BREIHOLZ, O., SHAH, M., REDICH, N., DHAMIJA, S., KRACHT, M. & HOLTSMANN, H. 2007. Functional Analysis of KSRP Interaction with the AU-Rich Element of Interleukin-8 and Identification of Inflammatory mRNA Targets. *Molecular and Cellular Biology*, 27, 8388-8400.
- WONG, N. & WANG, X. 2015. miRDB: an online resource for microRNA target prediction and functional annotations. *Nucleic Acids Res*, 43, D146-52.
-

-
- WU, B., KULKARNI, K., BASU, S., ZHANG, S. & HU, M. 2011. First-Pass Metabolism via UDP-Glucuronosyltransferase: a Barrier to Oral Bioavailability of Phenolics. *Journal of Pharmaceutical Sciences*, 100, 3655-3681.
- XU, N., CHEN, C.-Y. A. & SHYU, A.-B. 2001. Versatile Role for hnRNP D Isoforms in the Differential Regulation of Cytoplasmic mRNA Turnover. *Molecular and Cellular Biology*, 21, 6960-6971.
- XU, W., SAN LUCAS, A., WANG, Z. & LIU, Y. 2014. Identifying microRNA targets in different gene regions. *BMC Bioinformatics*, 15 Suppl 7, S4.
- YANG, C.-C., FAZLI, L., LOGUERCIO, S., ZHARKIKH, I., AZA-BLANC, P., GLEAVE, M. E. & WOLF, D. A. 2015. Downregulation of c-SRC kinase CSK promotes castration resistant prostate cancer and pinpoints a novel disease subclass. *Oncotarget*, 6, 22060-22071.
- YANG, J.-S. & LAI, E. C. 2010. Dicer-independent, Ago2-mediated microRNA biogenesis in vertebrates. *Cell Cycle*, 9, 4455-4460.
- YANG, J. S., PHILLIPS, M. D., BETEL, D., MU, P., VENTURA, A., SIEPEL, A. C., CHEN, K. C. & LAI, E. C. 2011. Widespread regulatory activity of vertebrate microRNA* species. *Rna*, 17, 312-26.
- YASAR, U., GREENBLATT, D. J., GUILLEMETTE, C. & COURT, M. H. 2013. Evidence for regulation of UDP-glucuronosyltransferase (UGT) 1A1 protein expression and activity via DNA methylation in healthy human livers. *J Pharm Pharmacol*, 65, 874-83.
- YE, G., FU, G., CUI, S., ZHAO, S., BERNAUDO, S., BAI, Y., DING, Y., ZHANG, Y., YANG, B. B. & PENG, C. 2011a. MicroRNA 376c enhances ovarian cancer cell survival by targeting activin receptor-like kinase 7: implications for chemoresistance. *J Cell Sci*, 124, 359-68.
- YE, W., LV, Q., WONG, C.-K. A., HU, S., FU, C., HUA, Z., CAI, G., LI, G., YANG, B. B. & ZHANG, Y. 2008. The Effect of Central Loops in miRNA:MRE Duplexes on the Efficiency of miRNA-Mediated Gene Regulation. *PLoS ONE*, 3, e1719.
- YE, X., HUANG, N., LIU, Y., PAROO, Z., HUERTA, C., LI, P., CHEN, S., LIU, Q. & ZHANG, H. 2011b. Structure of C3PO and mechanism of human RISC activation. *Nat Struct Mol Biol*, 18, 650-7.
- YU, D., GREEN, B., MARRONE, A., GUO, Y., KADLUBAR, S., LIN, D., FUSCOE, J., POGRIBNY, I. & NING, B. 2015a. Suppression of CYP2C9 by microRNA hsa-miR-128-3p in human liver cells and association with hepatocellular carcinoma. *Sci Rep*, 5, 8534.
- YU, D., GREEN, B., TOLLESON, W. H., JIN, Y., MEI, N., GUO, Y., DENG, H., POGRIBNY, I. & NING, B. 2015b. MicroRNA hsa-miR-29a-3p modulates CYP2C9 in human liver cells. *Biochem Pharmacol*, 98, 215-23.
- YU, X., DHAKAL, I. B., BEGGS, M., EDAVANA, V. K., WILLIAMS, S., ZHANG, X., MERCER, K., NING, B., LANG, N. P., KADLUBAR, F. F. & KADLUBAR, S. 2010. Functional genetic variants in the 3'-untranslated region of sulfotransferase isoform 1A1 (SULT1A1) and their effect on enzymatic activity. *Toxicol Sci*, 118, 391-403.
- YU, Z., LI, Z., JOLICOEUR, N., ZHANG, L., FORTIN, Y., WANG, E., WU, M. & SHEN, S. H. 2007. Aberrant allele frequencies of the SNPs located in microRNA target sites are potentially associated with human cancers. *Nucleic Acids Res*, 35, 4535-41.
-

-
- YUAN, L.-M., GAO, Z.-Z., SUN, H.-Y., QIAN, S.-N., XIAO, Y.-S., SUN, L.-L. & ZENG, S. 2016. Inter-isoform Hetero-dimerization of Human UDP-Glucuronosyltransferases (UGTs) 1A1, 1A9, and 2B7 and Impacts on Glucuronidation Activity. *Scientific reports*, 6, 34450-34450.
- YUEH, M. F., MELLON, P. L. & TUKEY, R. H. 2011. Inhibition of human UGT2B7 gene expression in transgenic mice by the constitutive androstane receptor. *Mol Pharmacol*, 79, 1053-60.
- ZEHAVI, L., AVRAHAM, R., BARZILAI, A., BAR-ILAN, D., NAVON, R., SIDI, Y., AVNI, D. & LEIBOWITZ-AMIT, R. 2012. Silencing of a large microRNA cluster on human chromosome 14q32 in melanoma: biological effects of mir-376a and mir-376c on insulin growth factor 1 receptor. *Mol Cancer*, 11, 44.
- ZENG, Y. & CULLEN, B. R. 2005. Efficient processing of primary microRNA hairpins by Drosha requires flanking nonstructured RNA sequences. *J Biol Chem*, 280, 27595-603.
- ZENG, Y.-B., LIANG, X.-H., ZHANG, G.-X., JIANG, N., ZHANG, T., HUANG, J.-Y., ZHANG, L. & ZENG, X.-C. 2016. miRNA-135a promotes hepatocellular carcinoma cell migration and invasion by targeting forkhead box O1. *Cancer Cell International*, 16, 63.
- ZHAN, J.-W., JIAO, D.-M., WANG, Y., SONG, J., WU, J.-H., WU, L.-J., CHEN, Q.-Y. & MA, S.-L. 2017. Integrated microRNA and gene expression profiling reveals the crucial miRNAs in curcumin anti-lung cancer cell invasion. *Thoracic cancer*, 8, 461-470.
- ZHANG, J., ZHOU, W., LIU, Y., LIU, T., LI, C. & WANG, L. 2018. Oncogenic role of microRNA-532-5p in human colorectal cancer via targeting of the 5'UTR of RUNX3. *Oncol Lett*, 15, 7215-7220.
- ZHANG, P., WU, W., CHEN, Q. & CHEN, M. 2019. Non-Coding RNAs and their Integrated Networks. *Journal of integrative bioinformatics*, 16, 20190027.
- ZHANG, S. Y., SURAPUREDDI, S., COULTER, S., FERGUSON, S. S. & GOLDSTEIN, J. A. 2012a. Human CYP2C8 is post-transcriptionally regulated by microRNAs 103 and 107 in human liver. *Mol Pharmacol*, 82, 529-40.
- ZHANG, W., WAGNER, B. J., EHRENMAN, K., SCHAEFER, A. W., DEMARIA, C. T., CRATER, D., DEHAVEN, K., LONG, L. & BREWER, G. 1993. Purification, characterization, and cDNA cloning of an AU-rich element RNA-binding protein, AUF1. *Molecular and Cellular Biology*, 13, 7652-7665.
- ZHANG, X., MORRISSEY, C., SUN, S., KETCHANDJI, M., NELSON, P. S., TRUE, L. D., VAKAR-LOPEZ, F., VESSELLA, R. L. & PLYMATE, S. R. 2011. Androgen receptor variants occur frequently in castration resistant prostate cancer metastases. *PLoS One*, 6, e27970.
- ZHANG, X., ZHANG, Q. Y., LIU, D., SU, T., WENG, Y., LING, G., CHEN, Y., GU, J., SCHILLING, B. & DING, X. 2005. Expression of cytochrome p450 and other biotransformation genes in fetal and adult human nasal mucosa. *Drug Metab Dispos*, 33, 1423-8.
- ZHANG, X., ZHU, J., XING, R., TIE, Y., FU, H., ZHENG, X. & YU, B. 2012b. miR-513a-3p sensitizes human lung adenocarcinoma cells to chemotherapy by targeting GSTP1. *Lung Cancer*, 77, 488-94.
- ZHAO, L., HUA, C., LI, Y., SUN, Q. & WU, W. 2015. miR-525-5p inhibits ADAMTS13 and is correlated with Ischemia/reperfusion injury-induced
-

-
- neuronal cell death. *International Journal of Clinical and Experimental Medicine*, 8, 18115-18122.
- ZHONG, X., FENG, J., XIAO, Y., WANG, P., FAN, Q., WU, R., HU, W. & HUANG, C. 2017. Uridine diphosphate-glucuronosyltransferase 2B15 D85Y gene polymorphism is associated with lower prostate cancer risk: a systematic review and meta-analysis. *Oncotarget*, 8, 52837-52845.
- ZHOU, S. F., LIU, J. P. & CHOWBAY, B. 2009. Polymorphism of human cytochrome P450 enzymes and its clinical impact. *Drug Metab Rev*, 41, 89-295.
- ZONG, C., WANG, J. & SHI, T. M. 2014. MicroRNA 130b enhances drug resistance in human ovarian cancer cells. *Tumour Biol*, 35, 12151-6.
- ZUCCONI, B. E. & WILSON, G. M. 2011. Modulation of neoplastic gene regulatory pathways by the RNA-binding factor AUF1. *Frontiers in bioscience (Landmark edition)*, 16, 2307-2325.

APPENDIX 2

Regulation of Human UGT2B15 and UGT2B17 by miR-376c in Prostate Cancer Cell Lines

Wijayakumara DD, Hu DG, Meech R, McKinnon RA, Mackenzie PI

The Journal of Pharmacology and Experimental Therapeutics: 2015
Sep;354(3):417-25

Removed due to copyright restriction

APPENDIX 3

Regulation of UDP-Glucuronosyltransferase 2B15 by miR-331-5p in prostate cancer cells involves canonical and non-canonical target sites

Wijayakumara DD, Mackenzie PI, McKinnon RA, Hu DG, Meech R

The Journal of Pharmacology and Experimental Therapeutics: 2018 Apr;365(1):48-59

Removed due to copyright restriction

APPENDIX 4

Regulation of UDP-Glucuronosyltransferases UGT2B4 and UGT2B7 by MicroRNAs in Liver Cancer Cells

Wijayakumara DD, McKinnon RA, Mackenzie PI, Hu DG, Meech R

The Journal of Pharmacology and Experimental Therapeutics: 2017 Jun;361(3):386-397.

Removed due to copyright restriction